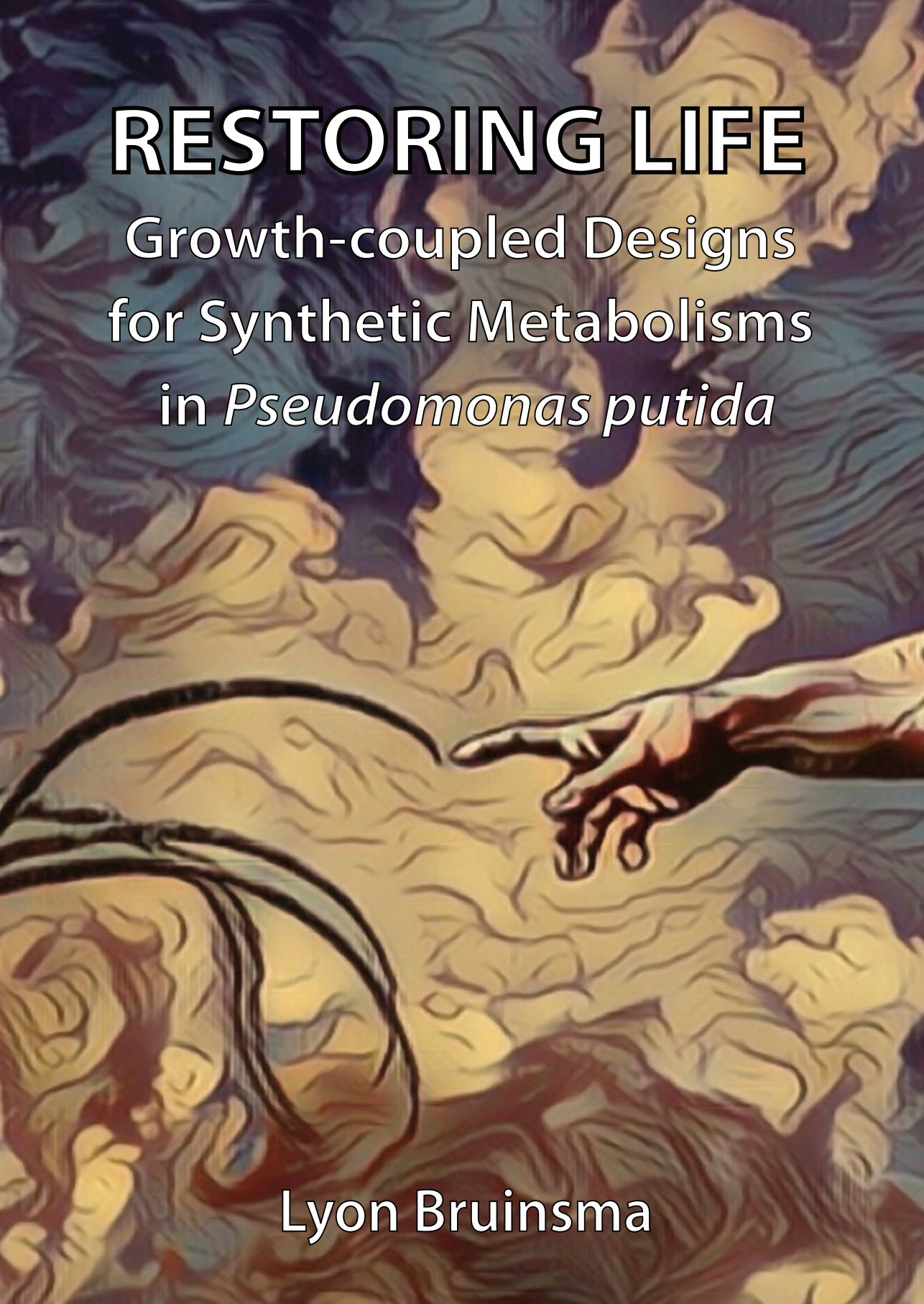
RESTORING LIFE
Growth-coupled Designs
for Synthetic Metabolisms
in *Pseudomonas putida*
Lyon Bruinsma

Propositions

1. Metabolic auxotrophies are excellent methods to implement synthetic modules.

   (this thesis)

2. Bacterial metabolism is remarkably plastic and often needs few modifications to adapt to novel lifestyles.

   (this thesis)

3. Only double-blind review ensures fairness of scientific publishing.
4. The underrepresentation of female opponents in Ph.D. defences is due to systemic biases and inadequate efforts to seek them out.
5. Keeping science conferences virtual offers the most inclusive and accessible format for researchers.
6. The monarchy should not receive special mention in proposition criteria.
7. Integrating ChatGTP in education will promote critical thinking and digital literacy skills among students.
8. Algorithms will help policymakers identify and prioritize issues based on objective data, rather than subjective opinions or biases.

Propositions belonging to this thesis, entitled

Restoring life: Growth-coupled designs for synthetic metabolisms in *Pseudomonas putida*

Lyon Bruinsma

Wageningen, 5 June 2023

RESTORING LIFE

GROWTH-COUPLED DESIGNS FOR SYNTHETIC METABOLISMS IN *PSEUDOMONAS PUTIDA*

Lyon Bruinsma

Thesis committee

Promotor

Prof. Dr Vitor A. P. Martins dos Santos
Personal Chair, Bioprocess Engineering
Wageningen University & Research

Other members

Prof. Dr D.Z. Machado de Sousa, Wageningen University & Research
Prof. Dr M. de Mey, Ghent University, Belgium
Dr S.K. Billerbeck, University of Groningen, The Netherlands
Prof. Dr M. Kisvaar, University of Tartu, Estonia

This research was conducted under the auspices of VLAG Graduate School (Biobased, Biomolecular, Chemical, Food and Nutrition Sciences).

RESTORING LIFE

GROWTH-COUPLED DESIGNS FOR SYNTHETIC METABOLISMS IN *PSEUDOMONAS PUTIDA*

Lyon Bruinsma

Thesis

submitted in fulfilment of the requirements for the degree of doctor
at Wageningen University
by the authority of the Rector Magnificus,
Prof. Dr A. P. J. Mol,
in the presence of the
Thesis Committee appointed by the Academic Board
to be defended in public
on Monday 5 June 2023
at 4 p.m. in the Omnia Auditorium.

Lyon Bruinsma
RESTORING LIFE
GROWTH-COUPLED DESIGNS FOR SYNTHETIC METABOLISMS IN *PSEUDOMONAS PUTIDA*,
232 pages.

PhD thesis, Wageningen University, Wageningen, the Netherlands (2023)
With references, with summary in English and Dutch

ISBN: 978-94-6447-648-4
DOI: 10.18174/590703

Contents

CHAPTER 1

General introduction and thesis outline

Lyon Bruinsma

"Together for implementation": the key message from the 2022 United Nations Climate Change Conference. It is an inarguable point that the world is on a rapid decline toward an irreversible catastrophe if actions are not taken soon. Our world has experienced unparallel economic growth since the discovery of fossil fuels in the Industrial revolution. Although unknown at the time, this growth led to disastrous consequences [1]. Our economy has been able to thrive at the cost of the planet: temperatures are rising, and biodiversity is declining. One could reason that we should quit fossil fuels immediately to protect the environment, yet any economist would disagree with that. In reality, economic growth is still highly prioritized over sustainability [2]. Therefore, we should strive for a "win-win" situation, where we can still ride on the flow of economic growth and at the same time achieve environmental protection [3]. This concept termed bioeconomy emerged in the 1970s as part of the broader movement toward sustainable development, which was a response to concerns about resource depletion, environmental degradation, and social inequality [4]. Its main focus lies on the revitalization of the economic system by transitioning toward the production of renewable biological resources and converting these resources into valuable products [5]. The importance of the bioeconomy has taken precedence as many countries have started to adopt its concept in their governmental policies [6][7]. This adoption is especially relevant as it can significantly aid them in achieving the sustainable development goals set by the United Nations [8]. While strong on paper, investments need to be made to establish a sustainable bioeconomy. Although composed of multilayered industries, industrial biotechnology is perceived as a major driving force for a successful bioeconomic model. [9][10][11].

Industrial biotechnology

When one sees a glass of beer or a wedge of cheese, one might not immediately think of biotechnological processes, yet both are products of biotechnological antiquity. Since ancient times, our ancestors used the innate fermentative capabilities of microorganisms as a tool for food preservation [12]. However, only since the last century has the biotechnological revolution begun when we started to leverage the overflow metabolism of microorganisms. For example, we advanced the medical

field, by using microorganisms for the production of penicillin and other antibiotics. [13]. We harnessed the power of the filamentous fungi *Aspergillus niger* to produce highly valuable citric acid for the food industry [14]. Moreover, we exploited the fermentative capabilities of *Clostridium acetobutylicum* to produce industrially relevant chemicals such as acetone, butanol, and ethanol [15]. All these examples encompass the concept of industrial biotechnology: leveraging the innate characteristics of enzymes or living organisms to produce high-value chemicals from renewable feedstocks.

Industrial biotechnology is especially interesting as it can be a key player in establishing a successful bioeconomy [10]. It has the potential to significantly reduce greenhouse gas emissions and mitigate the impacts of climate change, as many biobased products have a lower carbon footprint than their petrochemical counterparts [16]. Moreover, nearly all industrial materials currently produced with fossil resources could be substituted by biobased alternatives [17]. However, the costs of this greener approach often exceed those of conventional petrochemical processes. As mentioned earlier, economic growth is still highly prioritized over sustainability. Therefore, these processes need to be significantly optimized to be cost-competitive. For this optimization, a potential production host should meet the industrial TRY requirements indicated by: titer (g/L), rate (g/L/h), and yield (g product/g substrate) [18]. Due to these arduous requirements, only some biological processes that can compete with traditional processes have been realized on an industrial level. However, this is only a fraction of what can be attained, and more industrial processes are required to establish a sustainable bioeconomy. But how could we attain that goal?

Metabolic engineering and the DBTL cycle

So far, we discussed the usage of microorganisms to produce valuable compounds such as citric acid and butanol. These success stories can be attributed to the innate ability of these microorganisms to produce these chemicals as a byproduct of their central metabolism. Although these processes are established and commercialized, there is still substantial room for improvement for other microbial biobased processes. In most cases, microorganisms do not display natural production capac-

ities that are cost-competitive with conventional processes. Moreover, certain industrially relevant compounds cannot be naturally produced as part of the overflow metabolism. As a result, the development of new microbial cell factories through metabolic engineering is necessary to produce these compounds [19].

Metabolic engineering is a crucial concept in industrial applications because it focuses on the construction of microbial cell factories that can efficiently and cost-effectively produce valuable products [20][21]. One of the first landmark achievements in metabolic engineering was the production of human insulin in *Escherichia coli*, which greatly benefited human health for decades [22]. From here, several key achievements and discoveries of high impact have been made through metabolic engineering, such as the production of 1,3-propanediol by *E. coli* [23], and the anti-malaria drug artemisinin [24] and farnesene by engineered yeasts [25]. These studies showcase, often in combination with synthetic biology, how metabolic engineering can be utilized to produce important bioactive compounds that are only present in low quantities in nature. While promising, establishing new microbial cell factories generally encompasses multiple years of development and a considerable capital [18]. Introducing a pathway of interest in a foreign host is relatively easy, but making it thrive along the host's native metabolism and regulation is quite the task. Historically, metabolic engineering efforts have relied on a trial-and-error approach to develop a suitable strain. Luckily, the advent of exponentially improving technologies such as DNA synthesis, genome editing, high-throughput screening, and machine learning can facilitate the developmental process. However, the integration of these new methods calls for a systematic product-independent approach [26]. Therefore, an important concept within metabolic engineering for the design of microbial cell factories is the utilization of the design-build-test-learn (DBTL) cycle: an iterative framework that aids to increase the efficacy of metabolic engineering efforts [27]. (Figure 1.1).

The design phase typically starts with an analysis of the metabolic pathway involved in, for example, the production of the target compound or the consumption of a novel substrate. This often involves a detailed examination of the biochemical reactions and enzymes that are involved in the pathway, as well as an assessment of the regulatory mechanism that controls the production or consumption of the

Figure 1.1: Schematic representation of the design-build-test-learn (DBTL) cycle: adapted from the NWA-ORC project proposal of HARNESS – Hybrid Autotrophic Platform for Sustainable Polymers for a Clean, Circular Economy

target compound. This phase often goes accompanied by the usage of both kinetic and stochiometric models which aid in optimizing the metabolic network [28]. These models mathematically represent the cellular carbon flux and can give useful predictions for genetic alterations to achieve the set objective [29][30]. Based on this information, a first design can be produced which may involve the addition or deletion of specific genes, the modification of regulatory elements, or the introduction of new enzymes or metabolic pathways. Once the most optimal solution has been designed, the selected targets can be implemented in the build phase.

The build phase is critical for constructing microbial strains with the desired genetic modifications. Within the DBTL cycle, this phase can be rather challenging and time-consuming, as it requires expertise in molecular biology and genetic engineering. In addition, its success is often hampered due to other factors such as low transformation efficiency or toxicity of the introduced modules or modifications [31]. However, this phase is increasingly being facilitated since the emergence

of synthetic biology, which offers a wealth of standardized genetic parts and tools such as CRISPR-Cas9 [26][32].

The third phase is the test phase and is a critical step in the DBTL cycle to evaluate the performance of the constructed microbial strains and to identify the best candidates for the next cycle. However, just like the build phase, it can be time-consuming and moreover resource intensive. It often involves the evaluation of microbial performance under different conditions. Additionally, there may be unexpected challenges that arise during this phase, such as variability in growth rates or difficulties in measuring the concentration of the target compound [31]. However, new multi-omics systems are continuously being developed for high-throughput analysis, improving the speed and efficiency of the test phase [33][34]. In addition, the rise of synthetic biology sparked the emergence of *in vivo* biosensors to aid the test phase. These sensors can allow fast high throughput screening and facilitate the selection of a subset of strains with the best performance [35][36]. Moreover, this selection can be further improved by the establishment of biofoundries that can significantly accelerate the DBTL cycle through automation of the process [36][37].

At last, the cycle closes with the learning phase in which key insights are identified from the previous phases. This information is used to generate new hypotheses and refine the design for the microbial strains in future cycles. This phase generally comprises a set of *in-silico* tools to analyze the data from the test phase to make new predictions for the new design phase[21][38] Overall, the DBTL cycle allows researchers to rapidly design, construct, and evaluate microbial strains at an accelerated pace, and can be repeated until the set objective is accomplished [38].

Selecting a bioproduction host

Through the DBTL cycle, we can significantly accelerate the establishment of microbial hosts. But how do we determine the best hosts for bioproduction? As mentioned before, there are native production hosts that can produce industrially relevant chemicals due to overflow metabolism. However, these organisms often suffer from low genetic accessibility and more intricate compounds typically require the implementation and optimization of metabolic pathways [39]. There-

fore, a microbial production host or *chassis* is often desired with a clearly defined metabolism and multiple synthetic biology tools at its disposal for easy modification [40]. Moreover, they should have the ability to grow rapidly and robustly in defined laboratory and industrial conditions [41]. *E. coli* and *Saccharomyces cerevisiae* are typical hosts that are used for these purposes [42][43]. Both have been the center of attention for many years and a wide variety of tools has been developed for engineering and working with them [44][45]. Similarly, metabolic engineering strategies in these hosts have already been commercialized [46][47]. Albeit these historically grown organisms have advantageous traits, they are established hosts mostly due to their long history of tool development, compared to others [48]. However, nature is diverse and offers a plethora of potential hosts with attractive industrial characteristics that can be harnessed more efficiently and effectively if the right tools and knowledge are available.

***Pseudomonas putida*: a promising bioproduction host**

Industrial biotechnology is promising, but there are limitations in current industrial microbial processes such as expensive feedstocks, water usage, or low productivity due to product toxicity [49]. Phenotypic features to overcome these limitations are often polygenic and difficult to transplant into standardized hosts such as *E. coli* and *S. cerevisiae* [50]. Due to these difficulties, alternative microbial hosts are continuously being explored to tackle some of these limitations [48]. One of the potential candidates for industrial biocatalysis that has been up and coming is the gram-negative soil bacterium *Pseudomonas putida* KT2440 [51]. This bacterium has particularly gained industrial interest due to its natural high solvent tolerance, fast growth, low nutrient demands, and ability to withstand industrial conditions [52][53]. Moreover, its main carbon catabolism is a cyclic architecture composed of the Entner–Doudoroff, the Embden–Meyerhof–Parnas, and the Pentose Phosphate Pathway, which can lead to catabolic overproduction of NADPH [54]. This feature not only allows an increased oxidative stress endurance, frequently observed in an industrial setting, but it can also aid in establishing redox-demanding biocatalytic processes [55]. Because of its increasing popularity and relevant characteristics, several companies are already making use of *P. putida* to produce, for example,

2,5-furandicarboxylic acid (FDCA), polyhydroxyalkanoates, and rhamnolipids [55]. Moreover, there is an extensive repertoire of synthetic biology tools being developed to install *P. putida* as a microbial *chassis*, including promoters, vectors, and genome editing tools [56]. Additionally, both constrained-based and kinetic models have been developed [57][58]. The emergence of all these tools contributes to ushering *P. putida* as a potential industrial microbial platform for a much wider set of processes. However, while showcasing promising features, significant engineering strategies still need to be applied to further equip this bacterium with interesting metabolic features.

Accelerated cell factory development using growth-coupled selection

Traditional metabolic engineering strategies often rely on the introduction and overexpression of foreign or native genes. These strategies have allowed *P. putida* to grow on new carbon sources and to produce a plethora of valuable chemicals [59][60][61] . However, although this approach is efficient for certain modifications, engineering more intricate synthetic metabolic pathways in microbial hosts often requires more drastic metabolic rearrangements [62]. Adaptive laboratory evolution (ALE) is a powerful experimental technique to facilitate the establishment and optimization of new metabolic pathways in microbial hosts [63]. This technique relies on subjecting microbial hosts to selection pressure to allow the emergence of specific mutations to adapt to the desired conditions. ALE can equip microbial cell factories, in combination with rational metabolic engineering, with new and improved features at an accelerated rate significantly improving the DBTL cycle [64]. For example, *P. putida* was supplied with the catabolic pathway for xylose, a major constituent of lignocellulosic biomass [60]. However, the simple addition of the catabolic pathway resulted in poor growth, and further optimization through ALE was required to obtain an efficient catabolizing strain. In another study, ALE was used to increase the catabolism and tolerance of *P. putida* toward the aromatic compounds *p*-coumaric and ferulic acid [65]. Although both are great examples of ALE, they are quite straightforward and only required minimal selective pressure. Establishing and optimizing new features or production pathways is more arduous through ALE and requires substantially more evolutionary pressure. One way to

increase the pressure and accelerate the rate of evolution is by coupling ALE to growth.

Growth-coupled selections have been an up-and-coming method to drastically refactor metabolic networks, test synthetic modules, and accelerate cell factory development [66]. These strategies have shown to be quite efficient and have been deployed to optimize metabolic modules or radically refactor bacterial metabolism (Table 1.1). Moreover, they can be used to find alternatives for rate-limiting enzymes or establish production pathways [67]. The framework of these strategies is relatively simply divided. First, an auxotrophic strain is generated which cannot produce an essential precursor or reaction for cell proliferation. Second, a synthetic module is introduced for restoring growth again. In this scenario, growth is directly dependent on the efficacy of the introduced module and allows the optimization of gene expression, enzyme levels, and catalysis. These strategies are especially interesting for the traditional DBTL cycle. As we discussed in an earlier section, the test phase is often quite arduous as it generally requires laborious -omics analysis and analytics. However, in these selection strategies, microbial growth is measured as the output, and thus synthetic modules or microbial strains can be optimized *in vivo* at an accelerated rate. Moreover, if required, ALE could be applied to further optimize the synthetic modules and/or metabolism [62]. This approach has been shown to be very efficient in completely rewiring cellular metabolism to implement industrially relevant features. One key example is the establishment of a chemoautotrophic *E. coli*. By making xylose catabolism dependent on Rubisco carboxylation, the authors of the study were able to generate a strain that could generate all its biomass from CO_2 [68]. Apart from establishing new catabolic routes, growth coupling can even radically rearrange intrinsic pathways, tailoring industrial relevant features such as carbon conservation [69]. These examples showcase the tremendous plasticity of metabolic networks and how they can be radically rearranged for industrial purposes. The degree of control that we can exert nowadays over metabolism is immense and the usage of growth-coupled selections demonstrates how we can equip new microbial cell factories such as *P. putida* with novel functions at an accelerated rate.

Table 1.1: Selection of growth-coupled engineering strategies for new synthetic pathways or in vivo enzyme engineering. Adapted from [70]

Target	Auxotroph type	Selection/Engineering strategy	Sources
Synthetic metabolism			
Glycolysis alternative high carbon yield cycle (GATHCYC)	Pentose phosphate pathway	Deletion of the non-oxidative pentose phosphate pathway (*zwf1*) and transaldolase (*tal1*) and transketolase (*tkt1/2*) in *Saccharomyces cerevisiae*. A functional cycle relies on the functioning a promiscuous phosphoketolase and is required to supply the biomass precursor ribose-5-phosphate.	[69]
Ribulose monophosphate pathway	Pentose phosphate pathway	Deletion of *rpiAB* in *Escherichia coli*, making xylose catabolism dependent on methanol metabolism.	[71]
	Breakage of central carbon metabolism	Deletion of *tpiA* in *Escherichia coli* to interrupt gluconeogenesis, making pyruvate catabolism dependent on methanol metabolism.	[72]
Reductive glycine pathway	Glycine	Deletion of *phaC1 kbl ltaE glyA* to create a glycine auxotroph in *Cupriavidis necator*. Growth was restored by overexpressing the correct modules upon the presence of formate	[73]
		Deletion of *agx1, shm1,shm2, gly1* to create a glycine auxotroph in *Saccharomyces cerevisiae*. Growth was restored by overexpressing the correct modules upon the presence of formate	[74]
	Serine	Deletion of *kbl, ltaE, serA* to create a serine auxotroph in *Escherichia coli*. Growth was restored by overexpressing the correct modules upon the presence of formate	[75]
		Deletion of *serA*, PP_2533, *ltaE, aceA* to create a serine auxotroph in *Pseudomonas putida*. Growth was restored by overexpressing the correct modules upon the presence of methanol, formate, or CO_2.	[76]
Calvin Cycle	Breakage of central carbon metabolism	Deletion of *gpm* in *Escherichia coli* to create a metabolic cutoff, making pyruvate catabolism dependent on CO_2 assimilation by Rubisco.	[77]
Phosphoketolase bypass	Acetyl-CoA	Deletion of *bkdAA, ltaE,aceEF* to make acetyl CoA biosynthesis growth dependent on phosphoketolase activity.	[78]
Energy carrier			
NADH generation systems	NADH and ATP	Deletion of *lpd* involved in the pyruvate and 2-ketoglutarate dehydrogenase complex in *Escherichia coli*.	[79]
NADP-dependent formate dehydrogenase	NADPH	Deletion of NADPH-releasing reactions (*zwf, maeB, icd, sthA, pntAB*, and *maeA*) in *Escherichia coli*.	[80] [81]
***In vivo* enzyme engineering**			
D-ornithine racemase	L-arginine & L-ornithine	Deletion of *argA* in *Escherichia coli* to block L-arginine and L-ornithine biosynthesis.	[82]
Methyltransferases	Sulfur amino acids	Deletion of *cysE* in *Escherichia coli* to block methionine and cysteine biosynthesis and overexpression of the transsulfuration module from *Saccharomyces cerevisiae*.	[83]
Amine forming and converting enzymes	NH_3	Wild-type *Escherichia coli BL21*(DE3) in which the selected enzymes produced the nitrogen source in the form of ammonia or alanine.	[84]

Thesis outline and objectives

In this thesis, I aim to expand the metabolic repertoire of *P. putida* KT2440 with synthetic metabolisms for industrial biocatalysis predominantly through growth-coupled designs. In **chapter 1**, I thoroughly described the potential of *P. putida* and how growth-coupled designs can facilitate and accelerate the development of its metabolic repertoire.

Chapter 2 describes the set-up and incorporation of the assimilation of relevant C1 – feedstocks through the reductive glycine pathway. In this chapter, we created auxotrophic strains for C1 – moieties or the proteinogenic amino acid serine. Growth of these strains could only be complemented upon the introduction of assimilation pathways for industrially relevant C1 – feedstocks. Using this approach, we showed the functional complementation using methanol and formate. Moreover, for the first time, we showed synthetic CO_2 reduction through the reverse reaction of the formate dehydrogenase. This approach sets up the possibility for synthetic autotrophy by CO_2reduction through the reductive glycine pathway.

In **chapter 3** we further build upon the setup for synthetic autotrophy. To unlock the full potential of CO_2 fixation, a proper electron donor is required to provide the cell with reducing power and energy. We created a strain auxotrophic for NADH to examine the potential of several electron donors. Growth of this strain could only occur if the provided electron donor can suffice the whole cell with reducing power. A tight selection system was constructed and the feasibility of phosphite and hydrogen was assessed to supply the cell with reducing power. It was demonstrated that phosphite could serve as a phosphate donor, but not yet as an electron donor. Moreover, a synthetic module for hydrogen was created, genomically integrated, and transcribed. However, more research regarding its functionality and subsequent optimization as an electron donor is required.

A carbon conservation system in *P. putida* is described in **chapter 4**. This strategy relied on the overexpression of a highly active phosphoketolase, which circumvents the wasteful CO_2-releasing step of the pyruvate dehydrogenase. The introduced phosphoketolase shunt increased cellular fitness on both glycerol and xylose as the sole carbon source, achieving faster growth rates and higher cell densities. In addition, yields of mevalonate and malonyl-CoA on both carbon sources were im-

proved.

Chapter 5 describes the creation of a new-to-nature shikimate-dependent catabolism through radical reconfiguration of the whole metabolism of *P. putida*. Using a growth-coupled evolution strategy, we managed to acquire a superior strain with increased flux through the shikimate pathway. Further rational and model-driven engineering removed limiting steps and created a strain that uses the shikimate pathway as the dominant pathway for growth. This new-to-nature strain produced 4-hydroxybenzoate from glycerol as a by-product of growth and yielded 89.2% of the maximum theoretical yield. Moreover, we deliver a promising strain that can serve as a useful *chassis* to produce various shikimate pathway-derived compounds.

In **chapter 6**, we demonstrated for the first-time biological anisole production. Through a modular approach, we first showed anisole production from natural precursors and next extended this towards the production from glucose as the sole carbon source. Furthermore, we constructed an auxotrophic strain for *in vivo* growth-coupled evolution of methyltransferases. Using this strain, we evolved the methyltransferase responsible for anisole production and created a new superior variant.

In **chapter 7**, I summarize and discuss the work presented in this thesis and dive deeper into the bottlenecks that I encountered during my experiments as well as my vision of how I perceive the road should be paved for synthetic biology and metabolic engineering in industrial biotechnology.

Bibliography

1. Barañano, L., Unamunzaga, O., Garbisu, N., *et al.* Assessment of the Development of Forest-Based Bioeconomy in European Regions. *Sustainability (Switzerland)* **14,** 1–19 (2022).
2. Staffas, L., Gustavsson, M. & McCormick, K. Strategies and policies for the bioeconomy and bio-based economy: An analysis of official national approaches. *Sustainability (Switzerland)* **5,** 2751–2769 (2013).
3. Yang, Z., Gao, W. & Li, J. Can Economic Growth and Environmental Protection Achieve a "Win–Win" Situation? Empirical Evidence from China. *International Journal of Environmental Research and Public Health* **19** (2022).
4. Vivien, F. D., Nieddu, M., Befort, N., *et al.* The Hijacking of the Bioeconomy. *Ecological Economics* **159,** 189–197 (2019).
5. Aguilar, A., Twardowski, T. & Wohlgemuth, R. Bioeconomy for Sustainable Development. *Biotechnology Journal* **14** (2019).
6. Kuckertz, A. Bioeconomy transformation strategiesworldwide require stronger focus on entrepreneurship. *Sustainability (Switzerland)* **12** (2020).
7. Morone, P., D'Adamo, I. & Cianfroni, M. Inter-connected challenges: an overview of bioeconomy in Europe. *Environmental Research Letters* **17,** 114031 (2022).
8. El-Chichakli, B., von Braun, J., Lang, C., *et al.* Five cornerstones of a gloal bioeconomy. *Nature* **535,** 221–223 (2016).
9. Bugge, M. M., Hansen, T. & Klitkou, A. What is the bioeconomy? A review of the literature. *Sustainability (Switzerland)* **8** (2016).
10. Carus, M. & Dammer, L. The Circular Bioeconomy - Concepts, Opportunities, and Limitations. *Industrial Biotechnology* **14,** 83–91 (2018).
11. Heimann, T. Bioeconomy and SDGs: Does the Bioeconomy Support the Achievement of the SDGs? *Earth's Future* **7,** 43–57 (2019).
12. Paul Ross, R., Morgan, S. & Hill, C. Preservation and fermentation: Past, present and future. *International Journal of Food Microbiology* **79,** 3–16 (2002).
13. Pham, J. V., Yilma, M. A., Feliz, A., *et al.* A review of the microbial production of bioactive natural products and biologics. *Frontiers in Microbiology* **10,** 1–27 (2019).
14. Behera, B. C. Citric acid from Aspergillus niger: a comprehensive overview. *Critical Reviews in Microbiology* **46,** 727–749 (2020).
15. Riaz, S., Mazhar, S., Abidi, S. H., *et al.* Biobutanol production from sustainable biomass process of anaerobic ABE fermentation for industrial applications. *Archives of Microbiology* **204,** 1–9 (2022).
16. Correa, J. P., Montalvo-Navarrete, J. M. & Hidalgo-Salazar, M. A. Carbon footprint considerations for biocomposite materials for sustainable products: A review. *Journal of Cleaner Production* **208,** 785–794 (2019).
17. De Jong, E., Stichnothe, H., Bell, G., *et al. Bio-Based Chemicals: A 2020 Update* 1–79 (2020).
18. Nielsen, J. & Keasling, J. D. Engineering Cellular Metabolism. *Cell* **164,** 1185–1197 (2016).
19. Liu, Y. & Nielsen, J. Recent trends in metabolic engineering of microbial chemical factories. *Current Opinion in Biotechnology* **60,** 188–197 (2019).
20. Kim, G. B., Choi, S. Y., Cho, I. J., *et al.* Metabolic engineering for sustainability and health. *Trends in Biotechnology* **41,** 425–451 (2023).
21. Woolston, B. M., Edgar, S. & Stephanopoulos, G. Metabolic engineering: Past and future. *Annual Review of Chemical and Biomolecular Engineering* **4,** 259–288 (2013).

22. Goeddel, D. V., Kleid, D. G. & Bolivar, F. Expression in Escherichia coli of chemically synthesized genes for human insulin. *Proceedings of the National Academy of Sciences of the United States of America* **76,** 106–110 (1979).

23. Tong, I. T., Liao, H. H. & Cameron, D. C. 1,3-Propanediol production by Escherichia coli expressing genes from the Klebsiella pneumoniae dha regulon. *Applied and Environmental Microbiology* **57,** 3541–3546 (1991).

24. Paddon, C. J., Westfall, P. J., Pitera, D. J., *et al.* High-level semi-synthetic production of the potent antimalarial artemisinin. *Nature* **496,** 528–532 (2013).

25. Meadows, A. L., Hawkins, K. M., Tsegaye, Y., *et al.* Rewriting yeast central carbon metabolism for industrial isoprenoid production. *Nature* **537,** 694–697 (2016).

26. Opgenorth, P., Costello, Z., Okada, T., *et al.* Lessons from Two Design-Build-Test-Learn Cycles of Dodecanol Production in Escherichia coli Aided by Machine Learning. *ACS Synthetic Biology* **8,** 1337–1351 (2019).

27. Carbonell, P., Jervis, A. J., Robinson, C. J., *et al.* An automated Design-Build-Test-Learn pipeline for enhanced microbial production of fine chemicals. *Communications Biology* **1,** 1–10 (2018).

28. Chao, R., Mishra, S., Si, T., *et al.* Engineering biological systems using automated biofoundries. *Metabolic Engineering* **42,** 98–108 (2017).

29. Garcia-Albornoz, M. A. & Nielsen, J. Application of genome-scale metabolic models in metabolic engineering. *Industrial Biotechnology* **9,** 203–214 (2013).

30. Liao, X., Ma, H. & Tang, Y. J. Artificial intelligence: a solution to involution of design–build–test–learn cycle. *Current Opinion in Biotechnology* **75,** 102712 (2022).

31. Gurdo, N., Volke, D. C. & Nikel, P. I. Merging automation and fundamental discovery into the design–build–test–learn cycle of nontraditional microbes. *Trends in Biotechnology* **40,** 1148–1159 (2022).

32. Freemont, P. S. Synthetic biology industry: Data-driven design is creating new opportunities in biotechnology. *Emerging Topics in Life Sciences* **3,** 651–657 (2019).

33. Amer, B. & Baidoo, E. E. Omics-Driven Biotechnology for Industrial Applications. *Frontiers in Bioengineering and Biotechnology* **9,** 1–19 (2021).

34. Lawson, C. E., Harcombe, W. R., Hatzenpichler, R., *et al.* Common principles and best practices for engineering microbiomes. *Nature Reviews Microbiology* **17,** 725–741 (2019).

35. Campbell, K., Xia, J. & Nielsen, J. The Impact of Systems Biology on Bioprocessing. *Trends in Biotechnology* **35,** 1156–1168 (2017).

36. Zhang, J., Chen, Y., Fu, L., *et al.* Accelerating strain engineering in biofuel research via build and test automation of synthetic biology. *Current Opinion in Biotechnology* **67,** 88–98 (2021).

37. Holub, M. & Agena, E. Biofoundries and Citizen Science Can Accelerate Disease Surveillance and Environmental Monitoring. *SSRN Electronic Journal,* 1–7 (2022).

38. Chen, Y., Banerjee, D., Mukhopadhyay, A., *et al.* Systems and synthetic biology tools for advanced bioproduction hosts. *Current Opinion in Biotechnology* **64,** 101–109 (2020).

39. Bertsch, J. & Müller, V. Bioenergetic constraints for conversion of syngas to biofuels in acetogenic bacteria. *Biotechnology for Biofuels* **8,** 1–12 (2015).

40. De Lorenzo, V., Krasnogor, N. & Schmidt, M. For the sake of the Bioeconomy: define what a Synthetic Biology Chassis is! *New Biotechnology* **60,** 44–51 (2021).

41. Calero, P. & Nikel, P. I. Chasing bacterial chassis for metabolic engineering: a perspective review from classical to non-traditional microorganisms. *Microbial Biotechnology* **12,** 98–124 (2019).

42. Hong, K. K. & Nielsen, J. Metabolic engineering of Saccharomyces cerevisiae: A key cell factory platform for future biorefineries. *Cellular and Molecular Life Sciences* **69,** 2671–2690 (2012).

43. Pontrelli, S., Chiu, T. Y., Lan, E. I., *et al.* Escherichia coli as a host for metabolic engineering. *Metabolic Engineering* **50,** 16–46 (2018).

44. Chae, T. U., Choi, S. Y., Kim, J. W., *et al.* Recent advances in systems metabolic engineering tools and strategies. *Current Opinion in Biotechnology* **47,** 67–82 (2017).

45. Ren, J., Lee, J. & Na, D. Recent advances in genetic engineering tools based on synthetic biology. *Journal of Microbiology* **58,** 1–10 (2020).

46. McElwain, L., Phair, K., Kealey, C., *et al.* Current trends in biopharmaceuticals production in Escherichia coli. *Biotechnology Letters* **44,** 917–931 (2022).

47. Parapouli, M., Vasileiadis, A., Afendra, A. S., *et al. Saccharomyces cerevisiae and its industrial applications* **1,** 1–31 (2020).

48. Blombach, B., Grünberger, A., Centler, F., *et al.* Exploiting unconventional prokaryotic hosts for industrial biotechnology. *Trends in Biotechnology* **40,** 385–397 (2022).

49. Gong, Z., Nielsen, J. & Zhou, Y. J. Engineering Robustness of Microbial Cell Factories. *Biotechnology Journal* **12,** 1–9 (2017).

50. Thorwall, S., Schwartz, C., Chartron, J. W., *et al.* Stress-tolerant non-conventional microbes enable next-generation chemical biosynthesis. *Nature Chemical Biology* **16,** 113–121 (2020).

51. Nikel, P. I. & de Lorenzo, V. Pseudomonas putida as a functional chassis for industrial biocatalysis: From native biochemistry to trans-metabolism. *Metabolic Engineering* **50,** 142–155 (2018).

52. Ankenbauer, A., Schäfer, R. A., Viegas, S. C., *et al.* Pseudomonas putida KT2440 is naturally endowed to withstand industrial-scale stress conditions. *Microbial Biotechnology* **13,** 1145–1161 (2020).

53. Loeschcke, A. & Thies, S. Pseudomonas Putida - a Persatile Host for the Production of Natural Products. *Applied Microbiology and Biotechnology* **99,** 6197–6214 (2015).

54. Nikel, P. I., Chavarría, M., Fuhrer, T., *et al.* Pseudomonas putida KT2440 strain metabolizes glucose through a cycle formed by enzymes of the Entner-Doudoroff, embden-meyerhof-parnas, and pentose phosphate pathways. *Journal of Biological Chemistry* **290,** 25920–25932 (2015).

55. Weimer, A., Kohlstedt, M., Volke, D. C., *et al.* Industrial biotechnology of Pseudomonas putida: advances and prospects. *Applied Microbiology and Biotechnology* **104,** 7745–7766 (2020).

56. Martin-Pascual, M., Batianis, C., Bruinsma, L., *et al.* A navigation guide of synthetic biology tools for Pseudomonas putida. *Biotechnology Advances* **49,** 107732 (2021).

57. Nogales, J., Mueller, J., Gudmundsson, S., *et al.* High-quality genome-scale metabolic modelling of Pseudomonas putida highlights its broad metabolic capabilities. *Environmental Microbiology* **22,** 255–269 (2020).

58. Tokic, M., Hatzimanikatis, V. & Miskovic, L. Large-scale kinetic metabolic models of Pseudomonas putida KT2440 for consistent design of metabolic engineering strategies. *Biotechnology for Biofuels* **13,** 1–19 (2020).

59. Dvořák, P. & de Lorenzo, V. Refactoring the upper sugar metabolism of Pseudomonas putida for co-utilization of cellobiose, xylose, and glucose. *Metabolic Engineering* **48,** 94–108 (2018).

60. Elmore, J. R., Dexter, G. N., Salvachúa, D., *et al.* Engineered Pseudomonas putida simultaneously catabolizes five major components of corn stover lignocellulose: Glucose, xylose, arabinose, p-coumaric acid, and acetic acid. *Metabolic Engineering* **62,** 62–71 (2020).

61. Jha, R. K., Narayanan, N., Pandey, N., *et al.* Sensor-Enabled Alleviation of Product Inhibition in Chorismate Pyruvate-Lyase. *ACS Synthetic Biology* **8,** 775–786 (2019).

62. Cros, A., Alfaro-Espinoza, G., De Maria, A., *et al.* Synthetic metabolism for biohalogenation. *Current Opinion in Biotechnology* **74,** 180–193 (2022).

63. Mavrommati, M., Daskalaki, A., Papanikolaou, S., *et al.* Adaptive laboratory evolution principles and applications in industrial biotechnology. *Biotechnology Advances* **54,** 1–17 (2022).

64. Sandberg, T. E., Salazar, M. J., Weng, L. L., *et al.* The emergence of adaptive laboratory evolution as an efficient tool for biological discovery and industrial biotechnology. *Metabolic Engineering* **56,** 1–16 (2019).

65. Mohamed, E. T., Werner, A. Z., Salvachúa, D., *et al.* Adaptive laboratory evolution of Pseudomonas putida KT2440 improves p-coumaric and ferulic acid catabolism and tolerance. *Metabolic Engineering Communications* **11** (2020).

66. Orsi, E., Claassens, N. J., Nikel, P. I., *et al.* Growth-coupled selection of synthetic modules to accelerate cell factory development. *Nature Communications* **12,** 1–5 (2021).

67. Orsi, E., Claassens, N. J., Nikel, P. I., *et al.* Optimizing microbial networks through metabolic bypasses. *Biotechnology advances* **60,** 108035 (2022).

68. Gleizer, S., Ben-Nissan, R., Bar-On, Y. M., *et al.* Conversion of Escherichia coli to Generate All Biomass Carbon from CO2. *Cell* **179,** 1255–1263 (2019).

69. Hellgren, J., Godina, A., Nielsen, J., *et al.* Promiscuous phosphoketolase and metabolic rewiring enables novel non-oxidative glycolysis in yeast for high-yield production of acetyl-CoA derived products. *Metabolic Engineering* **62,** 150–160 (2020).

70. Chen, J., Wang, Y., Zheng, P., *et al.* Engineering synthetic auxotrophs for growth-coupled directed protein evolution. *Trends in Biotechnology* **40,** 773–776 (2022).

71. Chen, F. Y., Jung, H. W., Tsuei, C. Y., *et al.* Converting Escherichia coli to a Synthetic Methylotroph Growing Solely on Methanol. *Cell* **182,** 933–946 (2020).

72. Keller, P., Reiter, M. A., Kiefer, P., *et al.* Generation of an Escherichia coli strain growing on methanol via the ribulose monophosphate cycle. *Nature Communications* **13,** 1–13 (2022).

73. Claassens, N. J., Bordanaba-Florit, G., Cotton, C. A., *et al.* Replacing the Calvin cycle with the reductive glycine pathway in Cupriavidus necator. *Metabolic Engineering* **62,** 30–41 (2020).

74. Gonzalez De La Cruz, J., Machens, F., Messerschmidt, K., *et al.* Core Catalysis of the Reductive Glycine Pathway Demonstrated in Yeast. *ACS Synthetic Biology* **8,** 911–917 (2019).

75. Yishai, O., Bouzon, M., Döring, V., *et al. In Vivo Assimilation of One-Carbon via a Synthetic Reductive Glycine Pathway in Escherichia coli* 2018.

76. Bruinsma, L., Wenk, S., Claassens, N. J., *et al.* Paving the way for Synthetic C1 - metabolism in Pseudomonas putida through the reductive glycine pathway. *Metabolic Engineering,* 100585 (2023).

77. Antonovsky, N., Gleizer, S., Noor, E., *et al.* Sugar Synthesis from CO2 in Escherichia coli. *Cell* **166,** 115–125 (2016).

78. Wirth, N. T., Gurdo, N., Krink, N., *et al.* A synthetic C2 auxotroph of Pseudomonas putida for evolutionary engineering of alternative sugar catabolic routes. *Metabolic Engineering* **74,** 83–97 (2022).

79. Wenk, S. *Engineering formatotrophic growth in Escherichia coli* PhD thesis (Universität Potsdam, 2020), V, 107.

80. Calzadiaz-Ramirez, L., Calvó-Tusell, C., Stoffel, G. M., *et al.* In Vivo Selection for Formate Dehydrogenases with High Efficiency and Specificity toward NADP+. *ACS Catalysis* **10,** 7512–7525 (2020).

81. Lindner, S. N., Ramirez, L. C., Krüsemann, J. L., *et al.* NADPH-Auxotrophic E. coli: A Sensor Strain for Testing in Vivo Regeneration of NADPH. *ACS Synthetic Biology* **7,** 2742–2749 (2018).

82. Femmer, C., Bechtold, M., Held, M., *et al.* In vivo directed enzyme evolution in nanoliter reactors with antimetabolite selection. *Metabolic Engineering* **59,** 15–23 (2020).

83. Luo, H., Hansen, A. S. L., Yang, L., *et al.* Coupling S-adenosylmethionine–dependent methylation to growth: Design and uses. *PLoS Biology* **17,** 1–13 (2019).

84. Wu, S., Xiang, C., Zhou, Y., *et al.* A growth selection system for the directed evolution of amine-forming or converting enzymes. *Nature Communications* **13** (2022).

CHAPTER 2

PAVING THE WAY FOR SYNTHETIC C1 - METABOLISM IN *PSEUDOMONAS PUTIDA* THROUGH THE REDUCTIVE GLYCINE PATHWAY

Lyon Bruinsma, Sebastian Wenk,

Nico J. Claassens*, Vitor A. P. Martins dos Santos*

* Contributed equally

Adapted for publication as:

Paving the way for synthetic C1 - metabolism in Pseudomonas putida through the reductive glycine pathway,

2023, Metabolic Engineering

Abstract

One-carbon (C1) compounds such as methanol, formate, and CO_2 are alternative, sustainable microbial feedstocks for the biobased production of chemicals and fuels. In this study, we engineered the carbon metabolism of the industrially important bacterium *Pseudomonas putida* to modularly assimilate these three substrates through the reductive glycine pathway. First, we demonstrated the functionality of the C1-assimilation module by coupling the growth of auxotrophic strains to formate assimilation. Next, we extended the module in the auxotrophic strains from formate to methanol-dependent growth using both NAD and PQQ-dependent methanol dehydrogenases. Finally, we demonstrated, for the first time, engineered CO_2-dependent formation of part of the biomass through CO_2 reduction to formate by the native formate dehydrogenase, which required short-term evolution to rebalance the cellular NADH/NAD^+ ratio. This research paves the way to further engineer *P. putida* towards full growth on formate, methanol, and CO_2 as sole feedstocks, thereby substantially expanding its potential as a sustainable and versatile cell factory.

Introduction

Current biotechnological production of chemicals and fuels primarily depends on sugars and other plant biomass fractions as substrates. However, there are serious sustainability concerns related to these substrates due to their competition for land with biodiversity and food production [1]. Therefore, alternative microbial feedstocks need to be urgently considered. One-carbon (C1) feedstocks are considered prime sustainable alternatives, as CO_2 or reduced C1-feedstocks can be obtained from abundantly available atmospheric CO_2 or waste gas streams. CO_2 can be converted into chemicals and fuels by microorganisms when supplied with an inorganic energy source or a reduced C1-source.

Chemical (electro)catalytic methods are increasingly being developed to efficiently convert CO_2 into the soluble, reduced C1-molecules formate and methanol [2][3]. The production of e-methanol from CO_2 and electricity is already being scaled at an industrial scale in Iceland [4][5]. Both methanol and formate were identified as promising microbial feedstocks, given their liquid nature, and are therefore relatively easy to feed into the bioproduction process compared to the gaseous C1-molecules [1][4][6][7]. Energy-efficient conversion of C1-substrates into products can be achieved by anaerobic acetogenic bacteria. The bioproduction of ethanol from syngas (H_2, CO, and CO_2) has already been realized industrially, and the anaerobic production of some other products has been demonstrated [8][9]. However, these strictly anaerobic acetogens are relatively hard to modify genetically and can only generate a limited product spectrum due to their low availability of ATP [10]. Alternatively, the aerobic conversion of C1-substrates could be harnessed for a wider product spectrum, yet many aerobic C1-utilizers use energy-inefficient assimilation pathways and/or are hard to genetically modify [11][12].

Attractive aerobic biotechnological production organisms, such as *Escherichia coli*, *Saccharomyces cerevisiae*, and *Pseudomonas putida* are naturally unable to grow on C1-substrates. Nevertheless, in recent years efforts have been made in the former two organisms to establish synthetic methanol and formate assimilation. Especially efforts in *E. coli* have been successful, in which full synthetic methylotrophy and formatotrophy have been established [13][14][15]. However, the growth rates and yields of these *E. coli* strains on methanol and formate are not

sufficient yet for industrial performance. As an alternative bioproduction host, *P. putida* has emerged in recent years, as this soil bacterium is naturally endowed to withstand harsh conditions and physiochemical stresses. These features make it an industrially relevant microbe for which the generation of a plethora of products has been demonstrated [16][17][18][19]. *P. putida* cannot naturally grow on C1-substrates, and so far only the use of formate as an auxiliary energy source and the partial establishment of the Ribulose Monophosphate Pathway (RuMP) has been demonstrated [20][21]. The RuMP can allow for efficient growth on methanol, but this pathway does not allow for growth on formate or CO_2. Hence, to realize sustainable bioproduction using diverse C1-substrates in *P. putida*, efficient assimilation pathways must be established. Several pathways can be considered to establish C1-assimilation in this bacterium. Typical natural pathways for C1-assimilation such as the Calvin Cycle, RuMP, and Serine Cycle can allow for growth on CO_2, methanol, and/or formate [22][23] . However, all share the disadvantage of having a cyclic architecture in which a pathway metabolite needs to be regenerated for assimilation. Moreover, they have an intensive overlap with the host's native metabolism, making their engineering more challenging [13][14][24][25][26]. Additionally, the Calvin Cycle and the Serine Cycle are relatively energy-inefficient due to their high ATP consumption.

In recent years, the reductive glycine pathway (rGlyP) has been suggested as an alternative pathway for C1-assimilation in model microbes. This linear pathway was first designed as a synthetic pathway and recently found in nature as a CO_2 and formate assimilation pathway [24][27][28][29]. In the rGlyP, formate is converted to 5,10-methylene-THF through consecutive THF-ligation and reduction reactions. Next, 5,10-methylene-THF, together with CO_2, ammonia, and NADH produces glycine in the glycine cleavage system (GCS), which can operate in the reverse direction under elevated CO_2 concentrations. Then, glycine can be condensed with a second molecule of 5,10-methylene-THF to produce serine (Figure 2.1).

At last, serine can be converted to pyruvate through deamination and from thereon to biomass [24][30][31][32]. This formate assimilation pathway can be further extended towards methanol assimilation by adding a module containing a methanol and a formaldehyde dehydrogenase. Moreover, when equipped with a

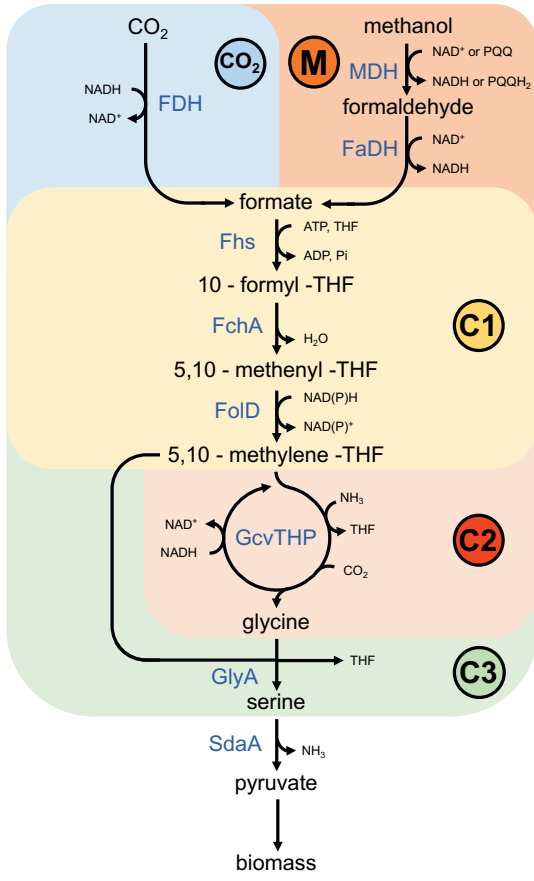

Figure 2.1: Core module of the reductive glycine pathway implemented in this study. The pathway is divided into several modules. The CO_2 and M modules convert CO_2 and methanol to formate, respectively. Formate is then converted to 5,10- methylene – THF in the C1 module. Subsequently, the 5,10 methylene-THF is converted to glycine by the C2 module comprising the reverse glycine cleavage system. In the C3 module, glycine is condensed with 5,10 methylene-THF to produce serine. Then, serine is deaminated to pyruvate where it provides the cell with the needed biomass. Abbreviations: (FDH), formate dehydrogenase, (MDH), methanol dehydrogenase, (FaDH), formaldehyde dehydrogenase, (Fhs), formate-THF-ligase, (FchA), formyltetrahydrofolate cyclohydrolase (FolD), bifunctionalmethylenetetrahydrofolate dehydrogenase/methenyltetrahydrofolate cyclohydrolase, (GcvTHP), glycine cleavage system, (GlyA), serine hydroxymethyltransferase, (SdaA), serine deaminase, (THF), tetrahydrofolate

CO_2-reducing formate dehydrogenase (FDH) and an additional energy source, the rGlyP could allow full growth on CO_2 as the sole substrate (Figure 2.1). Modular implementation of the rGlyP has recently led to the full establishment of this pathway in *E. coli* for growth on formate and methanol, and in *Cupriavidus necator* for

growth on formate [15][33]. Another recent work has demonstrated the establishment of the core of the rGlyP in *S. cerevisiae*, by converting formate into glycine [34]. The assimilation of CO_2 into the rGlyP has been proposed before, but it has not yet been demonstrated experimentally in an engineered strain [27]. The rGlyP is due to its high ATP-efficiency the aerobic pathway that can provide the highest theoretical yield on formate [4][24][35]. Also, for growth on CO_2 as the sole carbon source, the rGlyP is the most ATP-efficient aerobic pathway known; though there is an energetic disadvantage of this pathway due to the thermodynamics of the CO_2 to formate reduction reaction and its dependence on elevated CO_2. However, high-concentration CO_2 streams are commonly available and applied as a feed in industrial biotechnology [27][35]. For growth on methanol, the rGlyP is energetically only rivaled by the RuMP. Yet, the rGlyP can support higher yields than the RuMP for more oxidized products (e.g. pyruvate or lactate) as the rGlyP supports co-fixation of CO_2 with the highly reduced substrate methanol [4][35].

In this study, we establish the foundation for C1-assimilation by complementing biomass through the rGlyP for formate, methanol, and CO_2 in *P. putida*. We follow a growth-coupled modular engineering approach using specific auxotrophic strains to establish the core of the rGlyP [36]. We demonstrate the assimilation of formate, as well as methanol, through the core of the rGlyP into serine. Moreover, we demonstrate, for the first time, a growth-coupled selection for CO_2 fixation through reverse FDH activity into the rGlyP. Overall, this work demonstrates C1-assimilation of three highly promising C1-feedstocks in *P. putida*. The eventual establishment of complete C1-metabolism will substantially strengthen the position of *P. putida* as an industrial *chassis* in the bio-industry and thereby contribute to the transition to a biobased economy.

Results

Implementing the reductive glycine pathway

To implement the rGlyP, we split the pathway into three modules: C1, C2, and C3 (Figure 2.1). The C1 module converts formate to 5,10-methylene-THF, which is further converted to glycine via the reverse operation of the GCS in the C2 module. In the C3

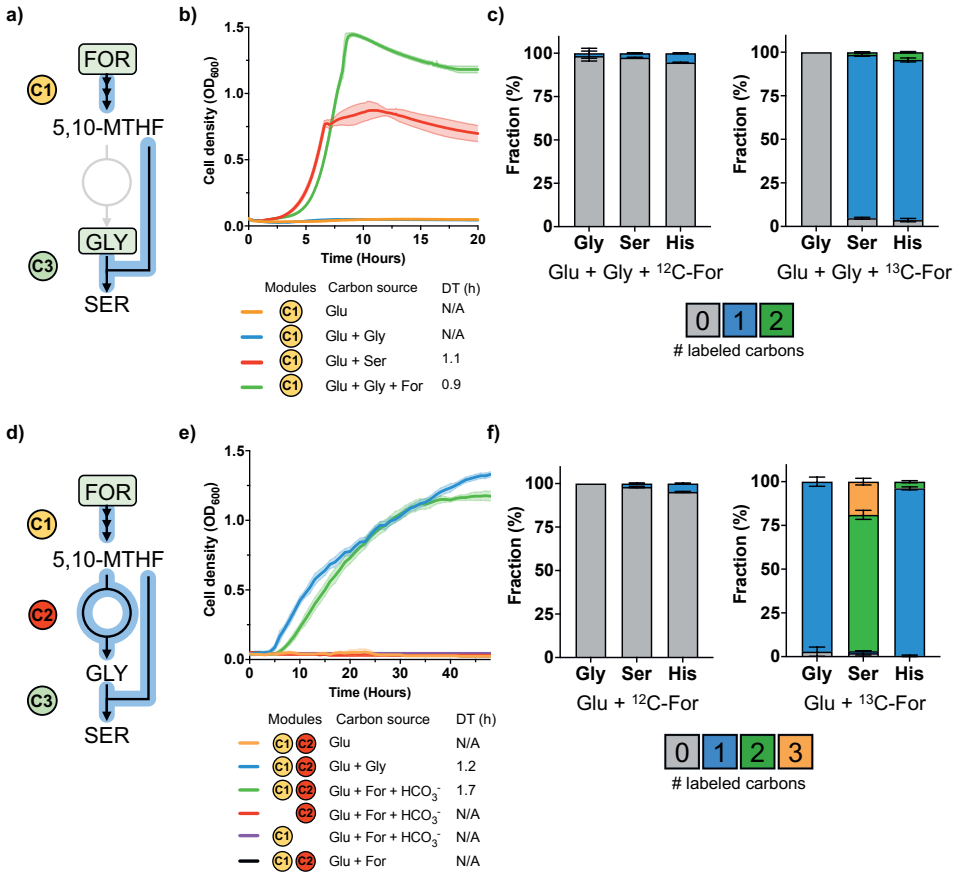

Figure 2.2: Formate-dependent growth. a) Selection of the C1 and C3 module in C1-S-aux. Growth is only possible when serine is supplemented to the medium or if both glycine and formate are present. b) Growth of C1-S-aux. Overexpression of the C1 module converts formate to replenish the cellular C1-moieties. The C3 module subsequently produces serine, restoring growth. c) ^{13}C labeling experiments confirm that cellular C1-moieties are produced from formate. d) Selection of the combined activity of the C1, C2, and C3 modules in C1-G-S-Aux. e) Growth of C1-G-S-Aux. Growth can solely be restored when glycine or formate are added to the medium (at elevated CO_2 levels through the addition of 100 mM sodium bicarbonate). f) ^{13}C labeling experiments confirm that cellular C1-moieties, glycine, and serine are produced from formate and CO_2. Abbreviations: (Gly), glycine, (Ser), serine, (His), histidine, (For), formate, (5,10-MTHF), 5,10-methylene-THF, (Glu), glucose, (HCO_3^-), bicarbonate, (N/A), not applicable, (DT), doubling time, (h) hours. Growth curves and labeling experiments represent the mean value ± SD from three biological replicates.

module, glycine is condensed with another 5,10-methylene-THF to serine. Finally, serine can be converted to pyruvate and from there to biomass. We constructed two auxotrophic strains in which the functionality of the modules could be coupled to growth, i.e., if the modules are functional the auxotrophy is relieved and the strains

will grow. To test the C1 and C3 modules, we constructed a growth-coupled design termed C1-S-Aux by deleting the genes of both GCSs (Δ*gcvTPH-I / II*) and the D-3-phosphoglycerate dehydrogenases (Δ*serA* / ΔPP_2533) (Figure 2.2 A). This strain is unable to produce serine and the C1-precursor molecules (e.g. 5,10-methylene-THF), which are essential for the biosynthesis of purines, thymidine, coenzyme A and methionine [31]. In this strain, growth on a canonical carbon source (e.g., glucose) can only be restored when serine is supplemented, or when both C1 and C3 modules are present and active with glycine and formate as substrates. In this case, the C1 module will convert formate into 5,10-methylene-THF, and the C3 module will condense 5,10-methylene-THF with glycine to form serine (Figure 2.2A).

To realize the heterologous expression of the C1 module, we created the pC1 plasmid by introducing the formate-THF ligase (*fhs*), 5,10-methenyl-THF cyclohydrolase (*fchA*), and the bifunctional 5,10-methenyl-THF cyclohydrolase / 5,10-methylene-THF dehydrogenase (*folD*) genes from *Clostridium ljunghdahlii* DSM13528 on a SEVAb24 backbone. We equipped the C1-S-Aux strain with pC1 and tested the growth of the strain on a medium containing glucose, glycine, and formate. We observed that the C1 and C3 module could carry enough flux into the C1-pool and serine to restore growth of C1-S-Aux. Growth occurred at a similar growth rate (doubling time ≈1 hour) and even a higher biomass yield than for the control medium with glucose and serine (Figure 2.2B). Overexpression of the C3 module was not necessary as endogenous activity was enough to restore growth. When formate was omitted from the medium, no growth was observed, which reflects its dependency on the assimilation of formate via the C1 module of the rGlyP. To confirm this dependency, we performed labeling experiments with ^{13}C-labeled formate and measured the labeling in the proteinogenic amino acids glycine, serine, and histidine (Figure 2.2C). If the C1 and C3 modules are functioning as expected, serine is derived from the condensation of unlabeled glycine with once-labeled 5,10-methylene-THF (derived from ^{13}C-formate). Histidine biosynthesis requires the incorporation of 10-formyl-THF, coming from formate in the C1 module, so it should also be labeled once. As expected, both serine and histidine were almost completely labeled once, confirming the activity of the C1 and C3 modules.

Next, we aimed to test the C2 module, which comprises the reverse operation

of the GCS. To test this module, we built a growth-coupled selection strain termed C1-G-S-Aux by deleting the genes encoding threonine aldolase (Δ*ltaE*), and isocitrate lyase (Δ*aceA*), as well as *serA* and PP_2533. This strain is unable to produce serine, glycine, and the C1-precursor molecules and requires external supplementation of serine or glycine for growth on glucose [32]. By the combined activity of the C1, C2, and C3 modules, formate together with CO_2 can generate glycine and subsequently serine to relieve the auxotrophy (Figure 2.2D). The GCS can run in the reverse direction at elevated CO_2 levels, which we created by supplementing the media with 100 mM sodium bicarbonate. It is unclear if the GCS uses CO_2 or bicarbonate, but these carbon species can be interconverted intracellularly by the native carbonic anhydrase (PP_0100). As the native expression level of the GCS is likely not high enough to sustain enough flux, we designed a plasmid to overexpress the native GCS system. We constructed plasmid pC2 (SEVAb65 backbone) overexpressing the endogenous *gcvT-I*, *gcvP-I*, and *gcvH-I* genes. We transformed C1-G-S-Aux with the plasmids pC1 and pC2 and were able to restore growth upon the addition of formate, at a slightly lower growth rate (doubling time 1.7 hours) and yield than for the glycine-supplemented control. (Figure 2.2E). No growth was observed when both modules were present and no bicarbonate was supplied, indicating that growth is not possible without elevated CO_2 levels. Similar to C1-S-Aux, the endogenous activity of the C3 module was sufficient to restore growth. Isotopic labeling of the proteinogenic amino acids glycine, serine, and histidine after growth on ^{13}C-formate further confirmed the combined activity of the rGlyP modules (Figure 2.2F). Glycine is produced by the condensation of labeled 5,10-methylene-THF and unlabeled CO_2 in the GCS and is expected to be labeled once. Almost all the glycine was labeled once, confirming the combined activity of the C1 and C2 modules. Serine is expected to be labeled twice as it is produced from once-labeled glycine plus a labeled 5,10-methylene-THF molecule. As expected, serine was predominantly labeled twice.

Extending the reductive glycine pathway with methanol assimilation

After demonstrating formate assimilation via the C1, C2, and C3 modules of the rGlyP we wanted to test if these modules could also serve to support methanol

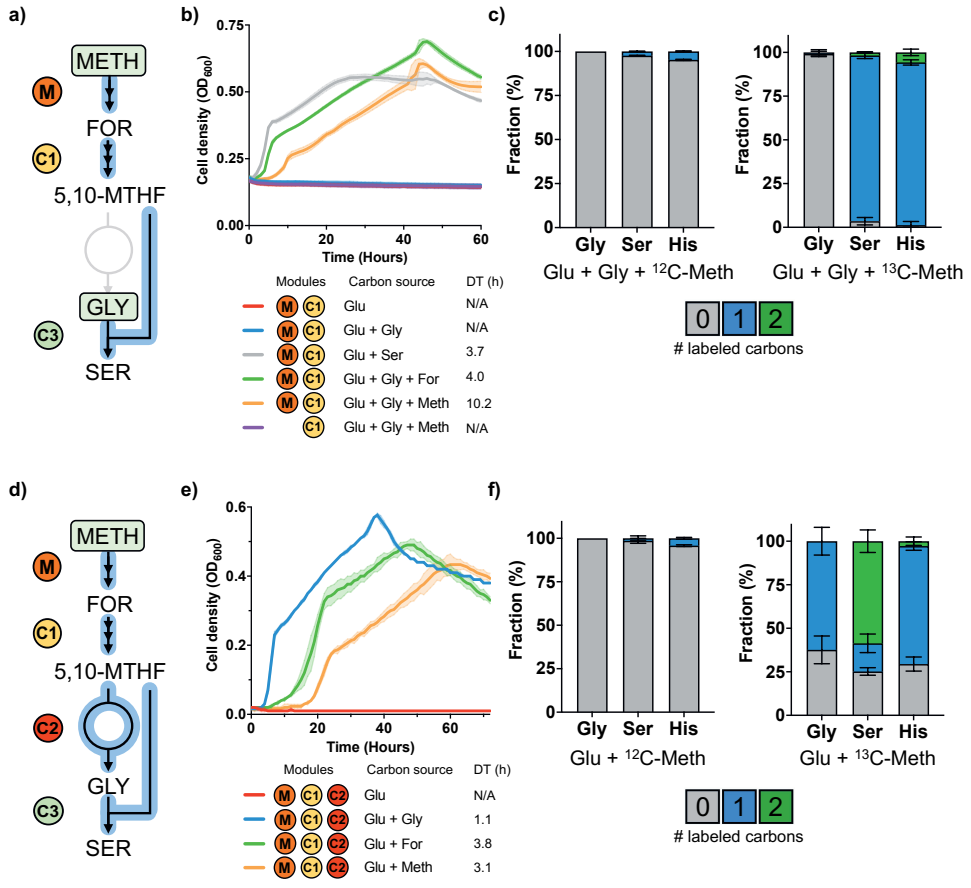

Figure 2.3: Methanol-dependent growth. a) Selection of the M, C, and C3 modules in C1-S-Aux. Growth is only possible when serine is supplemented to the medium or if both glycine and formate or methanol are present. b) Growth of C1-S-Aux expressing the MDH CT4-1 from Cupriavidus necator. Growth is only possible upon overexpression of the M and C1 module, which replenishes the cellular C1-precursor molecules. c) ^{13}C labeling experiments confirm that cellular C1-moieties are produced exclusively from methanol d) Selection of the combined effort of the M, C1, C2, and C3 modules in C1-G-S-Aux e) Growth of C1-G-S-Aux. Growth can solely be restored when glycine or methanol or formate are added to the medium (at elevated CO_2 levels through the addition of 100 mM sodium bicarbonate) f) ^{13}C labeling experiments confirm that cellular C1-moieties, glycine, and serine are produced mostly from methanol and CO_2. Abbreviations: (Gly) glycine, (Ser), serine, (His), histidine, (Meth), methanol, (For), formate (5,10-MTHF), 5,10-methylene-THF, (Glu), glucose, (N/A), not applicable, (DT), doubling time, (h) hours. Growth curves and labeling experiments represent the mean value ± SD from three biological replicates.

assimilation in *P. putida* (Figure 2.1). Like formate, methanol is a soluble microbial feedstock that can be efficiently generated from CO_2 and renewable electricity [37]. Methanol is converted to formate in two enzymatic steps. First, methanol is

oxidized to formaldehyde by a methanol dehydrogenase (MDH). Second, formaldehyde is further oxidized to formate by a formaldehyde dehydrogenase. From here on formate can be further assimilated through the engineered modules described before. To engineer methanol utilization in *P. putida*, we constructed the M-module comprising the necessary enzymes to oxidize methanol to formate. The genome of *P. putida* encodes for more than 20 alcohol dehydrogenases, yet none of them is annotated as an MDH. However, it was previously reported that some innate alcohol dehydrogenases could have a side activity towards methanol [20]. The first candidate is a pyrroloquinoline quinone (PQQ) dependent alcohol dehydrogenase, encoded by *pedE*, that showed activity towards methanol as a substrate [38]. The second candidate is a native alcohol dehydrogenase, encoded by *adhP*. Through BLAST analyses, we found that the *adhP* gene encodes a homolog of the MDH of *Corynebacterium glutamicum* (identity: 41.5%). Apart from these two candidates, we tested native or engineered enzymes originating from various organisms that were previously described to catalyze NAD-dependent methanol oxidation: *Bacillus methanolicus*, *Geobacillus stearothermophilus*, *C. glutamicum*, and *Cupriavidus necator* [39][40]. For the oxidation of formaldehyde to formate, we overexpressed the *fdhA* gene of *P. putida*, encoding a NAD-dependent formaldehyde dehydrogenase.

The various MDH candidate genes and *fdhA* were cloned into pC1, creating pM. We transformed C1-S-Aux with the various pM plasmids to assess which MDH candidate can sustain the highest flux and therefore growth. Without the plasmid expression of an MDH (M-module) no growth was observed. All MDH candidates were able to restore growth of the C1-S-Aux strain on glucose, glycine, and methanol, albeit with different growth patterns (Figure S2.1). The engineered MDH from *C. necator* was able to sustain the best growth (10 hrs. doubling time) with the shortest lag phase (Figure 2.3B). Next, growth was fastest restored using the MDH from *B. methanolicus* and *C. glutamicum*, followed by *adhP* and *G. stearothermophilus*. The PQQ-dependent alcohol dehydrogenase from *P. putida* was able to sustain growth (11 hrs. doubling time) despite its long lag phase compared to the strains expressing a NAD-MDH. As far as we know, this is the first time an overexpressed PQQ-dependent enzyme has been demonstrated for engineered methanol oxidation.

Methanol oxidation using PQQ instead of NAD^+ as an electron acceptor can be potentially advantageous as it has a larger thermodynamic driving force, -35.2 kJ/mol compared to 30.5 kJ/mol ($\Delta_r G'^m$, pH 7.5, ionic strength 0.25 M) [4][12]. NAD-MDH activity is notorious for being a thermodynamic, as well as a kinetic bottleneck for synthetic methylotrophy [41]. Even though we showed proof of principle for the PQQ-dependent operation of an MDH, the best NAD-MDH resulted in faster growth in C1-S-Aux. Still, further optimization of PQQ-MDHs, including for example upregulation of native *P. putida* PQQ biosynthesis, can possibly sustain faster growth rates and may be beneficial to support full methylotrophy. However, in this work, we further proceeded with the best-performing NAD-MDH from *C. necator* to demonstrate the potential of the rGlyP for synthetic methylotrophy in *P. putida* (Figure 2.3B). Just as with formate, methanol became essential for the growth of C1-S-Aux, and omitting it from the medium resulted in no growth. Labeling experiments with ^{13}C-methanol further confirmed the combined activity of the M, C1, and C3 modules. As expected, serine and histidine were both labeled once (Figure 2.3C).

We further tested methanol assimilation via the rGlyP till serine in the C1-G-S-Aux strain. Hereto, we tested pM with the engineered MDH from *C. necator* together with pC2. Experiments were performed at elevated CO_2 to reverse the GCS reaction by supplying 100 mM sodium bicarbonate to the medium. Through the combined effort of the M, C1, C2, and C3 modules, methanol together with CO_2 could potentially provide the cell with the necessary glycine and serine. As expected, growth was restored upon expression of all the modules and the addition of the required C1-compounds (Figure 2.3E). We performed labeling experiments to confirm the activity of the combined modules (Figure 2.3F). We note that a small fraction of all glycine and serine is unlabeled. Glycine can be produced by the amination of glyoxylate through promiscuous aminotransferase enzymes. However, the isocitrate lyase (*aceA*) is deleted in C1-G-S-Aux, making it unable to produce glyoxylate. We hypothesize that a latent unidentified reaction in *P. putida* can still produce glycine, e.g., from threonine, and was activated during growth of C1-G-S-Aux on methanol, contributing to the unlabeled fraction (≈37% of glycine). Nonetheless, taking the growth and labeling patterns into account, we can still conclude that methanol assimilation via the modules of the rGlyP carries most of the flux in C1-G-S-Aux.

Extending the reductive glycine pathway with CO_2 fixation

Apart from methanol oxidation, formate can be produced through CO_2 reduction [29][42][43][44][45][46]. FDHs commonly convert formate to CO_2, which is thermodynamically the most favorable direction. However, metal-dependent FDHs, using molybdenum or tungsten, can also serve in CO_2 fixation pathways by reducing CO_2 to formate [27][47]. The genome of *P. putida* accounts for two native FDHs. The genes *fdoGHI-fdhE* (PP_0489-0492) encode a membrane-bound FDH, which possibly uses quinol as a redox cofactor. The second FDH (PP_2183-2186) is a soluble NAD-dependent molybdenum-containing FDH [21]. We reasoned that the molybdenum-containing NAD-FDH from *P. putida* could be able to reduce CO_2 to formate and serve as an entry point for the rGlyP. To test this hypothesis, we constructed pCO_2 containing PP_2183-2186 on a SEVA83b backbone. We transformed C1-S-Aux with both pC1 and pCO_2 and grew the strain in sealed bottles containing 20 mM glucose, 10 mM glycine, and CO_2. The thermodynamics of CO_2 reduction are highly unfavorable ($\Delta_r G'^m$ = 14.4 kJ/mol, pH 7.5, ionic strength 0.25 M) [48]. Therefore, we filled the headspace of the bottles with 50% (v/v) CO_2 to push the reduction reaction. After a few weeks of incubation, we observed growth in one of the bottles. Reinoculation of this strain in fresh media with glucose, glycine, and 50% CO_2 enabled immediate growth (Figure S2.2). We cultivated this strain, termed C1-S-Evo, in a range of different CO_2 concentrations, from ambient (0.04%) to 50%, to examine the CO_2 dependency of this strain. We observed that growth was highly dependent on the concentration of CO_2 added to the headspace (Figure 2.4B). Fast growth was observed when the headspace was filled with 20-50% CO_2, with doubling times ranging from 13.7 down to 6.0 hours, respectively. Growth still occurred at 10% CO_2, albeit with a lower doubling time (39.7 hours). The clear dependency of the growth phenotype on the CO_2 concentration is likely related to the thermodynamic driving force of CO_2 reduction by FDH, which can be improved by increasing CO_2 concentrations. Growth was not observed when the pCO_2 plasmid was omitted, indicating that growth relies on the overexpression of FDH. Moreover, we noticed that this strain was able to grow at ambient CO_2 levels (Figure 2.4B, gray line). We hypothesized that the respiration of glucose (still proceeding to supply other biomass components than C1) increases the CO_2 concentration in the headspace, driving formate biosynthesis. To test this

hypothesis, we cultivated the strain in a closed and open environment, wherein the latter the CO_2 can freely escape. In both instances, growth occurred similarly (Figure S2.3). This indicates that the CO_2 present in the air and/or intracellularly generated from glucose respiration is enough to drive the reverse reaction toward formate production. To elucidate what changes had occurred during evolution to allow these CO_2-fixing phenotypes, the pC1 and pCO_2 plasmids of three growing isolates were sequenced.

We discovered a point mutation in the -35 box of the promoter of the CO_2 module, lowering its expression by 31.5-fold based on GFP fluorescence, indicating that the initial expression level of the promoter was too high (Figure S2.4). We transformed C1-S-Aux with pC1 and the mutated pCO_2 plasmid, to analyze if this mutation was the sole cause for growth. However, no immediate growth was observed (Data not shown). Therefore, genomic alterations likely contributed to establish this CO_2-dependent growth phenotype. We sequenced the genomes of three purified colonies from the evolved population and discovered four common mutations in all three isolates (Table S4). The most noticeable mutation was the introduction of a stop codon in the middle of the *nuoG* gene encoding the G subunit of the NADH-quinone oxidoreductase (complex I) in the electron transport chain. This complex is directly responsible for NADH oxidation and is needed to regenerate NAD^+ for glycolysis. The occurred mutation allows translation of only half of NuoG, probably either interrupting or decreasing the NADH oxidation activity complex I (Figure 2.4D). *P. putida* is an obligate aerobic bacteria, which relies on constitutive NADH dehydrogenase activity to oxidize NADH to NAD^+ [50]. This innate high NADH oxidation activity competes with FDH over NADH availability, likely preventing CO_2 reduction in the unevolved strain. Thus, we hypothesize that this mutation causes a redox perturbance that increases NADH levels for CO_2 reduction. We reverse-engineered the stop codon mutation in *nuoG* in C1-S-Aux to test the influence of this mutation and transformed the strain with pC1 and the mutated pCO_2 plasmid. After the introduction of this mutation, growth could occur at ambient and 50% CO_2 without the need for evolution, showcasing the beneficial effect of this mutation (Figure 2.4E). However, growth was still lagging compared to the evolved strain, so some of the other mutations may have contributed partly to the phenotype. To further prove

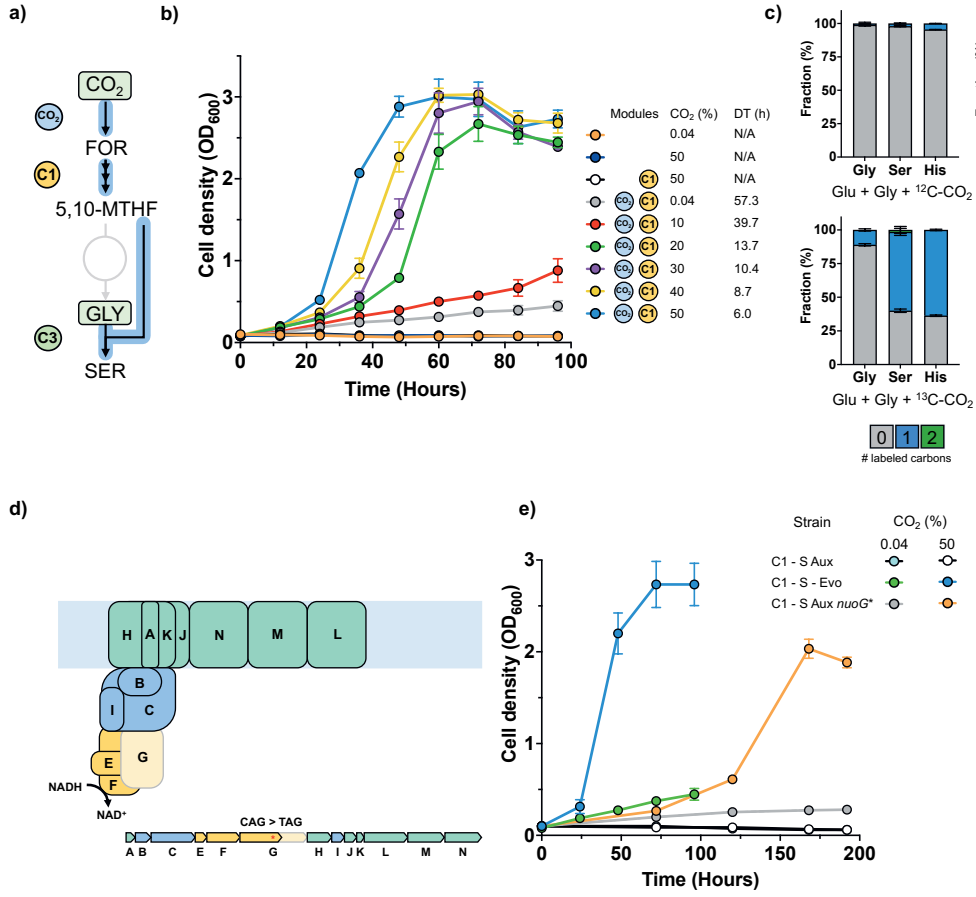

Figure 2.4: CO_2-dependent growth. A) Selection of the CO_2, C1, and C3 modules in C1-S-Aux/Evo. Growth is only possible when serine is supplemented to the medium or if both glycine and CO_2 are present. B) Growth of C1-S-Evo in different CO_2 concentrations. Growth is only possible upon overexpression of the CO_2 and C1 module, which replenishes the cellular C1-moieties. Growth is heavily dependent on the increasing CO_2 concentrations. C) ^{13}C labeling experiments confirm that cellular C1-moieties are produced mostly from CO_2. Data is derived from cells growing at 50% (v/v) CO_2. D) Localization of the NuoG protein within complex I of the electron transport chain. The acquired stop codon (CAG>TAG) during evolution allows translation of only half the NuoG protein. Figure adapted from (Chadwick et al., 2018) [49]. E) Retro engineering of the TAG stop codon in the nuoG gene in C1-S-Aux. Growth was restored due to this single mutation at ambient (0.04) and 50% (v/v) CO_2 by expressing the C1 and mutated CO_2 module. Abbreviations: (Gly) glycine, (Ser), serine, (His), histidine, (For), formate, (5,10-MTHF), 5,10-methylene-THF, (Glu), Glucose, (N/A), not applicable, (DT), doubling time, (h) hours. Growth curves and labeling experiments represent the mean value ± SD from three biological replicates.

CO_2 reduction and its entry into the rGlyP, we performed labeling experiments with ^{13}C-CO_2 (Figure 2.4C). Here, serine was expected to be completely labeled once, but

only ≈60% was once labeled. As glycine was labeled for ≈10%, this indicates that at least 50% of the labeled serine originates from labeled 5,10-methylene-THF. We demonstrated earlier that CO_2 released from glucose respiration is enough to drive the reverse FDH reaction resulting in slow growth (Figure S2.3). Therefore, it is likely that a mixture of labeled, as well as unlabeled intracellular CO_2 originating from glucose, is being fixed by the FDH, leading to mixed labeling patterns. This pattern is repeated for histidine, which should theoretically be fully labeled once. To estimate the intracellular labeling status of CO_2, we analyzed the proteinogenic amino acids proline and arginine (Figure S2.5). In the biosynthesis of arginine, one CO_2 is added through carboxylation, which is not present in proline. All other carbons of proline and arginine have the same origin [26]. Therefore, the difference in labeling between these two amino acids can be used to estimate the labeling of intracellular CO_2. This analysis showed that ≈76% of intracellular CO_2 is labeled. This explains part of the unlabeled serine and histidine, but one would expect somewhat higher labeling than 60% for serine. This may indicate some uncertainty in the method to determine intracellular CO_2 or some (small) contribution of other latent pathways to C1-biosynthesis other than CO_2 reduction. However, considering the dependency of growth on CO_2 and labeling patterns (≈50-60% for serine and histidine), we can conclude that CO_2 fixation via the reverse FDH reaction is the main contributor to C1-biosynthesis.

After establishing CO_2-dependent growth in the C1-S-Evo strain, we aimed to achieve the same in C1-G-S-Aux. For this purpose, we refactored the C1-S-Evo strain, instead of introducing the necessary mutations in C1-G-S-Aux. We deleted the ltaE and aceA genes to prevent glycine formation and reintroduced the C2 module in the genome. This strain, termed C1-G-S-Evo, was transformed with pC1 and the mutated pCO_2, and growth was assessed on 20 mM glucose and 50% CO_2. The strain expressing all three modules was able to sustain growth, albeit very slowly and with a low biomass yield (Figure S2.6). Although promising, further optimizations are needed to build toward strains that can generate all biomass from CO_2 via the thermodynamically challenging reduction by FDH.

Discussion

In this study, we successfully laid the foundation for synthetic C1-metabolism in the industrial workhorse *P. putida*. We were able to demonstrate formate, methanol, and CO_2 assimilation through heterologous expression of the core modules of the rGlyP in growth-coupled, auxotrophic selection strains. We show functional expression of all key modules of the rGlyP until serine using both formate and methanol as substrate. The demonstrated conversion in C1-G-S-Aux of methanol and formate into glycine and serine (together forming ≈11% of cellular biomass [11]) provides a strong basis for full formatotrophy and methylotrophy in *P. putida*. Full C1-dependent growth on both substrates can likely be achieved by a combination of genomic integration and further fine-tuning of the enzymes of the independent modules. Then, a combination of rational engineering and adaptive laboratory evolution can be used to optimize the complete metabolic network. This approach has been shown to be efficient in establishing full formatotrophy in both *E. coli* and *C. necator* [15][33][51].

Recently, the first proof of concept of bioproduction has been established with a synthetic formatotrophic *E .coli* [52]. Here they further optimized the bacterium through adaptive laboratory evolution and were able to produce lactate from formate at 10% of the theoretical maximum. The establishment of full C1-dependent growth in *P. putida* will also open many avenues for C1-based industrial biotechnology, given the many attractive properties, and demonstrated production pathways available for this bacterium. Establishing full formatotrophy in *P. putida* can benefit from its native catalytically fast, metal-dependent FDH, to provide energy to run the rGlyP. So far, full formatotrophic growth in *E. coli* was only demonstrated by heterologously expressing a kinetically slower non-metal-dependent FDH, likely limiting formatotrophic growth rates [15][24][26]. In parallel with this study, Turlin et al., (2022)[53] demonstrated formate assimilation in *P. putida* into most of its biomass via the full rGlyP, while acetate supplies energy and a small fraction of biomass. However, as *P. putida* contains a kinetically fast FDH, further evolution can potentially replace acetate with formate as the sole energy source, establishing full formatotrophic growth. Moreover, once equipped with the M or CO_2 module presented in this study, this future strain could be further evolved towards full

methylotrophy or chemolithoautotrophy.

In this work, we showcase a specific promising feature to engineer methanol conversion in *P. putida*, by demonstrating methanol-dependent growth through PQQ-dependent MDH activity. Methanol oxidation is frequently pinpointed as the major bottleneck during the ongoing efforts to establish synthetic methylotrophy in other organisms [22][54]. The NAD-dependent enzymes can lead to higher biomass yields but come with disadvantageous thermodynamics. The PQQ-dependent enzymes do cause a slight reduction in biomass yield, but their higher thermodynamics could lead to higher growth rates [4][12][30]. So far, none of the published metabolic engineering efforts toward synthetic methylotrophy has demonstrated the engineered expression of a PQQ-dependent MDH. As we demonstrate here, *P. putida* is a promising host to relatively easily establish PQQ-dependent synthetic methylotrophy, due to its native PQQ biosynthesis and PQQ-alcohol dehydrogenase that could execute PQQ-MDH activity [38]. So, it will be easier to establish PQQ-dependent methylotrophy in *P. putida* than in for example *E. coli*, which natively lacks PQQ-biosynthesis [55]. Although methanol-dependent growth in C1-S-Aux via PQQ-MDH is slower than via the NADH-MDH, these results establish the basis to further develop this industrially attractive phenotype. The native PQQ-MDH candidate enzyme used in this study could be further engineered through directed evolution toward higher specificity and activity on methanol. In summary, both NAD-and PQQ-dependent MDHs could be further explored to realize efficient and fast synthetic methylotrophy in *P. putida*.

This study shows engineered CO_2 fixation via the reverse activity of FDH. In recent years, CO_2 to formate reduction has been proposed for sustainable biotechnology as a promising feature for both engineered *in vitro* and *in vivo* CO_2 fixation. However, so far experimental evidence of engineered CO_2 fixation via FDH has only been shown for *in vitro* CO_2 reduction. These *in vitro* studies were based on metal-dependent FDH enzymes, from for example *C. necator* and *Rhodobacter capsulatus* [46][56]. The high *in vitro* catalytic rates found for CO_2 reduction to formate of these metal-dependent FDH enzymes (as opposed to slower non-metal-dependent FDHs) are a promising indication that engineered *in vivo* synthetic CO_2 fixation via metal-dependent FDH is achievable. However, engineered *in vivo* activ-

ity from CO_2 to formate by a metal-dependent FDH was not shown yet, possibly due to the complexity of overexpressing metal-dependent FDHs, which typically require chaperones and consist of multiple subunits. In addition, the reduction of CO_2 to formate by FDH is thermodynamically relatively challenging, likely requiring a very high substrate (CO_2 and NADH) to product (formate and NAD^+) ratio within the cell. We overcome these limitations by expressing the native metal-dependent FDH at elevated CO_2 levels, enabling FDH-mediated CO_2 reduction activity *in vivo*. By using a growth-coupled selection strategy, we show that the reaction can carry sufficient flux to supply the cell with the C1-precursors and the beta-carbon of serine (forming ≈4% of cellular biomass) [11]. However, this growth phenotype required short-term laboratory evolution, which resulted in fine-tuning of FDH expression and an essential early stop codon mutation in the NuoG subunit of complex I in the electron transport chain. This likely increased the $NADH/NAD^+$ ratio, facilitating the thermodynamics of CO_2 reduction to formate. In *E. coli*, it has been shown that a similar deletion rendered complex I non-functional, most likely resulting in an unbalanced $NADH/NAD^+$ ratio [57]. This indicates that the establishment of CO_2 fixation via FDH in *P. putida* and potentially other organisms require modulation of the $NADH/NAD^+$ ratio. Alternatively, metal-dependent NADPH-FDHs could be further developed for CO_2 reduction, as cells typically maintain a higher $NADPH/NADP^+$ ratio compared to $NADH/NAD^+$ [42]. Demonstrating efficient CO_2 reduction until serine in the C1-G-S-auxotroph was still not achieved. This likely reflects the more challenging redox requirements to realize this higher flux towards all C1-precursors, glycine, and serine in the cell. The reduction of CO_2 to formate could probably be further improved by redox-factor engineering approaches mentioned above and possibly with further expression and maturation optimization of FDH or other engineered or heterologous metal-dependent FDH candidates, which could be potentially even faster.

Overall, achieving growth with CO_2 as the sole carbon source (synthetic autotrophy) in *P. putida* via the rGlyP would be a very promising feature for sustainable industrial biotechnology. This would also require a suitable inorganic electron donor, for which hydrogen is an interesting candidate as it can be produced very efficiently from renewable electricity [6]. The soluble oxygen-tolerant NAD-reducing hydrogenase from *C. necator* has already been successfully expressed *in vivo* in *P. putida* as

an NADH regeneration system for product synthesis [58]. This NADH regeneration system combined with the here established CO_2 reduction could enable synthetic autotrophy in *P. putida* based on the rGlyP. If the FDH activity could be increased, which based on *in vitro* data could be faster than Rubisco [27], the rGlyP could possibly be a kinetically faster alternative to the naturally, ubiquitous Calvin cycle. This, together with the lower ATP costs of the rGlyP versus the Calvin Cycle makes it an attractive pathway to explore for synthetic autotrophy in *P. putida* and other organisms. Overall, this work widens the possibilities for engineered C1-assimilation based on the versatile rGlyP and shows the suitability of *P. putida* for C1-based biotechnology through lifestyle engineering. The successful establishment of synthetic C1-assimilation in *P. putida* is a key step towards its usefulness in contributing to realize a truly sustainable C1-based biotechnology.

Materials and methods

Plasmids, primers, and strains

All strains and plasmids used in the present study are listed in Table S1 and S2. Primers used for plasmid construction and gene deletions are listed in Table S3.

Bacterial strains and growth conditions

P. putida and *E. coli* cultures were incubated at 30°C and 37°C respectively. For cloning purposes, both strains were propagated in Lysogeny Broth (LB) medium containing 10 g/L NaCl, 10 g/L tryptone, and 5 g/L yeast extract. For the preparation of solid media, 1.5% (w/v) agar was added. Antibiotics, when required, were used at the following concentrations: kanamycin (Km) 50 μg/ml, gentamycin (Gm) 10 μg/ml, chloramphenicol (Cm) 50 μg/ml and apramycin (Apra) 50 μg/ml. All growth experiments were performed using M9 minimal medium (per Liter; 3.88 g K_2HPO_4, 1.63 g NaH_2PO_4, 2.0 g $(NH_4)_2SO_4$, pH 7.0. The M9 media was supplemented with a trace elements solution (10 mg/L ethylenediaminetetraacetic acid (EDTA), 0.1 g/L $MgCl_2 \cdot 6H_2O$, 2 mg/L $ZnSO_4 \cdot 7H_2O$, 1 mg/L $CaCl_2 \cdot 2H_2O$, 5 mg/L $FeSO_4 \cdot 7H_2O$, 0.2 mg/L $Na_2MoO_4 \cdot 2H_2O$, 0.2 mg/L $CuSO_4 \cdot 5H_2O$, 0.4 mg/L $CoCl_2 \cdot 6H_2O$, 1 mg/L $MnCl_2 \cdot 2H_2O$). Before the growth experiments, cells were pre-

grown in non-selective M9 media, containing 10 mM glucose and 2 mM serine, before being transferred to selective growth conditions. In all growth experiments, precultured strains were washed twice in M9 media without a carbon source before transfer and inoculated at an $OD600$ of 0.1. Selective growth conditions consisted of unless otherwise indicated, 10 mM glucose + 5 mM glycine (C1-S-Aux) or 10 mM glucose (C1-G-S-Aux) supplemented with relevant C1-substrates (30 mM formate or 500 mM methanol or 50% (v/v) CO_2). For the formate and methanol experiments with C1-G-S-Aux, 100 mM sodium bicarbonate was added to the medium to push the GCS in the reverse direction. Upon addition of sodium bicarbonate, the pH was readjusted to 7.0 with 1M HCl. Plate reader experiments were carried out in 200 μL of M9 medium using a Synergy plate reader (Biotek). Growth ($OD600$) was measured over time using continuous linear shaking (567 cpm, 3mm) and measurements were taken every five minutes. Plates were covered with a Breath-Easy sealing membrane (Sigma-Aldrich). For the CO_2-dependent growth experiments, 100 mL glass bottles were filled for 10% (10 mL) with liquid M9 media. Subsequently, the headspace (90%) was filled with the desired CO_2 concentration before autoclavation. Carbon sources and antibiotics were added after sterilization and cultures were incubated in a rotary shaker at 200 rpm at 30°C. All growth experiments were performed in biological triplicates and the represented growth curves show the average of these triplicates.

Plasmid construction

Plasmids were constructed using the standard protocols of the previously described SevaBrick Assembly [59]. All DNA fragments were amplified using Q5® Hot Start High-Fidelity DNA Polymerase (New England Biolabs). To construct the C1 module, DNA fragments of the *fhs*, *fchA*, and *folD* genes from *Clostridium ljungdahlli* DSM13528 were codon-optimized with the JCat tool [60] and synthesized through Genescript. The MDH genes from *Geobacillus stearothermophilus*, *Bacillus methanolicus*, *Corynebacterium glutamicum*, and an engineered variant from *Cupriavidus necator* [40] were codon-optimized and synthesized by IDT (Integrated DNA Technologies) (TableS5). All genes in this study were expressed under the control of a strong constitutive promoter (BBa_J23100) and RBS (BBa_B0034). All plas-

mids were transformed using heat shock in chemically competent *E. coli* DH5α λ*pir* and selected on LB agar with corresponding antibiotics. Colonies were screened through colony PCR with Phire Hot Start II DNA Polymerase (Thermo Fisher Scientific). Isolated plasmids were verified using Sanger sequencing (MACROGEN inc.) and subsequently transformed into *P. putida* via electroporation.

Genome modification

Genomic deletions in this study were performed using the protocol previously described by Wirth et al. (2020)[61]. Homology regions of ± 500 bp were amplified up and downstream of the target gene from the genome of *P. putida* KT2440. Both regions were cloned into the non-replicative pGNW vector and propagated in *E. coli* DH5α λ*pir*. Correct plasmids were transformed into *P. putida* by electroporation and selected on LB + Km plates. Successful co-integrations were verified by PCR. Hereafter, co-integrated strains were transformed with the pQURE6-H, and transformants were plated on LB + Gm containing 2 mM 3- methylbenzoic acid (3-mBz). This compound induces the XylS-dependent Pm promoter, regulating the I-SceI homing nuclease that cuts the integrated pGNW vector. Successful gene deletions were verified by PCR and Sanger sequencing (MACROGEN inc). Hereafter, the pQURE6-H was cured by removing the selective pressure and its loss was verified by sensitivity to gentamycin.

Promoter characterization

P. putida strains expressing GFP under the normal or mutated J23100 promoter or containing an empty vector were grown in biological triplicates in M9 medium + 10 mM glucose. Cell density $OD600$ and GFP fluorescence (excitation 485 nm, emission 512 nm, gain 50) were measured using a Synergy plate reader (Biotek) over time using continuous linear shaking, and measurements were taken every five minutes. The promoter strength was quantified based on fluorescence normalized per cell density (RFU/$OD600$) after 20 hours of cultivation when cells had reached the stationary phase. Values were corrected for background fluorescence of cells without GFP.

Whole-genome sequencing

Genomic DNA of the evolved mutants and the unevolved parent strain was isolated from LB overnight cultures using the GenElute™ Bacterial Genomic DNA Kit (Sigma-Aldrich St. Louis, MO). The extracted DNA was evaluated by gel electrophoresis and quantified by a NanoDrop spectrophotometer (Thermo Fisher Scientific). Samples were sent for Illumina sequencing to Novogene Co. Ltd. (Beijing, China). Raw Illumina reads were trimmed for low quality and adapters with fastp (v0.20.0). Mutations were identified by comparing the reads to the annotated reference genome of *P. putida* KT2440 (GCF_000007565.2) using breseq (v0.35.5) [62].

Carbon labeling

For stationary isotope tracing of the proteinogenic amino acids, cultures were grown in 10 ml of M9 media under the previously described experimental conditions. Media was composed of unlabeled (glucose and glycine) and labeled (formate-^{13}C, methanol-^{13}C, and $^{13}CO_2$) (Sigma, 99 atom%) carbon sources. Cells were cultivated in two successive cultures with labeled or unlabeled carbon to diminish the labeling effects of the preculture. Hereafter, the approximate cell volume was harvested that has the cellular biomass roughly equivalent to 1 mL with an $OD600$ of 1 was taken and pelleted down. The pellet was washed with 1 mL of pure water and pelleted down again. The pellet was resuspended in 1 ml of 6N HCl and incubated for 24 hours at 95°C. Then, the caps were opened, allowing evaporation under continuous airflow. The resulting pellet was resuspended in 1 mL of pure water and centrifugated for 5 minutes at full speed to remove residual particles. The hydrolysate was analyzed using ultra-performance liquid chromatography (UPLC) (Acquity, Waters) using an HSS T3 C18-reversed-phase column (Waters). The mobile phases were 0.1% formic acid in H2O (A) and 0.1% formic acid in acetonitrile (B). The flow rate was 400 μL/min and the following gradient was used: 0–1 min 99% A; 1–5 min gradient from 99% A to 82%; 5–6 min gradient from 82% A to 1% A; 6–8 min 1% A; 8–8.5 min gradient to 99% A; 8.5–11 min-re-equilibrate with 99% A. Mass spectra were acquired using an Exactive mass spectrometer (MS) (Thermo Scientific) in positive ionization mode. Data analysis was performed using Xcalibur (Thermo Scientific). The identification of amino acids was based on retention times

and m/z values obtained from amino acid standards (Sigma-Aldrich)

Acknowledgements

We are grateful to Iame Alves Guedes and Sara Cantera Ruiz de Pellon for their invaluable help with the CO_2-dependent experiments. We thank Bart Nijse for the analysis of the whole genome sequencing. This work was financed by the European Union's Horizon2020 Research and Innovation Program under grant agreement Nos. 635536 (EmPowerPutida) 730976 (IBISBA) and 101070281 (BIOS) to V.A.P.M.d.S.

Author contributions

L.B. conceived the study, performed growth experiments, and metabolome sampling; L.B., S.W and N.J.C designed the experiments; S.W. analyzed the ^{13}C tracer analysis; L.B. wrote the initial draft; L.B., S.W., N.J.C and V.A.P.M.d.S. reviewed and edited the manuscript; N.J.C. and V.A.P.M.d.S. provided supervision. V.A.P.M.d.S. arranged the funding.

Conflict of interest

The authors declare there are no conflicting interests.

Supplementary material

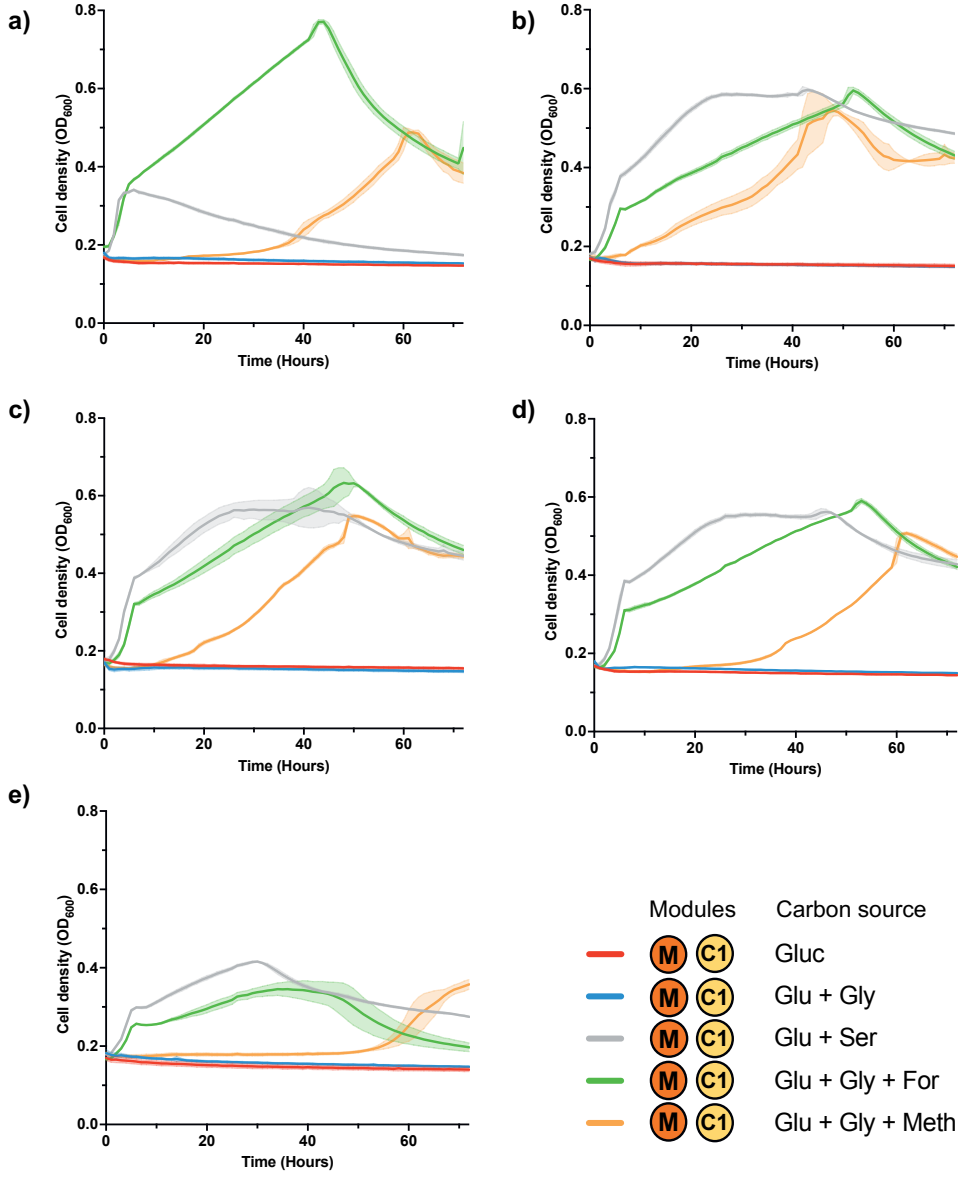

Figure S2.1: Methanol dependent growth with different methanol dehydrogenases a) G. stearothermophilus, b) B. methanolicus, c) C.glutamicum, d) adhP P. putida, e) pedE P. putida

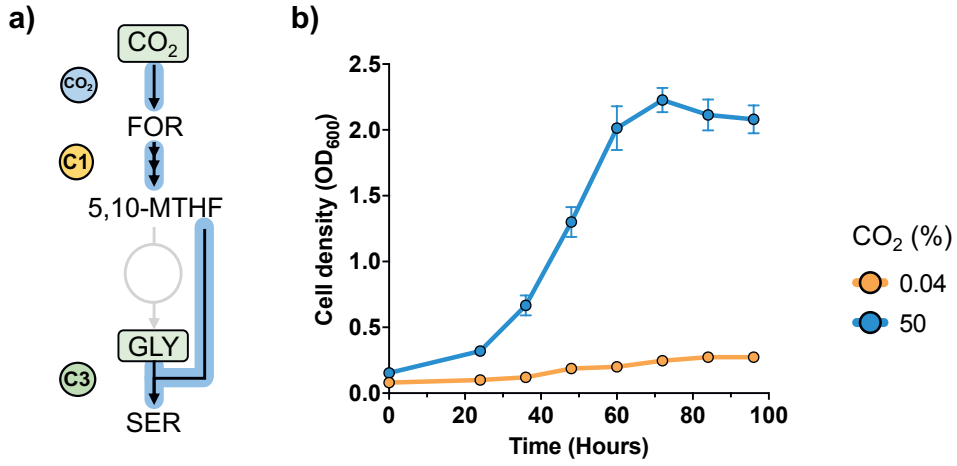

Figure S2.2: CO_2 dependent growth at ambient CO_2 with different cultivation systems. a) Selection of the CO_2 dependent growth in C1- S evo. b) Growth patterns of C1-S evo cultivated in closed anaerobic bottles and open falcon tubes where the CO_2 can freely escape

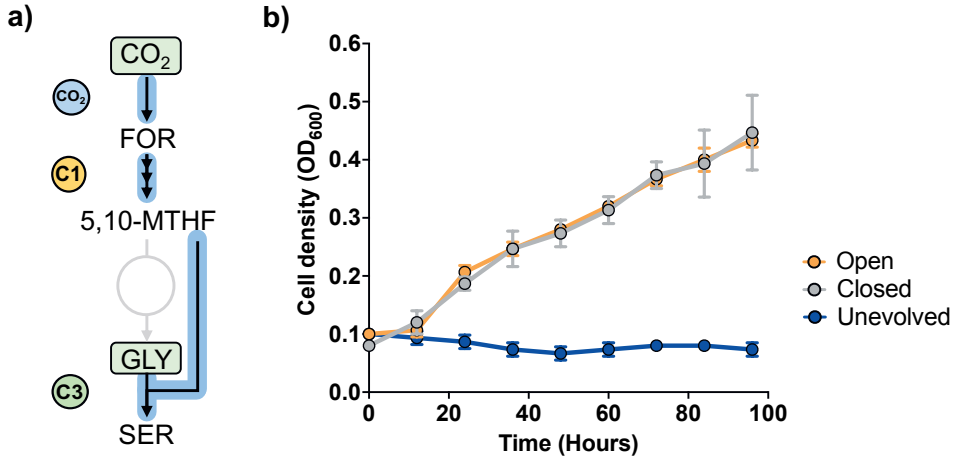

Figure S2.3: Reinoculation of evolved isolate in ambient and high CO_2 concentrations. a) Selection of the CO_2-dependent growth in the evolved isolate. b) Growth patterns of the evolved isolate cultivated in closed bottles with 0.04 or 50% CO_2. Growth curves represent the mean value ± SD from three biological replicates.

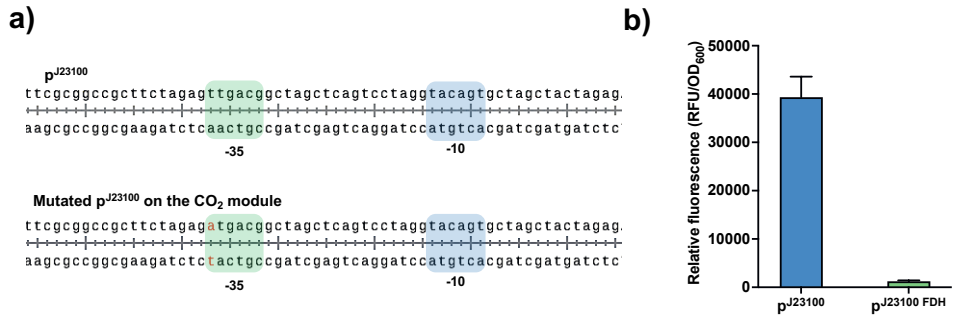

Figure S2.4: Characterization of the mutated CO_2 module during short term evolution. a). Promoter sequences of the J23100 promoter and the mutated CO_2 module. b). Characterization of the mutated J23100 promoter of the CO_2 module using fluorescence as output

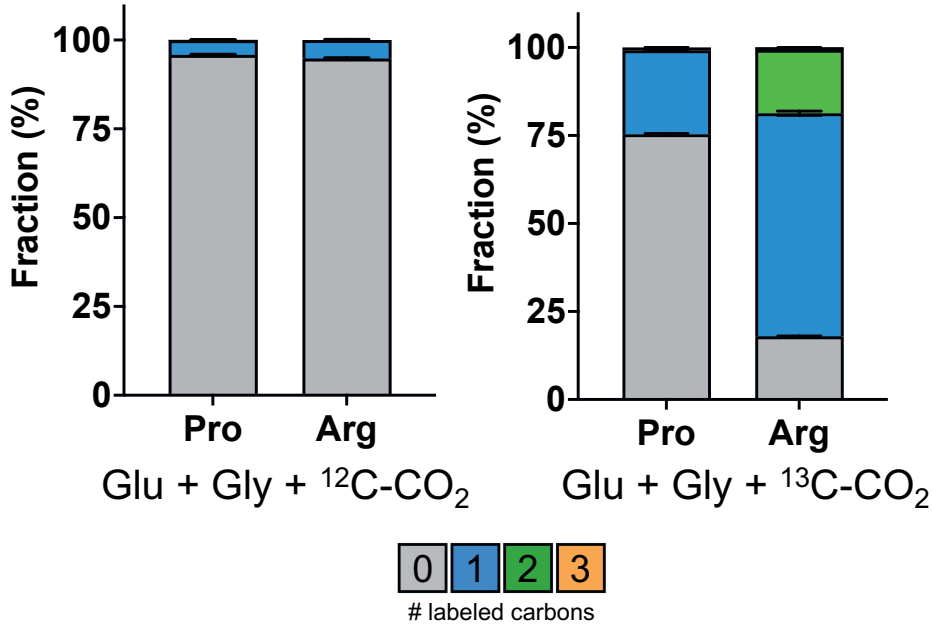

Figure S2.5: ^{13}C labeling of proline (Pro) and arginine (Arg) to determine intracellular CO_2 levels

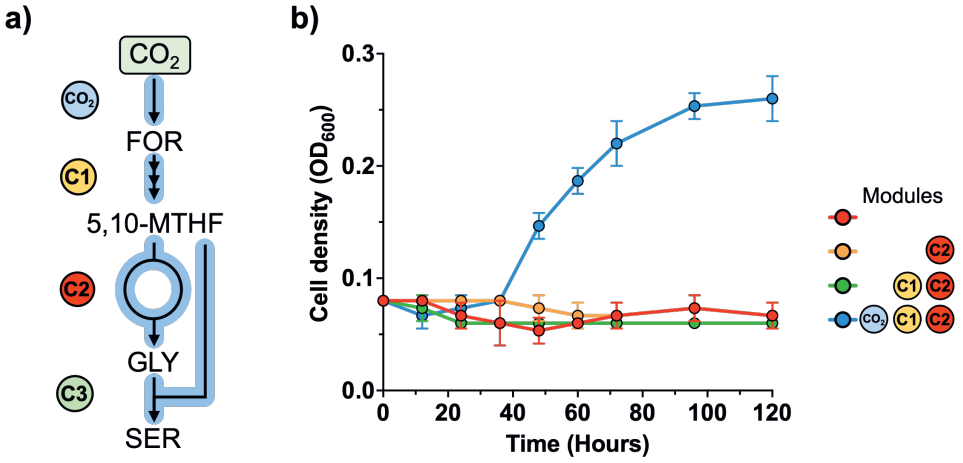

Figure S2.6: a) Selection of the combined effort of the CO_2, C1, and C2 modules in C1-G-S- Evo. b) Growth was solely restored when the CO_2, C1, and C2 modules are expressed.

The rest of the supplementary material of this chapter, including Supplementary Tables S1 to S5, can be accessed *via*:

https://www.sciencedirect.com/science/article/pii/S1096717623000241

Bibliography

1. Wendisch, V. F., Brito, L. F., Gil Lopez, M., *et al.* The flexible feedstock concept in Industrial Biotechnology: Metabolic engineering of Escherichia coli, Corynebacterium glutamicum, Pseudomonas, Bacillus and yeast strains for access to alternative carbon sources. *Journal of Biotechnology* **234,** 139–157 (2016).
2. Fan, L., Xia, C., Zhu, P., *et al.* Electrochemical CO2 reduction to high-concentration pure formic acid solutions in an all-solid-state reactor. *Nature Communications* **11,** 1–9 (2020).
3. Liu, Z., Wang, K., Chen, Y., *et al.* Third-generation biorefineries as the means to produce fuels and chemicals from CO2. *Nature Catalysis* **3,** 274–288 (2020).
4. Cotton, C. A., Claassens, N. J., Benito-Vaquerizo, S., *et al.* Renewable methanol and formate as microbial feedstocks. *Current Opinion in Biotechnology* **62,** 168–180 (2020).
5. Stöckl, M., Claassens, N. J., Lindner, S. N., *et al.* Coupling electrochemical CO2 reduction to microbial product generation – identification of the gaps and opportunities. *Current Opinion in Biotechnology* **74,** 154–163 (2022).
6. Claassens, N. J., Sánchez-Andrea, I., Sousa, D. Z., *et al.* Towards sustainable feedstocks: A guide to electron donors for microbial carbon fixation. *Current Opinion in Biotechnology* **50,** 195–205 (2018).
7. Naik, S. N., Goud, V. V., Rout, P. K., *et al.* Production of first and second generation biofuels: A comprehensive review. *Renewable and Sustainable Energy Reviews* **14,** 578–597 (2010).
8. Köpke, M. & Simpson, S. D. Pollution to products: recycling of 'above ground' carbon by gas fermentation. *Current Opinion in Biotechnology* **65,** 180–189 (2020).
9. Liew, F. E., Nogle, R., Abdalla, T., *et al.* Carbon-negative production of acetone and isopropanol by gas fermentation at industrial pilot scale. *Nature Biotechnology* **40,** 335–344 (2022).
10. Bertsch, J. & Müller, V. Bioenergetic constraints for conversion of syngas to biofuels in acetogenic bacteria. *Biotechnology for Biofuels* **8,** 1–12 (2015).
11. Claassens, N. J., He, H. & Bar-Even, A. Synthetic Methanol and Formate Assimilation Via Modular Engineering and Selection Strategies. *Methylotrophs and Methylotroph Communities* **5** (2019).
12. Whitaker, W. B., Sandoval, N. R., Bennett, R. K., *et al.* Synthetic methylotrophy: Engineering the production of biofuels and chemicals based on the biology of aerobic methanol utilization. *Current Opinion in Biotechnology* **33,** 165–175 (2015).
13. Chen, F. Y., Jung, H. W., Tsuei, C. Y., *et al.* Converting Escherichia coli to a Synthetic Methylotroph Growing Solely on Methanol. *Cell* **182,** 933–946 (2020).
14. Keller, P., Reiter, M. A., Kiefer, P., *et al.* Generation of an Escherichia coli strain growing on methanol via the ribulose monophosphate cycle. *Nature Communications* **13,** 1–13 (2022).
15. Kim, S., Lindner, S. N., Aslan, S., *et al.* Growth of E. coli on formate and methanol via the reductive glycine pathway. *Nature Chemical Biology* **16,** 538–545 (2020).
16. Ankenbauer, A., Schäfer, R. A., Viegas, S. C., *et al.* Pseudomonas putida KT2440 is naturally endowed to withstand industrial-scale stress conditions. *Microbial Biotechnology* **13,** 1145–1161 (2020).
17. Martin-Pascual, M., Batianis, C., Bruinsma, L., *et al.* A navigation guide of synthetic biology tools for Pseudomonas putida. *Biotechnology Advances* **49,** 107732 (2021).
18. Nikel, P. I. & de Lorenzo, V. Pseudomonas putida as a functional chassis for industrial biocatalysis: From native biochemistry to trans-metabolism. *Metabolic Engineering* **50,** 142–155 (2018).
19. Poblete-Castro, I., Becker, J., Dohnt, K., *et al.* Industrial biotechnology of Pseudomonas putida and related species. *Applied Microbiology and Biotechnology* **93,** 2279–2290 (2012).

20. Koopman, F. W., De Winde, J. H. & Ruijssenaars, H. J. C1 compounds as auxiliary substrate for engineered Pseudomonas putida S12. *Applied Microbiology and Biotechnology* **83,** 705–713 (2009).

21. Zobel, S., Kuepper, J., Ebert, B., *et al.* Metabolic response of Pseudomonas putida to increased NADH regeneration rates. *Engineering in Life Sciences* **17,** 47–57 (2017).

22. Antoniewicz, M. R. Synthetic methylotrophy: Strategies to assimilate methanol for growth and chemicals production. *Current Opinion in Biotechnology* **59,** 165–174 (2019).

23. Yu, H. & Liao, J. C. A modified serine cycle in Escherichia coli coverts methanol and CO2 to two-carbon compounds. *Nature Communications* **9** (2018).

24. Bar-Even, A., Noor, E., Flamholz, A., *et al.* Design and analysis of metabolic pathways supporting formatotrophic growth for electricity-dependent cultivation of microbes. *Biochimica et Biophysica Acta - Bioenergetics* **1827,** 1039–1047 (2013).

25. Barenholz, U., Davidi, D., Reznik, E., *et al.* Design principles of autocatalytic cycles constrain enzyme kinetics and force low substrate saturation at flux branch points. *eLife* **6,** 1–32 (2017).

26. Gleizer, S., Ben-Nissan, R., Bar-On, Y. M., *et al.* Conversion of Escherichia coli to Generate All Biomass Carbon from CO2. *Cell* **179,** 1255–1263 (2019).

27. Cotton, C. A., Edlich-Muth, C. & Bar-Even, A. Reinforcing carbon fixation: CO2 reduction replacing and supporting carboxylation. *Current Opinion in Biotechnology* **49,** 49–56 (2018).

28. Figueroa, I. A., Barnum, T. P., Somasekhar, P. Y., *et al.* Metagenomics-guided analysis of microbial chemolithoautotrophic phosphite oxidation yields evidence of a seventh natural CO2 fixation pathway. *Proceedings of the National Academy of Sciences of the United States of America* **115,** E92–E101 (2018).

29. Sánchez-Andrea, I., Guedes, I. A., Hornung, B., *et al.* The reductive glycine pathway allows autotrophic growth of Desulfovibrio desulfuricans. *Nature Communications* **11,** 1–12 (2020).

30. Claassens, N. J., Satanowski, A., Bysani, V. R., *et al.* Engineering the Reductive Glycine Pathway: A Promising Synthetic Metabolism Approach for C1-Assimilation (2022).

31. Yishai, O., Goldbach, L., Tenenboim, H., *et al.* Engineered Assimilation of Exogenous and Endogenous Formate in Escherichia coli. *ACS Synthetic Biology* **6,** 1722–1731 (2017).

32. Yishai, O., Bouzon, M., Döring, V., *et al. In Vivo Assimilation of One-Carbon via a Synthetic Reductive Glycine Pathway in Escherichia coli* 2018.

33. Claassens, N. J., Bordanaba-Florit, G., Cotton, C. A., *et al.* Replacing the Calvin cycle with the reductive glycine pathway in Cupriavidus necator. *Metabolic Engineering* **62,** 30–41 (2020).

34. Gonzalez De La Cruz, J., Machens, F., Messerschmidt, K., *et al.* Core Catalysis of the Reductive Glycine Pathway Demonstrated in Yeast. *ACS Synthetic Biology* **8,** 911–917 (2019).

35. Löwe, H. & Kremling, A. In-Depth Computational Analysis of Natural and Artificial Carbon Fixation Pathways. *BioDesign Research* **2021** (2021).

36. Orsi, E., Claassens, N. J., Nikel, P. I., *et al.* Growth-coupled selection of synthetic modules to accelerate cell factory development. *Nature Communications* **12,** 1–5 (2021).

37. Szima, S. & Cormos, C. C. Improving methanol synthesis from carbon-free H2 and captured CO2: A techno-economic and environmental evaluation. *Journal of CO2 Utilization* **24,** 555–563 (2018).

38. Wehrmann, M., Billard, P., Martin-Meriadac, A., *et al.* crossm Functional Role of Lanthanides in Enzymatic Activity and Transcriptional Regulation of Pyrroloquinoline Quinone- Dependent Alcohol Dehydrogenases in (2017).

39. Wenk, S. *Engineering formatotrophic growth in Escherichia coli* PhD thesis (Universität Potsdam, 2020), V, 107.

40. Wu, T. Y., Chen, C. T., Liu, J. T. J., *et al.* Characterization and evolution of an activator-independent methanol dehydrogenase from Cupriavidus necator N-1. *Applied Microbiology and Biotechnology* **100,** 4969–4983 (2016).

41. Woolston, B. M., King, J. R., Reiter, M., *et al.* Improving formaldehyde consumption drives methanol assimilation in engineered E. coli. *Nature Communications* **9** (2018).

42. Calzadiaz-Ramirez, L. & Meyer, A. S. Formate dehydrogenases for CO2 utilization. *Current Opinion in Biotechnology* **73,** 95–100 (2022).

43. Choe, H., Joo, J. C., Cho, D. H., *et al.* Efficient CO2-reducing activity of NAD-dependent formate dehydrogenase from Thiobacillus sp. KNK65MA for formate production from CO 2 gas. *PLoS ONE* **9,** 14–16 (2014).

44. Ragsdale, S. W. & Wood, H. G. Enzymology of the acetyl-coa pathway of CO2 fixation. *Critical Reviews in Biochemistry and Molecular Biology* **26,** 261–300 (1991).

45. Reda, T., Plugge, C. M., Abram, N. J., *et al.* Reversible interconversion of carbon dioxide and formate by an electroactive enzyme. *Proceedings of the National Academy of Sciences of the United States of America* **105,** 10654–10658 (2008).

46. Yu, X., Niks, D., Mulchandani, A., *et al.* Efficient reduction of CO2 by the molybdenum-containing formate dehydrogenase from Cupriavidus necator (Ralstonia eutropha). *Journal of Biological Chemistry* **292,** 16872–16879 (2017).

47. Maia, L. B., Moura, I. & Moura, J. J. Molybdenum and tungsten-containing formate dehydrogenases: Aiming to inspire a catalyst for carbon dioxide utilization. *Inorganica Chimica Acta* **455,** 350–363 (2017).

48. Flamholz, A., Noor, E., Bar-Even, A., *et al.* EQuilibrator - The biochemical thermodynamics calculator. *Nucleic Acids Research* **40** (2012).

49. Chadwick, G. L., Hemp, J., Fischer, W. W., *et al.* Convergent evolution of unusual complex I homologs with increased proton pumping capacity: energetic and ecological implications. *ISME Journal* **12,** 2668–2680 (2018).

50. Nies, S. C., Dinger, R., Chen, Y., *et al.* crossm Systems Analysis of NADH Dehydrogenase Mutants Reveals. **86,** 1–17 (2020).

51. Dronsella, B., Orsi, E., Benito-vaquerizo, S., *et al.* Engineered synthetic one-carbon fixation exceeds yield of the Calvin Cycle. *bioRxiv* (2022).

52. Kim, S., David Giraldo, N., Rainaldi, V., *et al.* Optimizing E. coli as a formatotrophic platform for bioproduction via the 1 reductive glycine pathway 2 (2022).

53. Turlin, J., Dronsella, B., Maria, A. D., *et al.* Integrated rational and evolutionary engineering of genome-reduced Pseudomonas putida strains empowers synthetic formate assimilation. *bioRxiv* **74,** 2022.07.10.499488 (2022).

54. Wang, Y., Fan, L., Tuyishime, P., *et al.* Synthetic Methylotrophy: A Practical Solution for Methanol-Based Biomanufacturing. *Trends in Biotechnology* **38,** 650–666 (2020).

55. Yang, X. P., Zhong, G. F., Lin, J. P., *et al.* Pyrroloquinoline quinone biosynthesis in Escherichia coli through expression of the Gluconobacter oxydans pqqABCDE gene cluster. *Journal of Industrial Microbiology and Biotechnology* **37,** 575–580 (2010).

56. Hartmann, T. & Leimkühler, S. The oxygen-tolerant and NAD+-dependent formate dehydrogenase from Rhodobacter capsulatus is able to catalyze the reduction of CO2 to formate. *FEBS Journal* **280,** 6083–6096 (2013).

57. Falk-Krzesinski, H. J. & Wolfe, A. J. Genetic analysis of the nuo locus, which encodes the proton- translocating NADH dehydrogenase in Escherichia coli. *Journal of Bacteriology* **180,** 1174–1184 (1998).

58. Lonsdale, T. H., Lauterbach, L., Honda Malca, S., *et al.* H2-driven biotransformation of n-octane to 1-octanol by a recombinant Pseudomonas putida strain co-synthesizing an O2-tolerant hydrogenase and a P450 monooxygenase. *Chemical Communications* **51,** 16173–16175 (2015).

59. Damalas, S. G., Batianis, C., Martin-Pascual, M., *et al.* SEVA 3.1: enabling interoperability of DNA assembly among the SEVA, BioBricks and Type IIS restriction enzyme standards. *Microbial Biotechnology* **13,** 1793–1806 (2020).

60. Grote, A., Hiller, K., Scheer, M., *et al.* JCat: A novel tool to adapt codon usage of a target gene to its potential expression host. *Nucleic Acids Research* **33,** 526–531 (2005).

61. Wirth, N. T., Kozaeva, E. & Nikel, P. I. Accelerated genome engineering of Pseudomonas putida by I-SceI—mediated recombination and CRISPR-Cas9 counterselection. *Microbial Biotechnology* **13,** 233–249 (2020).

62. Barrick, J. E., Colburn, G., Deatherage, D. E., *et al.* Identifying structural variation in haploid microbial genomes from short-read resequencing data using breseq. *BMC Genomics* **15,** 1–17 (2014).

CHAPTER 3

In vivo assessment of electron donors for synthetic autotrophy in *Pseudomonas putida*

Lyon Bruinsma, Nico J. Claassens*, Vitor A. P. Martins dos Santos*

* Contributed equally

Abstract

Heterotrophic microorganisms use organic feedstocks for growth and production, which has complications as it is in direct competition with food production. This problem can be circumvented by using sustainable alternative microbial feedstocks such as CO_2. However, to establish CO_2 as the sole carbon source, an efficient electron donor is required to supply the strain with NADH and ATP. In this study, we engineered the metabolism of *Pseudomonas putida* to assess *in vivo* the functionality of the electron donors phosphite and hydrogen to supply the whole cell with NADH. First, we created an NADH auxotrophic strain by deleting key genes within the tricarboxylic acid cycle and verified its functionality by formate supplementation. Next, we established phosphite as a phosphorus source and demonstrate that this module cannot supply the cell with enough reducing power in the current tested format. Lastly, we created, genome-integrated, and demonstrated transcription of a synthetic module containing a soluble hydrogenase. Although its functionality as an electron donor requires further research and optimization, this study paves the way to explore the potential of electron donors and their function as NADH regeneration systems in *P. putida*.

Introduction

Microorganisms are continuously being engineered for the biotechnological production of valuable chemicals such as fuels, solvents, and polymers [1]. For this purpose, most industrial biotechnology processes rely on the usage of heterotrophic organisms, which primarily consume sugar-based feedstocks. However, this can pose a problem as using these feedstocks for chemical production is often in direct competition with food production. Therefore, biotechnological production processes could become more sustainable without endangering food security if we could switch to non-competitive substrates such as CO_2 [2][3]. Autotrophic microorganisms have the ability to fix CO_2 as the sole carbon source for biomass. However, for this fixation, they require an energy source that is acquired through either light (photoautotrophy) or an inorganic electron donor (chemolithoautotrophy) [4][5].

The ability to use CO_2 as the sole carbon source for biomass and production is an attractive industrial feature and strides have been made to produce fuels and chemicals with autotrophic bacteria [6][7][8]. Although promising, autotrophic bacteria generally have less advanced toolboxes for genetic engineering than their heterotrophic counterparts [4][9]. Therefore, there are efforts underway to transplant CO_2 fixation pathways to heterotrophic hosts [10][11]. This transplantation has already led to full synthetic autotrophic growth through the Calvin cycle in both *Escherichia coli* and *Pichia pastoris* [12][13]. In these two strains, to supply the energy for carbon fixation, the organic electron donors formate and methanol were used, respectively. However, to establish synthetic autotrophy, inorganic donors should also be considered. The most promising and industrially relevant candidates are hydrogen and phosphite [14]. Hydrogen is a potent inorganic electron donor that supports autotrophic growth through the reductive acetyl-CoA pathway and Calvin cycle in, for example *Clostridium ljunghdahlii* and *Cupriavidus necator* using the respective pathways [15][16]. Phosphite serves as an electron donor for microbial autotrophy in *Desulfotignum phosphitoxidans* FiPS through the reductive acetyl-CoA pathway and in *Candidatus phopshitivorax* through potentially the reductive glycine pathway [17][18]. Since both can provide reducing power for the entire cell, their function in establishing synthetic autotrophy is noteworthy to explore.

In our previous work, we established CO_2 fixation through the reductive glycine

pathway in *Pseudomonas putida* through the reductive reaction of the native NAD-dependent molybdenum-containing formate dehydrogenase [19]. Through growth-coupled selection and short-term evolution, a strain was created that could generate ≈4% of its cellular biomass from CO_2. In this design, glucose was still used as an additional carbon and energy source. However, to establish a fully autotrophic regime, all cellular carbon should be produced from CO_2 rather than glucose. For this purpose, an efficient energy source is required that can provide *P. putida* with enough reducing power to convert CO_2 to formate and from thereon supply all biomass.

In this study, we laid the foundation for screening potential NADH regeneration systems for microbial CO_2 fixation in *P. putida*. We constructed an auxotrophic strain, which cannot generate the required reducing power when grown on acetate as the sole carbon source and requires the supplementation of external electron donors e.g., formate. Using this strain, we assessed the functionality of phosphite and hydrogen as potential electron donors to supply the cell with reducing power. We demonstrate the functionality of phosphite dehydrogenase as a phosphate source and show that it needs further optimization to serve as an energy source. Moreover, we successfully assembled and showed transcription of the soluble hydrogenase of *C. necator* in *P. putida*. However, more research is needed regarding its appropriate folding and its functionality as an electron donor. Nonetheless, this study's results pave the way for utilizing the described platform to engineer superior NADH regeneration systems for CO_2 fixation in *P. putida*, substantially strengthening its position as an industrial strain.

Results

Generating a *P. putida* strain auxotrophic for reducing energy

To test the potential of various electron donors as NADH regeneration systems, we created a *P. putida* strain auxotrophic in reducing power. We based this auxotrophic strain on a previously established design by Wenk et al., (2020) [20]. Their design relies on the deletion of the dihydrolipoyl dehydrogenase, encoded by *lpd*. This enzyme is key in the enzyme complexes: pyruvate dehydrogenase, 2-ketoglutarate

dehydrogenase, and the glycine cleavage system, where it is responsible for the regeneration of lipoic acid [20]. Once deleted, it efficiently blocks the oxidation of acetyl-CoA in the tricarboxylic acid (TCA) cycle. As a result, when using acetate as a carbon source, it can only be assimilated through the glyoxylate shunt when external electron donors are applied to supply reducing power. We deleted the dihydrolipoyl dehydrogenase encoding genes (*lpd*, *lpdG*, *lpdV*) from *P. putida* and examined if it could still grow using acetate as a carbon source. To our surprise, the strain was able to grow, indicating that it could still acquire reducing power from endogenous reactions (Figure S3.1). We hypothesized that the malate dehydrogenase, encoded by *mdh*, could still provide enough NADH to allow growth and aimed to remove it from the triple Δ*lpd* strain. However, the *lpd* deletions rendered this strain very fragile and any further attempts to engineer it were severely hampered. Thus, we decided on an alternative approach, by not deleting the *lpd* genes, but the core enzymes of the complexes in which they play a part. We deleted the *aceEF* and *sucAB* genes, encoding the pyruvate dehydrogenase and 2-ketoglutarate dehydrogenase respectively. Although *lpd* is part of the glycine cleavage system, we hypothesized that the native fluxes through this pathway are negligible to provide reducing power to support growth on acetate as the sole carbon source. Next, we deleted *mdh*, encoding a malate dehydrogenase, which can convert malate to oxaloacetate, releasing NADH in the process. However, this strain was still able to grow on acetate as the sole carbon source in minimal media (Figure 3.1B). Our next two targets were the malic enzyme and the soluble transhydrogenase encoded by *maeB* and *sthA*, respectively. The malic enzyme converts malate to pyruvate releasing primarily NADPH in the process. However, *in vivo* biochemical assays showed that it has also a very low affinity for NADH [21].

The soluble transhydrogenase (SthA) can efficiently convert NADPH to generate NADH [22]. We hypothesized that SthA in combination with the generated NADPH from malic enzyme (MaeB) or isocitrate dehydrogenase (ICD) might be able to restore growth. We assessed the growth of both strains in minimal media with acetate as the sole carbon source but observed that both strains were still able to grow (Figure 3.1B). We hypothesized that in the *maeB* mutant strain, NADH is still generated by the conversion of NADPH from ICD by the SthA. In the *sthA* mutant strain, the

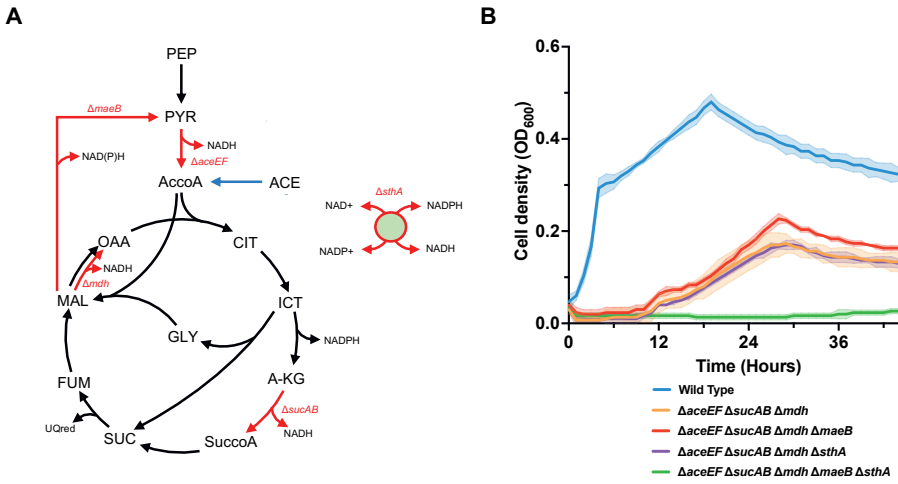

Figure 3.1: Construction of a platform strain auxotrophic for reducing energy a) Metabolic architecture of the central carbon metabolism of the constructed deletions. Red arrows indicated deleted reactions. b) Growth curves of the constructed mutants to establish E-Aux (green line). Abbreviations: (PEP), phosphoenolpyruvate, (PYR), pyruvate, (AccoA), acetyl-CoA, (OAA), oxaloacetate, (CIT), citrate, (ICT), isocitrate, (A-KG), alpha-ketoglutarate, (SuccoA), succinyl-CoA, (SUC), succinate, (FUM), fumarate, (MAL), malate, (GLY), glyoxylate, (ACE), acetate, (aceA), pyruvate dehydrogenase, (maeB), malic enzyme, (mdh), malate dehydrogenase, (sthA), soluble transhydrogenase, (sucAB), 2-ketoglutarate dehdyrogenase,. Growth curves represent the mean value ± SD from three independent experiments.

produced NADH most likely comes from MaeB, which produces possibly more NADH than previously described. Next, we combined the *maeB* and *sthA* deletions in the same strain. This strain termed E-Aux was unable to grow in minimal media with acetate as the sole carbon source, indicating that the major NADH-releasing fluxes were removed (Figure 3.1B). Therefore, we aimed to use this strain as a platform to test and compare different electron donors within *P. putida.*

Testing formate as an electron donor

The constructed E-aux strain is unable to produce reducing power when grown in minimal media with acetate and needs external supplementation of electron donors for NADH generation. As proof of principle, we used formate to validate the effectiveness of E-Aux as a platform to test potential electron donors. Formate has been described as a potential electron donor as its reduction potential is low enough to allow the direct reduction of cellular electron carriers [14]. The genome

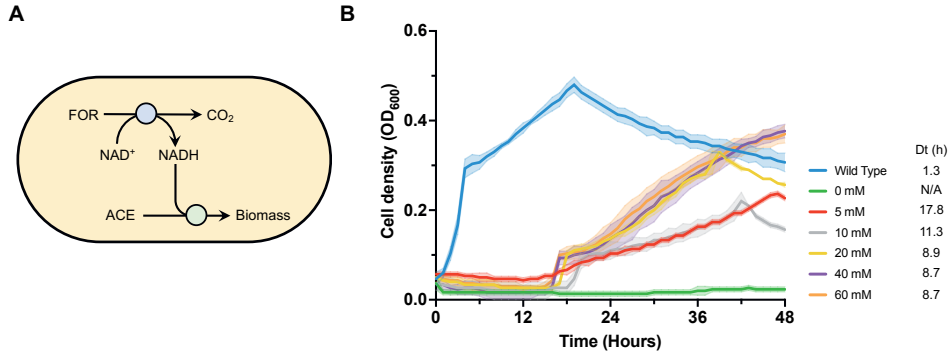

Figure 3.2: Validation of E-aux using formate as an electron donor. A) Metabolic schematic of the implemented strategy. Formate delivers reducing energy, which will allow growth on acetate as a sole carbon source to occur. B) Growth curves of E-Aux on different formate concentrations. Abbreviations: (FOR), formate, (ACE), acetate, (DT) doubling time, (h), hours. Growth curves represent the mean value ± SD from three independent experiments.

of *P. putida* accounts for two native formate dehydrogenases (FDH), of which one is NAD-dependent [23]. Moreover, this FDH contains molybdenum, which makes it kinetically faster than non-metal-containing FDHs [24]. Due to this favourable characteristic, we hypothesized that the addition of formate could restore the growth of E-Aux (Figure 3.2A). We added formate to the media in a dose-dependent manner and measured growth over time. As expected, the addition of formate was able to restore growth (Figure 3.2B). We observe that the lower formate concentrations, such as 5 and 10 mM, were able to restore growth on acetate, albeit with lower doubling times, and lower final cell densities. When the formate concentration was increased to 20 mM, the doubling time significantly improved to 8.9 hours and a higher cell density was achieved. A further increase to a formate concentration of 40 and 60 mM did not further decrease the doubling time but did increase the final achieved cell density (Figure 3.2B). Overall, the usage of formate confirms the dependency of E-aux on the supplementation of external electron donors and therefore its efficiency as a platform to test other NADH regeneration systems.

Testing phosphite as an electron donor

Having established E-aux as a selection strain, we aimed to examine the potential of phosphite as an electron donor. Phosphite is the most energetically favourable

biological electron donor with a redox potential of E'_0 of -650 mV, allowing direct reduction of the electron carriers NAD^+ and $NADP^+$ [14][17]. Given these favourable characteristics, this electron donor could be established as a potential NADH regeneration system in a biotechnological context. The biotechnological potential of phosphite as an external electron donor has been recently examined in *E. coli* [25]. Here, they observed a 1.8-fold increase in the intracellular NADH pool, showcasing the possibilities of phosphite as an additional NADH regeneration system. In *P. putida*, the usage of phosphite has so far only been established as a phosphate donor and biocontainment strategy [26]. Although only tested *in vivo* in cell lysates, increased production of NADH was observed upon the addition of phosphite. Therefore, we hypothesized that, like in *E. coli*, phosphite would lead to an increased NADH pool and could potentially supply the whole cell with reducing power.

To test this hypothesis, we cloned the *ptxD* gene from *Ralstonia sp*. 4506 on SEVAb23 plasmid and introduced it into the E-Aux strain. However, the plasmid burden was too extensive for the cells, and growth was even hindered in rich LB medium. Therefore, we opted for genomic expression and integrated the *ptxD* gene under the control of the constitutive J23100 promoter downstream of the PP_5322 gene, which has been described for its high basal expression, yet low impact on cellular fitness [27]. First, we assessed if the phosphite dehydrogenase (hereafter termed P – module) was active by growing the cells in 20 mM acetate with 60 mM formate and with phosphate or phosphite. In this scenario, formate would still provide the cell with reducing energy, whereas phosphite would supply the cell with phosphorus when the P – module is present (Figure 3.3A). When phosphate is supplied to the cell, we observed similar doubling times (4.7 hours) for the strains with and without the P – module, indicating that there is no protein burden (Figure 3.3B). When the cells were subjected to phosphite, only the strain expressing the P-module was able to grow, albeit at a slower doubling time (16.7 hours). This indicates that although the enzyme is expressed, there might be still some limitations. However, as we observed that the P – module is active and therefore can provide the cell with phosphorus, it can theoretically also supply the cell with reducing power. To test this hypothesis, we cultivated the cells in 20 mM acetate and 20 mM

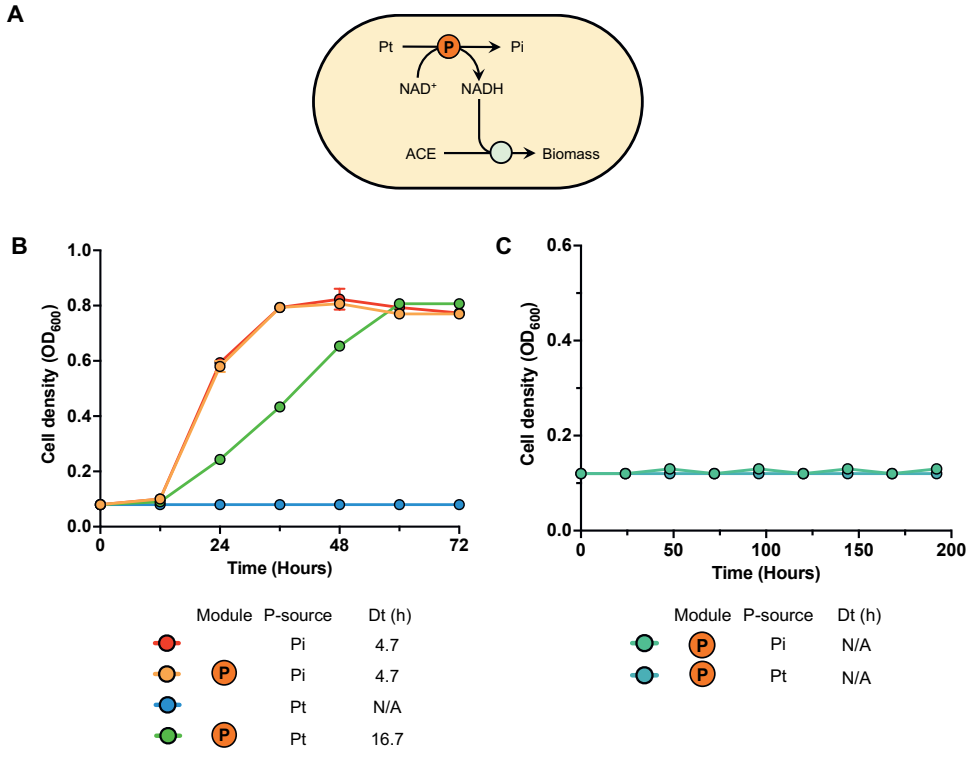

Figure 3.3: Testing phosphite as an electron donor A) Metabolic schematic of the implemented strategy. Phosphite delivers reducing energy and/or phosphate, allowing growth on acetate as a sole carbon source. B) Growth curves of E-Aux on acetate and formate with or without the P-module and different phosphorus sources. C) Growth of E-Aux on acetate with the P-module using phosphite as an electron donor. Abbreviations: (Pt), phosphite, (Pi), phosphate, (ACE), acetate, (DT) doubling time, (h), hours. Growth curves represent the mean value ± SD from three independent experiments.

phosphite or phosphate. However, we observed no growth after an incubation period of 8 days, indicating that in the current setup, the phosphite hydrogenase is not efficient enough yet to supply the whole cell with reducing power.

Testing hydrogen as an electron donor

Hydrogen is another potential electron donor for microbial C1 – fixation. Although its redox potential is slightly higher than phosphite (E'_0 of -410 mV compared to -650 mV), it still enables the direct reduction of the electron carriers NAD^+ and $NADP^+$ (E'_0 of -320 mV) [14]. Several bacteria can use hydrogen as an electron donor for autotrophic growth fixating CO_2 either through the reductive acetyl-CoA pathway or

the Calvin cycle [5]. A noticeable aerobic hydrogen-utilizing bacterium is *C. necator*, which uses hydrogen as an electron donor to fix CO_2 through the Calvin cycle. The genome of this bacterium encodes for three distinct hydrogenases, which unlike most hydrogenases are oxygen-tolerant [28][29]. Therefore, to test hydrogen as an electron donor, we aimed to express the oxygen-tolerant NAD^+ - reducing soluble [NiFe]-hydrogenase (SH) from *C. necator* in *P. putida*. This hydrogenase consists of multiple subunits and auxiliary proteins needed for the correct folding and maturation of the complex. As with the phosphite dehydrogenase, we aimed for genomic integration. For this purpose, we segmented all the different genes into two synthetic modules, the Hox and Hyp modules (Figure 3.4A). The Hox module consists of the seven genes *hoxFUYHWIN1*. The structural enzyme of SH consists of six subunits encoded by *hoxFUYHI* (Figure 3.4B). The genes *hoxFU* encode an NADH oxidoreductase module that is accompanied by a hydrogenase moiety encoded by *hoxYH*. The final two subunits are encoded by *hoxI*, a small homodimer bound to the NADH oxidoreductase module that serves as an NADPH activation site of the oxidized enzyme. The last two genes in the Hox module encode a specific endopeptidase to finalize the maturation process (*hoxW*) and a high-affinity nickel permease (*hoxN1*) [30].

The Hyp module consists of the seven auxiliary genes *hypA2B2F2C1D1E1X*, which are involved in the correct folding and maturation of the complex. The HypA2B2 and HypC1D1 proteins are required for the insertion of nickel and iron into HoxH, respectively. HypF2 is required for CN^- synthesis from carbamoyl phosphate and its delivery to HypE1 which delivers it to the HypC1D1 complex. The gene *hypX* encodes an additional maturase that is solely found in organisms that live in aerobic environments and is crucial for the oxygen tolerance of the enzyme [30]. We assembled all 14 genes on a bacterial artificial chromosome and placed both the Hox and Hyp module under the control of the constitutive pJ23100 promoter (Figure 3.4A). The plasmid was verified by sequencing and then integrated into E-aux. For this purpose, we integrated two *lox* sites downstream of the PP_5322 gene. Successful integration was confirmed with colony PCR (Figure S3.2) and strains were tested further for their ability to use hydrogen as an electron donor. For this purpose, we inoculated the strains in closed bottles containing 20 mM acetate and

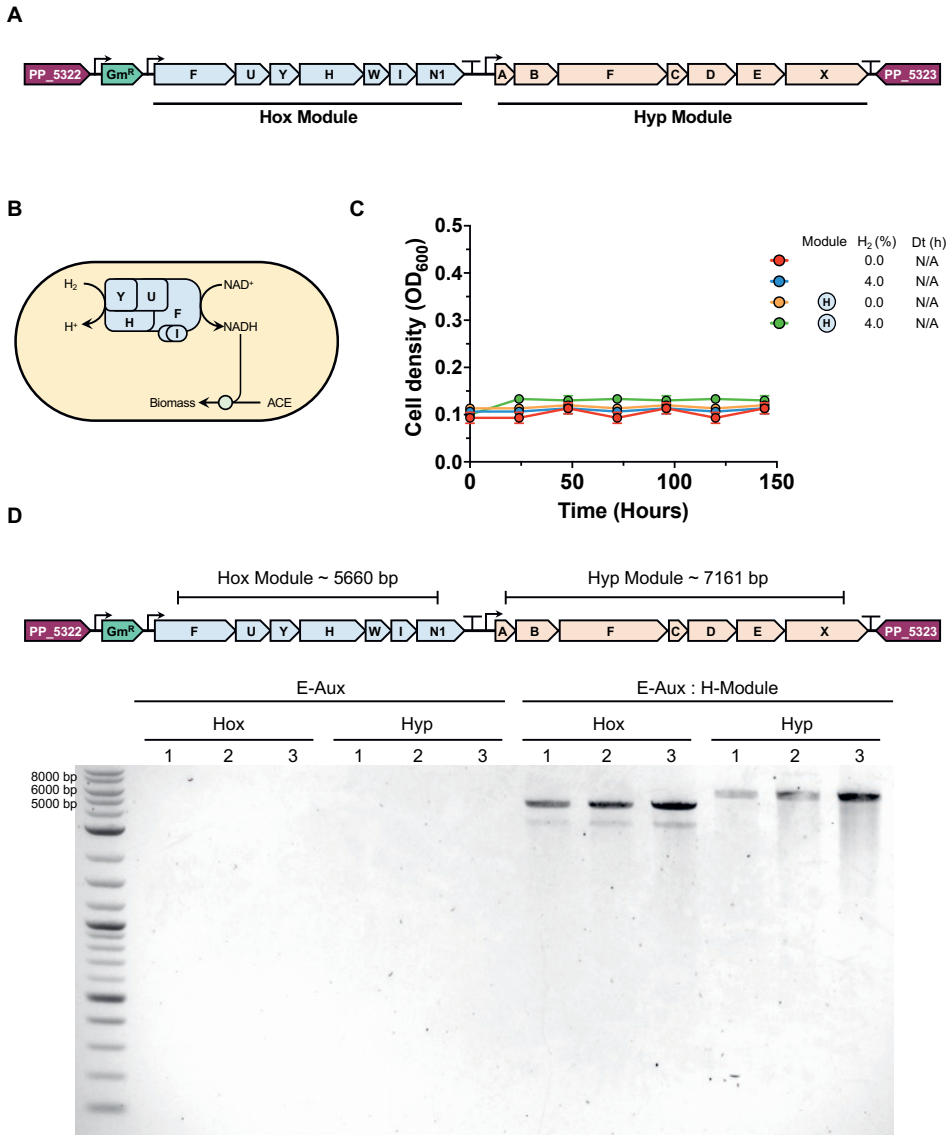

Figure 3.4: Testing hydrogen as an electron donor A) Genomic organization of the integration of the synthetic H-module consisting of the Hox and Hyp module containing all the necessary genes for the expression of the soluble hydrogenase from Cupriavidus necator. B) Metabolic schematic of the implemented strategy. Hydrogen delivers reducing energy, which will allow growth on acetate as a sole carbon source. C) Growth of E-Aux with and without the H-module using hydrogen as an electron donor. D) Gel electrophoresis gel of the amplified operons from the cDNA of E-aux with and without the H-module. Abbreviations: (ACE), acetate, (GmR), gentamicin resistance cassette, (N/A), not applicable, (DT) doubling time, (h), hours. Growth curves represent the mean value ± SD from three independent experiments.

hydrogen in the headspace. Hydrogen is very flammable in combination with oxygen and therefore the threshold was set at 4% (v/v) [31]. We grew E-aux with and without the H-module at 0 or 4% hydrogen. However, no growth was observed after 6 days in all tested conditions. We hypothesized that perhaps the genes were not transcribed and therefore not translated. To test this hypothesis, we created cDNA from strains with and without expressing the H – module. In the module, the Hox and Hyp operons are expressed as two operons and therefore should produce two polycistronic mRNAs. We used primers starting from the first gene of the operon and ending on the final gene to examine if all genes were expressed. As expected, both polycistronic mRNAs were detected, indicating that all the genes are at least transcribed (Figure 3.4D). However, further research is required to examine if all the enzymes are also translated.

Discussion

In this study, we tried to assess the functionality of potential electron donors as NADH regeneration systems in *P. putida*. We constructed an auxotrophic strain for reducing energy by deleting key reactions in the TCA cycle. This strain could only grow on acetate as the sole carbon source upon the supplementation of external electron donors for the generation of NADH. The first iteration of this strain relied on the deletions of *lpd*, encoding a dihydrolipoyl dehydrogenase. Although this mutation was efficient in turning *E. coli* auxotrophic for reducing energy, it did not do the trick for *P. putida* [20]. Therefore, in this study, we deleted individual reactions in which the Lpd enzyme exerts a function. Additionally, Mdh, encoding a malate dehydrogenase was removed, as it can convert malate to oxaloacetate releasing NADH in the process. Yet, this strain was still not auxotrophic, and it required the removal of both the MaeB and SthA enzymes. The malic enzyme is often described as a highly specific $NADP^+$-utilizing enzyme [32]. Even *in vitro* biochemical assays on cell-free extracts of *P. putida* using quasi *in vitro* conditions have indicated that this enzyme predominantly uses $NADP^+$ [21]. However, upon the deletion of SthA, which could convert the produced NADPH by MaeB to NADH, the cells were still able to grow on acetate as a sole carbon source. This indicates that MaeB might have a

higher affinity to NAD^+ than previously reported and can act as a source of NADH. Only the deletion of MaeB in combination with SthA rendered the strain fully auxotrophic for reducing energy. In general, the transcription and translation of the transhydrogenases are kept at a low-level in *P. putida* in a wide variety of carbon sources [22]. However, even with these low levels, enough activity was maintained to generate NADH from NADPH, likely derived from the ICD. Interestingly, according to biochemical assays, the ICD in *P. putida* has a higher cofactor specificity for NAD^+ than MaeB, with 11.1% to 3.5% respectively [21]. In the tested set-up of this study, the enzyme was not able to provide sufficient NADH to restore growth. However, if adaptive laboratory evolution would be performed using the E-Aux strain, there is a high chance that the cofactor specificity of this enzyme could change. Replacing a few residues in the active site can often already change the cofactor preference of an enzyme, changing it from NAD^+ to $NADP^+$ and vice versa [33][34][35]. The deletion of ICD would be an alternative, yet this would render the strain further auxotrophic, requiring supplementation of 2-ketoglutarate as a source for glutamate and derived amino acids [36]. Interestingly, all these candidates (*mdh*, *maeB*, *sthA* and *icd*) were still present in the auxotrophic *E. coli* strain, but most likely not able to sustain enough flux to rescue growth [20].

In this research, we tested the usage of both phosphite and hydrogen as electron donors. We observed that phosphite dehydrogenase is active in *P. putida*, as it can supply the cells with phosphorus. Yet, its usage to supply the whole cell with reducing power in the form of NADH was not achieved yet. In general, phosphite dehydrogenases are kinetically slower than their formate and hydrogen counterparts. Whereas phosphite dehydrogenases have been reported to display specific activities of 12.2 U/mg protein, formate dehydrogenases and hydrogenase activities are usually 5 to 10-fold higher [37][38][39]. However, these enzymatic activities were measured *in vitro* and do not necessarily reflect *in vivo* dynamics. For example, methanol dehydrogenases are kinetically slower than phosphite dehydrogenases, yet can provide the whole cell with the necessary reducing power [12][14][20]. Therefore, enzymes that can function better *in vivo* would need to be developed to install phosphite as the sole energy source for synthetic autotrophy in *P. putida*. The presented strain E-aux could be used to evolve such better en-

zymes as growth is coupled to NADH generation and growth could be used as a measurable output. This selection could either be performed through a random mutagenesis PCR library or adaptive laboratory evolution. If evolution would be applied to evolve kinetically faster enzymes, the previously mentioned ICD enzyme would need to be removed as a potential target to adapt during evolution. In addition, the membrane-bound proton-pumping transhydrogenase (PntAB) could be omitted from the selection system. Although this enzyme is mostly associated with the reoxidation of NADPH, it is theoretically reversible and could produce NADH [40]. Together, this could lead to superior variants that could eventually support the biotechnological exploitation of phosphite as an electron donor.

Apart from phosphite, we aimed to examine the feasibility of hydrogen as an electron donor. To this end, we repurposed the SH from *C. necator* in two synthetic operons and integrated this into the genome of *P. putida*. Although we observed successful integration and transcription, we did not observe growth. The next step would be to validate the translation of all the necessary subunits and auxiliary genes. A common approach that has been used to detect functional translation of hydrogenase subunits is by adding a Strep-tag, a synthetic peptide allowing the detection of proteins by affinity chromatography [30][41]. Another way would be to perform proteomics to assess the translation of the genes. However, even if all necessary genes would be translated, this would not necessarily indicate a functional complex. In general, *in vivo* maturation of SH is a very delicate process, with several steps to ensure proper folding and maturation [41]. Moreover, several factors, such as media, temperature, and carbon source can affect the specific activity of the enzyme [30]. The functional expression of the SH has already been established in *P. putida* [31]. Here, hydrogen was used as an NADH regeneration system to increase the production of 1-octanol for n-octane in carbon-free mineral media. The final observed titers after 24 hours were 36 mg/L and 101 mg/L in the absence and presence of hydrogen, respectively. However, this only accounts for a final increase of 0.5 mmol in the final octanol titer. As one NADH is needed to produce one 1-octanol, this would indicate that only a slight amount of reducing power was produced. Although the functional expression was sufficient to enhance production, our design demands a much higher level of NADH to provide all reducing power

and energy for growth on acetate. In the previous study, expression of the SH in *P. putida* led to a specific activity of 0.16 U/mg protein, whereas a maximized specific activity of 7.2 U/mg protein has been reported in *E. coli* [30][31]. Therefore, even if SH is functionally expressed in E-Aux, it might not be able to deliver enough reducing power to support growth. It is a possibility, that there are more unknown factors that are involved in functional expressing hydrogenases in a foreign host. Most conducted research focuses primarily on expressing hydrogenases in *E. coli* that contains four native hydrogenases by itself [30][42][43][44][45][46][47]. It has been speculated that the maturation factors have a high specificity towards their particular hydrogenase target and that they cannot be substituted by the foreign host native factors [47]. However, there is a possibility that other unknown factors are required for functional expression, which are not present in hosts without native hydrogenases. Therefore, more research is required on expressing a kinetically fast SH in *P. putida*.

In our work, we attempted to assess the feasibility of both phosphite and hydrogen as candidates for synthetic autotrophy. Yet, in both cases, the candidates have not been established yet as the sole supplier of reducing power. Both candidates have a low reduction potential allowing direct reduction of most cellular electron carriers. Nevertheless, both also come with disadvantages regarding implementation. Hydrogen is poorly soluble and highly explosive in combination with oxygen, posing a challenge to the aerobic nature of *P. putida*. Moreover, the successful maturation of SH is a delicate process involving many steps. Phosphite does not have solubility problems like hydrogen, but its dehydrogenases are kinetically slower than its hydrogen counterpart, a feature that should be further engineered. Phosphite metabolism does give a competitive advantage, allowing non-sterile fermentation conditions, and lowering overall production costs [26][48]. However, phosphite synthesis is more energy-intensive and environmentally hazardous compared to hydrogen synthesis, which can be more easily produced using electrochemistry, photochemistry, and biomass gasification [14][49]. As both electron donors have advantages and disadvantages, their implementation in *P. putida* requires further research beyond the work presented here. Yet, when functional, the synthetic NADH regeneration systems presented here could be easily applied

toward the implementation of the earlier established synthetic CO_2 fixation through the reductive glycine pathway [19]. This strain equipped with a strong module providing reducing energy, combined with long-term evolution, could equip *P. putida* with a synthetic chemolithoautotrophic lifestyle. This would further establish and enhance *P. putida* as a *chassis* in realizing a truly sustainable biotechnology. More broadly, this work has also laid a basis for further exploration of alternatives for the use of electron donors in C1-biotechnology.

Materials and methods

Plasmids, primers, and strains.

All strains and plasmids used in the present study are listed in Table S1 and Table S2, respectively. Primers used for plasmid construction and gene deletions are listed in Table S3.

Bacterial strains and growth conditions

P. putida and *E. coli* cultures were incubated at 30°C and 37°C respectively. For cloning purposes, both strains were propagated in Lysogeny broth (LB) medium containing 10 g/L NaCl, 10 g/L tryptone and 5 g/L yeast extract. For the preparation of solid media, 1.5% (w/v) agar was added. Antibiotics, when required, were used at the following concentrations: kanamycin (Km) 50 μg/ml, gentamycin (Gm) 10 μg/ml, and chloramphenicol (Cm) 50 μg/ml. While constructing the auxotrophic strains, 30 mM formate was added to the media to supply NADH. All growth experiments were performed using M9 minimal medium (per Liter; 3.88 g K_2HPO_4, 1.63 g NaH_2PO_4, 2.0 g $(NH_4)_2SO_4$, pH 7.0. The M9 media was supplemented with a trace elements solution (10 mg/L ethylenediaminetetraacetic acid (EDTA), 0.1 g/L $MgCl_2 \cdot 6H_2O$, 2 mg/L $ZnSO_4 \cdot 7H_2O$, 1 mg/L $CaCl_2 \cdot 2H_2O$, 5 mg/L $FeSO_4 \cdot 7H_2O$, 0.2 mg/L $Na_2MoO_4 \cdot 2H_2O$, 0.2 mg/L $CuSO_4 \cdot 5H_2O$, 0.4 mg/L $CoCl_2 \cdot 6H_2O$, 1 mg/L $MnCl_2 \cdot 2H_2O$). For the hydrogen experiment, the M9 media was further supplemented with 0.1 g/L ferric ammonium citrate and 1μM $NiCl_2 \cdot 6H_2O$ [30][50]. Phosphite experiments were conducted in MOPS media, previously described by Neidhardt et al (1974) [51]. In all growth experiments, cultures were preculture in 10 ml LB with corresponding antibiotics.

Then, the cultures were washed twice in M9 media without a carbon source or MOPS without a carbon and phosphorus source. Finally, the cultures were diluted to an $OD600$ of 0.1 to start the experiment. Plate reader experiments were carried out in a Synergy plate reader (Biotek) in which growth ($OD600$) was measured every five minutes over time using continuous linear shaking. Phosphite experiments were conducted in 50 mL Greiner tubes containing 10 mL of M9 media with the corresponding carbon and phosphorus sources. For the hydrogen-dependent growth experiments, glass bottles were filled for 10% with liquid M9 media. After sterilization, carbon sources were added, and the headspace was filled with 4% of hydrogen. Hereafter, the cultures were incubated in a rotary shaker at 200 rpm at 30 °C. All growth experiments were performed in biological triplicates and the represented growth curves show the average of these triplicates.

Plasmid construction

Plasmids were constructed using the previously described SevaBrick Assembly [52]. All DNA fragments were amplified using Q5® Hot Start High-Fidelity DNA Polymerase (New England Biolabs). All plasmids were transformed using heat shock in chemically competent *E. coli* DH5α λ*pir* and selected on LB agar with corresponding antibiotics. Colonies were screened through colony PCR with Phire Hot Start II DNA Polymerase (Thermo Fisher Scientific). Isolated plasmids were verified using Sanger sequencing (MACROGEN inc.) and subsequently transformed into *P. putida* via electroporation. The *ptxD* gene encoding phosphite dehydrogenase was obtained from Asin-Garcia et al., (2022) [26]. The soluble hydrogenase genes were obtained by PCR from a wild-type *Cupriavidus necator*. For the construction of the bacterial artificial chromosome, the *hox* and *hyp* genes were first removed from internal BsaI sites and cloned in the pSB1C3 repository vector. Hereafter, the *hox* and *hyp* operons were assembled on two separate pSEVAb23 plasmids. Hereafter, the operons were amplified and assembled in the pCC1FOS plasmid and verified by sequencing (MACROGEN inc.).

Strain construction

Genetic deletions in this study were performed using the protocol previously described by Wirth et al., (2020)[53]. Homology regions of ± 500 bp were amplified up and downstream of the target gene from the genome of *P. putida* KT2440. Both regions were cloned into the non-replicative pGNW vector and propagated in *E. coli* DH5α λ*pir*. Correct plasmids were transformed into *P. putida* by electroporation and selected on LB + Km plates. Successful co-integrations were verified by PCR. Hereafter, co-integrated strains were transformed with the pQURE6-H and transformants were plated on LB + Gm containing 2 mM 3- methylbenzoic acid (3-mBz). This compound induces the XylS – dependent Pm promoter, regulating the I-SceI homing nuclease that cuts the integrated pGNW vector. Succesful gene deletions were verified by PCR and Sanger sequencing (MACROGEN inc). Hereafter, the pQURE6-H was cured by removing the selective pressure and its loss was verified by sensitivity to gentamycin. The strain *P. putida* KT2440 Δ*aceEF* to construct E-Aux was obtained from Batianis et al., (2022) [54]. The hydrogen module was integrated into E-aux through conjugation. For this procedure, *P. putida* E-Aux, *E. coli* HB101 and *E. coli* containing the pCC1FOS-H-Module plasmid were cultured overnight at 30°C. The $OD600$ of the cultures was determined and adjusted to an $OD600$ of 1 in 1 mL using 1x PBS. The cells were centrifuged for 30 seconds at 7200 x g, the supernatant was discarded and subsequently, the cells were resuspended in 1 mL of 10 mM $MgSO_4$. Next, 150 μL of each of the bacterial cultures was combined and the mixture was centrifuged for 30 seconds at 7200 x g. The supernatant was discarded and the cells were resuspended in 15 μL of 10 mM $MgSO_4$, which was then transferred as a single drop to an LB plate. After incubating overnight at 30°C, biomass was collected in 1 mL of 10 mM $MgSO_4$ and 10 and 50 μL were plated on LB agar containing Gm and Cm and incubated at 30°C. Successful integration was verified through colony PCR with Phire Hot Start II DNA Polymerase (Thermo Fisher Scientific).

Validation of transcription of the H-module

RNA extraction was performed using the Maxwell® 16 LEV simply RNA Tissue kit (Promega). E-Aux with and without the integrated H-module were grown in LB media until an $OD600$ of ≈0.5-0.6 was reached. Cultures were centrifuged for 10

minutes at 4°C. Supernatant was discarded and 200 μL of chilled 1-thioglycerol / homogenization solution was added to the cell pellet and vortexed until the pellet dispersed. Hereafter, 200 μL of lysis buffer was added and vortexed vigorously for 15 seconds. All liquid was transferred to a LEV RNA cartridge and extraction was performed by a Maxwell MDx AS3000 machine (Promega) following the "simply RNA" protocol. RNA quantity was measured by Nanodrop (ThermoFisher). RNA quality was assessed by Qsep100 analyzer (Bioptic). RNA purity was further validated by PCR. Then, cDNA was synthesized using the RevertAid First Strain cDNA Synthesis Kit (ThermoFisher Scientific) according to the manufacturer's instructions. The produced cDNA was used to validate the transcription of the Hox and Hyp module within the H-module.

Author contributions

L.B. conceived and designed the study and performed the experiments. N.J.C and V.A.P.M.d.S. supervised this study. V.A.P.M.d.S. arranged funding.

Conflict of interest

The authors declare no conflict of interest.

Supplementary material

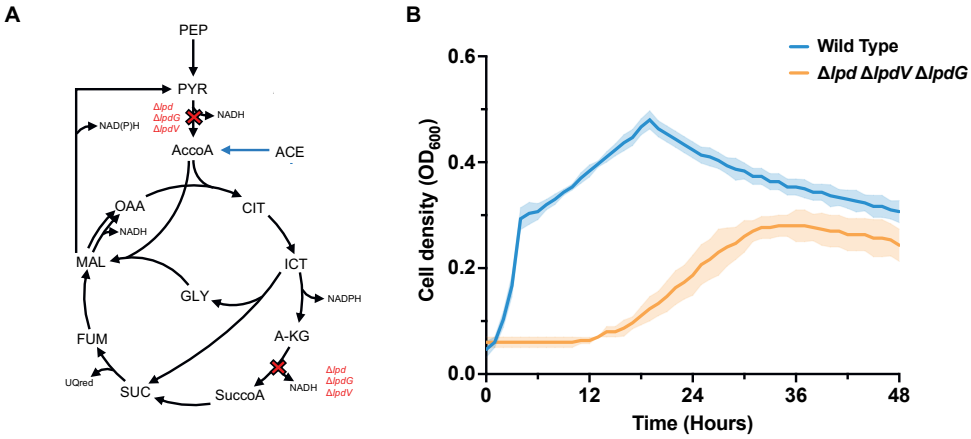

Figure S3.1: Characterization of a triple lpd knockout strain. A). The metabolic architecture of the central carbon metabolism of the constructed deletions. Red crosses indicated the reactions that become inactive by the deletion of the lpd genes. B) Growth curves of the Wild type P. putida strain (KT2440) and the constructed triple lpd knockout. Abbreviations: (PEP), phosphoenolpyruvate, (PYR), pyruvate, (AccoA), acetyl-CoA, (OAA), oxaloacetate, (CIT), citrate, (ICT), isocitrate, (A-KG), alpha-ketoglutarate, (SuccoA), succinyl-CoA, (SUC), succinate, (FUM), fumarate, (MAL), malate, (GLY), glyoxylate, (ACE), acetate. Growth curves are averages from biological triplicates

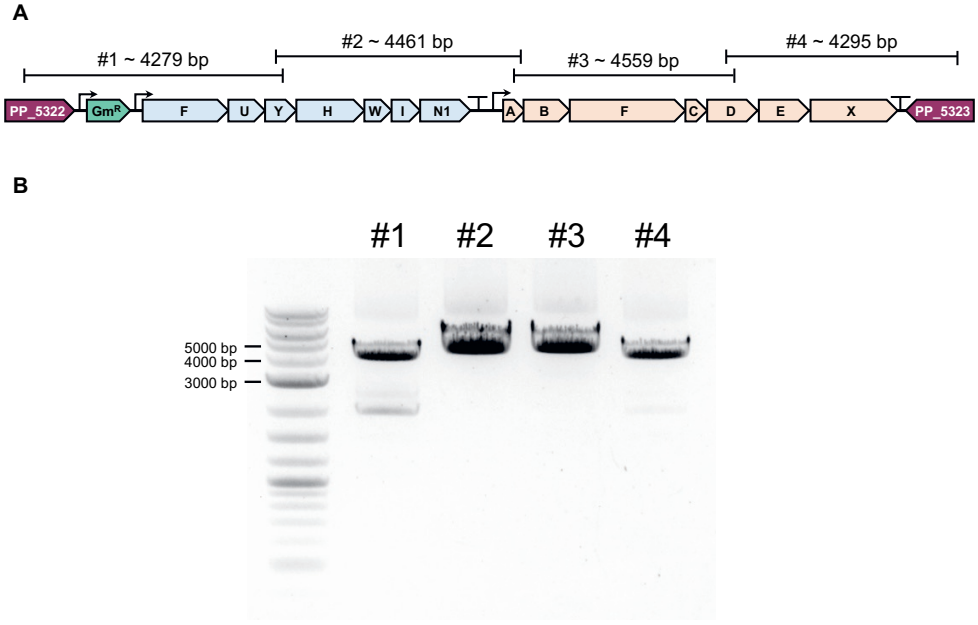

Figure S3.2: Integration of the soluble hydrogenase in Pseudomonas putida A). The metabolic architecture of the integrated bacterial artificial chromosome in the PP_5322 locus of P. putida. Indicated by the parenthesis are the fragments used to validate successful integration. B) Gel electrophoresis gel of the integrated H-module

The rest of the supplementary material of this chapter, including Supplementary Tables S1 to S3, can be accessed *via*:

https://figshare.com/s/b423cac14284c6320972

Bibliography

1. Nielsen, J. & Keasling, J. D. Engineering Cellular Metabolism. *Cell* **164,** 1185–1197 (2016).
2. Satanowski, A. & Bar-Even, A. A one-carbon path for fixing CO 2. *EMBO reports* **21,** 1–6 (2020).
3. Wendisch, V. F., Brito, L. F., Gil Lopez, M., *et al.* The flexible feedstock concept in Industrial Biotechnology: Metabolic engineering of Escherichia coli, Corynebacterium glutamicum, Pseudomonas, Bacillus and yeast strains for access to alternative carbon sources. *Journal of Biotechnology* **234,** 139–157 (2016).
4. Claassens, N. J., Sousa, D. Z., Dos Santos, V. A., *et al.* Harnessing the power of microbial autotrophy. *Nature Reviews Microbiology* **14,** 692–706 (2016).
5. Santos Correa, S., Schultz, J., Lauersen, K. J., *et al.* Natural carbon fixation and advances in synthetic engineering for redesigning and creating new fixation pathways. *Journal of Advanced Research* (2022).
6. Müller, J., MacEachran, D., Burd, H., *et al.* Engineering of Ralstonia eutropha H16 for autotrophic and heterotrophic production of methyl ketones. *Applied and Environmental Microbiology* **79,** 4433–4439 (2013).
7. Rodrigues, J. S. & Lindberg, P. Metabolic engineering of Synechocystis sp. PCC 6803 for improved bisabolene production. *Metabolic Engineering Communications* **12** (2021).
8. Ueki, T., Nevin, K. P., Woodard, T. L., *et al.* Converting carbon dioxide to butyrate with an engineered strain of Clostridium ljungdahlii. *mBio* **5,** 19–23 (2014).
9. Nybo, S. E., Khan, N. E., Woolston, B. M., *et al.* Metabolic engineering in chemolithoautotrophic hosts for the production of fuels and chemicals. *Metabolic Engineering* **30,** 105–120 (2015).
10. Gong, F., Liu, G., Zhai, X., *et al.* Quantitative analysis of an engineered CO2-fixing Escherichia coli reveals great potential of heterotrophic CO2 fixation. *Biotechnology for Biofuels* **8** (2015).
11. Mattozzi, M. d., Ziesack, M., Voges, M. J., *et al.* Expression of the sub-pathways of the Chloroflexus aurantiacus 3-hydroxypropionate carbon fixation bicycle in E. coli: Toward horizontal transfer of autotrophic growth. *Metabolic Engineering* **16,** 130–139 (2013).
12. Gassler, T., Sauer, M., Gasser, B., *et al.* The industrial yeast Pichia pastoris is converted from a heterotroph into an autotroph capable of growth on CO2. *Nature Biotechnology* **38,** 210–216 (2020).
13. Gleizer, S., Ben-Nissan, R., Bar-On, Y. M., *et al.* Conversion of Escherichia coli to Generate All Biomass Carbon from CO2. *Cell* **179,** 1255–1263 (2019).
14. Claassens, N. J., Sánchez-Andrea, I., Sousa, D. Z., *et al.* Towards sustainable feedstocks: A guide to electron donors for microbial carbon fixation. *Current Opinion in Biotechnology* **50,** 195–205 (2018).
15. Köpke, M., Held, C., Hujer, S., *et al.* Clostridium ljungdahlii represents a microbial production platform based on syngas. *Proceedings of the National Academy of Sciences of the United States of America* **107,** 13087–13092 (2010).
16. Liu, C., Colon, B. C., Ziesack, M., *et al.* Water splitting–biosynthetic system with CO2 reduction efficiencies exceeding photosynthesis. *Science* **352,** 1210–1213 (2016).
17. Figueroa, I. A., Barnum, T. P., Somasekhar, P. Y., *et al.* Metagenomics-guided analysis of microbial chemolithoautotrophic phosphite oxidation yields evidence of a seventh natural CO2 fixation pathway. *Proceedings of the National Academy of Sciences of the United States of America* **115,** E92–E101 (2018).
18. Schink, B. & Friedrich, M. Phosphite oxidation by sulphate reduction. *Nature* **406,** 37 (2000).
19. Bruinsma, L., Wenk, S., Claassens, N. J., *et al.* Paving the way for Synthetic C1 - metabolism in Pseudomonas putida through the reductive glycine pathway. *Metabolic Engineering,* 100585 (2023).
20. Wenk, S. *Engineering formatotrophic growth in Escherichia coli* PhD thesis (Universität Potsdam, 2020), V, 107.

21. Nikel, P. I., Chavarría, M., Fuhrer, T., *et al.* Pseudomonas putida KT2440 strain metabolizes glucose through a cycle formed by enzymes of the Entner-Doudoroff, embden-meyerhof-parnas, and pentose phosphate pathways. *Journal of Biological Chemistry* **290,** 25920–25932 (2015).

22. Nikel, P. I., Pérez-Pantoja, D. & de Lorenzo, V. Pyridine nucleotide transhydrogenases enable redox balance of Pseudomonas putida during biodegradation of aromatic compounds. *Environmental Microbiology* **18,** 3565–3582 (2016).

23. Zobel, S., Kuepper, J., Ebert, B., *et al.* Metabolic response of Pseudomonas putida to increased NADH regeneration rates. *Engineering in Life Sciences* **17,** 47–57 (2017).

24. Maia, L. B., Moura, I. & Moura, J. J. Molybdenum and tungsten-containing formate dehydrogenases: Aiming to inspire a catalyst for carbon dioxide utilization. *Inorganica Chimica Acta* **455,** 350–363 (2017).

25. Hu, G., Guo, L., Gao, C., *et al.* Synergistic Metabolism of Glucose and Formate Increases the Yield of Short-Chain Organic Acids in Escherichia coli. *ACS Synthetic Biology* **11,** 135–143 (2022).

26. Asin-Garcia, E., Batianis, C., Li, Y., *et al.* Phosphite synthetic auxotrophy as an effective biocontainment strategy for the industrial chassis Pseudomonas putida. *Microbial Cell Factories* **21,** 1–17 (2022).

27. Chaves, J. E., Wilton, R., Gao, Y., *et al.* Evaluation of chromosomal insertion loci in the Pseudomonas putida KT2440 genome for predictable biosystems design. *Metabolic Engineering Communications* **11,** e00139 (2020).

28. Burgdorf, T., Lenz, O., Buhrke, T., *et al.* [NiFe]-hydrogenases of Ralstonia eutropha H16: Modular enzymes for oxygen-tolerant biological hydrogen oxidation. *Journal of Molecular Microbiology and Biotechnology* **10,** 181–196 (2006).

29. Schuchmann, K., Chowdhury, N. P. & Müller, V. Complex multimeric [FeFe] hydrogenases: Biochemistry, physiology and new opportunities for the hydrogen economy. *Frontiers in Microbiology* **9,** 1–22 (2018).

30. Schiffels, J., Pinkenburg, O., Schelden, M., *et al.* An Innovative Cloning Platform Enables Large-Scale Production and Maturation of an Oxygen-Tolerant [NiFe]-Hydrogenase from Cupriavidus necator in Escherichia coli. *PLoS ONE* **8** (2013).

31. Lonsdale, T. H., Lauterbach, L., Honda Malca, S., *et al.* H2-driven biotransformation of n-octane to 1-octanol by a recombinant Pseudomonas putida strain co-synthesizing an O2-tolerant hydrogenase and a P450 monooxygenase. *Chemical Communications* **51,** 16173–16175 (2015).

32. Huergo, L. F., Araújo, G. A., Santos, A. S., *et al.* The NADP-dependent malic enzyme MaeB is a central metabolic hub controlled by the acetyl-CoA to CoASH ratio. *Biochimica et Biophysica Acta - Proteins and Proteomics* **1868,** 140462 (2020).

33. Bouzon, M., Döring, V., Dubois, I., *et al.* Change in cofactor specificity of oxidoreductases by adaptive evolution of an escherichia coli nadph-auxotrophic strain. *mBio* **12** (2021).

34. Cahn, J. K., Werlang, C. A., Baumschlager, A., *et al.* A General Tool for Engineering the NAD/NADP Cofactor Preference of Oxidoreductases. *ACS Synthetic Biology* **6,** 326–333 (2017).

35. Sellés Vidal, L., Kelly, C. L., Mordaka, P. M., *et al.* Review of NAD(P)H-dependent oxidoreductases: Properties, engineering and application. *Biochimica et Biophysica Acta - Proteins and Proteomics* **1866,** 327–347 (2018).

36. Lindner, S. N., Ramirez, L. C., Krüsemann, J. L., *et al.* NADPH-Auxotrophic E. coli: A Sensor Strain for Testing in Vivo Regeneration of NADPH. *ACS Synthetic Biology* **7,** 2742–2749 (2018).

37. Garcia Costas, A. M., White, A. K. & Metcalf, W. W. Purification and Characterization of a Novel Phosphorus-oxidizing Enzyme from Pseudomonas stutzeri WM88. *Journal of Biological Chemistry* **276,** 17429–17436 (2001).

38. Niks, D., Duvvuru, J., Escalona, M., *et al.* Spectroscopic and kinetic properties of the molybdenum-containing, NAD+-dependent formate dehydrogenase from Ralstonia eutropha. *Journal of Biological Chemistry* **291,** 1162–1174 (2016).

39. Van Der Linden, E., Burgdorf, T., Bernhard, M., *et al.* The soluble [NiFe]-hydrogenase from Ralstonia eutropha contains four cyanides in its active site, one of which is responsible for the insensitivity towards oxygen. *Journal of Biological Inorganic Chemistry* **9,** 616–626 (2004).

40. Graf, S. S., Hong, S., Müller, P., *et al.* Energy transfer between the nicotinamide nucleotide transhydrogenase and ATP synthase of Escherichia coli. *Scientific Reports* **11,** 1–12 (2021).

41. Germer, F., Zebger, I., Saggu, M., *et al.* Overexpression, isolation, and spectroscopic characterization of the bidirectional [NiFe] hydrogenase from Synechocystis sp. PCC 6803. *Journal of Biological Chemistry* **284,** 36462–36472 (2009).

42. Akhtar, M. K. & Jones, P. R. Deletion of iscR stimulates recombinant clostridial Fe-Fe hydrogenase activity and H2-accumulation in Escherichia coli BL21(DE3). *Applied Microbiology and Biotechnology* **78,** 853–862 (2008).

43. Fan, Q., Waldburger, S., Neubauer, P., *et al.* Implementation of a high cell density fed-batch for heterologous production of active [NiFe]-hydrogenase in Escherichia coli bioreactor cultivations. *Microbial Cell Factories* **21,** 1–11 (2022).

44. Kim, J. Y., Jo, B. H. & Cha, H. J. Production of biohydrogen by recombinant expression of [NiFe]-hydrogenase 1 in Escherichia coli. *Microbial Cell Factories* **9,** 1–10 (2010).

45. Laffly, E., Garzoni, F., Fontecilla-Camps, J. C., *et al.* Maturation and processing of the recombinant [FeFe] hydrogenase from Desulfovibrio vulgaris Hildenborough (DvH) in Escherichia coli. *International Journal of Hydrogen Energy* **35,** 10761–10769 (2010).

46. Maeda, T., Tran, K. T., Yamasaki, R., *et al.* Current state and perspectives in hydrogen production by Escherichia coli: roles of hydrogenases in glucose or glycerol metabolism. *Applied Microbiology and Biotechnology* **102,** 2041–2050 (2018).

47. Wells, M. A., Mercer, J., Mott, R. A., *et al.* Engineering a non-native hydrogen production pathway into Escherichia coli via a cyanobacterial [NiFe] hydrogenase. *Metabolic Engineering* **13,** 445–453 (2011).

48. Shaw, A. J., Lam, F. H., Hamilton, M., *et al.* Metabolic engineering of microbial competitive advantage for industrial fermentation processes. *Science* **353,** 583–586 (2016).

49. Zhai, F., Xin, T., Geeson, M. B., *et al.* Sustainable Production of Reduced Phosphorus Compounds: Mechanochemical Hydride Phosphorylation Using Condensed Phosphates as a Route to Phosphite. *ACS Central Science* **8,** 332–339 (2022).

50. Yu, J. & Munasinghe, P. Gas fermentation enhancement for chemolithotrophic growth of Cupriavidus necator on carbon dioxide. *Fermentation* **4** (2018).

51. Neidhardt, F. C., Bloch, P. L. & Smith, D. F. Culture medium for Enterobacteria. *JOURNAL OF BACTERIOLOGY* **119,** 736–747 (1974).

52. Damalas, S. G., Batianis, C., Martin-Pascual, M., *et al.* SEVA 3.1: enabling interoperability of DNA assembly among the SEVA, BioBricks and Type IIS restriction enzyme standards. *Microbial Biotechnology* **13,** 1793–1806 (2020).

53. Wirth, N. T., Kozaeva, E. & Nikel, P. I. Accelerated genome engineering of Pseudomonas putida by I-SceI—mediated recombination and CRISPR-Cas9 counterselection. *Microbial Biotechnology* **13,** 233–249 (2020).

54. Batianis, C., van rosmalen, R., Major, M., *et al.* A tunable metabolic valve for precise growth control and increased product formation in Pseudomonas putida. *Metabolic Engineering,* 118159 (2022).

CHAPTER 4

INCREASING CELLULAR FITNESS AND PRODUCT YIELDS IN *PSEUDOMONAS PUTIDA* THROUGH AN ENGINEERED PHOSPHOKETOLASE SHUNT

Lyon Bruinsma, Maria Martin-Pascual, Kesi Kurnia, Marieken Tack
Simon Hendriks, Richard van Kranenburg, Vitor A. P. Martins dos Santos

Abstract

Pseudomonas putida has received increasing interest as a cell factory due to its remarkable features such as fast growth, a versatile and robust metabolism, an extensive genetic toolbox and its high tolerance to oxidative stress and toxic compounds. This interest is driven by the need to improve microbial performance to a level that enables biologically possible processes to become economically feasible, thereby fostering the transition from an oil-based economy to a more sustainable bio-based one. To this end, one of the current strategies is to maximize the product-substrate yield of an aerobic biocatalyst such as *P. putida* during growth on glycolytic carbon sources, such as glycerol and xylose. We demonstrate that this can be achieved by implementing the phosphoketolase shunt, through which pyruvate decarboxylation is prevented, and thus carbon loss is minimized.

In this study, we introduced the phosphoketolase shunt in the metabolism of *P. putida* KT2440. To maximize the effect of this pathway, we first tested and selected a phosphoketolase (Xfpk) enzyme with high activity in *P. putida*. Results of the enzymatic assays revealed that the most efficient Xfpk was the one isolated from *Bifidobacterium breve*. Using this enzyme, we improved the *P. putida* growth rate on glycerol and xylose by 44 and 167%, respectively, as well as the biomass yield quantified by $OD600$ by 50 and 30%, respectively. Finally, we demonstrated the impact on product formation and achieved a 38.5% increase in mevalonate and a 25.9% increase in flaviolin yield from glycerol. A similar effect was observed on the mevalonate-xylose and flaviolin-xylose yields, which increased by 48.7 and 49.4%, respectively.

P. putida with the implemented Xfpk shunt grew faster, reached a higher final $OD600$ and provided better product-substrate yields than the wild type. By reducing the pyruvate decarboxylation flux, we significantly improved the performance of this important workhorse for industrial applications. These enhanced properties of *P. putida* will be crucial for its subsequent use in a range of industrial processes.

Introduction

There is a pressing need to transition to a sustainable and biobased economy [1]. The deployment of micro-organisms to produce chemicals currently derived from fossil fuels is a promising green alternative to this end [2]. One of the key challenges when using micro-organisms as cell factories is the optimization of the titer, rate, and yield (TRY) to make the production process competitive with the petrochemical industry [3]. *Pseudomonas putida* is an attractive host that is increasingly being developed as a cell factory for a wide range of biotechnological applications [4][5]. Its high metabolic versatility, ability to tolerate environmental stresses and wide use of a variety of carbon sources make this bacterium one of the laboratory workhorses that can fulfil the demands of industrial biotechnology [6][7]. In current industrial cultivation processes, feedstock costs remain one of the major bottlenecks [8]. Therefore, the substrate-to-product ratio must be as close to the theoretical maximum as possible. Many high-value products, such as isoprenoids, butanol, and polyketides, are derived from the intermediate acetyl–CoA, a key compound connecting the glycolysis and the tricarboxylic acid (TCA) cycle [9]. *P. putida*, like many other bacteria grown on glycolytic carbon sources, produces acetyl-CoA through pyruvate decarboxylation. However, in this process, carbon is lost in the form of CO_2, lowering the theoretical carbon yield.

Nature has cunning ways to resolve this problem by itself, through the usage of phosphoketolases (Xfpks). These enzymes are widely distributed among *Bifidobacteria*. These bacteria lack the aldolase and glucose-6-phosphate $NADP^+$ oxidoreductase enzymes and use an alternative route to metabolize carbohydrates, in which phosphoketolases are key. These enzymes irreversibly cleave the sugar phosphates xylulose-5-phosphate (X5P) and fructose-6-phosphate (F6P) to glyceraldehyde-3-phosphate (G3P) and erythrose-4-phosphate (E4P) respectively, releasing an acetyl-phosphate (AcP) in the process. This AcP is then converted by the phosphotransacetylase (Pta) to acetyl-CoA, circumventing pyruvate carboxylation [10]. One of the most famous examples of using this enzyme is the non-oxidative glycolysis (NOG) [11][12]. The NOG pathway generates acetyl-CoA from sugars or sugar phosphates without carbon loss. To such an end, the Xfpk catalyzes the two aforementioned reactions, in which E4P and G3P are formed. To achieve

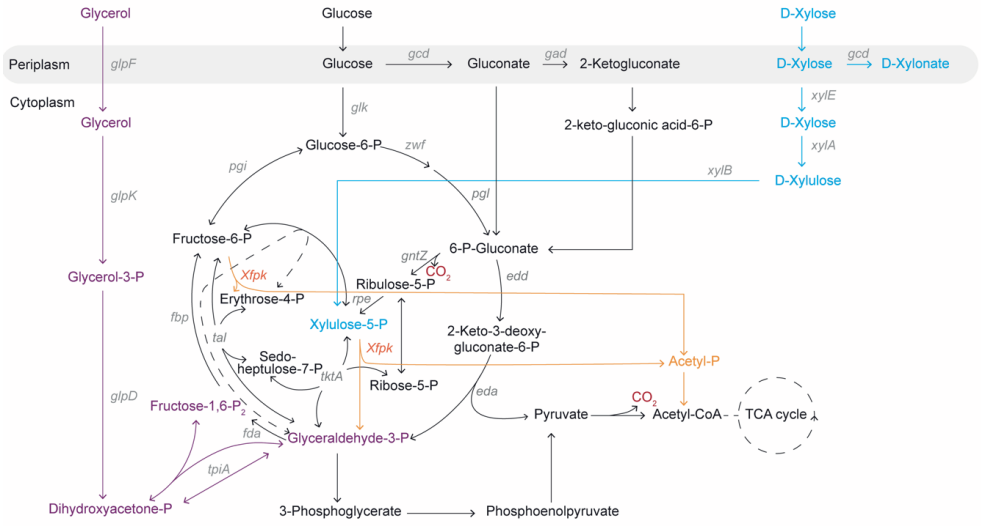

Figure 4.1: Metabolism of P. putida with the phosphoketolase shunt. Native metabolism of P. putida when glycerol (purple), glucose (black) and xylose (blue) are used as carbon sources. Rewired metabolism of P. putida when the phosphoketolase (Xfpk) is implemented (orange)

complete carbon conservation, three molecules of F6P are needed.

These are broken down into three AcP and two E4P molecules. The E4P molecules need to undergo carbon rearrangement by the transaldolase and transketolase reactions to regenerate two molecules of F6P. Recent metabolic engineering efforts have shown that the implementation of a phosphoketolase can improve carbon yields and the production of acetyl-CoA–derived products. For instance, the introduction of a phosphoketolase from *B. adolescentis* into *E. coli* showed improved yields for poly-β-hydroxybutyrate (PHB) (63.7 %), fatty acid (14.36 %) and mevalonate (64.3 %) [13]. Overexpression of the phosphoketolase gene from *B. animalis* in a *Corynebacterium glutamicum* strain resulted in a 14% increase in the glutamic acid yield from glucose as well as suppression of CO_2 emission [14]. Similarly, Meadows et al., (2016) [15] combined a xylulose-5-phosphate-specific phosphoketolase and three other heterologous enzymes to rewire the central carbon metabolism for more acetyl-CoA supply in *S. cerevisiae*, resulting in engineered strains that produce more farnesene and require less oxygen. In this study, we first characterized several Xfpk enzymes from *Bifidobacterium* species through *in vitro* assays. Secondly, we demonstrate that the introduction of the phosphoke-

tolase shunt in *P. putida* KT2440 can improve biomass formation on glycerol and xylose, consuming less substrate in the process. At last, we prove that the carbon-conserving pathway can significantly increase the yield of the acetyl-CoA-derived compounds, such as malonyl-CoA and mevalonate.

Results

Selecting the best phosphoketolase candidate

To maximize carbon conservation in *P. putida*, we introduced the phosphoketolase shunt in its central metabolism. Xfpk cleaves the respective sugar phosphates F6P and X5P and releases AcP in the process, which can be directly converted to acetyl-CoA. We hypothesized that through this introduction, pyruvate decarboxylation would be circumvented, and the carbon loss minimized (Figure 4.1). To select an Xfpk candidate with high enzymatic activity, an *in vitro* assay was performed. We cloned all candidate genes (*xfpk* from *B. adolescentis*, *B. animalis* and *B. breve*) under the control of a strong constitutive promoter (BBa_J23100) and RBS (0034) in the medium copy number pSEVAb83 vector. Functional expression of all enzymes in *P. putida* was assessed by the detection of AcP generated from F6P in cell-free extracts (Figure 4.2). The Xfpk enzymes from *B. adolescentis* and *B. animalis* produced

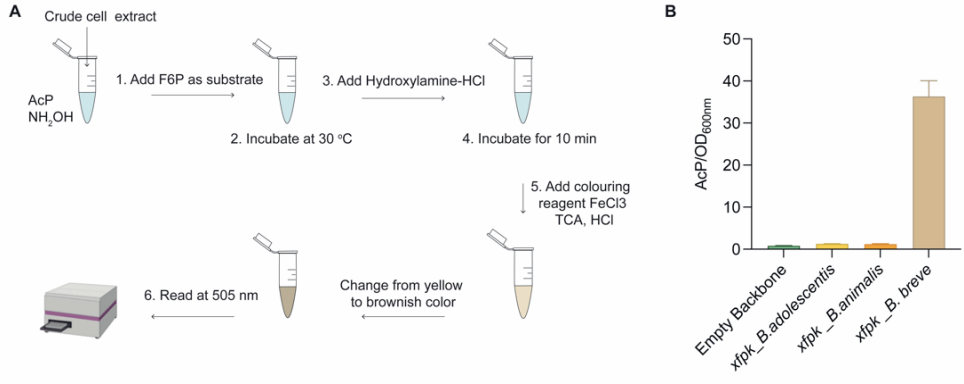

Figure 4.2: in vitro essay characterization of Xfpks. A) Workflow of the ferric hydroxamate method used for Acp quantification. B) Acp production from F6P in cell-free extracts by the three isolated Xfpk enzymes. Abbreviations: (AcP), acetyl-phosphate, (F6P), fructose-6-phosphate, (TCA), trichloroacetic acid. Bar graphs represent the mean value ± SD from three independent experiments.

1.26 and 1.19 mM AcP/$OD600$, respectively. Both only produced amounts slightly higher compared to the empty vector control (0.80 mM). This suggests that both enzymes are active, yet do not cleave F6P with high efficiency. However, the Xfpk from *B. breve* displayed high reactivity towards F6P. An AcP concentration of 36.25 mM/$OD600$ was measured, roughly 30-fold higher than the concentrations of the other two candidates. Therefore, the Xfpk from *B. breve* was selected for further experiments to assess growth and production.

Effect of the phosphoketolase on the glycerol metabolism of *P putida* KT2440

To determine whether the expression of the Xfpk from *B. breve* impacts the fitness of *P. putida*, we assessed its effect on cells grown on glycerol. Glycerol is a major waste product of the biodiesel industry and has a higher degree of reduction than glucose, making it an excellent substrate for microbial fermentation [6]. To facilitate growth on glycerol, we constructed a *glpR* knockout mutant. This gene encodes a glycerol repressor and causes inconsistent lag phases when cultured on glycerol [16]. Subsequently, *P. putida* Δ*glpR* strains, harbouring either an empty pSEVAb83 plasmid or the pSEVAb83 encoding the *xfpk* gene from *B. breve*, were grown in M9 minimal medium supplemented with 200 mM glycerol. The growth experiments revealed that Xfpk overexpression resulted in a 44.3% increase in specific growth rate from 0.12 to 0.18 h^{-1}. Moreover, the introduction of the Xfpk increased the maximum $OD600$ from 4.4 to 6.6, an increase of 50% (Figure 4.3B). We assumed that this increase could be an effect of enhanced glycerol consumption. However, both strains consumed glycerol to a similar extent, implying that most formed biomass is a direct result of carbon conservation (Figure 4.3B). To use the phosphoketolase shunt to a further extent, we overexpressed the fructose-1,6-biphosphatase (Fbp) to increase the flux towards F6P. However, this did not have any added benefit over overexpressing the Xfpk alone (Data not shown).

Exploiting the phosphoketolase shunt for the production of acetyl-CoA derived compounds from glycerol

After demonstrating the beneficial effect of the Xfpk on growth, we shifted to leverage this advantageous strain to produce acetyl-CoA-derived compounds from glyc-

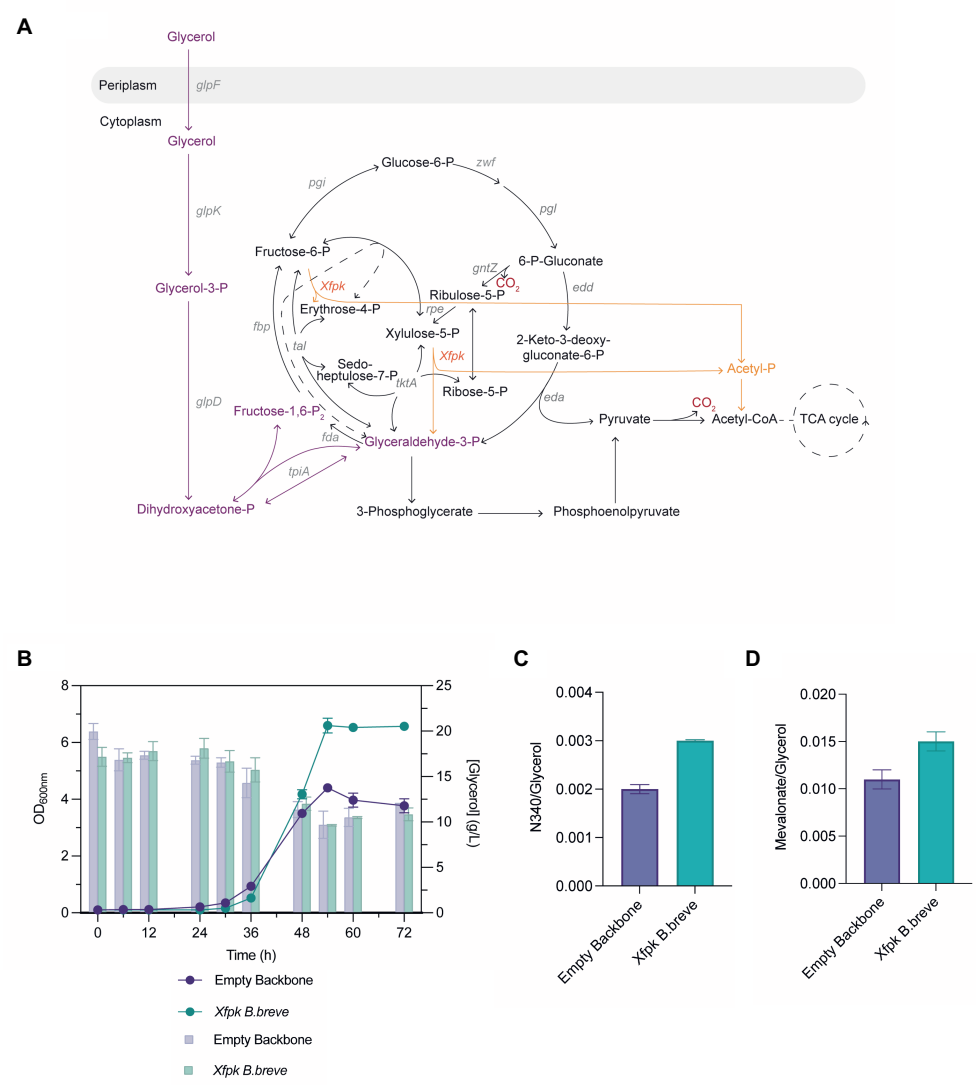

Figure 4.3: The effect of Xfpk expression on glycerol metabolism A) Architecture of the metabolism of P. putida with the Xfpk when it is grown on glycerol, B) growth patterns of strain growing on glycerol expressing an empty plasmid or the Xfpk. Lines present optical density and bars glycerol concentration, C) Flaviolin yield, D) Mevalonate yield. Data points and bar graphs represent the mean value ± SD from three independent experiments.

erol. A wide variety of interesting valuable compounds can be derived from the intermediate acetyl-CoA e.g., isoprenoids, 1-butanol, and polyketides [9]. As described previously, in a normal glycolytic regime, acetyl-CoA is produced by pyruvate decarboxylation. In this conversion, carbon is lost in the form of CO_2, nega-

tively impacting the yield of acetyl-CoA-derived products. By rewiring the metabolic flux through the phosphoketolase shunt, this loss can be prevented, improving yields in the process. To assess this beneficial effect, we took two acetyl-CoA-derived compounds, malonyl-CoA, and mevalonate, as a proof of concept. Malonyl-CoA is a malonic acid that can be used to produce fatty alcohols and is derived directly from acetyl-CoA by the enzyme acetyl-CoA carboxylase consisting of four subunits (AccABCD). For easy detection of increased malonyl-CoA levels, we used the previously repurposed type III polyketide synthase RppA [17]. This enzyme converts five molecules of malonyl-CoA to 1,3,6,8-tetrahydroxynapthaene, which is subsequently nonenzymatically oxidized to flaviolin. The produced flaviolin is red-coloured by itself, allowing spectrophotometrically quantification at a wavelength of 340 nm. Within our experiments, we overexpressed both RppA as well as all the several native subunits in *P. putida*.

The second acetyl-CoA-derived compound, mevalonate, is a key compound in industrial biochemistry. It is a metabolic precursor for terpenoids, which can be used in the production of cosmetics and biofuels [18]. Mevalonate is produced from acetyl-CoA in a three-step process. First one acetyl-CoA is converted to acetoacetyl-CoA. Secondly, a second acetyl-CoA will condense with acetoacetyl-CoA to form 3-hydroxy-3-methylglutaryl-CoA (HMG-CoA). Finally, this HMG-CoA is converted to mevalonate. For our experiments, we used the *mvaE* and *mvaS* genes from *Enterococcus faecalis*. The *mvaE* gene encodes a bifunctional protein that catalyzes both the first and last reaction in the mevalonate production pathway [18]. For the production experiments, we relocated the *xfpk* gene to a pSEVA62b vector and all product expression genes were cloned under a constitutive J23100 promoter into a pSEVA23b vector. The production experiments for malonyl-CoA revealed a yield of 0.002 and 0.003 (absolute absorbance flaviolin / consumed glycerol) for *P. putida* Δ*glpR* with an empty plasmid and with the Xfpk shunt, respectively (Figure 4.3C). Therefore, *P. putida* Δ*glpR* with the Xfpk shunt produced 38.5% more than the control. Similar results were obtained for mevalonate production, in which *P. putida* Δ*glpR* with an empty plasmid had a yield of 0.011 and with the Xfpk shunt of 0.015 mol/mol: 25.9% higher (Figure 4.3D).

Effect of the phosphoketolase on engineered xylose metabolism in P putida KT2440

The Xfpk is a promiscuous enzyme, which besides cleaving the sugar-phosphate F6P, also cleaves X5P. As X5P is the breakdown product of xylose degradation, we hypothesized that introducing the phosphoketolase shunt could enhance growth on xylose. Xylose is a major constituent of hemicellulose which has been proposed as an alternative microbial feedstock [19]. Xylose utilization requires a combination of two genes, *xylA* encoding xylose isomerase and *xylB* encoding xylulokinase. Additional overexpression of *xylE* which encodes a xylose/H^+ symporter has been described to improve the growth on xylose even further [20][21]. The xylose utilization genes, derived from *E. coli*, were codon-optimized for *P. putida* using the Jcat tool (Table S3). The *xylABE* genes alone and together with the *xfpk* were cloned in the low copy number vector pSEVAb62 under the expression of the strong constitutive BBa_J23100 promoter. Both plasmids were transformed in a *P. putida* strain with a Δ*gcd* background. The *gcd* gene encodes a glucose dehydrogenase, which has been reported to break down xylose to xylonate, a dead-end product [20].

Plasmid-born expression of the xylose utilization genes resulted in very long lag phases (>312 h) and irregular growth patterns (Data not shown). Therefore, we decided to chromosomally express the operons. The xylose operons, both with and without the *xfpk*, and under the control of the constitutive Ptac promoter were chromosomally integrated into KT2440Δ*gcd* downstream of the PP_5322 gene, resulting in strains KT2440Δ*gcd-xylABE* and KT2440Δ*gcd-xylABE-xfpk*. This locus has been described for its high basal expression, yet low impact on cellular fitness [22]. These new plasmid-free strains showed a reduced lag phase of 12 hours. Corresponding with the results of the glycerol experiment, strains expressing the Xfpk, showed a faster growth rate and higher cell density compared to their non-expressing counterpart. KT2440Δ*gcd-xylABE* grew with a specific growth rate of 0.02 h^{-1} and reached the stationary phase after 216 hours at an $OD600$ of 5.73. On the contrary, KT2440Δ*gcd-xylABE-xfpk* had a specific growth rate of 0.05 h^{-1} and a final $OD600$ of 7.4; an increase of 167% and 30.2%, respectively. Moreover, KT2440Δ*gcd-xylABE-xfpk* reached a higher OD while using less substrate than its non-expressing counterpart, highlighting the major impact carbon conservation has (Figure 4.4B).

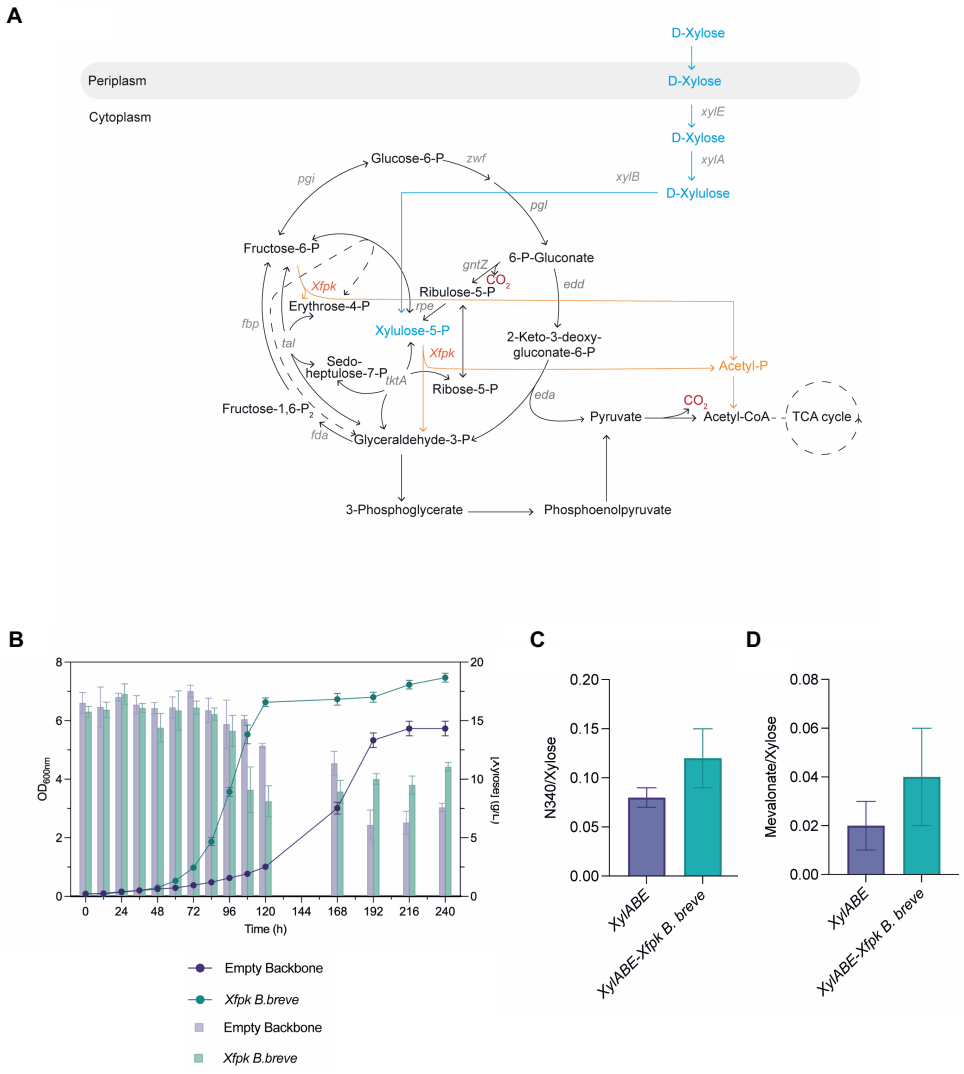

Figure 4.4: The effect of Xfpk expression on engineered xylose metabolism A) Architecture of the metabolism of P. putida with the Xfpk when grown on xylose. B) growth patterns of strains growing on xylose expressing an empty plasmid or the Xfpk. Lines present optical density and bars xylose concentration. C) Flaviolin yield, D) Mevalonate yield. Data points and bar graphs represent the mean value ± SD from three independent experiments.

As with glycerol, we equipped the xylose strains with the plasmids to produce malonyl and mevalonate. The production experiments for malonyl-CoA revealed a yield of 0.08 and 0.12 (absolute absorbance flaviolin / consumed xylose) for KT2440Δ*gcd-xylABE* and KT2440Δ*gcd-xylABE-xfpk*, respectively (Figure 4.4C). There-

fore, KT2440Δ*gcd-xylABE-xfpk* produced 49,4% more than the control. Similar results were obtained for mevalonate production, in which KT2440Δ*gcd-xylABE* had a yield of 0.022 and KT2440Δ*gcd-xylABE-xfpk* 0.042 mol/mol: 48,7% higher (Figure 4.4D).

Discussion

In this study, we showed that the introduction of the phosphoketolase shunt increased the cellular fitness of *P. putida*, enabling it to reach higher cell densities and growth rates. Additionally, yields were enhanced due to carbon conservation. Although we only showcase its beneficial effect on glycerol and xylose, we believe its catabolic repertoire can be further extended. Hemicellulose, of which xylose is a major constituent, contains other promising substrates that would profit from the phosphoketolase shunt, such as arabinose, mannose, and galactose [19]. For arabinose, Elmore et al., (2020) [21] recently engineered both the oxidative and isomerase pathway in *P. putida*. The oxidative pathway breaks down arabinose to the TCA intermediate 2-ketoglutarate, whilst the isomerase pathway is analogous to the xylose pathway. Therefore, for the Xfpk shunt to be used to its maximum efficiency, only the isomerase pathway, which has X5P as a product, would suffice. The other two substrates, mannose, and galactose, both break down to F6P, allowing full utilization of the Xfpk shunt as well.

The Xfpk shunt, as described in this study, could be further enhanced towards a full NOG or the recently engineered GATCHYC (glycolysis alternative high carbon yield cycle) [11][23]. Both cycles display full carbon conservation with a 100% acetyl-CoA yield from its designated substrate. However, the NOG pathway contains two bidirectional steps (transaldolase and transketolase), which kinetically limits the pathway [24]. On the other hand, the GATCHYC relies mostly on unidirectional steps and the promiscuous activity of the Xfpk, which would cleave the sugar-phosphate sedoheptulose-7-phosphate (S7P) as well. The Xfpk from *B. breve* has been reported to use X5P and F6P in a 3:2 ratio [25]. It is likely that it also possesses a side activity towards S7P, making the implementation of the GATCHYC noteworthy. However, whereas full conversion of substrate to acetyl-CoA is a major benefit in both path-

ways, their major bottleneck is the insufficient formation of redox cofactors. To resolve this problem, alternative electron donors could potentially be added. One of the most promising candidates is formate, which can be directly derived from the electrochemical reduction of CO_2 [26]. Moreover, it has already been showcased that supplementation of formate to *P. putida* KT2440 drastically increased NADH formation [27]. Therefore, a combination of this carbon conservation pathway with formate might yield a superior platform strain.

Another recently engineered route to overcome the redox limitation of the NOG is the EP-bifido pathway [13]. This route was demonstrated with glucose as a carbon source and pushes the flux towards the oxidative pentose phosphate pathway. In this pathway, NADPH is generated at the expense of 1 CO_2. However, due to the introduction of the Xfpk, more carbon loss was eventually prevented, and product yield was enhanced. The metabolism of *P. putida* consists of a cyclic architecture, termed EDEMP, merged from the Enter-Doudoroff (ED), the Embden-Meyerhof-Parnas (EMP) and the Pentose Phosphate Pathway (PPP) [28]. This cycle recycles hexose phosphates, generating reducing equivalents in the form of NADPH. Replacing the EDEMP with the EP- bifido pathway could have great implications for the metabolism of *P. putida* as it would produce reducing equivalents whilst conserving carbon. This synergistic effect could further enhance product formation. Moreover, as NADPH is a well-known combater of oxidative stress, it could even further increase *P. putida* as an industrial workhorse [29].

Materials and methods

Bacterial strains and growth conditions

P. putida and *E. coli* cultures were incubated at 30°C and 37°C respectively. For genetic modification and plasmid isolation, strains were cultured in Lysogeny broth (LB) medium containing 10 g/L NaCl, 10 g/L tryptone and 5 g/L yeast extract, unless otherwise indicated. For the preparation of solid media, 1.5% (w/v) agar was added. Antibiotics were used whenever required at the following concentrations: kanamycin (Km) 50 μg/ml, gentamycin (Gm) 10 μg/ml, chloramphenicol (Cm) 50 μg/ml and apramycin (Apra) 50 μg/ml. All growth experiments were per-

formed using M9 minimal medium (per Liter: 3.88 g K_2HPO_4, 1.63 g NaH_2PO_4, 2.0 g $(NH_4)_2SO_4$), pH 7.0. The M9 media was supplemented with a trace elements solution (10 mg/L ethylenediaminetetraacetic acid (EDTA), 0.1 g/L $MgCl_2 \cdot 6H_2O$, 2 mg/L $ZnSO_4 \cdot 7H_2O$, 1 mg/L $CaCl_2 \cdot 2H_2O$, 5 mg/L $FeSO_4 \cdot 7H_2O$, 0.2 mg/L $Na_2MoO_4 \cdot 2H_2O$, 0.2 mg/L $CuSO_4 \cdot 5H_2O$, 0.4 mg/L $CoCl_2 \cdot 6H_2O$, 1 mg/L $MnCl_2 \cdot 2H_2O$).In these experiments, strains were precultured in 10 ml LB with corresponding antibiotics. Then, the cultures were washed twice in M9 media or MOPS without a carbon source. Finally, the cultures were diluted to an $OD600$ of 0.1 to start the experiment and incubated in a rotary shaker at 200 rpm at 30°C. Samples were taken at various time points for quantification of cell density and HPLC analysis.

Plasmid construction

DNA fragments were amplified using Q5 Hot Start High Fidelity DNA Polymerase (New England Biolabs) and separated by electrophoresis using a 1% (w/v) agarose gel. DNA was purified by the NucleoSpin Gel and PCR clean-up kit (Macharey-Nagel, Germany). Plasmids were constructed using Golden Gate using the SEVA assembly protocol or through Gibson Assembly [30]. The phosphoketolase genes were obtained from the genomic DNA of the *Bifidobacterium* strains: *B. animalis* DSM 10140, *B. adolescentis* ATCC 15703, *B. breve* DSM 21213 (Table 3, Supplementary data). The *rppA* gene from *Streptomyces Griseus* and all *accA-D* genes from *P. putida* KT2440 were taken from an in-house plasmid (Batianis et al., unpublished). The *mvaE* and *mvaS* genes were derived from pSMART-MEV1 ordered from Addgene (pSMART-Mev1 was a gift from Michael Lynch (Addgene plasmid #65815; http://n2t.net/addgene:65815; RRID:Addgene_65815)). All plasmids were transformed via heat shock in chemically competent *E. coli* DH5α λ*pir* and transformants were selected on LB plates with corresponding antibiotics. Colonies were screened by colony PCR using Phire Hot Start II DNA Polymerase (Thermo Fisher Scientific Inc. Waltheim, MA, USA). The plasmids from successful screenings were extracted and verified by Sanger DNA sequencing (MACROGEN Inc, the Netherlands). Correct plasmids were transformed into *P. putida* using electroporation.

Strain construction

The deletion and introduction of genes in the genome were performed using the protocol previously described by Wirth et al., 2020 [31]. First, regions of approximately 500 bp upstream and downstream of the target genes were amplified from the genomic DNA of *P. putida* KT2440. The TS1 and TS2 fragments were cloned into the non-replicative pGNW plasmid and propagated into *E. coli* DH5α λ*pir*. Positive colonies were transformed into *P. putida* via electroporation and successful cointegrations were screened by PCR. For the chromosomal integration of the xylose operon, the TS1 and TS2 regions of the PP5322 locus were amplified. The xylose operon was assembled using the standard protocols of the previously described SevaBrick assembly [30]. Subsequently, this operon was cloned together with the TS1 and TS2 regions of the PP_5322 locus in the pGNW vector for chromosomal integration. The second plasmid pQURE6-H [32] was introduced to the selected co-integrate. The transformants were grown on an LB agar plate with Gm and induced with 2 mM 3-methylbenzoic acid (3-mBz). The 3-mBz was used to induce the XylS-dependent Pm promoter, driving the expression of the I-SceI homing nuclease. Deletions and insertions were confirmed by colony PCR. Successful recombinants were cured of pQURE6-H by omitting 3-mBz from the medium and selected for antibiotic sensitivity.

Crude cell extraction

Cell-free extracts were obtained from 25 ml of culture broth in 50 ml Greiner Tubes and cultivated at 30°C, 200 rpm orbital shaking until an $OD600$ of ca. 0.5-0.6. The cultures were pelleted by centrifugation for 10 min at 4°C. Cell pellets were washed once with 50 ml of precooled 1X PBS buffer (pH = 7.0) with 10 mM 2-mercaptoethanol at 4°C. The pellets were resuspended in 750 μL of pre-cooled 1X PBS buffer (pH = 7.0) with 10 mM 2-mercaptoethanol. After that, the cell suspension was transferred to a pre-chilled tube with 0.5 mm silica beads and homogenized using a FastPrep®-24 (MP Biomedicals, SantaAna, CA, USA) (2 cycles of 30 s, 5 min resting on ice in between runs). The homogenized mixture was centrifuged at 7,500 x g for 30 min at 4°Cto remove insoluble cell debris. The cell-free extracts were stored at –20°C for further use.

Phosphoketolase activity assay

Phosphoketolase activity was measured using the ferric hydroxamate method, based on the chemical conversion of enzymatically produced acetyl-phosphate into ferric acetyl hydroxamate, according to the protocol from Wang et al., (2019) [13]. The standard reactions were carried out in 1.5 mL of Eppendorf tube in a total assay volume of 100 μL consisting of 50 mM Tris (pH 7.5), 5 mM $MgCl_2$, 5 mM potassium phosphate, 1 mM thiamine pyrophosphate and 10 mM F6P as a substrate. The crude cell-free extract was added to start the reaction and incubated at 30°C for 1 hour. To stop the enzymatic reaction, 60 μL hydroxylamine hydrochloride (2 M, pH 6.5) was added to 40 μL of assay solution. After incubation for 10 min at room temperature, 120 μL colouring reagent consisting of 15% (w/v) trichloroacetic acid, 4 M HCl, and $FeCl_3 \cdot 6H_2O$ (5% [w/v] in 0.1 M HCl) were added to generate ferric hydroxamate, which was then spectrophotometrically quantified at 505 nm by comparing to a series of lithium potassium acetyl-phosphate standards (Sigma).

Analytical Methods

Extracellular metabolite concentrations were determined by high-performance liquid chromatography (HPLC). Glycerol, xylose and mevalonate concentrations were detected and quantified using an ICS5000 HPLC (Thermo Scientific) with a refractive index detector (Shodex RI-101, sample frequency 5 Hz) and a Thermo UV/VIS detector (λ = 210nm) coupled to an Animex HPX-87H column (BioRad) at 60 °C. Separations were performed using 0.016 N H_2SO_4 as an eluate at a flow rate of 0.6 mL/min. Culture samples were centrifuged at 16,000 x g for 15 min. Supernatant and standards were mixed with 6 mM propionic acid as an internal standard at a ratio of 4:1. The flaviolin in the supernatant was quantified in triplicate in a Synergy microplate reader (Biotek Instruments) at a wavelength of 340 nm. The relative flaviolin production (N340) was determined by normalizing the measured absolute values (A340) by the cell density ($OD600$).

Acknowledgements

We would like to thank Marina Fassarella for providing us with the *Bifidobacterium* strains.

Author contributions

L.B. conceptualization; L.B., M.M.P., K.K., M.T and S.H. methodology; L.B. and M.M.P. writing-initial draft; L.B., M.M.P., K.K., M.T, S.H., R.v.K and V.A.P.M.d.S. writing-review and editing; R.v.K. and V.A.P.M.d.S. supervision.

Conflict of interest

The authors declare no conflict of interest.

Supplementary material

The rest of the supplementary material of this chapter, including Supplementary Tables S1 to S4, can be accessed *via*:

https://microbialcellfactories.biomedcentral.com/articles/10.1186/s12934-022-02015-9

Bibliography

1. Staffas, L., Gustavsson, M. & McCormick, K. Strategies and policies for the bioeconomy and bio-based economy: An analysis of official national approaches. *Sustainability (Switzerland)* **5,** 2751–2769 (2013).
2. Paula, L. & Birrer, F. Including public perspectives in industrial biotechnology and the biobased economy. *Journal of Agricultural and Environmental Ethics* **19,** 253–267 (2006).
3. Nielsen, J. & Keasling, J. D. Engineering Cellular Metabolism. *Cell* **164,** 1185–1197 (2016).
4. Poblete-Castro, I., Becker, J., Dohnt, K., *et al.* Industrial biotechnology of Pseudomonas putida and related species. *Applied Microbiology and Biotechnology* **93,** 2279–2290 (2012).
5. Martin-Pascual, M., Batianis, C., Bruinsma, L., *et al.* A navigation guide of synthetic biology tools for Pseudomonas putida. *Biotechnology Advances* **49,** 107732 (2021).
6. Nikel, P. I., Kim, J. & de Lorenzo, V. Metabolic and regulatory rearrangements underlying glycerol metabolism in Pseudomonas putidaKT2440. *Environmental Microbiology* **16,** 239–254 (2014).
7. Ankenbauer, A., Schäfer, R. A., Viegas, S. C., *et al.* Pseudomonas putida KT2440 is naturally endowed to withstand industrial-scale stress conditions. *Microbial Biotechnology* **13,** 1145–1161 (2020).
8. Caspeta, L. & Nielsen, J. Economic and environmental impacts of microbial biodiesel. *Nature Biotechnology* **31,** 789–793 (2013).
9. Central metabolic nodes for diverse biochemical production. *Current Opinion in Chemical Biology* **35,** 37–42 (2016).
10. Henard, C. A., Smith, H. K. & Guarnieri, M. T. Phosphoketolase overexpression increases biomass and lipid yield from methane in an obligate methanotrophic biocatalyst. *Metabolic Engineering* **41,** 152–158 (2017).
11. Bogorad, I. W., Lin, T. S. & Liao, J. C. *Synthetic non-oxidative glycolysis enables complete carbon conservation* 2013.
12. Lin, P. P., Jaeger, A. J., Wu, T. Y., *et al.* Construction and evolution of an Escherichia coli strain relying on nonoxidative glycolysis for sugar catabolism. *Proceedings of the National Academy of Sciences of the United States of America* **115,** 3538–3546 (2018).
13. Wang, Q., Xu, J., Sun, Z., *et al.* Engineering an in vivo EP-bifido pathway in Escherichia coli for high-yield acetyl-CoA generation with low CO2 emission. *Metabolic Engineering* **51,** 79–87 (2019).
14. Chinen, A., Kozlov, Y. I., Hara, Y., *et al.* Innovative metabolic pathway design for efficient l-glutamate production by suppressing CO2 emission. *Journal of Bioscience and Bioengineering* **103,** 262–269 (2007).
15. Meadows, A. L., Hawkins, K. M., Tsegaye, Y., *et al.* Rewriting yeast central carbon metabolism for industrial isoprenoid production. *Nature* **537,** 694–697 (2016).
16. Nikel, P. I., Romero-Campero, F. J., Zeidman, J. A., *et al.* The glycerol-dependent metabolic persistence of Pseudomonas putida KT2440 reflects the regulatory logic of the GlpR repressor. *mBio* **6,** 1–13 (2015).
17. Yang, D., Kim, W. J., Yoo, S. M., *et al.* Repurposing type III polyketide synthase as a malonyl- CoA biosensor for metabolic engineering in bacteria. *Proceedings of the National Academy of Sciences of the United States of America* **115,** 9835–9844 (2018).
18. Yoon, S. H., Lee, S. H., Das, A., *et al.* Combinatorial expression of bacterial whole mevalonate pathway for the production of β-carotene in E. coli. *Journal of Biotechnology* **140,** 218–226 (2009).
19. Scapini, T., dos Santos, M. S., Bonatto, C., *et al.* Hydrothermal pretreatment of lignocellulosic biomass for hemicellulose recovery. *Bioresource Technology* **342** (2021).
20. Dvořák, P. & de Lorenzo, V. Refactoring the upper sugar metabolism of Pseudomonas putida for co-utilization of cellobiose, xylose, and glucose. *Metabolic Engineering* **48,** 94–108 (2018).

21. Elmore, J. R., Dexter, G. N., Salvachúa, D., *et al.* Engineered Pseudomonas putida simultaneously catabolizes five major components of corn stover lignocellulose: Glucose, xylose, arabinose, p-coumaric acid, and acetic acid. *Metabolic Engineering* **62,** 62–71 (2020).

22. Chaves, J. E., Wilton, R., Gao, Y., *et al.* Evaluation of chromosomal insertion loci in the Pseudomonas putida KT2440 genome for predictable biosystems design. *Metabolic Engineering Communications* **11,** e00139 (2020).

23. Hellgren, J., Godina, A., Nielsen, J., *et al.* Promiscuous phosphoketolase and metabolic rewiring enables novel non-oxidative glycolysis in yeast for high-yield production of acetyl-CoA derived products. *Metabolic Engineering* **62,** 150–160 (2020).

24. Andersen, J. L., Flamm, C., Merkle, D., *et al.* Chemical transformation motifs-modelling pathways as integer hyperflows. *IEEE/ACM Transactions on Computational Biology and Bioinformatics* **16,** 510–523 (2019).

25. Bergman, A., Siewers, V., Nielsen, J., *et al.* Functional expression and evaluation of heterologous phosphoketolases in Saccharomyces cerevisiae. *AMB Express* **6** (2016).

26. Claassens, N. J., Sánchez-Andrea, I., Sousa, D. Z., *et al.* Towards sustainable feedstocks: A guide to electron donors for microbial carbon fixation. *Current Opinion in Biotechnology* **50,** 195–205 (2018).

27. Zobel, S., Kuepper, J., Ebert, B., *et al.* Metabolic response of Pseudomonas putida to increased NADH regeneration rates. *Engineering in Life Sciences* **17,** 47–57 (2017).

28. Nikel, P. I., Chavarría, M., Fuhrer, T., *et al.* Pseudomonas putida KT2440 strain metabolizes glucose through a cycle formed by enzymes of the Entner-Doudoroff, embden-meyerhof-parnas, and pentose phosphate pathways. *Journal of Biological Chemistry* **290,** 25920–25932 (2015).

29. Nikel, P. I., Fuhrer, T., Chavarría, M., *et al.* Reconfiguration of metabolic fluxes in Pseudomonas putida as a response to sub-lethal oxidative stress. *ISME Journal* **15,** 1751–1766 (2021).

30. Damalas, S. G., Batianis, C., Martin-Pascual, M., *et al.* SEVA 3.1: enabling interoperability of DNA assembly among the SEVA, BioBricks and Type IIS restriction enzyme standards. *Microbial Biotechnology* **13,** 1793–1806 (2020).

31. Wirth, N. T., Kozaeva, E. & Nikel, P. I. Accelerated genome engineering of Pseudomonas putida by I-SceI—mediated recombination and CRISPR-Cas9 counterselection. *Microbial Biotechnology* **13,** 233–249 (2020).

32. Volke, D. C., Friis, L., Wirth, N. T., *et al.* Synthetic control of plasmid replication enables target- and self-curing of vectors and expedites genome engineering of Pseudomonas putida. *Metabolic Engineering Communications* **10,** e00126 (2020).

CHAPTER 5

SHIKIMATE PATHWAY-DEPENDENT CATABOLISM ENABLES HIGH-YIELD PRODUCTION OF AROMATICS

Lyon Bruinsma*, Christos Batianis* Sara Moreno-Paz, Kesi Kurnia
Job J. Dirkmaat, Ruud A. Weusthuis, Vitor A. P. Martins dos Santos
* Contributed equally

Abstract

The biotechnological application of microorganisms to replace fossil-based processes is a global necessity. To fully leverage their potential, high titers, rates, and yields are required for commercial processes. This generally involves radical reprogramming of the intrinsic metabolism. In this study, we demonstrate a combination of metabolic modeling, rational engineering, and adaptive laboratory evolution to radically refactor bacterial metabolism. We created a new-to-nature shikimate pathway-dependent catabolism in *Pseudomonas putida* by reprogramming the shikimate pathway as the dominant pathway for growth. This new strain diverts it's the vast majority of its carbon catabolism flux through the shikimate pathway and produced 0.35 mol/mol 4-hydroxybenzoate in glycerol minimal medium during growth, achieving 89.2% of the maximum predicted pathway yield. We demonstrate that the shikimate pathway can act as the main catabolic route and deliver a promising strain that can serve as a useful *chassis* to produce various shikimate pathway-derived compounds..

Introduction

Metabolism defines the lifestyle of any organism that we know [1]. Despite the considerable diversity among organisms, there is a primary central carbon metabolism shared by almost all of them. This primary metabolism, often consisting of glycolysis, the tricarboxylic acid (TCA) cycle, and the pentose phosphate pathway is used to convert carbon sources to precursor molecules necessary to synthesize all cellular constituents for growth and maintenance [2]. As a result, the primary metabolism is often viewed as a rigid network, and any deviation from it can lead to reduced cell viability or even cell death [3]. This is unfortunate as we can leverage this network to produce a plethora of fuels and chemicals, replacing petroleum-derived processes [4]. Therefore, for the sake of the bioeconomy, we need to be able to efficiently manipulate these networks to produce chemicals with high titers, rates, and productivity [5]. To achieve this goal, microorganisms need to be radically refactored to ensure a high flux towards the product of interest. Yet, the introduction of a production pathway often interferes directly with the main metabolism, and fluxes are not easily diverted [6]. Moreover, extra complexity is added as many inherent pathways are subjected to tight regulation and therefore carry considerably low fluxes [5]. One of these pathways is the shikimate pathway, the biochemical source of numerous aromatic molecules including aromatic amino acids. While a myriad of valuable molecules can be derived from this pathway, its biotechnological exploitation remains a mounting metabolic engineering challenge [7][8][9].

Standard metabolic engineering strategies rely on simple gene overexpressions and flux alterations in the central carbon metabolism. However, these modifications compete directly with cellular fitness and often do not result in economically feasible yields [10]. Therefore, a paradigm shift is essential to fully reshape the rigid carbon metabolism and exert the potential of the shikimate pathway. In recent years, growth-coupled selections have emerged as powerful tools to redesign cell factories for the production or consumption of new substrates or to establish new metabolic architectures [11][12][13][14]. This approach combined with laboratory evolution has the power to completely reprogram cellular metabolism, creating industrially relevant cell factories. One key example is the establishment of a chemo-autotrophic *Escherichia coli* that can generate all its biomass from CO_2 [15].

By introducing essential deletions in xylose catabolism, bacterial growth became dependent on the carboxylation reaction by Rubisco. Eventually, this dependency was able to establish full autotrophic growth after several rounds of laboratory evolution. Using a similar approach, a synthetic methylotrophic *E. coli* strain was engineered [16]. Here, methanol utilization was coupled to xylose catabolism, which after evolution yielded a strain that could generate all biomass and energy from this promising C1-feedstock. Apart from introducing foreign pathways in a microbial host, growth-coupled selection systems can be used to fully rearrange native metabolic architectures. Iacometti et al., (2022) [17] demonstrated the flexibility of bacterial metabolism by establishing silent glycolytic routes in *E. coli*. Using growth-coupled evolution they acquired a strain in which the canonical Embden-Meyerhof-Parnas (EMP) pathway was replaced by a serine shunt. Therefore, we believe that these growth-coupled scenarios can be deployed as a metabolic engineering strategy for the shikimate pathway.

In this study, we describe how we rigorously rearranged the intrinsic metabolic network of the industrially relevant bacterium *Pseudomonas putida*, creating a shikimate pathway-dependent catabolism (SDC) (Figure 5.1). We established a model-driven rearrangement of the main carbon metabolism through pyruvate-driven laboratory evolution using the innate pyruvate-releasing reactions from the shikimate pathway with the aid of a selective biosensor. Whole genome sequencing and reverse engineering revealed that a perturbation in the signaling network was key in realizing this drastic metabolic shift. Further optimization of SDC was achieved using a rational and model-driven approach, resulting in the first strain ever constructed which uses the shikimate pathway as the dominant catabolic pathway and can serve as a useful *chassis* to produce various aromatic compounds. Our findings highlight the tremendous plasticity of metabolic networks and how growth-coupled strategies can be exploited to install new-to-nature metabolisms for industrial biotechnology.

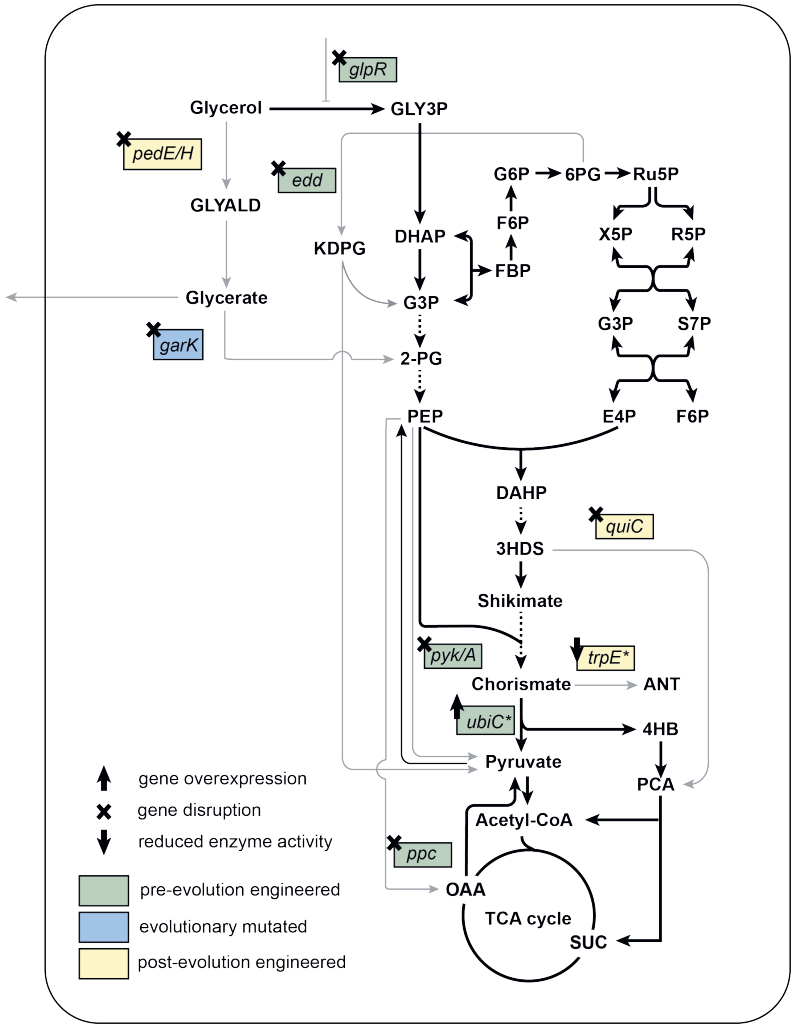

Figure 5.1: Metabolic architecture of the shikimate pathway-dependent catabolism. Pathways and mutations that were engineered pre- and post-evolution to establish the final SDC strain. Abbreviations: GLY3P, sn-glycerol-3-phosphate; GLYALD, glyceraldehyde; DHAP, dihydroxyacetone phosphate; G3P, glyceraldehyde-3-phosphate; 2-PG, 2-phosphoglycerate; KDPG, 2-keto-3-deoxy-6-phosphogluconate; PEP, phosphoenolpyruvate; FBP, fructose bisphosphate, F6P, fructose-6-phosphate; G6P, glucose-6-phosphate; 6PG, 6-phosphogluconate; Ru5P, ribulose-5-phosphate; R5P, ribose-5-phosphate; X5P, xylose-5-phosphate; S7P, sedoheptulose-7-phosphate; E4P, erythrose-4-phosphate; DAHP, 3-deoxy-d-arabinoheptulosonate-7-phosphate; 3HDS, 3-dehydroshikimate; ANT, anthranilate; 4HB, 4-hydroxybenzoate; PCA, protocatechuate; SUC, succinate; OAA, oxaloacetate; glpR, glycerol regulon repressor; edd, phosphogluconate dehydratase; pedE/H, PQQ - dependent alcohol dehydrogenases; garK, glycerate kinase; pyk/A, pyruvate kinase; quiC, dehydroshikimate dehydratase; ubiC, chorismate pyruvate lyase; ppc, phosphoenolpyruvate carboxylase; trpE. anthranilate synthase

Results

Metabolic design and *in-silico* assessment of SDC

Pyruvate is a key node in central metabolism predominantly produced in *P. putida* via the Entner-Doudoroff (ED) and lower Embden–Meyerhof–Parnas (EMP) pathway. Yet apart from the main carbon metabolism, pyruvate is produced by several other innate reactions, some derived from the shikimate pathway. Therefore, to increase the flux through the shikimate pathway, we aimed to establish it as the main source of cellular pyruvate creating SDC. We used iJN1462, the genome-scale model (GEM) of *P. putida*, to find all the pyruvate-releasing reactions present. We analyzed the ability of each of these reactions to support *in-silico* growth as the sole pyruvate source using glycerol as a carbon source (Figure 5.2A). The model predicted the highest growth rate using a shikimate pathway reaction when chorismate pyruvate lyase (CHRPL) was the sole pyruvate source. This reaction cleaves chorismate, the final product of the shikimate pathway, to pyruvate and 4-hydroxybenzoate (4HB) (Figure 5.2B). When CHRPL is the sole pyruvate source, the *in-silico* growth rate reduces by 17.8% compared to the wild-type (*P. putida* KT2440). Still, it allows 26.1% faster growth than the other pyruvate-releasing shikimate reactions and was therefore chosen as the most efficient candidate to establish SDC. To further evaluate the feasibility of SDC, we calculated the overall chemical equations from glycerol to pyruvate in terms of its ability to generate reduced cofactors and ATP compared to the native metabolism (Supplementary Data). For this purpose, native and SDC metabolism were simulated with flux balance analysis (FBA) in which pyruvate production was set as the main objective using glycerol as the carbon source. During native metabolism, glycerol is equimolarly converted to pyruvate, generating reducing equivalents in the process. As *P. putida* is an aerobic bacterium, a large surplus of ATP can be generated in the electron transport chain. In contrast, the SDC metabolism is energetically poor compared to the native metabolism. The shikimate pathway is an anabolic pathway and requires the incorporation of NADPH and ATP to reach the end product chorismate. Moreover, there is a net production of CO_2 reducing the pyruvate yield. Nonetheless, with the production of reducing equivalents, a surplus of 0.23 ATP can be generated for growth and maintenance.

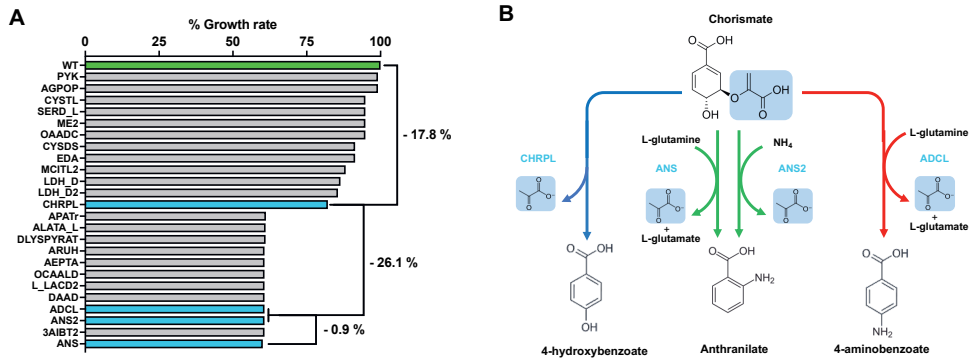

Figure 5.2: In-silico assessment of SDC A) Growth rate predictions using FBA with glycerol as carbon source. Each pyruvate-releasing reaction was set as the sole pyruvate source. All reactions are compared to the growth rate of the wild-type which was set as 100% (μmax= 0.235 h^{-1}). B) Metabolic scheme of the pyruvate-releasing reactions derived from the shikimate pathway. PYK, pyruvate kinase; AGPOP, DGTP:pyruvate 2-O-phosphotransferase; CYSTL, cystathionine b-lyase; SERD_L, L-serine deaminase; ME2, malic enzyme (NADP); OAADC, oxaloacetate decarboxylase; CYSDS, cysteine desulfhydrase; EDA, 2-dehydro-3-deoxy-phosphogluconate aldolase; MCITL2, methylisocitrate lyase; LDH_D, D-lactate dehydrogenase; LDH_D2, D-lactate dehydrogenase (q8); CHRPL, chorismate pyruvate lyase; APATr, B-alanine pyruvate aminotransferase; ALATA_L, L-alanine transaminase; DLYSPYRAT, D-lysinepyruvate aminotransferase; ARUH, L-arginine pyruvate transaminase; AEPTA, 2-aminoethylphosphonate pyruvate transaminase; OCAALD, 4-oxalcitromalate aldolase; L_LACDS, L-lactate dehydrogenase (ubiquinone); DAAD, D-amino acid dehydrogenase; ADCL, 4-aminobenzoate synthase; ANS2, anthranilate synthase 2; 3AIBT2, L-3 aminoisobutyrate transaminase; ANS, anthranilate synthase.

Creating a growth-coupled scenario to establish SDC

Our *in-silico* analysis demonstrates the feasibility of SDC. However, its prediction relies solely on stoichiometry. Microbial metabolism is tightly regulated, and a metabolic reconfiguration of this extent is impossible to attain through rational engineering. Adaptive laboratory evolution (ALE) is a microbial engineering method commonly used to achieve desired phenotypes that cannot be obtained using the rational approach [18]. Therefore, to install CHRPL as the major pyruvate source, we established a pyruvate auxotrophic strain (Δ*pyr*) to allow for growth-coupled evolution (Figure 5.3A). At first, we deleted *edd*, encoding a 6-phosphogluconate dehydratase. This reaction is part of the ED pathway together with the sequential pyruvate-releasing step, encoded by *eda*, and the deletion of *edd* will render the whole pathway inactive. Next, we decoupled pyruvate from phosphoenolpyruvate (PEP), by deleting the pyruvate kinases encoded by *pyk* and *pykA*. The last

major pyruvate node was removed by deleting phosphoenolpyruvate carboxylase, encoded by *ppc*. This reaction converts PEP into oxaloacetate, which subsequently can be converted to pyruvate by the oxaloacetate decarboxylase (PP_1389). It is important to note, that the deletion of *pyk*, *pykA*, and *ppc* not only disrupts the flow to pyruvate but also increases the intracellular PEP pool for the shikimate pathway. At last, we deleted *glpR*, which encodes the transcriptional repressor of the glycerol catabolic operon. We termed this final strain Δ*pyr* and evaluated whether it exhibited pyruvate auxotrophy by growing it in glycerol minimal media supplemented with increasing concentrations of pyruvate. As expected, Δ*pyr* was not able to grow in glycerol minimal medium without the addition of pyruvate, indicating that biomass formation is exclusively dependent on its external supplementation (Figure 5.3B). Albeit this strain can serve as a base strain for ALE, our *in-silico* simulations indicated additional pyruvate-releasing reactions (AGPOP, CYSTL, SERD_L, ME2, OAADC, CYSDS, MCITL2, LDH_D, LDH_D2) that are more favorable and can allow faster growth rates than when using CHRPL (Figure 5.2A). Although the removal of these reactions would benefit evolution, they might affect cellular fitness. Moreover, the other chorismate-derived pyruvate-releasing reactions cannot be removed, as this would render the strain auxotrophic for both tryptophan and folate (Figure 5.2B). Therefore, by only selecting on growth, there is an increased possibility that undesired phenotypes might develop.

To circumvent this problem, we implemented a second layer of screening by incorporating a previously established 4HB – responsive sensor [19]. This sensor constitutes a double mutant pobR enzyme from *Acinetobacter baylyi* ADP1, which binds to 4HB upon detection and expresses sfGFP. We further adapted this biosensor by including an LAA degradation tag, to decrease leakiness and increase tunability (Figure 5.3C). We cloned the sensor in a pSEVAb83 backbone and tested its efficacy in *P. putida* KT2440 in glycerol minimal media supplemented with increasing concentrations of 4HB. As expected, the sensor displayed dose-dependent *sfgfp* expression to exogenous 4HB concentrations indicating a strong selection method for ALE (Figure 5.3D). Using this method, superior strains can be isolated that exhibit fast growth rates and a high flux towards 4HB formation.

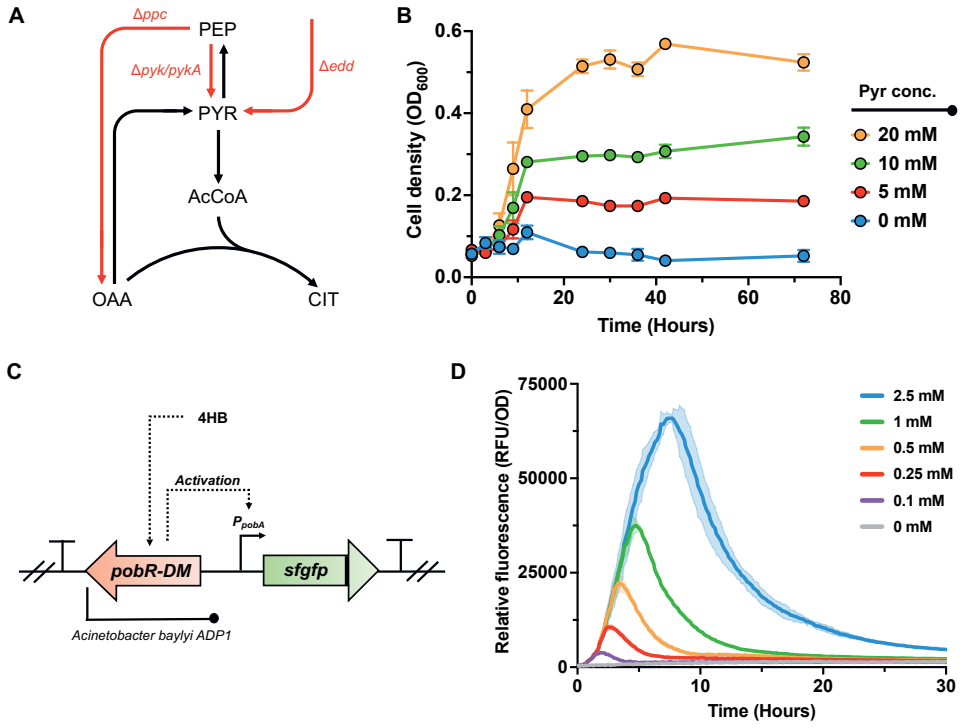

Figure 5.3: Setting up the base strain and biosensor for adaptive laboratory evolution. A) Metabolic scheme of the genetic basis of Δpyr. All major pyruvate-releasing reactions that were deleted are denoted in red. B) Growth curve of Δpyr in glycerol minimal media supplemented with various concentrations of pyruvate. C) Graphical representation of the 4HB-responsive biosensor used in this study. The PobR enzyme from Acinetobacter baylyi ADP1 binds to 4HB upon its presence. This in turn activates PpobA expressing the sfgfp gene. The gene is equipped with an LAA degradation tag, to reduce leakiness of the system D) Relative fluorescence profiles of P. putida ΔglpR equipped with the 4HB-sensor upon exposure to increasing 4HB levels in glycerol minimal medium. Abbreviations: PEP, phosphoenolpyruvate; PYR, pyruvate; AcCoA, acetyl-CoA; OAA, oxaloacetate; CIT, citrate; 4HB, 4-hydroxybenzoate. Data points represent the mean value ± SD from three independent experiments.

Establishing SDC through laboratory evolution

The establishment of SDC requires rigorous rearrangement of the complete metabolic network. So far, we established a pyruvate auxotrophic strain to make the shikimate pathway the major source for pyruvate and a 4HB – responsive sensor to select superior isolates. To further drive evolution, we incorporated a feedback-inhibition-resistant CHRPL [19]. To maintain high levels of CHRPL, we placed the corresponding gene (*ubiC*$^{E31Q/M34V}$) under the control of the constitutive J23100 promoter downstream of the biosensor in the same transcriptional operon. Through

this design, the 4HB produced by CHRPL creates a positive feedback loop and will increase its own transcription, likely aiding the evolution of SDC. We equipped *P. putida* Δ*pyr* with the modified biosensor and started evolution by cultivating the strain in glycerol minimal medium in two independent experiments. Growth in the population emerged in the first phase after roughly 20-24 days in both experiments (Figure 5.4A). After this initial passage, growth rates quickly increased with the next passage, indicating that crucial adaptations occurred in the initial phase. In total, the cultures in the two independent experiments were serially diluted for ≈50 days in 13 to 18 passages and plated on minimal media with glycerol.

Forty colonies were selected per ALE experiment based on fluorescence and selected for further characterization. The isolated mutants showed a diverse range of growth rates and fluorescence profiles (Figure S5.1). Within the isolated population, we observed fast-growing mutants with low fluorescent profiles. Most likely, these strains evolved through alternative salvage pathways to restore growth. This finding highlights the importance of the implemented 4HB-responsive biosensor during evolution to select superior strains. From the heterogeneous mixture of mutants, we isolated SDC.1 (Figure 5.4B). This strain demonstrated fast growth among the isolated mutants (0.099 h^{-1}), albeit significantly slower than the wild-type (0.210 h^{-1}) (Figure S5.1A). However, SDC.1 displayed high levels of fluorescence among the isolated mutants and a 10-fold increase in relative fluorescence compared to the

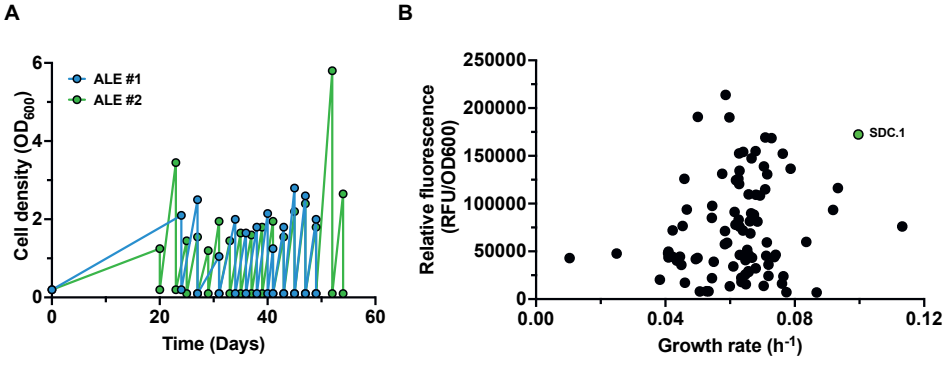

Figure 5.4: Isolation of SDC.1 after adaptive laboratory evolution. A) Growth curves of ALE passages in glycerol minimal medium. B) Relative fluorescence profiles (RFU/OD_{600}) plotted against the growth rate (h^{-1}) of the selected mutants after ALE in glycerol minimal medium. Every dot in the graph indicates a single isolated mutant.

wild-type (Figure S5.1B). This indicates that the fast-growing mutant SDC.1 carries a high flux through the shikimate pathway towards 4HB biosynthesis.

Genomic characterization of SDC

To elucidate the genetic basis of SDC, we sequenced the genomes and plasmids of the most efficiently evolved strains. We focused solely on isolates that displayed high relative fluorescence. This is because these strains should display a high carbon flux through the shikimate pathway irrespective of the growth rate. From each evolution experiment, we chose ten mutants. At first, we sequenced the biosensor plasmids to check for alterations. However, no mutations occurred in the plasmids of all twenty isolates, indicating that growth occurred solely due to genomic alterations. All isolates from the two individual evolution experiments contained mutations in the *miaA* and *mexT* genes at various positions (Figure 5.5A).

MiaA is a tRNA dimethylallyl transferase and has been known to affect the expression of various genes related to the central and secondary metabolism [20]. In *P. putida* specifically, it was reported that the removal of *miaA*, dramatically increased the expression of the *trpE* and *trpGDC* genes, both involved in tryptophan biosynthesis [21]. MiaA has been further studied in *Pseudomonas chlororaphis*, where its inactivation led to the upregulation of the *trp* genes and *aroF*. The latter encodes a 3-deoxy-7-phosphoheptulonate synthase, which catalyzes the first reaction of the shikimate pathway [22].

The *mexT* gene encodes a transcriptional regulator that has mostly been studied in *Pseudomonas aeruginosa* in which it has been shown to repress the entire quinolone biosynthetic pathway and the first reaction of tryptophan biosynthesis [23]. Another major mutation that occurred in 12 out of the 20 isolates was a perturbation in *garK*, encoding a glycerate kinase. However, as the *garK* perturbation did not occur in all isolates, we deemed this one as non-universal and focused solely on *miaA* and *mexT*. To assess the importance of these mutations, we deleted the *miaA* and *mexT* genes from Δ*pyr* and assessed their growth in glycerol minimal medium. Surprisingly, the removal of the *miaA* gene allowed growth without the need for evolution (Figure 5.5B). The deletion of *mexT* did not result in immediate growth. However, in combination with Δ*miaA*, its deletion led to higher growth rates and a

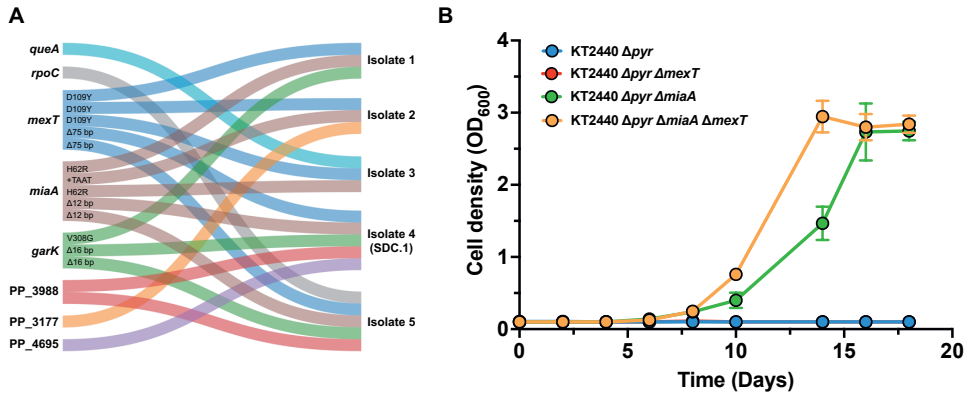

Figure 5.5: Exploring the genetic basis of SDC for further optimization. A) Genomic alterations that were discovered in the five strains with the highest relative fluorescence after laboratory evolution. B) Growth curves of the reverse-engineered strains. The miaA and mexT genes were deleted separately and in combination from Δpyr. Abbreviations: queA, S-adenosylmethionine:tRNA ribosyltransferase-isomerase; rpoC, DNA-directed RNA polymerase subunit beta; mexT, Transcriptional regulator MexT; miaA, tRNA dimethylallyltransferase; garK, glycerate kinase; SDC, shikimate pathway-dependent catabolism. Data points represent the mean value ± SD from three independent experiments.

shorter lag phase than the single Δ*miaA* mutant. As the inactivation of only *miaA* allowed growth in minimal medium with glycerol in Δ*pyr*, we speculate that it is key in regulating the shikimate pathway and could be a potential target for metabolic engineering strategies in other organisms.

Evaluation of metabolic fluxes in SDC

Strain SDC.1 was selected from the heterogeneous mix based on its growth rate and fluorescence profile. Next, we aimed to determine the flux increase through the shikimate pathway of this strain compared to the wild type. Chorismate, the final product of the shikimate pathway, is equimolarly cleaved into 4HB and pyruvate by chorismate pyruvate lyase. Therefore, we set out to quantify 4HB production to evaluate whether SDC.1 uses the shikimate pathway as its main metabolic route for growth. In theory, the higher the yield of 4HB, the more flux is diverted into the shikimate pathway. FBA analysis predicts a maximum pathway yield of 0.39 mol 4HB / mol glycerol. In this scenario, there is no bacterial growth, and all carbon, including the released pyruvate by CHRPL, is directed toward 4HB synthesis. Therefore, we set this as our attainable maximum. To assess 4HB production, we

deleted the *pobA* gene in both the wild type and SDC.1, creating SDC.2. This gene encodes a *p*-hydroxybenzoate hydroxylase and is responsible for the degradation of 4HB to protocatechuate (PCA), which can be further degraded to fuel the TCA cycle. The removal of the *pobA* gene had a negligible effect on wild-type growth. However, growth of SDC.2 was severely stunted, requiring 14 days to reach the stationary phase compared to 4 days for SDC.1 (Figure 5.6A). Moreover, a lower final cell density was observed indicating that SDC.2 metabolism is highly dependent on the activity of the shikimate pathway and that the produced 4HB cannot be recycled back for cell proliferation. The obtained yield for SDC.2 was 0.06 mol 4HB / mol glycerol, a 13.8 – fold increase compared to the wild type Δ*pobA*, confirming a significantly increased carbon flux through the shikimate pathway (Figure 5.6B). However, this flux only comprises 15.4% of the predicted maximum theoretical flux, implying that other routes are still taking a significant portion of the intracellular fluxes.

We focused particularly on the shikimate pathway to further optimize SDC.2. We hypothesized that *quiC*, encoding 3-dehydroshikimate (3HDS) dehydratase, was siphoning off carbon from the shikimate pathway towards the TCA cycle. When growth was simulated for SDC.2, the model predicted that 54% of the flux entering the shikimate pathway is redirected through this reaction, converting the shikimate pathway intermediate 3DHS to PCA, efficiently circumventing the *pobA* deletion. As such, we created SDC.3 by deleting *quiC* from SDC.2 and assessed its growth and 4HB production. It became apparent that this reaction indeed was a major metabolic bypass. The SDC.3 strain displayed even further stunted growth compared to SDC.2, reaching the stationary phase after 10 days with a concomitant significantly lower biomass formation (Figure 5.6A). The final 4HB yield increased 2.4 – fold to 0.14 mol 4HB / mol glycerol (Figure 5.6D), indicating a further increase in the flux through the final reactions of the shikimate pathway.

Although the optimized strain SDC.3 demonstrated increased fluxes through the shikimate pathway, it only reaches 36.7% of the attainable predicted maximum yield. Therefore, we further simulated the SDC metabolism to identify bottlenecks. Our simulations predicted that 19.7% of the total consumed glycerol is excreted as glycerate. As mentioned earlier, 12 out of 20 isolates contained mutations in the

garK gene. The isolated SDC.1 and its derivates contain a 16 bp deletion within the gene resulting in a frameshift. The *garK* gene encodes glycerate kinase, which is responsible for the phosphorylation of glycerate to glycerate-2-phosphate, which can then enter the main metabolism. We hypothesized that the frameshift renders the enzyme inactive and allows glycerate to accumulate. We quantified glycerate production in SDC.3 and confirmed our hypothesis as 18.3% of the total amount of glycerol was excreted as glycerate, decreasing the total carbon flux towards the shikimate pathway (Figure 5.6C).

According to model simulations, pyruvate production from glycerol using SDC only yields 6.1% of ATP compared to the ED pathway (Supplementary Data). Aerobic bacteria like *P. putida* generate most electron carriers in the TCA cycle, which can then feed the electron transport chain and produce ATP through oxidative phosphorylation. However, in the SDC strains, the connection between glycolysis and TCA is disrupted and the TCA cycle can only be reached through the ATP-consuming shikimate pathway. Model predictions show that in native metabolism, glycerol is catabolized to the glycolytic intermediate dihydroxyacetone-P (DHAP) (Figure 5.1). This process costs 1 ATP per glycerol and yields 1 reduced quinone. However, in SDC, the model predicts NAD-dependent oxidation of glycerol to glycerate by AldB-1, PP_2694, or FrmA. Therefore, the activation of the alternative glycerol utilization pathway most likely serves as an additional source of reducing equivalents which can be oxidized in the electron transport chain to generate a proton motive force for additional ATP. In addition, the GarK enzyme also requires the utilization of ATP. Therefore, it is likely that *garK* has mutated to conserve additional ATP. Although the model predicts NAD-dependent oxidation of glycerol to glycerate, the first step in glycerate production from glycerol in *P. putida* is initiated by the PQQ - dependent alcohol dehydrogenases encoded by *pedE* and *pedH* [24]. Like NADH, $PQQH_2$ gets oxidized in the electron transport chain, generating ATP. The ability to generate ATP by converting glycerol into glycerate, therefore, reduces the required SDC-dependent flux towards the TCA cycle.

To abolish glycerate production, we deleted both *pedH* and *pedE* from SDC.3, creating SDC.4. This deletion extended the lag phase slightly but did not have a significant impact on the growth rate (Figure 5.6A). Glycerate production was com-

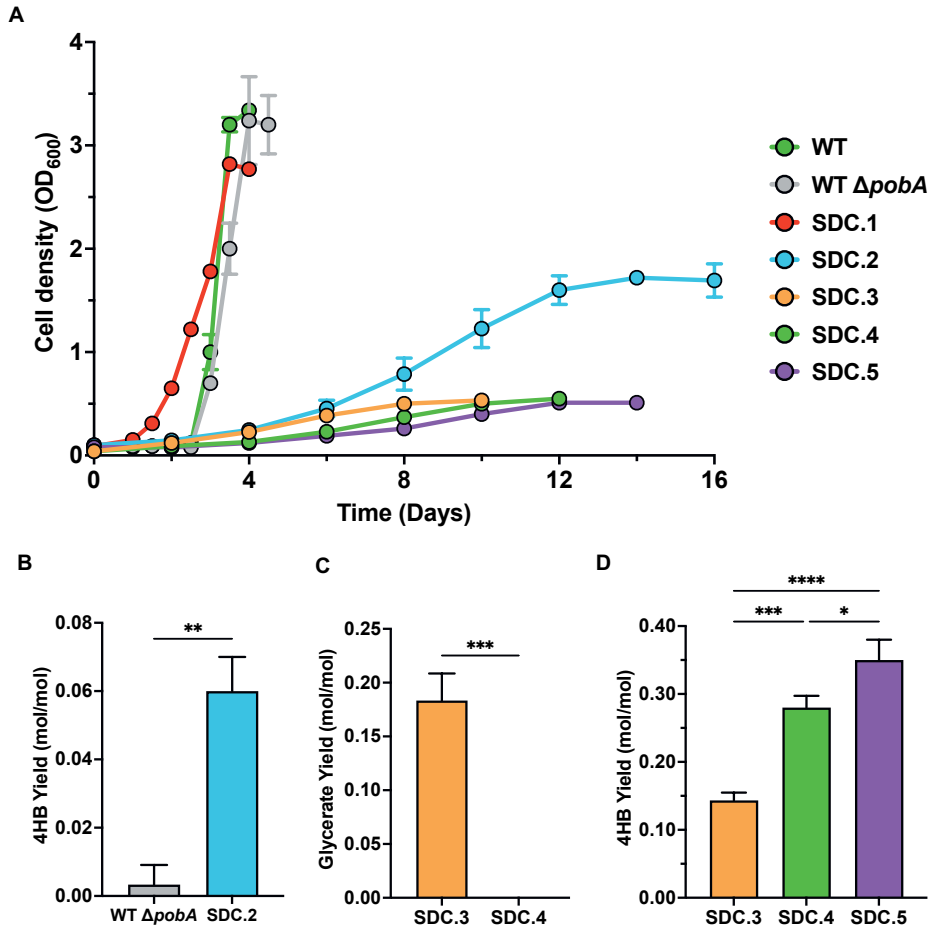

*Figure 5.6: A) Growth curves of the wild-type strain and WT ΔpobA compared to the SDC strains. B) Quantification of 4HB yields in the WT ΔpobA vs SDC.2. C) Quantification of glycerate yields in SDC.3 vs SDC.4. D) Quantification of 4HB yields in SDC.3 vs SDC.4 vs SDC.5. Data points and bar graphs represent the mean value ± SD from three independent experiments. *, p <0.1; **, p <0.01; ***, p <0.001; ****, p <0.0001 determined by an unpaired Student's t-test.*

pletely abolished and revealed to be a major metabolic bottleneck as its removal increased the yield from 0.14 to 0.28 mol 4HB/mol glycerol (Figure 5.6D). This accounts for 71.0% of the maximum predicted pathway yield and indicates that a significant flux in SDC.4 is diverted through the shikimate pathway.

For further optimization, we focused on branching pathways from the shikimate pathway. Within the isolated mutants, we discovered mutations in the genes *miaA* and *mexT* and have previously shown their impact on establishing SDC. Both their

encoded proteins have been reported to directly influence tryptophan biosynthesis by regulating anthranilate synthase (ANS), encoded by *trpE* in *P. putida*. We hypothesized that the SDC.1 strain and its further derivatives may display increased ANS activity due to the mutations in *miaA* and *mexT*. Like CHRPL, the TrpE enzyme cleaves chorismate releasing pyruvate in the process. However, this reaction requires additional L-glutamine or ammonia as an amine donor, which according to our *in-silico* assessment results in lower growth rates (Figure 5.2A). Yet, the removal of this reaction is unwanted as it would render the strain auxotrophic for tryptophan. Therefore, we aimed to reduce its activity by introducing a P290S point mutation in the *trpE* gene of SDC.4. This specific mutation has been reported to lower the activity of the TrpE enzyme [25]. This new strain, termed SDC.5, has a slower growth rate (0.008 ± 0.000 h^{-1}) compared to SDC.4 (0.011 ± 0.000 h^{-1}) yet reached similar final cell densities (Figure 5.6A). However, the 4HB yield increased from 0.28 to 0.35 mol 4HB/mol glycerol (Figure 5.6D). This accounts for 89.2% of the maximum predicted pathway yield and indicates that SDC.5 diverts most of its glycerol metabolism through the shikimate pathway

Genomic integration and characterization of a stable SDC strain

So far, we quantified the flux through the shikimate pathway using 4HB as output. By reaching the predicted maximum, we can conclude that all major bottlenecks are removed and that we successfully established SDC. Therefore, we aimed to produce a stable strain that could serve as a *chassis* for shikimate pathway-derived products. For this purpose, we integrated the feedback resistant $ubiC^{E31Q/M34V}$ gene in SDC.5 under the control of a bicistronic design at the innocuous PP_5322 site [26]. Furthermore, we restored the *pobA* gene to create the final SDC.6 strain in which 4HB can once more fuel biomass production (Figure 5.7A). We determined the growth characteristics of SDC.6 and compared them to the wild type as both strains have different pathways to convert glycerol to pyruvate. Moreover, we used SDC.1 as a second control to examine the impact of all further modifications on growth. As expected, the wild type using the canonical glycerol metabolism grew fast and reached the stationary phase within 24 hours. Our genomically stable SDC.6 strain had a lower specific growth rate than SDC.1, 0.038 ± 0.001 h^{-1} vs 0.052 ± 0.007 h^{-1},

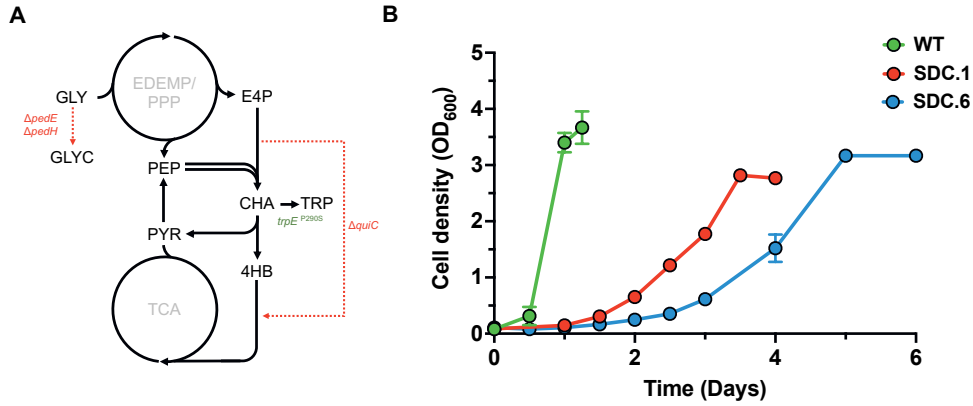

Figure 5.7: A) Graphical representation of the genetic modifications in SDC6. The pedE and pedH genes were deleted to abolish glycerate formation as a byproduct. The quiC gene was deleted to avoid splitting of the shikimate pathway and the P290S point mutation in trpE was introduced to lower fluxes toward tryptophan biosynthesis. B) Growth curves of the wild type (KT2440), the first isolated SDC.1 and optimized SDC.6 strain. Abbreviations: GLY, glycerol; GLYC, glycerate; E4P, erythrose-4-phosphate; PEP phosphoenolpyruvate; PYR, pyruvate; CHA, chorismate; TRP, tryptophan; 4HB, 4-hydroxybenzoate; EDEMP, Entner-Doudoroff-Embden-Meyerhof-Parnas pathway; PPP, pentose phosphate pathway; TCA, tricarboxylic acid cycle. Data points represent the mean value ± SD from three independent experiments.

respectively (Figure 5.7B). We hypothesize that the lower growth rate of SDC.6 is the result of i) the absence of QuiC, which allowed a quick bypass in SDC.1 from the shikimate pathway toward the TCA cycle, ii) the removal of glycerate production, which allowed higher ATP generation, and iii) fewer pyruvate production due to elevated TrpE activity (Figure 5.7A). Although slower, SDC.6 reached a final $OD600$ of 3.17, which is 14.5% higher than SDC.1. This can be attributed to the removal of glycerate formation in SDC.6 which can now be funneled towards biomass production (Figure 5.7A).

However, this removal likely increased the lag phase in SDC.6. The PedE and PedH enzymes are part of the alternative glycerol metabolism in *P. putida* and their removal has been demonstrated to strongly prolong the lag phase [24]. Yet, SDC.6 is still superior to SDC.1 as it is devoid of all the bottlenecks described above and can therefore lead to higher yields for shikimate pathway-derived products. Next, we used the model to calculate the maximum specific growth rate in SDC.6. For this analysis, we set the maximum glycerol uptake rate at 3.95 mmol/g_{CDW}/h, the same as in KT2440. However, the model predicts a lower glycerol uptake rate for

this strain, with a maximum of 3.36 mmol/g_{CDW}/h, probably indicating a limitation in cofactor regeneration. Moreover, the model predicts a maximum specific growth rate of 0.16 h^{-1}, which is 4.2 – fold higher than the actual growth rate we observed. Therefore, there is still room for improvement to establish SDC.6 as a true *chassis* for shikimate pathway-derived products.

Discussion

In this study, we created a new-to-nature shikimate pathway-dependent catabolism in *P. putida*. Based on model simulations and rational engineering, we constructed a growth-coupled scenario. Next, through pyruvate-driven evolution coupled with a biosensor-assisted selection strategy, the superior mutant SDC.1 was isolated. This strain showed a fast growth rate and a high relative fluorescence profile among all isolates. We discovered that SDC.1 displayed a 13.8-fold higher flux through the shikimate pathway than the WT, reaching a 4HB yield of 15.2% of the maximum predicted pathway yield. Through further model-driven and rational engineering, we removed all potential bottlenecks and created SDC.5 which reached 89.2% of the maximum predicted pathway yield, demonstrating a massive catabolic and anabolic flux through the shikimate pathway. By reintroducing 4HB degradation, we established SDC.6, the first strain ever constructed which uses the shikimate pathway as the dominant pathway for glycerol catabolism and therefore growth. Moreover, the SDC.5 strain presented in this study can be equipped with other pyruvate-releasing steps to achieve high yields for valuable molecules such as maleate [27], 3-hydroxybenzoate [28], para-aminobenzoate [29], and salicylate [30].

Growth-coupled bioproduction of shikimate-derived products using pyruvate-releasing reactions has been theorized before [7] and has recently also been proven [30][31]. However, although both strategies were effective, they still relied on the external supplementation of aromatic amino acids and yeast extract, which would substantially increase operating costs. The fact that the carbon flux in these designs could not support growth could potentially be attributed to the complex regulatory network of the shikimate pathway. The shikimate pathway is regulated on differ-

ent levels e.g., transcriptional repression, attenuation, and feedback inhibition [32], which has made traditional metabolic engineering strategies rather challenging. In this study, we showcase that indeed regulation is the biggest bottleneck. The SDC was established due to a small number of mutations that most likely broke the regulatory network of the shikimate pathway. Various genomic alterations were discovered in all sequenced isolates in the genes *miaA* and *mexT*. Both encoded enzymes appear to have a regulatory function regarding the shikimate pathway, yet their exact regulatory mechanism remains elusive. Deletion of *miaA* was able to restore growth without the need for evolution and the subsequent deletion of *mexT* further improved growth rates and reduced lag phases. Therefore, we believe that it is noteworthy to examine these genes as metabolic engineering targets for the shikimate pathway in other industrial organisms.

In this work, FBA analysis was frequently used to support our hypothesis. One noteworthy example is the prediction of glycerate as a by-product. This phenotype was attributed to a 16 bp deletion in SDC.1 in the *garK* gene, encoding a glycerate kinase. This enzyme is responsible for the phosphorylation of glycerate to glycerate-2-phosphate, which can then enter the main metabolism. The production of glycerate from glycerol produces two molecules of $PQQH_2$ [24], which yields two molecules of ATP in the electron transport chain. However, the GarK enzyme requires the usage of one molecule of ATP. As SDC is energetically poor, this deletion likely inactivated the enzyme to conserve ATP, which allowed glycerate to accumulate. Moreover, glycerate production results in the generation of reduced cofactors which can be used for respiration, decreasing the required catabolic flux over the SDC. In general, ATP seems to be the most limiting factor. The final product of SDC is 4HB and pyruvate. The latter can be oxidized in the TCA cycle to generate reducing equivalents or be converted back into PEP. The SDC.5 strain reaches up to 89.2% of the predicted pathway yield. This indicates that the majority of the released pyruvate is recycled back to PEP and reintroduced into the shikimate pathway. However, this step also requires the incorporation of ATP. Although this is efficient for eventual product formation, it does not aid in growth. Therefore, to increase the ATP pool in SDC, external electron donors could be applied to generate NADH, which then can be oxidized in the electron transport chain to provide ATP. Formate is a

formidable candidate, as *P. putida* already encodes a kinetically fast formate dehydrogenase [33]. Another potential electron donor is phosphite, whose potential has recently been explored in *P. putida* [34]. Although its dehydrogenase is kinetically slower than its formate counterpart [35], it was able to increase the NADH pool in *P. putida*. Moreover, compared to formate, phosphite metabolism gives a competitive advantage, allowing non-sterile fermentation conditions, and lowering overall production costs [36]. Therefore, both electron donors are worthy of investigation to further improve the SDC.

To further realize the full potential of the SDC, optimization is an unavoidable challenge. Although the yield is significantly increased, productivity is still limited in SDC.5 and most likely also in SDC.6 upon the overexpression of external pathways. In our current design, the shikimate pathway carries the whole metabolic regime with only a single overexpression. Thus, further optimization of the shikimate pathway would be a necessity to further increase the fluxes. This could either be achieved through genomic overexpression or a second round of laboratory evolution. In our first evolution experiment, we identified *miaA* and *mexT* as key players involved in the shikimate pathway. However, the strain still had many bottlenecks that, although facilitated growth, decreased the shikimate pathway flux. The streamlined SDC.5 strain has a maximized flux through the shikimate pathway where the released pyruvate is the only junction between glycerol catabolism and the TCA cycle. This strain would be an excellent candidate for another round of evolution. Not only would this stringent selection system lead to increased fluxes through the shikimate pathway, but it may also lead to the identification of other unknown bottlenecks.

A second way to optimize the fluxes in SDC is through rational, model-guided engineering. We demonstrated the power of *in-silico* simulations to aid the experimental design, identify metabolic bottlenecks, and guide optimization based on maximum yields and optimal growth rates. Unlike the wild type, our SDC strain has a more complicated glycerol to pyruvate node with many more enzymatic steps that make rational engineering nontrivial. For an optimal flux, a fine balance in erythrose-4-phosphate (E4P) and phosphoenolpyruvate (PEP) is required. We hypothesize that the main limitation of SDC is the availability of E4P, as the PEP pool

is already significantly increased through the blockage of its degradation nodes in the initial Δ*pyr* strain. Like the shikimate pathway, the pentose phosphate pathway is predominantly used for anabolic reactions in *P. putida*, likely displaying low native fluxes [37]. However, to fully realize the potential of metabolic modeling, more information regarding the metabolic fluxes would need to be gathered. Recently, Ling et al., (2022) [38] used an intracellular metabolomic analysis to identify potential bottlenecks for the production of *cis*,*cis*-muconic acid in *P. putida*. They measured the accumulation of intermediates in the EDEMP cycle or shikimate pathway and therefore could analyze the effect of certain genetic overexpressions. This approach could be applied here as well and would yield valuable metabolic information crucial in enhancing the traditional DBTL (design-build-test-learn) cycle, and supporting the often-limiting learning step [39]. All this information could be fed back into the model to further speed up the establishment of a superior SDC strain with high yields and productivity. Moreover, it can identify the rate-limiting steps currently present in SDC.6 to improve growth. Our model predicts a maximum growth rate for 0.16 h^{-1} for SDC.6 compared to 0.235 h^{-1} for the wild-type. The SDC relies solely on the shikimate pathway and requires substantially more enzymes than the native pathway of *P. putida* to reach pyruvate from glycerol. Therefore, more resources need to be allocated towards protein synthesis and growth rates can never reach the level of the wild type. In our current design, we rely on native protein expression levels and only overexpress the *ubiC* gene in addition to establish growth. However, to improve growth, more potential candidates should be expressed. For example, high expression of the pentose phosphate pathway and shikimate pathway could theoretically increase the metabolic flux, but the resource allocation toward protein synthesis will only reduce the growth rate [40]. Therefore, the previously mentioned metabolomic approach can be applied to identify rate-limiting enzymes and select these candidates for overexpression without causing too much protein burden.

This work highlights the plasticity of bacterial metabolism and how a combination of model-driven design, rational engineering, and laboratory evolution can create novel metabolisms. We repurposed the shikimate route as the major catabolic route and demonstrate that it can carry the whole cellular flux for growth.

Moreover, we believe that the SDC strain presented in this study will open many potential practical applications for the high-yield synthesis of industrial valuable aromatic compounds.

Material & Methods

Plasmids, primers, and strains

All strains and plasmids used in the present study are listed in Table S2. Primers used for plasmid construction and gene deletions are listed in Table S3.

Culture conditions and medium

P. putida and *E. coli* cultures were incubated at 30°C and 37°C respectively. For cloning purposes, both strains were propagated in Lysogeny Broth (LB) medium containing 10 g/L NaCl, 10 g/L tryptone, and 5 g/L yeast extract. For the preparation of solid media, 1.5% (w/v) agar was added. Antibiotics, when required, were used at the following concentrations: kanamycin (Km) 50 μg/ml, gentamycin (Gm) 10 μg/ml, chloramphenicol (Cm) 50 μg/ml and apramycin (Apra) 50 μg/ml. All growth experiments were performed using M9 minimal medium (per Liter; 3.88 g K_2HPO_4, 1.63 g NaH_2PO_4, 2.0 g $(NH_4)_2SO_4$, pH 7.0. The M9 media was supplemented with a trace elements solution (per Liter; 10 mg/L ethylenediaminetetraacetic acid (EDTA), 0.1 g/L $MgCl_2 \cdot 6H_2O$, 2 mg/L $ZnSO_4 \cdot 7H_2O$, 1 mg/L $CaCl_2 \cdot 2H_2O$, 5 mg/L $FeSO_4 \cdot 7H_2O$, 0.2 mg/L $Na_2MoO_4 \cdot 2H_2O$, 0.2 mg/L $CuSO_4 \cdot 5H_2O$, 0.4 mg/L $CoCl_2 \cdot 6H_2O$, 1 mg/L $MnCl_2 \cdot 2H_2O$). In these experiments, strains were precultured in 10 ml LB with corresponding antibiotics. Then, the cultures were washed twice in M9 media without a carbon source. Finally, the cultures were diluted to an $OD600$ of 0.1 to start the experiment. Flask experiments were performed in 250 ml Erlenmeyer flasks filled with 25 ml of M9 minimal medium with 40 (SDC characterization) or 200 (ALE experiment) mM glycerol and the cultures were incubated in a rotary shaker at 200 rpm at 30°C.

Cloning procedures

Plasmids were constructed using the standard protocols of the previously described SevaBrick assembly [41]. All DNA fragments were amplified using Q5® Hot Start High-Fidelity DNA Polymerase (New England Biolabs). To construct the plasmids pSensor and pSensorEvo, the 4HB-responsive regulator and promoter (PobR/PpobA) were synthesized by Integrated DNA Technologies (IDT), and the *ubiC*$^{E31Q/M34V}$ was amplified from the genome of *E. coli* with primers to introduce the E31Q and M34V mutations. All parts were integrated into the pSB1C3 repository and subsequently assembled into pSEVAb83 following the standard procedures of the SevaBrick assembly. All plasmids were transformed via heat shock in chemically competent *E. coli* DH5α λ*pir* cells and via electroporation or conjugation in *P. putida* (Thermo Fisher Scientific). Transformants were selected on LB agar plates with corresponding antibiotics and colonies were tested by colony PCR with Phire Hot Start II DNA polymerase (Thermo Fisher Scientific). After extraction, all constructs were verified by Sanger DNA sequencing (MACROGEN Inc.).

Genome modifications

Genomic modifications in this study were performed using the protocol previously described by Wirth et al. (2020)[42]. Homology regions of ± 500 bp were amplified up and downstream of the target gene from the genome of *P. putida* KT2440. Both regions were cloned into the non-replicative pGNW vector and propagated in *E. coli* DH5α λ*pir*. Correct plasmids were transformed into *P. putida* by electroporation and selected on LB + Km plates. Successful co-integrations were verified by PCR. Hereafter, co-integrated strains were transformed with the pQURE6-H, and transformants were plated on LB + Gm containing 2 mM 3-methylbenzoic acid (3-mBz). This compound induces the XylS – dependent Pm promoter, regulating the I-SceI homing nuclease that cuts the integrated pGNW vector. Successful gene deletions were verified by PCR and Sanger sequencing (MACROGEN inc). The P290S modification in *trpE* was verified by MASC PCR as described by Wang & Church, (2011) [43]. Hereafter, the pQURE6-H was cured by removing the selective pressure and its loss was verified by sensitivity to gentamycin.

Analytical methods

Cell growth was determined by measuring the optical density at 600 nm ($OD600$) using an $OD600$ DiluPhotometer spectrophotometer (IMPLEN) or a Synergy plate reader (BioTek Instruments). Analysis of glycerol and pyruvate in supernatants was performed using high-performance liquid chromatography (HPLC) (Thermo Fisher Scientific) equipped with an Aminex HPX-87H column. The mobile phase was 5 mM of H_2SO_4 at a flow rate of 0.6 ml/min, the column temperatures were held at 60 °C and the compounds were detected using a Shodex RI-101 detector (Shodex). The amount of produced 4HB was determined using HPLC (Shimadzu) with a C18 column (4.6 mm × 250 mm) and a UV/vis detector set at 472 nm. The mobile phase consisted of Milli-Q water (A), 100 mM formic acid (B), and acetonitrile (C) with a flow rate of 1 ml/min at 30 °C. Chromatographic separation of analytes was attained using the following gradient program: t = 0 - 5min: A-55%, B-10%, and C-35%; from t = 5 - 10min ramp to A-10%, B-10%, and C-80% and held until 15 min. Then from t = 15 – 16 min, the gradient was returned to A-55%, B-10%, and C-35% and maintained isocratic for a total run time of 18 min. For quantification, calibration curves were prepared using pure standards (99% purity) purchased from Sigma-Aldrich.

Adaptive laboratory evolution

Strain Δ*pyr* was inoculated in two 250 ml shake flasks with M9 minimal medium supplemented with 200 mM glycerol as the sole carbon source and incubated in a rotary shaker at 200 rpm at 30°C. The starting cell density was set at $OD600$ = 0.1 and cells were diluted back to the same $OD600$ after they reached an $OD600$ of >1.0. Evolved strains were selected on M9 agar plates with 40 mM glycerol and characterized in 200 μL of M9 medium with 40 mM glycerol using a Synergy plate reader (BioTek Instruments). Cell density ($OD600$) and GFP fluorescence (excitation 485 nm, emission 512 nm, gain 50) were measured over time using continuous linear shaking (567 cpm, 3mm), and measurements were taken every fifteen minutes. A customized Python script was programmed to calculate the growth rates taking the natural log of the $OD600$ values.

Whole-genome sequencing

The genomic DNA of the evolved mutants was isolated from LB overnight cultures using the GenElute™ Bacterial Genomic DNA Kit (Sigma-Aldrich St. Louis, MO). The extracted DNA was evaluated by gel electrophoresis and quantified by a NanoDrop spectrophotometer (Thermo Fisher Scientific). Samples were sent for Illumina sequencing to Novogene Co. Ltd. (Beijing, China). Raw Illumina reads were trimmed for low quality and adapters with fastp (v0.20.0). Mutations were identified by comparing the reads to the annotated reference genome of *Pseudomonas putida* KT2440 (GCF_000007565.2) using breseq (v0.35.5) [44].

Genome-scale metabolic modeling

Computational analysis was performed using COBRApy (version 0.18.1) and Python (version 3.6, Python Software Foundation). We used iJN1462, the latest developed genome-scale model (GEM) of *P. putida* to rank pyruvate-releasing reactions and to simulate native and SDC metabolism [45]. In all simulations, glycerol was used as the sole carbon source with a maximum uptake rate of 3.95 mmol/g_{CDW}/h [46]. All metabolic reactions able to produce pyruvate in the iJN1462 GEM were evaluated for their capacity to support growth as the sole pyruvate source. The upper and lower bounds of all pyruvate-releasing reactions were constrained to zero except for two essential reactions: ANS2 (*trpE*, *pabA*) and ADCL (*pabC*). Iteratively, the flux through each reaction was unconstrained making it the main available source of pyruvate in the model. The growth rate, represented by the BIOMASS_KT2440_WT3 reaction, was maximized. Reactions were ranked according to the predicted maximum growth rates relative to the wild-type growth rate (100%). iJN1462 was modified to correctly simulate SDC and wild-type metabolism (Table S4) [47]. When simulating SDC, a pFBA-like constraint was applied such that the sum of all the predicted fluxes cannot exceed the sum of all predicted fluxes in native metabolism. Besides, as a base for SDC simulation, we constrained to zero the flux through reactions EDD, PYK, AGPOP, ME2, OAAFC, SERD_L, CYSTL, CYSDS, MCITL2, LDH_2, and LDH_D2 to reproduce the result of the biosensor-assisted ALE that made CHRPL the main pyruvate source. Model modifications that allowed the simulation of the different SDC strains are presented in Table S5. Maximum theoretical 4HB yields were calculated

maximizing the 4HB exchange reaction (EX_4hbz_e). The optimal metabolism of the SDC strains and their maximum growth rates were simulated maximizing biomass production (BIOMASS_KT2440_WT3).

Statistical analysis

All reported experiments are derived from independent biological replicates. Figures represent the mean values of corresponding biological triplicates and the standard deviation. The level of significance of the difference when comparing results was evaluated by an unpaired Student's t-test

Author contributions

C.B conceived this study. C.B and L.B designed the study. C.B, L.B, K.K and J.J.D conducted the experiments. S.M.P conducted the computations. V.A.P.M.d.S. and R.A.W supervised this study. V.A.P.M.d.S. arranged funding.

Conflict of interest

The authors declare there are no conflicting interests.

Supplementary Data

Energy generation by SDC

We calculated overall equations from glycerol to pyruvate to study the feasibility of SDC in terms of its ability to generate reduced cofactors and ATP compared to native metabolism. Native and SDC metabolism were simulated with flux balance analysis (FBA) with pyruvate production (EX_pyr_e) as maximization objective. Then, reduced models were generated containing only predicted active reactions of central carbon metabolism (Table S5.1), as well as exchange reactions for nadh_c, nadph_c, atp_c, nad_c, nadp_c, pyr_c, h_c, h2o_c, q8_c, q8h2_c, o2_c, coa_c, co2_c, and pi_c. To find the most efficient overall reaction in terms of ATP generation, pyruvate exchange was set as the objective to maximize and the bounds of its exchange reaction were constrained to the optimal value. Then, the ATP exchange reaction was set as a new objective to maximize. A glycerol uptake of 1 mmol/g_{CDW}/h was used and the fluxes through the different exchange reactions are defined as coefficients in the overall equations. According to iJN1462 oxidation of NADH via NADH dehydrogenase (reaction NADH16pp) allows the export of 3 H^+ to the periplasm. The reduction of ubiquinone-8 (q8) to ubiquinol (q8h2), and oxidation of q8h2 by cytochrome oxidase (CYTVo3_4pp) allows the export of 4 H^+ to the periplasm. Generation of ATP by the ATP synthase (ATPS4rpp) requires the import of 4 H^+ from the cytoplasm resulting in a yield of 1 ATP per oxidation of 1 q8h2 and 1.75 ATP per oxidation of NADH.

Overall equation native metabolism (KT2440):

1 Glycerol + 1 Q_8 + 1 NAD^+ + 1 ATP + Pi –> 1 PYR + 1 Q_8H_2 + 1 NADH + H^+ + 2 ATP

Simplified equation (conversion of reduced cofactors to ATP in the respiratory chain):

1 Glycerol –> 1 PYR + 3.75 ATP

Overall equation SDC:

1 Glycerol + 1.8 Q_8 + 1.4 NAD^+ + 1.1 NADPH + 1.1 O_2 + 2.1 ATP + 1.3 H_2O –> 0.55 PYR + 1.8 Q_8H_2 + 1.4 NADH + 1.4 CO_2 + 2.1 ADP + 2.1 Pi + 2.9 H^+

Simplified equation (assuming conversion of NADH to NADPH and generation of ATP by oxidation of reduced cofactors in the respiratory chain):

1 Glycerol + 1.1 O_2 –> 0.55 PYR + 1.4 CO_2 + 0.23 ATP

Note: the O_2 in this equation is not used in the respiratory chain but in the first two reactions converting 4HB into TCA intermediates.

Supplementary material

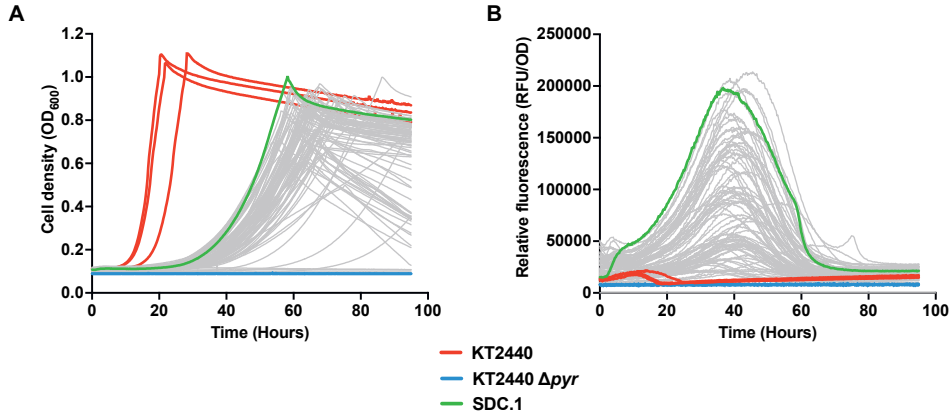

Figure S5.1: Characterization of isolated mutants after adaptive laboratory evolution. A) Growth curves of selected mutants after ALE in glycerol minimal medium. B) Relative fluorescence profiles of the selected mutants after ALE in glycerol minimal medium. All strains in the depicted graphs are equipped with the 4HB responsive biosensor, and the evolved mutants were compared to the wild type (red) and the parental Δpyr strain (blue). Every line indicates a single strain

The rest of the supplementary material of this chapter, including Supplementary Tables S1 to S5, can be accessed *via*:

https://figshare.com/s/58b42e88689c5dbfa3c1

Bibliography

1. Yu, T., Liu, Q., Wang, X., *et al.* Metabolic reconfiguration enables synthetic reductive metabolism in yeast. *Nature Metabolism* **4** (2022).
2. Noor, E., Eden, E., Milo, R., *et al.* Central Carbon Metabolism as a Minimal Biochemical Walk between Precursors for Biomass and Energy. *Molecular Cell* **39,** 809–820 (2010).
3. Stephanopoulos, G. & Vallino, J. J. Network Rigidity and Metabolic Engineering in Metabolite Overproduction. *Science* **252,** 1675 (1991).
4. Staffas, L., Gustavsson, M. & McCormick, K. Strategies and policies for the bioeconomy and bio-based economy: An analysis of official national approaches. *Sustainability (Switzerland)* **5,** 2751–2769 (2013).
5. Nielsen, J. & Keasling, J. D. Engineering Cellular Metabolism. *Cell* **164,** 1185–1197 (2016).
6. Orsi, E., Claassens, N. J., Nikel, P. I., *et al.* Optimizing microbial networks through metabolic bypasses. *Biotechnology advances* **60,** 108035 (2022).
7. Averesch, N. J. & Krömer, J. O. Metabolic engineering of the shikimate pathway for production of aromatics and derived compounds-Present and future strain construction strategies. *Frontiers in Bioengineering and Biotechnology* **6** (2018).
8. Fujiwara, R., Noda, S., Tanaka, T., *et al.* Metabolic engineering of Escherichia coli for shikimate pathway derivative production from glucose–xylose co-substrate. *Nature Communications* **11,** 1–7 (2020).
9. Li, Z., Wang, H., Ding, D., *et al.* Metabolic engineering of Escherichia coli for production of chemicals derived from the shikimate pathway. *Journal of Industrial Microbiology and Biotechnology* **47,** 525–535 (2020).
10. Braga, A. & Faria, N. Bioprocess Optimization for the Production of Aromatic Compounds With Metabolically Engineered Hosts: Recent Developments and Future Challenges. *Frontiers in Bioengineering and Biotechnology* **8** (2020).
11. Kim, S., Lindner, S. N., Aslan, S., *et al.* Growth of E. coli on formate and methanol via the reductive glycine pathway. *Nature Chemical Biology* **16,** 538–545 (2020).
12. Nielsen, J. R., Weusthuis, R. A. & Huang, W. E. Growth-coupled enzyme engineering through manipulation of redox cofactor regeneration. *Biotechnology Advances* **63,** 108102 (2023).
13. Orsi, E., Claassens, N. J., Nikel, P. I., *et al.* Growth-coupled selection of synthetic modules to accelerate cell factory development. *Nature Communications* **12,** 1–5 (2021).
14. Yu, T., Zhou, Y. J., Huang, M., *et al.* Reprogramming Yeast Metabolism from Alcoholic Fermentation to Lipogenesis. *Cell* **174,** 1549–1558 (2018).
15. Gleizer, S., Ben-Nissan, R., Bar-On, Y. M., *et al.* Conversion of Escherichia coli to Generate All Biomass Carbon from CO2. *Cell* **179,** 1255–1263 (2019).
16. Chen, F. Y., Jung, H. W., Tsuei, C. Y., *et al.* Converting Escherichia coli to a Synthetic Methylotroph Growing Solely on Methanol. *Cell* **182,** 933–946 (2020).
17. Iacometti, C., Marx, K., Hönick, M., *et al.* Activating Silent Glycolysis Bypasses in Escherichia coli. *BioDesign Research* **2022,** 1–17 (2022).
18. Wu, Y., Jameel, A., Xing, X. H., *et al.* Advanced strategies and tools to facilitate and streamline microbial adaptive laboratory evolution. *Trends in Biotechnology* **40,** 38–59 (2022).
19. Jha, R. K., Narayanan, N., Pandey, N., *et al.* Sensor-Enabled Alleviation of Product Inhibition in Chorismate Pyruvate-Lyase. *ACS Synthetic Biology* **8,** 775–786 (2019).
20. Koshla, O., Yushchuk, O., Ostash, I., *et al.* Gene miaA for post-transcriptional modification of tRNAXXA is important for morphological and metabolic differentiation in Streptomyces. *Molecular Microbiology* **112,** 249–265 (2019).

21. Olekhnovich, I. & Gussin, G. N. Effects of mutations in the Pseudomonas putida miaA gene: Regulation of the trpE and trpGDC operons in P. putida by attenuation. *Journal of Bacteriology* **183,** 3256–3260 (2001).

22. Yu, J. M., Wang, D., Pierson, L. S., *et al.* Disruption of MiaA provides insights into the regulation of phenazine biosynthesis under suboptimal growth conditions in Pseudomonas chlororaphis 30-84. *Microbiology (United Kingdom)* **163,** 94–108 (2017).

23. Tian, Z. X., Fargier, E., Mac Aogáin, M., *et al.* Transcriptome profiling defines a novel regulon modulated by the LysR-type transcriptional regulator MexT in Pseudomonas aeruginosa. *Nucleic Acids Research* **37,** 7546–7559 (2009).

24. Wehrmann, M., Toussaint, M., Pfannstiel, J., *et al.* The cellular response to lanthanum is substrate specific and reveals a novel route for glycerol metabolism in pseudomonas putida kt2440. *mBio* **11,** 1–14 (2020).

25. Lenzen, C., Wynands, B., Otto, M., *et al.* High-yield production of 4-hydroxybenzoate from glucose or glycerol by an engineered Pseudomonas taiwanensis VLB120. *Frontiers in Bioengineering and Biotechnology* **7,** 1–17 (2019).

26. Chaves, J. E., Wilton, R., Gao, Y., *et al.* Evaluation of chromosomal insertion loci in the Pseudomonas putida KT2440 genome for predictable biosystems design. *Metabolic Engineering Communications* **11,** e00139 (2020).

27. Noda, S., Shirai, T., Mori, Y., *et al.* Engineering a synthetic pathway for maleate in Escherichia coli. *Nature Communications* **8,** 1–7 (2017).

28. Zhou, Y., Li, Z., Wang, X., *et al.* Establishing microbial co-cultures for 3-hydroxybenzoic acid biosynthesis on glycerol. *Engineering in Life Sciences* **19,** 389–395 (2019).

29. Averesch, N. J. & Rothschild, L. J. Metabolic engineering of Bacillus subtilis for production of para-aminobenzoic acid – unexpected importance of carbon source is an advantage for space application. *Microbial Biotechnology* **12,** 703–714 (2019).

30. Noda, S., Mori, Y., Fujiwara, R., *et al.* Reprogramming Escherichia coli pyruvate-forming reaction towards chorismate derivatives production. *Metabolic Engineering* **67,** 1–10 (2021).

31. Wang, J., Zhang, R., Zhang, Y., *et al.* Developing a pyruvate-driven metabolic scenario for growth-coupled microbial production. *Metabolic Engineering* **55,** 191–200 (2019).

32. Li, M., Liu, C., Yang, J., *et al.* Common problems associated with the microbial productions of aromatic compounds and corresponding metabolic engineering strategies. *Biotechnology Advances* **41,** 107548 (2020).

33. Zobel, S., Kuepper, J., Ebert, B., *et al.* Metabolic response of Pseudomonas putida to increased NADH regeneration rates. *Engineering in Life Sciences* **17,** 47–57 (2017).

34. Asin-Garcia, E., Batianis, C., Li, Y., *et al.* Phosphite synthetic auxotrophy as an effective biocontainment strategy for the industrial chassis Pseudomonas putida. *Microbial Cell Factories* **21,** 1–17 (2022).

35. Claassens, N. J., Sánchez-Andrea, I., Sousa, D. Z., *et al.* Towards sustainable feedstocks: A guide to electron donors for microbial carbon fixation. *Current Opinion in Biotechnology* **50,** 195–205 (2018).

36. Shaw, A. J., Lam, F. H., Hamilton, M., *et al.* Metabolic engineering of microbial competitive advantage for industrial fermentation processes. *Science* **353,** 583–586 (2016).

37. Elmore, J. R., Dexter, G. N., Salvachúa, D., *et al.* Engineered Pseudomonas putida simultaneously catabolizes five major components of corn stover lignocellulose: Glucose, xylose, arabinose, p-coumaric acid, and acetic acid. *Metabolic Engineering* **62,** 62–71 (2020).

38. Ling, C., Peabody, G. L., Salvachúa, D., *et al.* Muconic acid production from glucose and xylose in Pseudomonas putida via evolution and metabolic engineering. *Nature communications* **13,** 4925 (2022).

39. Shimizu, H. & Toya, Y. Recent advances in metabolic engineering–integration of in silico design and experimental analysis of metabolic pathways. *Journal of Bioscience and Bioengineering* **132,** 429–436 (2021).

40. Baldazzi, V., Ropers, D., Gouze, J.-L., *et al.* Resource allocation accounts for the large variability of rate-yield phenotypes across bacterial strains (2023).

41. Damalas, S. G., Batianis, C., Martin-Pascual, M., *et al.* SEVA 3.1: enabling interoperability of DNA assembly among the SEVA, BioBricks and Type IIS restriction enzyme standards. *Microbial Biotechnology* **13,** 1793–1806 (2020).

42. Wirth, N. T., Kozaeva, E. & Nikel, P. I. Accelerated genome engineering of Pseudomonas putida by I-SceI—mediated recombination and CRISPR-Cas9 counterselection. *Microbial Biotechnology* **13,** 233–249 (2020).

43. Wang, H. H. & Church, G. M. *Multiplexed genome engineering and genotyping methods: Applications for synthetic biology and metabolic engineering* 1st ed., 409–426 (2011).

44. Barrick, J. E., Colburn, G., Deatherage, D. E., *et al.* Identifying structural variation in haploid microbial genomes from short-read resequencing data using breseq. *BMC Genomics* **15,** 1–17 (2014).

45. Nogales, J., Mueller, J., Gudmundsson, S., *et al.* High-quality genome-scale metabolic modelling of Pseudomonas putida highlights its broad metabolic capabilities. *Environmental Microbiology* **22,** 255–269 (2020).

46. Nikel, P. I., Kim, J. & de Lorenzo, V. Metabolic and regulatory rearrangements underlying glycerol metabolism in Pseudomonas putidaKT2440. *Environmental Microbiology* **16,** 239–254 (2014).

47. Batianis, C., van rosmalen, R., Major, M., *et al.* A tunable metabolic valve for precise growth control and increased product formation in Pseudomonas putida. *Metabolic Engineering,* 118159 (2022).

CHAPTER 6

Establishing microbial production of anisole

Lyon Bruinsma, Christos Batianis, Vitor A. P. Martins dos Santos

Abstract

Anisole is extensively used for the manufacturing of a plethora of industrial products. However, its production is currently only limited to petroleum-based processes. Here, we report, for the first time, the microbial production of anisole by a metabolically engineered *Pseudomonas putida* strain. First, we establish anisole production through a modular approach, first from phenol, then 4-hydroxybenzoate, and at last glucose. Second, we employed a growth-coupled selection design based on the proteinogenic amino acids cysteine and methionine. Using this selection system, we converted a chavicol *O*-methyltransferase to display significantly better kinetics toward phenol as a substrate. The metabolic engineering strategies presented here will be useful to enable a switch on the production of anisole from a chemical to a sustainable biological one.

Introduction

The vast majority of industrially valuable chemicals are produced through chemical synthesis. Although efficient, many compounds needed for this synthesis are still petroleum derived. This approach is highly unsustainable and comes with many environmental issues [1]. Therefore, sustainable alternative synthesis methods are desired. In recent years, microbial cell factories have gained considerable interest in the biobased production of chemicals [2]. Microorganisms can use renewable start materials and are more selective, efficient and less environmentally hazardous compared to traditional chemical synthesis [3]. For this reason, microbial cell factories, such as *Escherichia coli*, *Saccharomyces cerevisiae* and *Pseudomonas putida* are constantly being metabolically expanded to produce chemicals non-native to the host [4][5][6]. Although promising, the use of microbial cell factories is often limited to the known biochemical space, whereas many industrially relevant compounds can still be produced only through chemical synthesis. However, many relevant compounds are only a single reaction step away from a known biological or bioactive compound [7].

Recently, underground metabolism has been highlighted as a way to establish novel metabolic pathways [3]. It relies on the promiscuous activity of enzymes, which can be explored to establish novel biochemistries. Although many chemical processes could be turned biological, often no enzymes are known for their conversion. To bridge this knowledge gap, retrosynthesis has been established as a means to identify novel biosynthetic pathways [8]. These methods rely on enzymatic reaction rules, which describe the pattern of the reactive sites of compounds that are recognized by promiscuous enzymes [9]. In this way, retrosynthesis can predict novel biosynthetic pathways for uncommon or new-to-nature compounds, moving them from the chemical to the biological space.

In this study, we focus on transplanting anisole toward the biological space. Anisole is an aromatic ether found in certain plants where it contributes to floral scents [10] and it is also a key industrial intermediate product in the manufacturing of perfumes, dyes, drugs, fabric softeners, pesticides, water treatment and photographic chemicals [11]. Anisole is usually synthesized by liquid phase processes in an alkaline environment [12]. However, these processes have become restricted

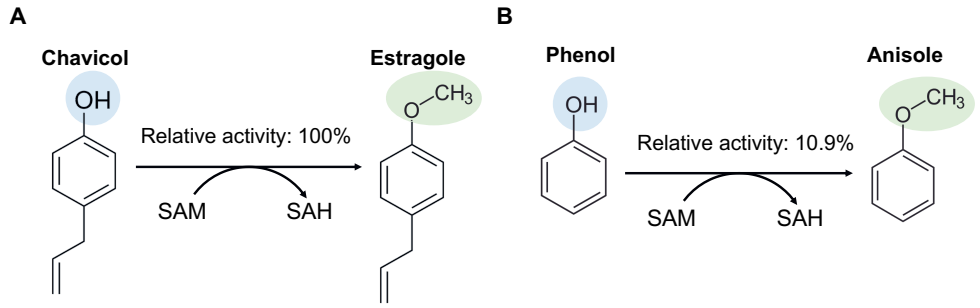

Figure 6.1: Figure 1 Enzymatic conversion by CVOMT1 from Ocimum basilicum. A) Native chavicol O-methyltransferase activity of CVOMT1 converting chavicol to estragole. B) Low promiscuous activity of CVOMT1 converting phenol to anisole. Relative activities are derived from Gang et al., (2002)[14].

in recent years, as the alkali are harmful to the environment. Moreover, the raw chemicals used in these processes are extremely toxic and dangerous to human health [11]. Currently, a greener method is used in which anisole is synthesized by vapour phase methylation. However, apart from anisole, this can lead to impurities by creating side products such as *o*-cresol, *p*-cresol and *p*-xylene [12]. Moreover, in this process, phenol is the used substrate and is predominantly still produced from petroleum-derived feedstocks [13]. Therefore, a more efficient and cleaner process is desirable.

According to Axelrod & Daly (1968) [15] , anisole can be biologically produced from phenol by the enzyme phenol *O*-methyltransferase (EC 2.1.1.25). Although this enzyme is known to be present in mammals, currently no coding sequence is known [15]. In a previous study by Pham et al, (2020) [16] the Selenzyme tool was deployed to search for promiscuous enzymes that could act as a phenol *O*-methyltransferase. Using this approach, they discovered the CVOMT1 enzyme from *Ocimum basilicum* [14]. CVOMT1 is a chavicol *O*-methyltransferase (EC 2.1.1.146) which transfers the methyl group from S-adenosyl-L-methionine (SAM) to the hydroxyl group on the benzene ring of chavicol, producing estragole. However, this enzyme was reported to display low activity towards phenol as a substrate (10.7% relative activity in enzymatic assays compared to chavicol: 100%) (Figure 6.1). Although phenol was tested as a substrate, the production of anisole was not described by CVOMT1. Yet, since the reaction centres and cofactors used by CVOMT1

and phenol *O*-methyltransferase are similar, we hypothesized that anisole is the produced product.

In this study, we established, for the first time, biological anisole production in a microbial cell factory. We followed a modular engineering approach to establish anisole production using glucose as the sole feedstock. In addition, we constructed a growth-coupled selection system to optimize the kinetic parameters of CVOMT1 towards phenol as a substrate. Using this system, we created a new significantly more efficient variant with a higher affinity towards phenol, laying the foundation to create a kinetically fast phenol *O*-methyltransferase enzyme for the bioproduction of anisole. Overall, this work demonstrates the power of microbial cell factories to replace fully chemical processes with biological ones.

Results

Pseudomonas putida is a robust host to produce aromatics compounds

The production of aromatic compounds often comes with unwanted toxicity. One way of circumventing this is the utilization of microbial hosts with high tolerance towards aromatic compounds [17]. *P. putida* KT2440 is generally regarded as an excellent candidate, due to its inherent high tolerance to a range of toxic compounds including aromatics [18]. It is known to reconfigure its metabolic fluxes resulting in a significant surplus of NADPH as a response to combat oxidative stress [19]. Phenol is a highly toxic chemical, and its presence generally poses a burden on the microbial vitality [20][21]. For anisole, as far as we know, there is no data yet regarding its microbial toxicity. Therefore, we subjected *P. putida* KT2440 to different phenol and anisole concentrations to examine the tolerance of the strain towards these two aromatics. The strain was able to withstand up to 5 mM of phenol (Figure 6.2A). Growth rates did not deviate up to 2 mM of phenol and even reached a higher cell density. However, at concentrations of 3 mM and above, phenol starts to have a detrimental effect, affecting growth rate and final cell density (Figure 6.2A). On the contrary, the presence of anisole did not show any detrimental effects on growth (Figure 6.2B). The presence of phenolic hydroxyl groups has been associated with the inhibition of microbial enzymes and the damage of the bacterial membrane

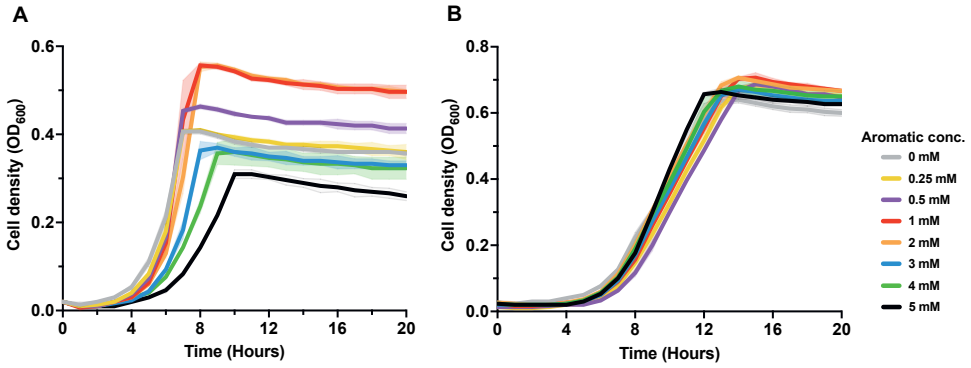

Figure 6.2: Toxicity analyses. A) Growth curves of P. putida KT2440 subjected to different phenol concentrations. B) Growth curves of P. putida KT2440 subjected to different anisole concentrations. Growth curves represent the mean value ± SD from three independent experiments.

[22]. Since the hydroxyl group of phenol is replaced by a methyl group in anisole, the unwanted side effects might not exist.

Testing CVOMT1 for anisole production

To examine the potential of CVOMT1 to establish anisole production, we codon-optimized the *cvomt1* gene and placed it on a pSEVA23b backbone. We transformed *P. putida* KT2440 with this plasmid or an empty vector and fed the strains 50 mM glucose and 1 mM of phenol to determine anisole production. The empty vector control consumed 0.01 mM phenol after 24 hours, whereas CVOMT1 consumed 0.12 mM phenol (Figure 6.3B). Although we detect that CVOMT1 uses phenol as a substrate, no anisole was detected in the samples. For the efficient conversion of phenol to anisole, SAM is required as a cofactor. We hypothesized that its availability might be limited, hampering the conversion of phenol. To increase SAM availability, we added 1 mM methionine to the media, the direct precursor to SAM biosynthesis (Figure 6.3A). We observed that this drastically improved phenol consumption and were finally able to detect anisole production (Figure 6.3C). However, anisole yielded only 15.5% mol/mol of the converted phenol. Anisole is a volatile compound and most likely abiotically escapes the culture media. To examine this, we cultivated overnight three flasks containing 2 mM anisole in M9 minimal media. We observed that the anisole indeed escaped the media, as 89% of the anisole disap-

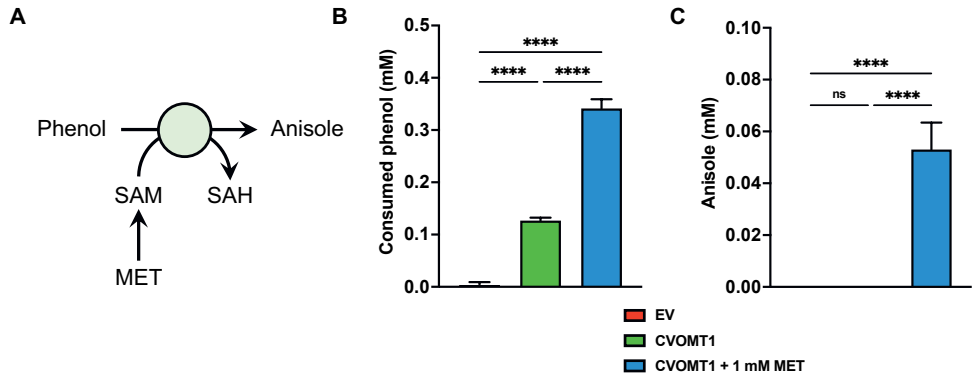

*Figure 6.3: Anisole production by CVOMT1. A) Schematical representation of phenol O-methyltransferase activity by CVOMT1. B) Phenol consumption in 24 hours. C) Anisole production after 24 hours. Abbreviations: (SAM), S-adenosyl-l-methionine, (SAH), S-adenosyl-L-homocysteine, (MET), methionine, (EV), empty vector. Data points and bar graphs represent the mean value ± SD from three independent experiments. ****, p <0.0001 determined by an unpaired Student's t-test.*

peared overnight (Figure S6.1). Unfortunately, current strategies to capture anisole from fermentation broth are not yet known and require further research.

Establishing anisole production from glucose

To achieve anisole production from glucose, we first attempted to establish phenol production. Phenol is predominantly produced by two different reactions which both derive from the shikimate pathway. The first reaction is performed by tyrosine phenol-lyase, in which tyrosine is cleaved to pyruvate, phenol, and ammonia. The second reaction produces phenol through the decarboxylation of 4-hydroxybenzoate (4HB). We performed flux balance analysis (FBA) to determine which pathway would obtain higher yields. Our analysis indicated that anisole production through tyrosine would obtain a slightly higher yield than through 4HB: 0.534 compared to 0.531 mol/mol glucose, respectively. However, tyrosine production contains more enzymatic steps and its biosynthesis is tightly regulated [23]. Moreover, the tyrosine phenol-lyase is feedback inhibited by phenol, which would further limit anisole production [17]. Therefore, we chose the 4HB variant to establish phenol production. We attempted to clone the *BscBCD* operon from *Bacillus subtilis*, which encodes a 4HB decarboxylase complex [24]. However, as phenol

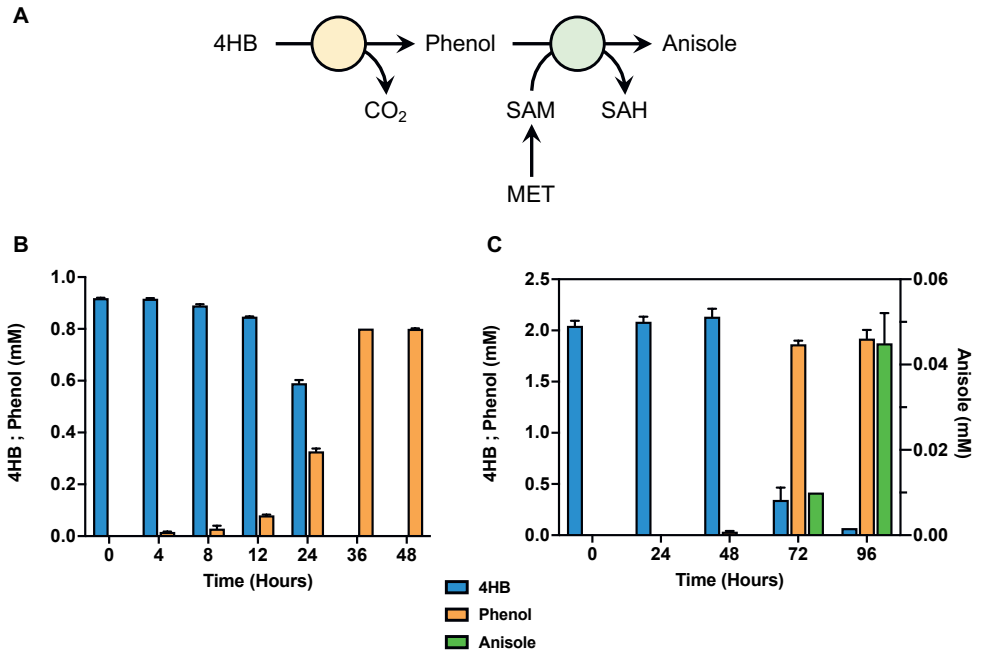

Figure 6.4: Anisole production from 4-hydroxybenzoate. A) Schematical representation of anisole production from 4HB. Phenol is produced by the 4HB decarboxylase from Bacillus subtilis. Anisole is produced by the chavicol O-methyltransferase from Ocimum basilicum. B) Phenol production from 4HB over the course of two days. C) Anisole production from 4HB over the course of four days. Abbreviations: (4HB), 4-hydroxybenzoate, CO_2, (carbon dioxide), (SAM), S-adenosyl-l-methionine, (SAH), S-adenosyl-L-homocysteine, (MET), methionine. Bar graphs represent the mean value ± SD from three independent experiments.

production is quite toxic, plasmid-born expression of the operon was unsuccessful. Therefore, we created a genomic landing pad based on the Cre/*lox* system. To allow high transcription levels similar to plasmid-borne expression, we integrated the T7-RNA polymerase and its depending promoter in the landing pad. We integrated the landing pad in KT2440 Δ*pobA* to assess phenol production. The *pobA* gene encodes a *p*-hydroxybenzoate hydroxylase which is responsible for 4HB degradation to protocatechuate (PCA). Therefore, in this setup, 4HB cannot be degraded and can only be converted towards phenol. We supplemented the strain with 50 mM glucose and 1 mM 4HB and measured phenol production over time.

Although we observed a hard restraint on growth and 4HB conversion, most likely attributed to the toxicity of phenol, all 4HB was converted to phenol over the course of 2 days (Figure 6.4B). With phenol production established, we aimed to

produce anisole using 4HB as the precursor. We cloned the *cvomt1* gene and the 4HB decarboxylase in the same plasmid and transformed this into KT2440 Δ*pobA*. Although the construction of the previous phenol module on a plasmid was unsuccessful due to phenol toxicity, we did not observe this for this anisole module. It is most likely that CVOMT1 is detoxifying the intracellular phenol towards the less toxic anisole, allowing plasmid-born expression. We grew KT2440 Δ*pobA* in 50 mM glucose supplemented with 2 mM of 4HB and methionine. The strains started to consume 4HB after 48 hours and within 24 hours the majority was converted towards phenol with minor production of anisole (0.01 mM). After 96 hours, almost all 4HB was converted towards phenol. However, a fraction of anisole could be detected (0.045 mM), demonstrating the successful production of anisole from 4HB as the precursor (Figure 6.4C).

After demonstrating the successful conversion of 4HB to phenol and anisole, we aimed to establish 4HB production from glucose. The production of 4HB is catalyzed by the enzyme chorismate pyruvate lyase, which cleaves chorismate equimolarly into 4HB and pyruvate. To establish 4HB production, we took the feedback-resistant gene ($ubiC^{E31Q/M34V}$) from *E. coli* [25]. To push the flux in the shikimate pathway, we added the feedback-resistant $aroG^{D146N}$ gene from *E. coli* and cloned both genes on a pSEVAb23 vector. To further enhance the flux through the shikimate pathway, we deleted the *quiC* gene in KT2440 Δ*pobA*, which encodes a 3-dehydroshikimate (3DHS) dehydratase (Figure 6.5A). This enzyme converts the shikimate pathway intermediate 3DHS to PCA, diverting the flux away from 4HB production. We grew this strain with 50 mM glucose and measured 4HB production. Although produced, the 4HB yield was rather low (0.035 mol 4HB / mol glucose) (Figure 6.5B). We hypothesized that there might be a precursor limitation. The shikimate pathway requires one mole of erythrose-4-phosphate (E4P) and two moles of phosphoenolpyruvate (PEP) to synthesize chorismate, the final product and precursor to 4HB. To increase PEP availability, we first deleted the gene *pykA*. This gene encodes a pyruvate kinase, which cleaves PEP to pyruvate (Figure 6.5A). This was deemed effective as we measured a yield of 0.057 mol/mol, an increase of 63,4%. To further increase the PEP pool, we deleted the *ppc* gene encoding a phosphoenolpyruvate carboxylase, which converts PEP to oxaloacetate. However, this deletion did not further increase

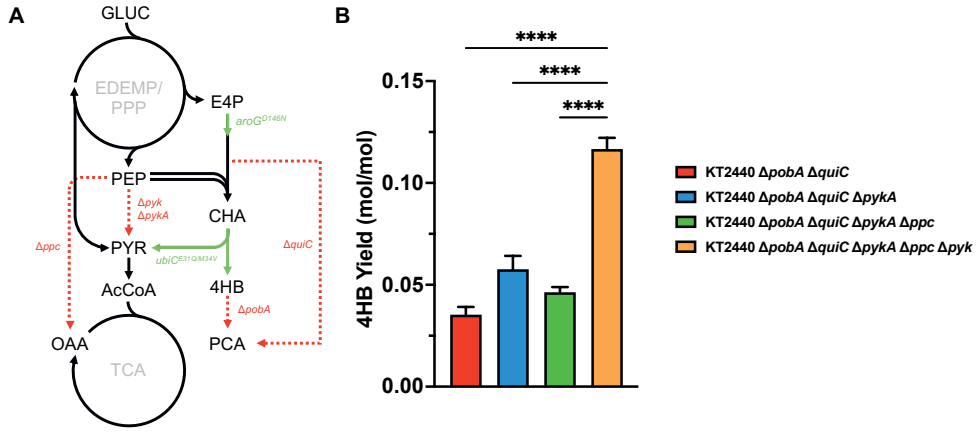

Figure 6.5: 4-Hydroxybenzoate production from glucose. A) Schematical representation of the 4HB production pathway in P. putida KT2440. Mutations are denoted by the red square dotted arrows. Overexpressed genes are denoted by green arrows. B) Aromatic yields detected during 4HB production from glucose. Abbreviations: (GLUC), glucose, (E4P), erythrose-4-phosphate, (PEP) phosphoenolpyruvate, (CHA), chorismate, (PYR), pyruvate, (4HB), 4-hydroxybenzoate, (PCA), protocatechuate, (AcCoA), acetyl-CoA, (OAA), oxaloacetate. Bar graphs represent the mean value ± SD from three independent experiments.

yield and rather reduced it. At last, we deleted the gene *pyk*, the second isoenzyme for pyruvate kinase. This deletion completely decouples all metabolic nodes from PEP, leaving the shikimate pathway as the sole entry point. As expected, this was deemed the most effective, yielding 0.116 mol/mol, an increase of 232,6% compared to KT2440 Δ*pobA* Δ*quiC* strain.

So far, we demonstrated that we can produce anisole from 4HB as a precursor. In addition, 4HB production from glucose was established. Therefore, we aimed to connect these two modules and produce anisole from glucose as the sole carbon source. We combined the $aroG^{D146N}$ and $ubiC^{E31Q/M34V}$ genes from *E. coli*, the *BscBCD* operon from *B. subtilis* and the *cvomt1* gene from *O. basilicum* on a pSEVAb23 vector (Figure 6.6A). For the production experiment, the highest 4HB-producing strain KT2440 Δ*pobA* Δ*quiC* Δ*pyk* Δ*pykA* Δ*ppc* was selected. We equipped this strain with the anisole production plasmid and grew it in minimal media containing 50 mM glucose and 2 mM methionine to increase the intracellular SAM pool. This strain produced 0.067 mM anisole, showcasing biological anisole production from glucose as a feedstock (Figure 6.6B). However, proportional quantities of 4HB

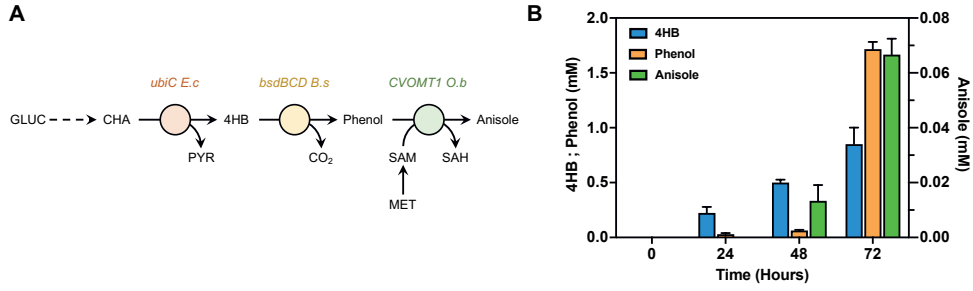

Figure 6.6: Anisole production from glucose A) Schematical representation of the anisole production pathway in P. putida KT2440. B) Aromatic titers detected during anisole production from glucose. Abbreviations: (GLUC), Glucose, (CHA), Chorismate, (4HB), 4-hydroxybenzoate, (PYR), pyruvate, (SAM), S-adenosyl-l-methionine, (SAH), S-adenosyl-L-homocysteine, (MET), methionine. Bar graphs represent the mean value ± SD from three independent experiments.

and phenol were still detected, 0.85 and 1.72 mM respectively. This indicates that both the 4HB decarboxylase and the CVOMT1 enzyme are still bottlenecks in biological anisole production from glucose. We hypothesize that the feedback-resistant UbiC generates 4HB at a faster rate than the 4HB decarboxylase can convert it, allowing 4HB accumulation. Therefore, promoters of both reactions should be fine-tuned to allow a smooth conversion from glucose to phenol. Phenol is most likely accumulated because it is a poor substrate for CVOMT1, and the enzyme needs to be subjected to further optimization to enhance its substrate specificity towards phenol.

Developing a growth-coupled selection system

To optimize the substrate specificity of CVOMT1 towards phenol, we deployed a selection system in which growth is coupled to SAM methylation [26]. This design relies on the conversion of methionine to cysteine through the intermediate homocysteine with the aid of a SAM-dependent methyltransferase. Exogenously added methionine is converted to SAM, which would subsequently be converted to S-adenosyl-l-homocysteine (SAH) by CVOMT1 (Figure 6.8C). Then, SAH is converted to homocysteine and subsequently to cysteine by reverse transsulfuration restoring growth in the process. Thus, the better the kinetics of CVOMT1 towards phenol, the faster growth would be restored.

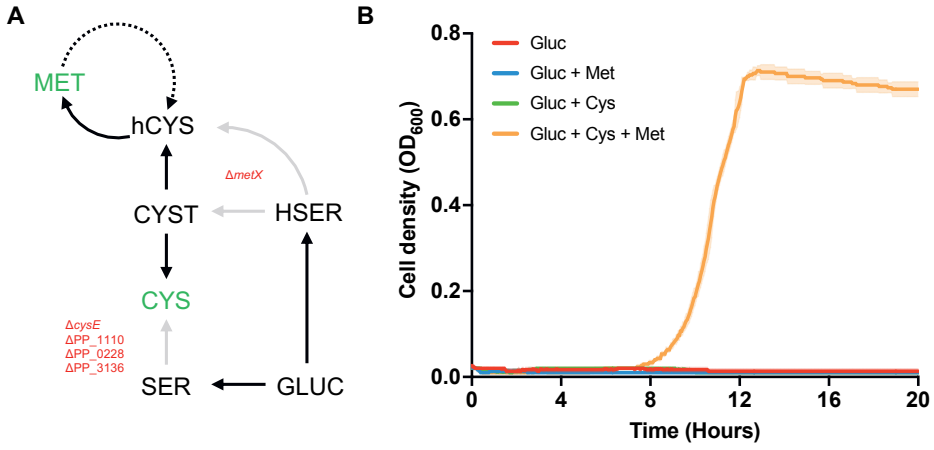

Figure 6.7: Construction of a cysteine and methionine auxotroph. A) Schematic representation of the constructed knockouts. B) Growth curves of CM-Aux. Growth can only occur when both the amino acids cysteine and methionine are added to the media. Abbreviations: (GLUC), glucose, (CYS), cysteine, (MET), methionine, (hCYS), homocysteine, (CYST), cystathionine, (HSER), homoserine, (SER), serine. Growth curves represent the mean value ± SD from three independent experiments.

For this design, we aimed to construct a double auxotrophic strain for the amino acids cysteine and methionine (Figure 6.7A). Cysteine biosynthesis is derived from serine and is catalyzed by serine *O*-acetyltransferases. According to the KEGG database, this reaction is encoded by the genes *cysE*, PP_1110, PP_0228, and PP_3136, of which the latter two are putative. First, we examined the effect of only removing the annotated *cysE* and PP_1110 genes. However, this strain was still able to grow in minimal media with glucose, indicating a flux towards cysteine biosynthesis (Figure S6.2A). Next, we individually deleted the PP_0228 and PP_3136 from this strain to test whether these putative genes are involved in cysteine biosynthesis. The deletion of PP_3136 had no effect, and growth in minimal media with glucose could still occur (Figure S6.2B). However, the deletion of PP_0228 rendered the strain unable to synthesize cysteine, making it dependent on supplementation (Figure S6.2C). This would indicate that the PP_3136 gene is misannotated, not expressed, or involved in cysteine biosynthesis but not able to sustain enough flux to rescue growth. Nonetheless, we deleted PP_3136 to ensure a tight selection and fully decouple our module from the main metabolism. Apart from being derived from serine, cysteine can be produced through the transsulfuration of cystathion-

ine, an intermediated within methionine biosynthesis. In theory, cysteine could still be produced through this pathway in *P. putida*, yet we observe that the intracellular flux cannot rescue growth (Figure S6.2D). To completely uncouple methionine and cysteine biosynthesis from the central metabolism we deleted the *metX* gene, encoding a homoserine *O*-acetyltransferase. The growth of this strain, termed CM-Aux, could only be restored through the addition of both cysteine and methionine, indicating a tight selection system (Figure 6.7B).

Testing the synthetic modules

Next, we aimed to install the reverse transsulfuration module which will convert homocysteine to the amino acid cysteine. This is a two-step process, catalyzed by the enzymes cystathionine-β-synthase and cystathionine-γ-lyase. We created

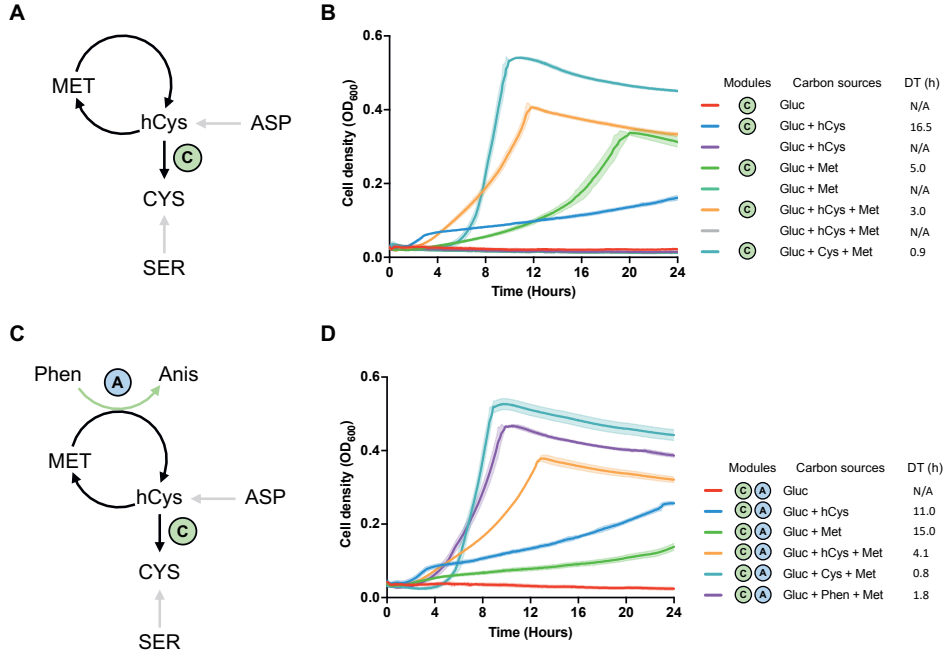

Figure 6.8: Establishing a growth-coupled methyltransferase selection system A) Selection of the C-Module in CM-Aux. B) Growth curves of CM-Aux with the implemented C-Module. C) Selection of the C and A-Module in CM-Aux. D) Growth curves of CM-Aux with the implemented C and A-Module. Abbreviations: (GLUC), glucose, (CYS), cysteine, (MET), methionine, (hCYS), homocysteine, (CYST), cystathionine, (ASP), aspartate, (SER), serine, (Phen), phenol, (Anis), anisole, (N/A), not applicable, (DT), doubling time, (h) hours. Growth curves represent the mean value ± SD from three independent experiments.

the C-module by cloning the cystathionine-β-synthase (Cys4) from *S. cerevisiae* and the cystathionine-γ-lyase (PA0400) from *Pseudomonas aeruginosa* on a pSEVAb62 backbone. We equipped the CM-Aux strain with the C-module and assessed the growth of the strain in minimal media. In all cases, growth could only occur upon the expression of the C-module. This module converts homocysteine to methionine, and if active, produces cysteine, restoring growth (Figure 6.8A). The addition of homocysteine only led to minor cell growth with a doubling time of 16.5 hours. When methionine was supplied together with homocysteine, growth was improved to a doubling time of 3 hours. As methionine is externally applied in this scenario, all homocysteine can be converted towards cysteine, most likely supporting higher growth rates. Interestingly, also with methionine as the sole supplementation, growth could occur with a doubling time of 5 hours. This indicates that the native methyltransferases of *P. putida* have sufficient activity to restore growth. Although this side activity renders the selection less tight, cells with kinetically fast CVOMT1 enzymes should theoretically still grow faster. To validate this hypothesis, we implemented the A-Module (the native CVOMT1 enzyme) together with the C-module in CM-Aux (Figure 6.8C). We observed that with both modules, the growth with homocysteine was improved (doubling time 11 hours), yet growth with methionine as sole supplementation was reduced to a doubling time of 15 hours. However, upon the addition of phenol and methionine, a doubling time of 1.8 hours was observed (Figure 6.8D). In this scenario, the CVOMT1 enzyme converts phenol and SAM to anisole and SAH. Then the SAH is converted into homocysteine and subsequently to cysteine, restoring growth. We observe that the CVOMT1 enzyme is active and that its activity can be coupled with growth (Figure 6.8D; purple line).

Evolution of CVOMT1

Having established a growth-coupled selection strategy, we aimed to evolve kinetically better CVOMT1 enzymes. In our current selection system, growth with CVOMT1 is relatively fast compared with the control (doubling time of 1.8 and 0.8 hours, respectively) (Figure 6.8D). Here, we supply 1 mM of methionine and phenol which most likely saturates the enzyme, thereby favouring kinetics and limiting the selection. We varied the methionine and phenol concentrations to find the optimal

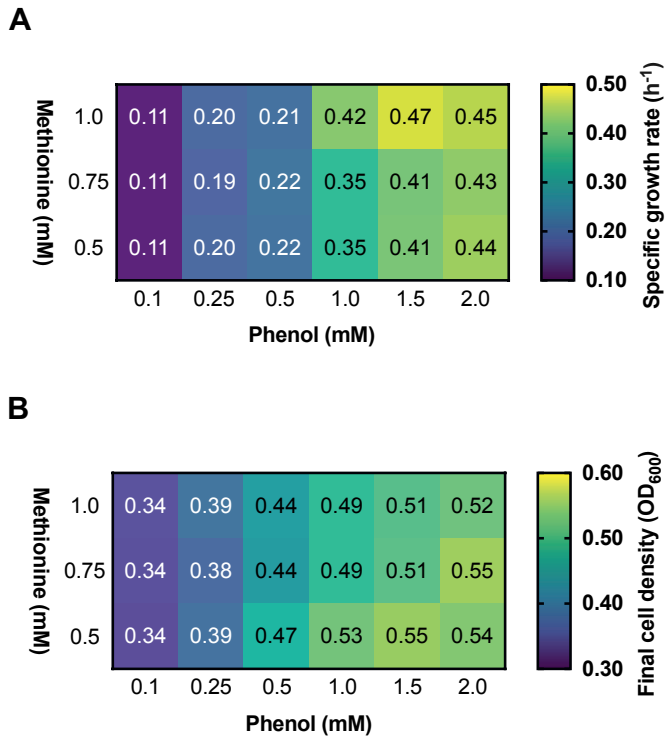

Figure 6.9: Optimization of the parameters for growth coupled selection. A) Heatmap of the specific growth rates of CM-Aux expressing the C and A-Module at different methionine and phenol concentrations. B) Heatmap of the final acquired cell densities of CM-Aux expressing the C and A-Module at different methionine and phenol concentrations. All values represent the average from three independent experiments.

conditions to select kinetically better CVOMT1 enzymes (Figure 6.9). Methionine supplies SAM and its availability did not seem to hamper enzyme kinetics and therefore growth. This is in accordance with the literature, as CVOMT1 naturally has a Michaelis constant (K_m) of 6 nM for SAM [14]. Therefore, the main limitation is phenol which is a poor substrate for CVOMT1. We observed that with increasing phenol concentrations, growth accelerates, as phenol is more rapidly converted and can supply the cell with cysteine for growth (Figure 6.9A). The less phenol is added, the less cysteine will be produced, which is reflected in the final observed cell density (Figure 6.9B). For biological anisole production, we need fast enzymes with a high affinity towards phenol and therefore a low K_m. This is especially important as a high K_m would require the build-up of intracellular phenol which might ham-

per bioproduction. Therefore, to screen potential better candidates, we selected a phenol concentration of 0.1 mM.

The optimization of CVOMT1 could be performed through either random mutagenesis PCR or adaptive laboratory evolution. Although both are efficient, in the latter one there is the possibility that native methyltransferases will be able to rescue growth, a phenomenon that has been observed by Luo et al., (2019) [26]. In their study, they actively improved two methyltransferases regarding melatonin biosynthesis, yet noticed the contribution of native methyltransferases to bacterial growth. In our study, we also observed minor growth using native methyltransferases when methionine was the sole supplementation (Figure 6.8D, green line). Therefore, we deployed a randomized approach using error-prone PCR on the *cvomt1* gene from *O. basilicum*. We transformed this library into CM-Aux containing the C-module and grew it overnight in minimal media with 10 mM glucose, 1 mM methionine, and 0.1 mM phenol to reduce the population that harbours kinetically slower enzymes. Hereafter, we plated the culture on minimal agar with the same carbon sources. In total, 92 visible large variants were selected, and their growth was compared to the wild-type CVOMT1 enzyme. We observed that all variants grew significantly faster compared to the wild-type enzyme (Figure S6.3A). However, the growth rates between the isolates were not as diverse as we would have expected. Therefore, we reduced the phenol concentration by ten-fold to 0.01 mM to further tighten the selection system and screen for variants with high selectivity towards phenol. The reduction of phenol proved to be effective, as the growth rates of the isolates were more diverse (Figure S6.3B).

Evalution of isolated mutants

We sequenced the *cvomt1* gene of the five fastest-growing isolates and discovered that all genes had the same mutation in which aspartic acid (Asp) at position 264 was substituted with asparagine (Asn). According to Gang et al., (2002) [14], the aminoacidic residues His-263, Asp-264 and Glu-322 in CVOMT1 are implicated in catalysis. Asparagine is the amide form of aspartic acid and has a high propensity to form hydrogen bonds [27]. The three-dimensional structure of the evolved enzyme reveals that the replaced Asn-264 is now able to form hydrogen bonds with Met-314,

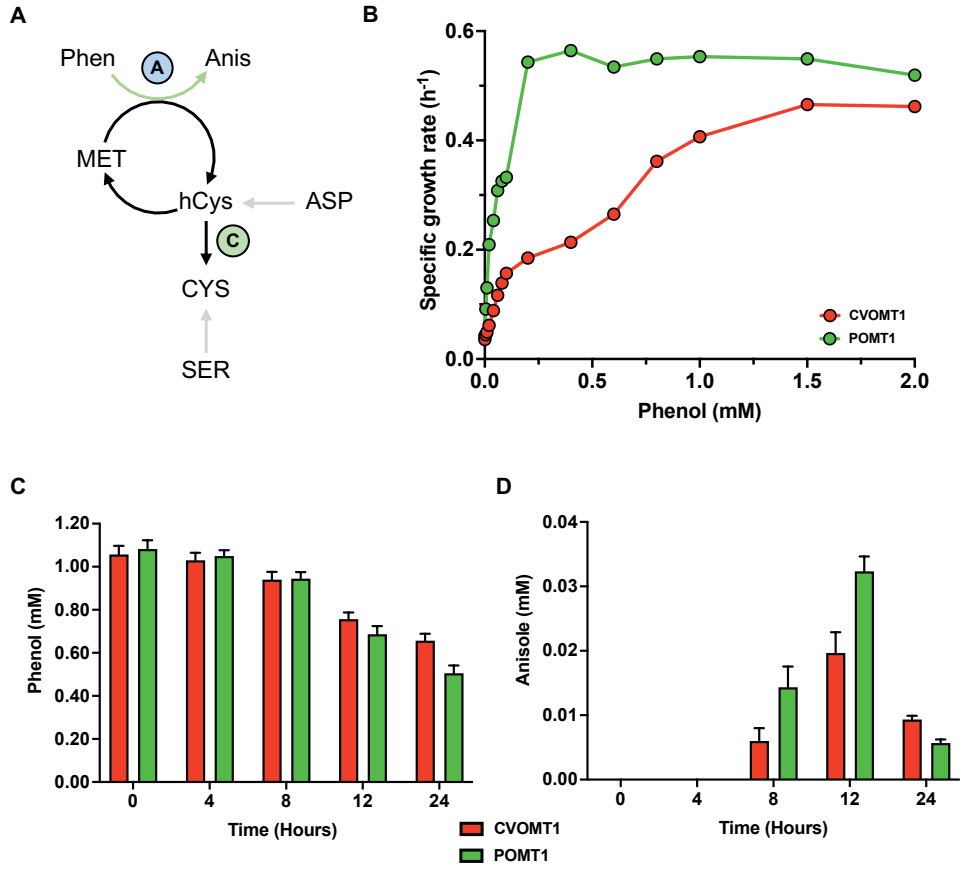

Figure 6.10: Characterization of POMT1. A) Selection of the C and A-Module in CM-Aux. B) Specific growth rates of CM-Aux equipped with CVOMT1 or POMT1 at different phenol concentrations. C) Phenol consumption of CVOMT1 vs POMT1. D) Anisole production of CVOMT1 vs POMT1. Abbreviations: (GLUC), glucose, (CYS), cysteine, (MET), methionine, (hCYS), homocysteine, (CYST), cystathionine, (ASP), aspartate, (SER), serine, (Phen), phenol, (Anis), anisole. Data points represent the mean value ± SD from three independent experiments.

causing a conformational change of Phe-310 (Figure S6.4). Both Phe-310 and Met-314 are involved in substrate binding of the isoflavone *O*-methyltransferase of *Medicago sativa*, which is distantly related to *cvomt1* from *O. basilicum* [14]. Therefore, it could be possible that this conformational change allows an increased binding affinity towards phenol. Moreover, it is likely that Asn-264 supports the stabilization of phenol in the active site. Hydrogen bonds are generally considered to play a key role in protein-ligand binding and enzyme catalysis [28]. In CVOMT1, Asp-264 is less favourable to making hydrogen bonds and substrate stabilization is performed by

His-263 alone [14]. However, to validate the biochemical reason for the enhanced enzyme kinetics, further research would be required.

Chracterization of POMT1

We rebranded the newly evolved variant as POMT1 (phenol *O*-methyltransferase 1) and analyzed its substrate binding affinities in CM-Aux using 1 mM of methionine and different phenol concentrations (Figure 6.10B). POMT1 outcompetes CVOMT1 on all supplied phenol concentrations, reaching its maximum growth rate at a concentration of 0.2 mM, highlighting its superior kinetics. Next, we aimed to examine the anisole production rate of POMT1 compared to CVOMT1. We transformed *P. putida* KT2440 with either candidate and fed the strains 1 mM of phenol and methionine to determine anisole production. Over the course of 24 hours, CVOMT1 consumed 0.40 mM phenol (Figure 6.10C). POMT1 consumed 45% more within 24 hours, with a total of 0.58 mM. Both candidates produced anisole over the course of the experiment, with CVOMT1 at a maximum of 0.019 mM and POMT1 at a maximum of 0.032 mM at 12 hours (Figure 6.10D). However, the total anisole titre is strongly reduced at 24 hours again. Therefore, although POMT1 is kinetically better towards phenol and could produce anisole at a faster rate, the volatility of anisole remains a bottleneck

Discussion

Nature offers us a myriad of enzymes to catalyze a plethora of metabolic reactions. Although we see these enzymes as quite rigid, they are often quite promiscuous by nature. This promiscuity can be harnessed to engineer enzymes that catalyze reactions that differ from its primary biological function. This concept, together with the power of retrobiosynthesis, can enable us to modify and optimize enzymatic pathways or design new one. However, determining new characteristics of novel enzymes is generally a difficult task requiring extensive analysis. Therefore, growth-coupled strategies are a great alternative to significantly accelerate the discovery of novel enzymes. In this study, we used the concept of synthetic biology to establish a novel enzyme and foster the transition of anisole production from a chemical to a biological industry. Although we present significant strides towards biological

anisole production, several other parameters and bottlenecks must be taken into consideration to fully exploit its potential. We demonstrated the successful production of anisole from glucose. This was partly accomplished by an increase in the PEP pool for the shikimate pathway by deleting the competing pathways. However, another important cofactor of the shikimate pathway is the precursor E4P. This compound is derived from the pentose phosphate pathway and has been reported to likely display low native fluxes in *P. putida* [29]. Therefore, an effective strategy to increase the intracellular E4P pool would be the upregulation of the transketolase and transaldolase of the pentose phosphate pathway [30]. This strategy with the increased PEP pool could drastically improve the flux through the shikimate pathway.

Additionally, our production still relies upon the external supplementation of methionine to the culture media for increased SAM biosynthesis. To decouple this external supplementation, SAM should be produced intracellularly from the intrinsic metabolism. Yet, the shikimate pathway like methionine biosynthesis is highly subjected to feedback inhibition, limiting its production. Homoserine *O*-acetyltransferase, encoded by *metX*, is reported to be inhibited by both methionine and SAM. Moreover, methionine biosynthesis uses L-cysteine as a precursor, which biosynthesis is also significantly inhibited by cysteine. Fortunately, feedback-resistant enzymes have been engineered for both pathways and deployed in recent years [26][31]. Using both these variants would significantly contribute to methionine biosynthesis. However, in addition to this, the native methionine adenosyltransferase (*metK*), converting methionine to SAM, and the adenosylhomocysteinase (*ahcY*) should be overexpressed. The latter is deemed crucial as it recycles the produced SAH back for SAM regeneration, which has been described as the major limiting step in deploying heterologous methyltransferases [31]. All these strategies could drastically push the metabolic fluxes towards the shikimate pathway and SAM biosynthesis and therefore anisole biosynthesis.

However, the last intracellular bottleneck would be the conversion of phenol to anisole. In this study, we constructed a growth-coupled selection system to optimize the CVOMT1 enzyme from *O. basilicum* to have a greater affinity towards phenol. Through high throughput screening, we created POMT1, an enzyme with

superior kinetics towards phenol compared to its ancestor. This stronger affinity was obtained using only a single amino acid substitution in the catalytic centre of the enzyme. Due to this single mutation, growth in our selection system could be restored with smaller amounts of phenol, demonstrating better affinities. Currently, during anisole production from glucose, large amounts of phenol are still accumulated due to the poor specificity of CVOMT1 towards phenol. Although it remains to be tested, the POMT1 enzyme could partially remove this bottleneck due to its better specificity. Yet further optimization of POMT1 would still be beneficial to create more superior variants with stronger affinities and faster conversion rates for biological anisole production. Additionally, the CM-Aux strain presented in this study could be further used to optimize a wide range of methyltransferases for interesting, methylated compounds. For example, many methylated plant-derived compounds have distinct biological activities and pharmacological properties [32]. However, plant-derived *O*-methyltransferases such as CVOMT1 generally accept a broad range of substrates, yet with different specificities [33]. As we show in this study, the substrate preference of these enzymes could be easily changed and most likely be made more specialized to a certain target compound. The high throughput screening system which we used to engineer POMT1 could be used to engineer a variety of other methyltransferases. An immense error-prone library could be subjected to the precursor of choice and with growth as output could lead to the discovery of new enzymes with high substrate specificities.

Above are presented the bottlenecks for optimizing anisole production intracellularly. Yet the main limitation of biological anisole production that remains to be addressed is its volatility, which occurs extracellularly. Because of this, it removes the ideal scenario of a traditional “end of the pipe” fermentation approach, in which a substrate-depleted, anisole-rich broth would be subjected to further processing. Instead, a biphasic fermentation system would be required for *in situ* anisole removal during bioreactor operation [34]. In these bioreactor systems, an organic solvent is often added to the aqueous medium to capture the product. Octanol and tributyrin are frequently used organic solvents during microbial fermentations [35]. Moreover, an *in situ* two-phase extractive fermentation using tributyrin has been reported in both *E. coli* and *Corynebacterium glutamicum* for the volatile

aromatic ester, methyl anthranilate [5]. Another potential candidate that could be considered as an extractant is oleyl alcohol. This alcohol has recently been deployed as an extractant for the water-insoluble compound bisdemethoxycurcumin and could potentially be aidful in capturing the partially water-insoluble anisole [36]. Alternatively, for producing and extracting volatile organic compounds (VOC), vacuum-based membrane techniques such as pervaporation, vacuum membrane distillation or vapour permeation could be applied. These techniques are increasingly being developed to remove VOCs from industrial wastewater and fermentation broth and could be an alternative for the organic solvent phase [37]. However, as there is no data available for biological anisole production, these options are all simply considerations and more research would be needed.

Overall, this work sets a significant step towards the microbial production of anisole. Moreover, it demonstrates the power of growth-coupled design, to engineer novel enzymes in an accelerated manner, setting up the possibility for other novel biosynthetic pathways. All of this will facilitate the conversion from chemical processes towards biological ones, which is an environmental and societal necessity, and the work presented here makes a great stride towards realizing this.

Material & Methods

Plasmids, primers, and strains

All strains and plasmids used in the present study are listed in Table S1. Primers used for plasmid construction and gene deletions are listed in Table S2.

Bacterial strains and growth conditions

P. putida and *E. coli* cultures were incubated at 30°C and 37°C respectively. For cloning purposes, both strains were propagated in Lysogeny Broth (LB) medium containing 10 g/L NaCl, 10 g/L tryptone, and 5 g/L yeast extract. For the preparation of solid media, 1.5% (w/v) agar was added. Antibiotics, when required, were used at the following concentrations: kanamycin (Km) 50 μg/ml, gentamycin (Gm) 10 μg/ml, chloramphenicol (Cm) 50 μg/ml and apramycin (Apra) 50 μg/ml. All growth experiments were performed using M9 minimal medium (per Liter; 3.88 g K_2HPO_4, 1.63 g NaH_2PO_4, 2.0 g $(NH_4)_2SO_4$, pH 7.0. The M9 media was supplemented

with a trace elements solution (10 mg/L ethylenediaminetetraacetic acid (EDTA), 0.1 g/L $MgCl_2 \cdot 6H_2O$, 2 mg/L $ZnSO_4 \cdot 7H_2O$, 1 mg/L $CaCl_2 \cdot 2H_2O$, 5 mg/L $FeSO_4 \cdot 7H_2O$, 0.2 mg/L $Na_2MoO_4 \cdot 2H_2O$, 0.2 mg/L $CuSO_4 \cdot 5H_2O$, 0.4 mg/L $CoCl_2 \cdot 6H_2O$, 1 mg/L $MnCl_2 \cdot 2H_2O$). In these experiments, strains were precultured in 10 ml LB with corresponding antibiotics. Then, the cultures were washed twice in M9 media without a carbon source. Finally, the cultures were diluted to an $OD600$ of 0.1 to start the experiment. In all plate reader experiments, a glucose concentration of 10 mM was used. Unless otherwise indicated, the supplementary carbon sources, cysteine, methionine, homocysteine, and phenol were added at a concentration of 1 mM. Plate reader experiments were carried out in 200 μL of M9 medium using an ELx808 plate reader (Biotek). Growth ($OD600$) was measured over time using continuous shaking and measurements were taken every three minutes. Flask experiments were performed in 250 ml Erlenmeyer flasks filled with 25 ml of M9 minimal medium containing 50 mM of glucose. Unless otherwise indicated, the supplementary carbon sources, 4HB, phenol and methionine were added at a concentration of 1 mM. The cultures were incubated in a rotary shaker at 200 rpm at 30°C.

Plasmid construction

Plasmids were constructed using the previously described SevaBrick Assembly (Damalas et al., 2020)[38]. All DNA fragments were amplified using Q5® Hot Start High-Fidelity DNA Polymerase (New England Biolabs). The *cvomt1* gene from *Ocimum basilicum* was codon-optimized with the JCat tool (Grote et al., 2005) and synthesized through Genescript (Table S3). The *ubiC* gene was amplified from the genomic DNA from *E. coli* and the feedback-resistant mutations were introduced during PCR. The feedback-resistant *aroG* gene was obtained from an in-house plasmid. The *BsdBCD* genes were amplified from the genomic DNA of *Bacillus subtilis*. All genes were expressed using the Biobrick BBa_J23100 promoter and BBa_B0034 RBS. For genomic integration, the phenol operon was amplified by PCR from the assembled plasmid and cloned into a pGNW containing *lox* sites. The T7 RNA polymerase and Cre recombinases were amplified from in-house plasmids. All plasmids were transformed using heat shock in chemically competent *E. coli* DH5α λ*pir* and selected on LB agar with corresponding antibiotics. Colonies were screened

through colony PCR with Phire Hot Start II DNA Polymerase (Thermo Fisher Scientific). Isolated plasmids were verified using Sanger sequencing (MACROGEN inc.) and subsequently transformed into *P. putida* via electroporation.

Strain construction

Genetic deletions in this study were performed using the protocol previously described by Wirth et al., (2020)[39]. Homology regions of ± 500 bp were amplified up and downstream of the target gene from the genome of *P. putida* KT2440. Both regions were cloned into the non-replicative pGNW vector and propagated in *E. coli* DH5α λ*pir*. Correct plasmids were transformed into *P. putida* by electroporation and selected on LB + Km plates. Successful co-integrations were verified by PCR. Hereafter, co-integrated strains were transformed with the pQURE6-H and transformants were plated on LB + Gm containing 2 mM 3- methylbenzoic acid (3-mBz). This compound induces the XylS – dependent Pm promoter, regulating the I-SceI homing nuclease that cuts the integrated pGNW vector. Succesful gene deletions were verified by PCR and Sanger sequencing (MACROGEN inc). Hereafter, the pQURE6-H was cured by removing the selective pressure and its loss was verified by sensitivity to gentamycin.

Analytical methods

Cell growth was determined by measuring the optical density at 600 nm ($OD600$) using an $OD600$ DiluPhotometer spectrophotometer (IMPLEN) or a Synergy plate reader (BioTek Instruments). Analysis of glucose in supernatants was performed using high-performance liquid chromatography (HPLC) (Thermo Fisher Scientific) equipped with an Aminex HPX-87H column. The mobile phase was 5 mM of H_2SO_4 at a flow rate of 0.6 ml/min, the column temperatures were held at 60 °C and the compounds were detected using a Shodex RI-101 detector (Shodex). The amount of produced 4HB, phenol and anisole was determined using HPLC (Shimadzu) with a C18 column (4.6 mm × 250 mm) and a UV/vis detector set at 472 nm. The mobile phase consisted of Milli-Q water (A), 100 mM formic acid (B) and acetonitrile (C) with a flow rate of 1 ml/min at 30 °C. Chromatographic separation of analytes was attained using the following gradient program: t = 0 - 5min: A-55%, B-10% and C-35%; from t = 5 - 10min ramp to A-10%, B-10% and C-80% and held until 15 min.

Then from t = 15 – 16 min, the gradient was returned to A-55%, B-10% and C-35% and maintained isocratic for a total run time of 18 min. For quantification, calibration curves were prepared using pure standards (99% purity) purchased from Sigma-Aldrich.

High throughput screening of CVOMT1 varieties

The CVOMT1 library was generated using the GeneMorph II Random Mutagenesis Kit (Agilent Technologies) following the manufacturer's protocol. In short, 50 ng of *cvomt1* DNA was taken as the template for error-prone PCR and amplified with the primers CVOMT_ALE_FW and CVOMT_ALE_RV. The error-prone PCR was carried out for 30 thermal cycles and the PCR product was gel purified and cloned into a pSEVAb23 vector. Next, the library was transformed by electroporation into the CM-Aux strain containing the C-module and grown overnight in LB media with the corresponding antibiotics. The next day, cells were washed twice with M9 minimal media without a carbon source. Then, cells were reinoculated at an $OD600$ of 0.1 in 10 ml of M9 containing 10 mM glucose, 1 mM methionine and 0.1 mM phenol and grown overnight. This culture was subsequently plated on M9 agar containing the same carbon sources. After 2 days of growth, 92 visible large colonies were picked and inoculated in a 96-well plate filled with 200 μL of LB supplemented with the appropriate antibiotics. Two wells contained CM-Aux with the unevolved CVOMT1 enzyme as positive control and two were left blank as a negative control. The plate was incubated for 24 hours at 30°C in an ELX808 plate reader. The next day, 5 μL was transferred to a new 96-well plate containing 200 μL M9 with 10 mM glucose, 1 mM methionine and 0.1 mM phenol and incubated for 24 hours at 30°C$\dot{\text{G}}$rowth ($OD600$) was measured every three minutes over time using continuous shaking.

Modelling Anisole production

We used iJN1462, the latest developed genome-scale model (GEM) of *P. putida* for anisole production and added the reactions for phenol-*O*-methyltransferase, 4HB decarboxylase and tyrosine phenol-lyase. Flux balance analysis was used to calculate the maximum theoretical by setting anisole production as the objective.

Structural protein analysis

Structural models of CVOMT1 and POMT1 were generated using the open-source software ColabFold [40]. Visualization and analysis of the protein 3D structures were performed in the Mol* 3D viewer of the RCSB protein data bank

Statistical analysis

All reported experiments are derived from independent biological replicates. Figures represent the mean values of corresponding biological triplicates and the standard deviation. The level of significance of the difference when comparing results was evaluated by an unpaired Student's t-test

Author's contributions

L.B and C.B conceived and designed this study. L.B conducted the experiments. V.A.P.M.d.S. provided supervision and arranged funding.

Conflict of interest

The authors declare there are no conflicting interests.

Supplementary material

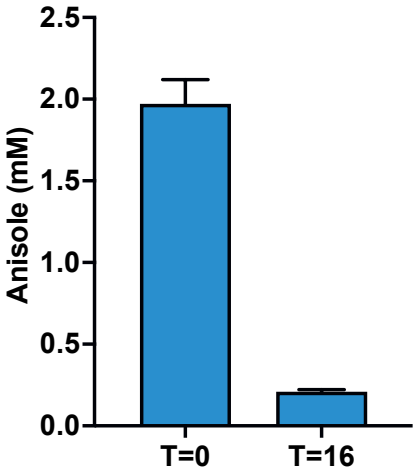

Figure S6.1: Abiotic degradation of anisole. Three independent flaks containing M9 minimal media with 2 mM anisole were incubated overnight (16 hours). Bar graphs represent the mean value ± SD from three independent experiments.

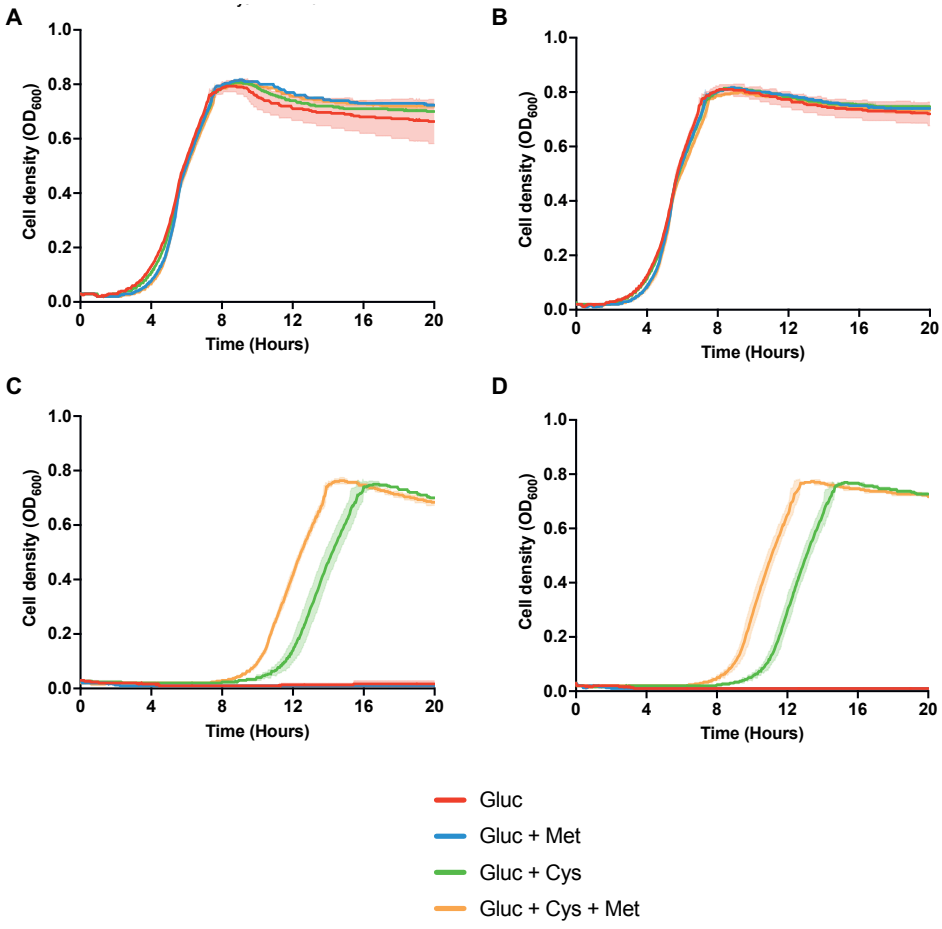

Figure S6.2: Construction and characterization of a cysteine auxotroph. A) KT2440 ΔcysE ΔPP_1110. B) KT2440 ΔcysE ΔPP_1110 ΔPP_3136 C) KT2440 ΔcysE ΔPP_1110 ΔPP_0228. D) KT2440 ΔcysE ΔPP_1110 ΔPP_0228 ΔPP_3136. Abbreviations: (Gluc), glucose, (Cys), cysteine, (Met), methionine. Growth curves represent the mean value ± SD from three independent experiments.

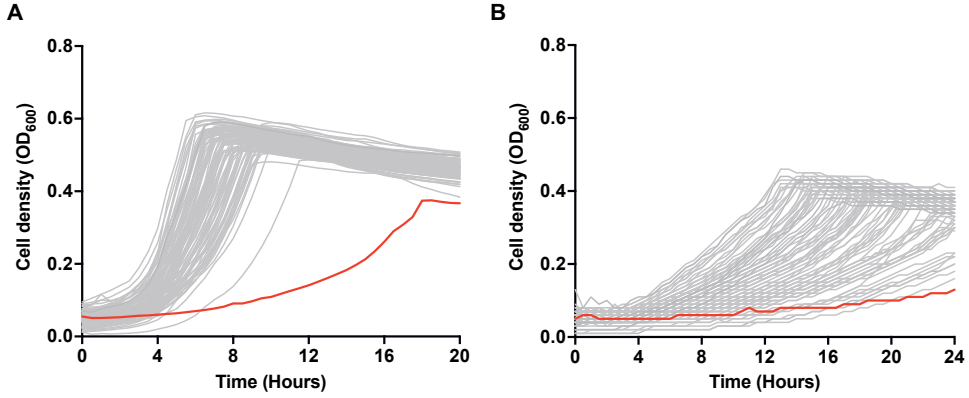

Figure S6.3: Selection of kinetically superior CVOMT1 enzymes. A) Growth curves of CM-Aux with the implemented C and the mutated A-Module at a phenol concentration of 0.1 mM. A) Growth curves of CM-Aux with the implemented C and the mutated A-Module at a phenol concentration of 0.01 mM. Every line represents a single isolate. Growth coupled selection with the unevolved CVOMT1 enzyme is indicated in red.

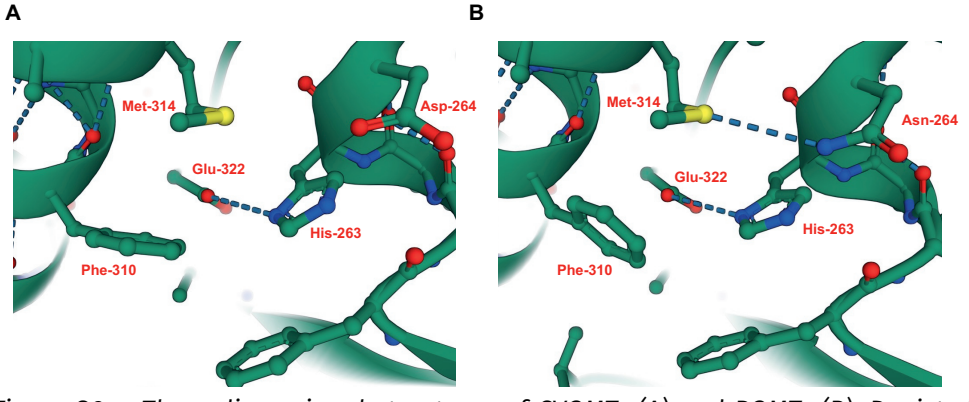

Figure S6.4: Three-dimensional structures of CVOMT1 (A) and POMT1 (B). Depicted is the active site of the proteins and the conformational change of Phe-310 that occurred due to the Asn-264 introduction.

The rest of the supplementary material of this chapter, including Supplementary Tables S1 to S3, can be accessed *via*:

https://figshare.com/s/3bc936b293e24b17d226

Bibliography

1. Mori, R. Replacing all petroleum-based chemical products with natural biomass-based chemical products: a tutorial review. *RSC Sustainability* (2023).
2. Nielsen, J. & Keasling, J. D. Engineering Cellular Metabolism. *Cell* **164,** 1185–1197 (2016).
3. Rosenberg, J. & Commichau, F. M. Harnessing Underground Metabolism for Pathway Development. *Trends in Biotechnology* **37,** 29–37 (2019).
4. Batianis, C., van rosmalen, R., Major, M., *et al.* A tunable metabolic valve for precise growth control and increased product formation in Pseudomonas putida. *Metabolic Engineering,* 118159 (2022).
5. Luo, Z. W., Cho, J. S. & Lee, S. Y. Microbial production of methyl anthranilate, a grape flavor compound. *Proceedings of the National Academy of Sciences of the United States of America* **166,** 10749–10756 (2019).
6. Zhang, J., Hansen, L. G., Gudich, O., *et al.* A microbial supply chain for production of the anti-cancer drug vinblastine. *Nature* **609,** 341–347 (2022).
7. MohammadiPeyhani, H., Hafner, J., Sveshnikova, A., *et al.* Expanding biochemical knowledge and illuminating metabolic dark matter with ATLASx. *Nature Communications* **13,** 1–12 (2022).
8. Lin, G. M., Warden-Rothman, R. & Voigt, C. A. Retrosynthetic design of metabolic pathways to chemicals not found in nature. *Current Opinion in Systems Biology* **14,** 82–107 (2019).
9. Hadadi, N., MohammadiPeyhani, H., Miskovic, L., *et al.* Enzyme annotation for orphan and novel reactions using knowledge of substrate reactive sites. *Proceedings of the National Academy of Sciences of the United States of America* **116,** 7298–7307 (2019).
10. Maia, A. C. D., De Lima, C. T., Navarro, D. M. D. A. F., *et al.* The floral scents of Nymphaea subg. Hydrocallis (Nymphaeaceae), the New World night-blooming water lilies, and their relation with putative pollinators. *Phytochemistry* **103,** 67–75 (2014).
11. Dang, D., Wang, Z., Lin, W., *et al.* Synthesis of anisole by vapor phase methylation of phenol with methanol over catalysts supported on activated alumina. *Cuihua Xuebao/Chinese Journal of Catalysis* **37,** 720–726 (2016).
12. Vani, B., Pabba, M., Kalyani, S., *et al.* Separation of Anisole and Valuable Byproducts from Liquid Reaction Mixtures by Solvent Extraction and Multicomponent Distillation. *Journal of Solution Chemistry* **50,** 160–177 (2021).
13. Weber, V. & Gmbh, I. P. Phenol. *Encyclopedia of industrial chemistry* (2020).
14. Gang, D. R., Lavid, N., Zubieta, C., *et al.* Characterization of phenylpropene O-methyltransferases from sweet basil: Facile change of substrate specificity and convergent evolution within a plant O-methyltransferase family. *Plant Cell* **14,** 505–519 (2002).
15. Axelrod, J. & Daly, J. Enzymatic O-methylation of phenol by mammalian liver A guinea pig homogenate was incubated with S-adenosylLMe-14Cimethionine. *Biochimica et Biophysica Acta* **25,** 472–478 (1968).
16. Nhung Pham. Evaluating and deploying genome-scale metabolic models for microbial cell factories. *Wageningen University* (2020).
17. Li, M., Liu, C., Yang, J., *et al.* Common problems associated with the microbial productions of aromatic compounds and corresponding metabolic engineering strategies. *Biotechnology Advances* **41,** 107548 (2020).
18. Loeschcke, A. & Thies, S. Pseudomonas Putida - a Persatile Host for the Production of Natural Products. *Applied Microbiology and Biotechnology* **99,** 6197–6214 (2015).
19. Nikel, P. I., Fuhrer, T., Chavarría, M., *et al.* Reconfiguration of metabolic fluxes in Pseudomonas putida as a response to sub-lethal oxidative stress. *ISME Journal* **15,** 1751–1766 (2021).
20. Krastanov, A., Alexieva, Z. & Yemendzhiev, H. Microbial degradation of phenol and phenolic derivatives. *Engineering in Life Sciences* **13,** 76–87 (2013).

21. Wierckx, N. J., Ballerstedt, H., De Bont, J. A., *et al.* Engineering of solvent-tolerant pseudomonas putida S12 for bioproduction of phenol from glucose. *Applied and Environmental Microbiology* **71,** 8221–8227 (2005).

22. Miklasińska-Majdanik, M., Kpa, M., Wojtyczka, R. D., *et al.* Phenolic compounds diminish antibiotic resistance of staphylococcus aureus clinical strains. *International Journal of Environmental Research and Public Health* **15** (2018).

23. Miao, L., Li, Q., Diao, A., *et al.* Construction of a novel phenol synthetic pathway in Escherichia coli through 4-hydroxybenzoate decarboxylation. *Applied Microbiology and Biotechnology* **99,** 5163–5173 (2015).

24. Lupa, B., Lyon, D., Shaw, L. N., *et al.* Properties of the reversible nonoxidative vanillate/4-hydroxybenzoate decarboxylase from Bacillus subtilis. *Canadian Journal of Microbiology* **54,** 75–81 (2008).

25. Jha, R. K., Narayanan, N., Pandey, N., *et al.* Sensor-Enabled Alleviation of Product Inhibition in Chorismate Pyruvate-Lyase. *ACS Synthetic Biology* **8,** 775–786 (2019).

26. Luo, H., Hansen, A. S. L., Yang, L., *et al.* Coupling S-adenosylmethionine–dependent methylation to growth: Design and uses. *PLoS Biology* **17,** 1–13 (2019).

27. Vennelakanti, V., Qi, H. W., Mehmood, R., *et al.* When are two hydrogen bonds better than one? Accurate first-principles models explain the balance of hydrogen bond donors and acceptors found in proteins. *Chemical Science* **12,** 1147–1162 (2021).

28. Chen, D., Oezguen, N., Urvil, P., *et al.* Regulation of protein-ligand binding affinity by hydrogen bond pairing. *Science Advances* **2** (2016).

29. Elmore, J. R., Dexter, G. N., Salvachúa, D., *et al.* Engineered Pseudomonas putida simultaneously catabolizes five major components of corn stover lignocellulose: Glucose, xylose, arabinose, p-coumaric acid, and acetic acid. *Metabolic Engineering* **62,** 62–71 (2020).

30. Ling, C., Peabody, G. L., Salvachúa, D., *et al.* Muconic acid production from glucose and xylose in Pseudomonas putida via evolution and metabolic engineering. *Nature communications* **13,** 4925 (2022).

31. Kunjapur, A. M., Hyun, J. C. & Prather, K. L. Deregulation of S-adenosylmethionine biosynthesis and regeneration improves methylation in the E. coli de novo vanillin biosynthesis pathway. *Microbial Cell Factories* **15,** 1–17 (2016).

32. Cui, H., Song, M. C., Ban, Y. H., *et al.* High-yield production of multiple O-methylated phenylpropanoids by the engineered Escherichia coli-Streptomyces cocultivation system. *Microbial Cell Factories* **18,** 1–13 (2019).

33. Liu, Y., Fernie, A. R. & Tohge, T. Diversification of Chemical Structures of Methoxylated Flavonoids and Genes Encoding Flavonoid-O-Methyltransferases. *Plants* **11** (2022).

34. Teke, G. M., Tai, S. L. & Pott, R. W. Extractive Fermentation Processes: Modes of Operation and Application. *ChemBioEng Reviews* **9,** 146–163 (2022).

35. Wynands, B., Lenzen, C., Otto, M., *et al.* Metabolic engineering of Pseudomonas taiwanensis VLB120 with minimal genomic modifications for high-yield phenol production. *Metabolic Engineering* **47,** 121–133 (2018).

36. Incha, M. R., Thompson, M. G., Blake-Hedges, J. M., *et al.* Leveraging host metabolism for bisdemethoxycurcumin production in Pseudomonas putida. *Metabolic Engineering Communications* **10,** e00119 (2020).

37. Fatima, S., Govardhan, B., Kalyani, S., *et al.* Extraction of volatile organic compounds from water and wastewater by vacuum-driven membrane process: A comprehensive review. *Chemical Engineering Journal* **434,** 134664 (2022).

38. Damalas, S. G., Batianis, C., Martin-Pascual, M., *et al.* SEVA 3.1: enabling interoperability of DNA assembly among the SEVA, BioBricks and Type IIS restriction enzyme standards. *Microbial Biotechnology* **13,** 1793–1806 (2020).

39. Wirth, N. T., Kozaeva, E. & Nikel, P. I. Accelerated genome engineering of Pseudomonas putida by I-SceI—mediated recombination and CRISPR-Cas9 counterselection. *Microbial Biotechnology* **13,** 233–249 (2020).

40. Mirdita, M., Schütze, K., Moriwaki, Y., *et al.* ColabFold: making protein folding accessible to all. *Nature Methods* **19,** 679–682 (2022).

CHAPTER 7

General discussion and future perspectives

Lyon Bruinsma

Industrial biotechnology has the power to reshape the bioeconomy to deliver a more sustainable future [1]. For this exact reason, the demand for industrial processes using microorganisms is ever-increasing [2]. Currently, native and synthetic microbial processes have been utilized and commercialized. Yet we have only scraped the surface of the ever-growing possibilities. We are in a scientific revolution in which we can exert immense control over metabolic networks, transplanting and creating metabolic traits how we desire. Relevant industrial traits can be reposited within a potential industrial host to elevate its efficiency for the bioindustry. Within the scope of this thesis, I used predominantly growth-coupled designs to equip the soil bacterium and potential industrial "*chassis*" *Pseudomonas putida* KT2440 with synthetic metabolic structures.

The first part of the research described in this thesis involves the incorporation of new metabolic features for the assimilation of C1 compounds and the incorporation of external electron donors for CO_2 fixation. Both strategies use the rational approach of a growth-coupled design for the characterization of new features. This growth-coupled pipeline offers a key advantage as it can not only improve the implemented synthetic module but go on to improve the strain itself. From a personal point of view, this strategy is incredibly useful as it immediately reflects *in vivo* dynamics. This became especially apparent in **chapter 3**, in which we tried to transplant a phosphite dehydrogenase or the soluble hydrogenase from *Cupriavidus necator* to *P. putida*. Although both were unfortunately not yet working as desired, the growth-coupled selection allowed fast screening which under normal circumstances would have been impossible. Moreover, through the Darwinian principles of "survival of the fittest", we can harness the power of evolution to circumvent metabolic bottlenecks and even create novel biochemistries. In **chapter 6**, we utilized an auxotrophic *P. putida* strain to significantly improve the kinetics of an anisole-producing enzyme. The fact that this optimization was obtained with only a single round of evolution, highlights the key advantage of growth-coupled strategies for creating novel biochemistries. These advantages became more apparent in **chapter 2**, where short-time evolution established for the first time synthetic reductive CO_2 fixation through the innate formate dehydrogenase of *P. putida*. Here, evolution not only altered the introduced module but also the strain itself. How-

ever, this phenomenon of "life finds a way" came truly to fruition in **chapter 5**, in which we used evolution to alter the whole metabolism. Here, we converted the normally anabolic shikimate pathway into a catabolic regime, which is a radical, large-scale metabolic rearrangement not previously achieved.

Throughout this discussion chapter, I will further discuss the general impact of the presented research regarding growth-coupling strategies and how they can be further utilized and improved. Moreover, I will comment on the nomenclature of industrial *chassis*, and the future of *P. putida* itself. Lastly, I will share my perspective on how I envision the future of synthetic biology and metabolic engineering in industrial biotechnology.

A bright future for growth-coupled selections

Throughout this thesis, I utilized growth-coupled designs for the assessment of introduced modules (**chapters 2 & 3**), the screening of an *in vitro* mutagenesis library (**chapter 6**), and the rearrangement of the entire metabolic network (**chapter 5**). As demonstrated in these chapters, these nifty designs can significantly accelerate the development of microbial cell factories as growth becomes the measurable output. Therefore, I envision the future of growth-coupled designs as a bright one. The efficiency of these strategies is continuously being recognized by the scientific community and explored to expand metabolic networks. One example is the manipulation of enzymes toward the utilization of non-canonical cofactors [3]. These cofactors are beneficial as they have limited crosstalk between the native redox cofactor usage in cellular metabolism and can therefore be exploited to achieve higher yields. Another example is the incorporation of halogenated compounds such as fluorine, chlorine, bromine, and iodine in the main metabolism [4]. The incorporation of these halogenated compounds in the main metabolism is generally problematic due to their toxic and, for the microbe, alien nature [5]. Therefore, growth-coupled selections have been suggested as the way forward to incorporate these burdensome reactions into the metabolic network [4]. This, paired with evolution, can accelerate the creation of novel biochemistries, thereby potentially opening new avenues for biocatalysis.

Various growth-coupled scenarios combined with evolution have been used to deeply refactor the main metabolism (Table 1.1). A few key examples are the establishment of C1 metabolisms or the shikimate pathway-dependent metabolism described in **chapter 5** [6][7][8][9][10]. However, more often these growth-coupled designs are used for the assessment of *in vitro* libraries [11][12]. In some instances though, when the synthetic module can be coupled to a stringent selection system, continuous *in vivo* mutagenesis could be explored for automated directed evolution [13]. Nevertheless, the ability to do so is still a case-by-case study to determine if this can be applied or not. Metabolism is remarkably plastic and evolutionary pressure might lead to "cheating" cells that emerge outside of the applied pressure. For example, in **chapter 2**, we established CO_2 fixation through short-term evolution. This evolution was possible as the metabolic auxotroph was quite stringent. It relied on the production of 5,10-methylene-THF through the introduced modules and there was no other supplier than CO_2. However, in **chapter 5**, we created a metabolic auxotroph that was less stringent and could potentially evolve in other ways than through the shikimate pathway. After adaptive laboratory evolution, we indeed noticed fast-growing strains with low fluorescent profiles, most likely indicating that these strains evolved through other alternative pathways. By utilizing the biosensor, we were able to selectively isolate the desired strain. However, it should be noted that the possibility of other dominant pathways emerging underscores the potential of growth-coupled evolution. For example, we also used the pyruvate auxotrophic strain for the redirection of metabolic fluxes toward other interesting pathways. Simultaneously, with the establishment of the shikimate pathway-dependent catabolism (SDC), we created a serine-dependent pathway (Data not shown in this thesis). In this metabolic scenario, the catabolic fluxes are diverted towards serine biosynthesis to create pyruvate by serine deamination. Serine is an industrially important chemical with a fast-growing market demand [14]. Thus, like SDC, this new catabolic pathway could be exploited to produce serine in a growth uncoupled fashion.

Although the pyruvate auxotroph is less stringent than the one described in **chapter 2**, both are still prime examples of how this non-stringent genotype can be exploited to establish interesting phenotypes. This also became apparent **chap-**

ters 3 and **6** in which we used other less stringent auxotrophic strains. In **chapter 3**, we created an auxotrophic strain for reducing power by deleting core NADH-releasing reactions within the TCA cycle. In **chapter 6**, we created an auxotrophic strain for the sulfur amino acids cysteine and methionine. Both these strains are useful for the fast characterization of introduced modules but would be less favorable concerning evolution. Cofactor promiscuity would be the undoing of the NADH-auxotrophic strain. Often the replacement of a few residues in the active site can already change the cofactor preference of an enzyme, changing it from NAD^+ to $NADP^+$ and vice versa [15][16][17]. Under evolutionary pressure, not just the target enzyme, but all redox cofactor enzymes are capable of evolution resulting in "cheating" cells. The strain could become more stringent by deleting the majority of NADH and NADPH-producing reactions, yet I question how viable this selection system would be. The same principle goes for the amino acid auxotroph described in **chapter 6**. In our experiments, we observed that the activity from innate methyltransferases was sufficient to restore growth. Thus, also in this instance, evolution would be out of the question as it might lead to unwanted phenotypes. Both auxotrophic strains are however still highly useful in assessing the efficacy of synthetic modules created through *in vitro* mutagenesis and can significantly accelerate the slower test and learn phase of the DBTL cycle. This became especially apparent in **chapter 6** in which we isolated a superior enzyme for anisole biosynthesis in a single round of selection.

The next steps for growth-coupled selections

As aforementioned, growth-coupled selections have been shown to be highly efficient. It is therefore no wonder that their incorporation in biofoundries is highly desired [18]. Biofoundries aim at increasing the development of microbial cell factories for product formation through automation and high-throughput screening [19]. The incorporation of growth-coupled modules could significantly reduce screening times as the only measurable parameter is growth. This strategy would be particularly useful to construct novel cell factories or to engineer and optimize novel enzymes as described in **chapter 6**. Especially the latter is highly interesting, as many chemical compounds could be produced by biological means [20].

When possible, these novel enzymes could be coupled to microbial growth following a similar scheme. However, to fully exert this potential, the incorporation of computational metabolic network analysis is a must [21]. Despite some successful examples, including those present in this thesis, the potential for these growth-coupled designs remains untapped. Currently, most auxotrophic strains are based on intuition and often lack the incorporation of an *in-silico* analysis [22]. This type of approach limits the creativity of the construction of auxotrophic strains and the integration of metabolic models could generate novel counterintuitive, complex designs of growth-coupled scenarios. The model can predict the necessary reactions that need to be removed to abolish cell growth while integrating the necessary complementing reaction that will restore growth. Algorithms have already predicted that growth-coupled overproduction is feasible for almost all metabolites in different production hosts [23]. This particularly highlights the necessity of computational integration and how this approach could be useful for both optimizing native networks and installing novel bioproduction pathways [24]. In conclusion, growth-coupled designs hold a lot of promise for a bright future of industrial biotechnology, and ongoing research and development in this field are likely to lead to a wide range of new and improved production processes and enzymes in the coming years.

Establishing *P. putida* as industrial *chassis*: the way forward

The *chassis* delusion

Within the scope of this thesis, I aimed to expand the metabolic repertoire of *P. putida*, a soil bacterium generally regarded as a "*chassis*" for metabolic engineering applications. Beyond this, a plethora of independent microorganisms is being developed as *chassis* for metabolic engineering purposes [25]. The scientific community tends to aim for diversification instead of unification, where often similar catabolic or anabolic reactions are carried out in a wide variety of hosts, such as C1 – assimilation pathways [10][26][27] or xylose catabolism [28][29][30] . But does this diversification advance or hinder the progress of industrial biotechnology? Moreover, is this diversification a waste of time and money, or can it generate useful

information to create a superior organism for the bioindustry?

Over the years, several organisms such as *Escherichia coli*, *Saccharomyces cerevisiae*, and *Bacillus subtilis* have been engineered as microbial *chassis* for biotechnological purposes [31][32][33]. The reason for their popularity is well understood, as these organisms were one of the first characterized and therefore are well-studied with plenty of synthetic biology tools at their disposal [31]. Even *P. putida* is increasingly being developed as a *chassis* and its set of genetic and *in-silico* tools is continuously being expanded [34]. However, one could consider that the notion that any of these cell factories is a microbial *chassis* is a delusion. Webster's dictionary describes *chassis* as "the frame and working parts exclusive of the body or housing". If we would talk about a car, this would mean that the metal frame stays the same, whereas the interior design can be exchanged to the user's liking. If we would translate this analogy to microbial cell factories, this would indicate that the cell envelope is the only asset that would remain intact. Yet, with most microbial "*chassis*" the entire interior is never replaced. In most cases, only a new chair is added, or the rearview mirrors are replaced. So, is it accurate to call them *chassis* if most of the "vehicle" stays the same?

The term *chassis* in synthetic biology often only refers to a microbial platform that can act as a framework to support foreign biological parts and components [35][36]. But even in the world of synthetic biology, the term *chassis* is often widely used in different contexts [35]. These *chassis* are often selected and justified based on one or more interesting traits. For example, *P. putida* is often highlighted due to its high solvent tolerance and its ability to withstand industrial-scale stress conditions [36][37][38][39]. One key feature attributed to its tolerance is its ability to recycle hexose sugars to replenish the NADPH pool to combat oxidative stress [40]. Yet, what happens if we incorporate new metabolic pathways for assimilation or production? Does the newly implemented pathway intervene with NADPH generation and decrease the tolerance or is NADPH generation in the EDEMP cycle still preferred and does it hamper production? Recently, *P. putida* was equipped with a linear glycolysis by disrupting the native EDEMP cycle [41]. While this pathway generates more NADH and ATP, it removes the one thing that made *P. putida* unique. Of course, the solvent tolerance is not only attributed to an increased NADPH pool.

Some of the main features that make *P. putida* tolerant are its highly efficient efflux pumps and the change in lipid composition of the cell membrane upon solvent exposure [42]. These features are polygenic by nature and can be difficult to transplant to other hosts [43]. In that regard, *P. putida* is still an interesting host for biomanufacturing purposes. Additionally, this bacterium has been shown to be naturally endowed to withstand industrial-scale stress conditions, a feature that other, more widely used industrial hosts such as *E. coli* only offer to a lesser extent [37]. Therefore, due to its previously mentioned favorable characteristics, *P. putida* remains a good candidate for industrial biotechnology. However, it is still too much of an enigma to be called a microbial *chassis* and there is still substantial room for improvement to establish it as one.

Towards the domestication of *P. putida* as a *chassis*.

A microbial *chassis* provides the basic framework upon which new functions or products can be engineered and should be easy to engineer, robust, and moreover predictable in behavior. Reconfiguring a microbial cell factory towards a microbial *chassis* requires a fast amount of development, ranging from the characterizations of genetic tools to the creation of metabolic models and physiological characterization, e.g., provided by techniques like transcriptomics, proteomics, and metabolomics [44]. The progress in installing *P. putida* as a potential *chassis* has been years in the making and numerous genetic engineering and *in-silico* tools, as well as genetic safeguards for biocontainment, have been developed [34]. However, even despite these efforts, *P. putida* is still away from what is now publicly regarded as a "*chassis*". One feature that particularly stands out in this bacterium is its metabolic capacity. Yet this trait has also been described as "too much of a good thing", as this very metabolic endowment may hinder the deployment of useful production pathways due to the catabolism of intermediates and the existence of yet uncharacterized (iso)enzymes [45]. However, I believe this accounts for almost any organism. Currently, we adapt microbes for the industry that are loaded with unwanted metabolic capacities. If we produce compound X from glucose, then one could reason it would not need the enzymes from xylose and arabinose catabolism. Extra protein burden has been associated with slower growth

and productivity in *E. coli* [46]. Hence, when talking about microbial production platforms, one should consider the substrate and product and remove any unnecessary genetic and metabolic information [47]. By removing the unnecessary burden, metabolic resources could be better allocated toward the product of interest, which eventually can increase yield and improve the efficiency of production processes.

In this regard, there have been various efforts to streamline metabolic capacity and control through genome reduction of *P. putida*. Through a rational approach, a first iteration was created, termed EM42, which had its genome reduced by 4.3%, eliminating functions unnecessary in industrial applications such as prophages and the flagellar machinery [48] . This strain demonstrated along with superior growth properties a net increase in ATP and NADPH availability. Recently, the genome of this strain was even further reduced by removing antibiotic resistance cassettes, improving the biosafety [49]. The genome of this final iteration was only reduced by 4.76%, whereas there are many more unnecessary parts that could potentially be removed. Of course, this is still a tedious task, as many proteins still have uncharacterized functions [50]. Therefore, unlike the rational approach mentioned above, a random approach could be used to streamline the genome. In a previous study, customized mini transposons combined with a specific recombination system were used to reduce the genome of *P. putida* by 7.4% [51]. Although this study used a randomized approach using the Tn5 transposons, new technologies such as the CRISPR-transposon could enable targeted deletion of entire genomic regions [52]. This in turn can deliver a wealth of fundamental knowledge to generate genome-reduced variants that are a more stable and predictable *chassis*.

Moreover, genome reduction would be beneficial to establish new synthetic metabolisms in a growth-coupled manner as well, as there would be less variability and interference from other metabolic pathways. This decrease in variability could aid in using growth-coupled selections with less chance of creating “cheating” cells. In **chapter 2**, we created a strain auxotrophic in glycine and serine by deleting the threonine aldolase, which can convert threonine to glycine. However, when we attempted to evolve this strain on CO_2 as the feedstock, we noticed that most likely a latent unidentified reaction could perform the same reaction, circumventing the

auxotrophy. This is not uncommon as enzymes are promiscuous by nature and often crucial for the emergence of novel metabolic pathways [53] . Hench, to establish *P. putida* as a microbial *chassis* that is predictable in behavior and metabolic capacity, removing as much of this metabolic redundancy would be a way forward.

Towards standardization and transplantation

As we move forward toward the domestication of *P. putida* as a microbial *chassis*, we ought to look beyond its existing capabilities. Although *P. putida* displays favorable characteristics, there are plenty of other traits displayed in other *chassis* that are not inherent to this bacterium. Due to this, there is reoccurring research on installing nonconventional hosts for industrial purposes [54]. A trend nowadays is to apply genetic engineering tools to nonconventional hosts, because like *P. putida*, they contain attractive industrial features [54]. But one might ask the question if it is easier to adopt these nonconventional hosts or to transfer their attractive properties to a more established one.

For example, the assimilation of C1 – compounds is a very interesting feature, yet native assimilators are limited in their genetic toolbox and therefore restricted in their engineering efforts [55]. However, these traits could be relatively easily transferred to an easier-to-handle host. In **chapter 2** we demonstrate how part of the reductive glycine pathway for C1 – assimilation could be transferred into *P. putida* allowing growth with methanol, formate, or CO_2. Further engineering would then lead to a fully synthetic C1-utilizing bacterium. This bacterium could then already benefit from the wide array of standardized production pathways that have been installed over the years. Yet, this transplantation is not always as easy as it sounds. The linear pathway transplanted in **chapter 2** is relatively easy because it has minimal overlap with the native metabolism. The same concept is extended to other linear assimilation pathways, such as the xylose catabolism described in **chapter 4**. These are, however, just some examples of transplantable traits. If we would aim to construct an ideal synthetic *chassis*, we would probably envision a minimal cell capable of self-propagation with a library of available genetic modules containing structural and metabolic functions appropriate to the desired industrial setting [56][57]. Therefore, the concept of synthetic biology should aim for the standardiza-

tion of genetic parts encoding metabolic and structural industrial features [58][59]. We often refrain from this standardization and continue with diversification, installing multiple organisms as potential "*chassis*" [44]. However, traversing the "Valley of Death" and introducing novel microbes into production processes often does not gain traction in the industry [60]. Therefore, for the sake of synthetic biology in industrial biotechnology, it would be more interesting to focus on transplantable industrial traits. It is no surprise that a plethora of interesting features for the new industrial age lies in extremophilic microorganisms. These microbes thrive in inhospitable environments where other living beings would succumb such as extreme acidity, alkalinity, temperature, or a high concentration of toxic compounds [61][62]. These extreme environments made these organisms incredibly resilient, and their microbial properties are therefore highly advantageous for industrial biotechnology. For example, temperatures in an industrial-scale bioreactor can vary a lot due to uneven mixing and varying variables, and significantly affect the microbial production [63][64]. Thus the ability to withstand high temperatures or fluctuations is an important and interesting industrial feature [43].

Another beneficial extremophilic property is halotolerance: the ability to withstand high osmotic pressures. This beneficial property would allow seawater-based fermentation, removing the need for sterilization and reducing the chance of microbial contamination [65][66]. However, just like the efflux pumps of *P. putida*, these interesting extremophilic traits are often polygenic and difficult to engineer into established biotechnological workhorses [54]. Extremophilic features such as thermotolerance have been attempted to be engineered using adaptive laboratory evolution (ALE). While evolution is a powerful approach for installing these new industrial features, it often stagnates at a certain level. For example, *E. coli* was evolved to withstand temperatures up to 48°C [67]. Nonetheless, tolerance to even higher temperatures was unfeasible as the native proteome of *E. coli* became incredibly unstable [68]. Therefore, in the quest towards programmable chemistry, it is noteworthy to further unravel the genomic and metabolic black box of extremophilic features and discover if we can modularize these features to transplant them into more conventional hosts.

Diversification or unification?

Nowadays, similar, and sometimes identical metabolic features are being put in a wide variety of microbial cell factories. Hereupon we have to ask ourselves the question once more: "does this diversification advance or hinder the progress of industrial biotechnology"? My answer would be the former. Synthetic biology aims to develop microbial cell factories *de novo* with all the desired characteristics we want, just like how Victor Frankenstein built his monster out of independent parts aiming to create the perfect being. However, to achieve this point of *de novo* construction, we need the genetic "Lego bricks" to create a more complex system. This requires standardized transplantable traits of which we need to know how they work. For example, in **chapter 3**, I aimed at transplanting the soluble hydrogenase from *C. necator* towards *P. putida*, which unfortunately did not come to fruition. Even in literature, the transplantation of hydrogenases is questioned, showing lesser activity in hosts that do not possess native hydrogenase than those that do [69]. So, for the sake of synthetic biology, which aims towards standardization, this part would be insufficient. Accordingly, one might reason that, within synthetic biology, functional transplantable parts need to be validated in several genetic and metabolic backgrounds. Although it seems redundant, it will generate information to further streamline the parts for the *chassis* of the future. Modularity is key in synthetic biology and therefore more projects should focus on the characterization of biological components [70]. All the data obtained from these characterizations can fuel computational models to provide predictions to get a better understanding of biological parts. In that regard, diversification is still needed to eventually lead to unification. We often focus on applied science and disregard the fundamental core. I find that this collection of new information on the functioning of cells is crucial and could significantly aid to develop new parts for future strains. In conclusion, all these sources of information will provide us with all the tools to create microbial cell factories for chemical production using renewable substrates.

Synthetic metabolisms for industrial biotechnology: A not so futuristic view

Rethinking the metabolic blueprint

Apart from the industrially relevant physiological features mentioned above, metabolic features should also be considered. Metabolic engineering efforts in current microbial cell factories often solely rely on the exploitation of their inherent metabolic networks [71][72]. However, these networks have evolved for millions of years and are programmed to support growth and not production. Moreover, many interesting pathways are subjected to tight regulation and therefore carry considerably low fluxes [72]. This became apparent in **chapter 5**, in which we evolved a strain to grow solely on the shikimate pathway for glycerol catabolism. At first, we speculated a tremendous number of alterations in what we perceived as logical sites, e.g., promoters of genes within the shikimate pathway or pentose phosphate pathway or coding sequences to create feedback inhibition shikimate pathway enzymes. To our surprise, only minor modifications emerged during evolution and the only universal mutated candidates were regulators that most likely abolished the metabolic regulation of this network.

Even if we disregard metabolic regulation, we often see the inherent metabolic networks as the standard blueprint to which we should adhere. But microbes have so far evolved to thrive in natural environments, not in industrial biotechnology settings. However, just like how Leonardo da Vinci applied his scientific talents to advance the fields of painting, sculpture, and anatomy, we, as metabolic engineers, can apply our understanding of biology to redesign and optimize these metabolic blueprints. For example, we often see native glycolytic pathways as the standard, even though they are not optimized for production. In **chapter 4**, we demonstrate this through the introduction of a phosphoketolase shunt which circumvents the pyruvate decarboxylation step, preserving carbon in the process. This introduction not only increased cellular fitness but also improved product formation from acetyl-CoA. This concept is especially important for industrial processes, as the final yield is crucial to compete with the petrochemical industry [73]. Consequently, an optimal pathway would need to reach as close to the theoretical yield as possible. This concept has been explored using the previously mentioned

phosphoketolase strategy. The prime example is the establishment of the designed non-oxidative glycolysis (NOG). This synthetic cyclic pathway relies on the carbon-conserving strategy of the phosphoketolase shunt combined with the carbon rearrangements of the pentose phosphate pathway [74]. Through this arrangement, the NOG enables full carbon conservation during sugar catabolism, achieving theoretical yields of 100% of acetyl-CoA from glucose. Though first designed *in vitro* and partially *in vivo*, it has recently been established as a functional metabolism in *E. coli* [75]. Moreover, an improved version of the NOG, termed the glycolysis alternative high carbon yield cycle (GATHCYC), has recently been implemented in *S. cerevisiae* [76]. This new cycle relies on the promiscuity of the phosphoketolase to omit the transaldolase and transketolase steps of the pentose phosphate pathway. Both these reactions are bidirectional and require two substrates for carbon rearrangements and were therefore pinpointed as a major bottleneck. Another milestone regarding synthetic metabolisms is the CO_2 fixating crotonyl-CoA/ethylmalonyl-CoA/hydroxybutyryl-CoA (CETCH) cycle [77]. Here, the authors combined 17 enzymes from nine different organisms of all domains of life to create this new metabolic route. Moreover, they recently extended this cycle to support *in vitro* polyketide synthesis [78]. All the pathways mentioned above are wonderful examples of metabolic marvels and they are probably only the tip of the iceberg in the extent of how we can (re)design metabolic pathways.

Redesigning the metabolic blueprint

A big player that has emerged for the redesign of pathways is retrosynthesis. This method relies on enzymatic reaction rules, which describe the pattern of the reactive sites of compounds that are recognized by promiscuous enzymes [79]. In this way, retrosynthesis can not only predict novel biosynthetic pathways for uncommon or new-to-nature compounds but potentially also reinvent new alternatives for the central carbon metabolism, such as the NOG and the GATHCYC [80]. Potentially, we could create even better catabolic and anabolic pathways for production, which are currently unknown. Novel catabolic pathways such as the NOG and the GATHCYC are very useful, but they still rely on existing biochemistries. However, one could reason that we are thereby limiting the possibilities and ought to dream big-

ger. The biochemical network is immense and could be deployed to predict alternative, perhaps better routes for industrial production [50]. In general, central carbon metabolism has been described as a minimal walk between 12 essential precursors that form all the essential building blocks and some pathways could even already have shortcuts [81]. But how can we create such a novel network? This is where the power of computational modeling comes into play. One example of the usefulness of modeling is described in **chapter 5**. Here, we used an *in-silico* approach that was efficient in establishing and optimizing the SDC, by predicting the best pyruvate-releasing reactions and byproduct formation. Computational approaches are increasingly being developed to aid metabolic engineering efforts with applications such as pathway construction and optimization [82][83]. Their implementation is a must and can take metabolic engineering to full maturation. Especially the rise of artificial intelligence will usher in a new era. We could design and tailor the microbial cell factories of the future while taking the input (carbon source) and output (product) in mind. The connectivity between those nodes can then be predicted to be as minimal and efficient as possible to obtain the desired titers, rates, and yield.

The challenges of transplanting functional C1 assimilation pathways

The valorization of C1-feedstocks, such as methanol, formate, CO_2, and CO, has gained an increasing amount of interest over the last years [84]. Their emergence can be attributed to the increase in sugar prices, the always ongoing food vs. fuel debate, and the desire for a sustainable bioeconomy [85]. This led to an increasing number of C1 assimilation pathways that are continuously being implemented in potential production hosts, one depicted in **chapter 2** within this thesis. The most focus on implementation is put on the ribulose monophosphate pathway for methanol [6][86], the reductive glycine pathway for methanol, formate, and CO_2 [10][26][27], and the Calvin cycle for CO_2 [8][9]. Even though the implementation of C1 metabolism in existing hosts is becoming more prevalent, only a few examples exist of their functional implementation, and often they required drastic metabolic rearrangements [6][86].

In this thesis, I describe the partial implementation of the reductive glycine pathway in **chapter 2**, though full growth on formate and methanol has not been

successful yet and probably requires extensive evolution. Moreover, I have attempted to install the ribulose monophosphate pathway in *P. putida*, but unfortunately, this has also been unsuccessful with the same reasoning. This might raise the question of how efficient these radical lifestyle changes are for a microbial cell factory and how this would affect eventual production. In total, a few synthetic C1 microbes have been designed, but so far, only one has been used for C1-based production. The previously engineered formatotrophic *E. coli* with the reductive glycine pathway was utilized for the production of lactate from formate, reaching 10% of the theoretical maximum [87]. Although this first proof-of-concept application is promising, lactate is still an easy bulk chemical to produce compared to others which are more intricate. So, if these strains can be used for efficient C1-based production of more complex chemicals is a question that remains to be answered in the future.

Nonetheless, this does not refrain from the fact that C1 substrates are potentially the microbial feedstock of the future. Energy-efficient conversion of C1 substrates into products can already be achieved by anaerobic acetogenic bacteria and has been realized industrially, for example, for the bioproduction of ethanol from syngas [88][89]. However, these strictly anaerobic acetogens are relatively hard to genetically modify and can only generate a limited product spectrum due to their low availability of ATP [55]. This is one of the major reasons that sparked the C1 revolution of transplanting assimilation pathways to heterotrophic microbial hosts. In this context, I ponder the question if this is the most efficient way forward. While C1 feedstocks are useful, changing the substrate preference from sugar to methanol, formate or CO_2 requires such a radical metabolic rearrangement that it might only be feasible for a few hosts, which greatly limits the possibilities. And even then, the question remains how efficient these strains will be for bioproduction. In my opinion, we should rethink C1 – metabolism and find a way to make it easier and more applicable to a wider repertoire of microbial cell factories.

A new approach for C1 – metabolism

The popularity of C1 metabolism sparked the development of novel C1 and carbon fixation pathways. Computational models and retrosynthesis can particularly be

useful to aid in the development of these novel metabolisms. However, the prediction of these pathways often uses existing biochemistries containing enzymes that are already known, for example from the KEGG (Kyoto Encyclopedia of Genes and Genome) database [90][91]. This approach is quite limited as the biochemical network is bigger than we can imagine. To establish novel biochemical pathways such as the CETCH cycle, we need to look further than what is known and strive toward what can become. Fortunately, these strides are progressively being made. The most noticeable one is the birth of the ATLAS database of biochemistry [92]. Through a computational design, a repository was created of all possible biochemical reactions by taking the known biochemical reactions in the KEGG database [92]. This database contained 130 000 hypothetical enzymatic reactions that had never been reported in any living organisms, greatly improving the possibilities for designing novel pathways. However, ATLAS only included compounds present in the KEGG database, most likely limiting the possibilities that could be achieved. Recently, an updated version termed ATLASx was created which unified 14 different databases into one curated dataset providing a platform to explore novel biosynthetic pathways [50].

Especially for the sake of C1 metabolism, the ATLAS database has been deemed useful. Novel C1 assimilation pathways have been systemically designed and *in vitro* validated [93]. These non-natural pathways were designed for the assimilation of methanol-derived formaldehyde. Even more recently, a novel C1 assimilation pathway for the assimilation of glycolaldehyde has been constructed *in vitro* [94]. Glycolaldehyde can directly be derived from formaldehyde and novel enzymes have been developed for their conversion [95][96]. However, these enzymes often still have a low substrate affinity toward formaldehyde. This is particularly a problem as formaldehyde is extremely toxic for living organisms and the concentrations presently used for these enzymes would be lethal [97]. So, although these pathways have only been realized *in vitro*, they could be extended toward microbial cell factories through further enzyme engineering efforts and potentially growth-coupled designs. In **chapter 6**, I demonstrated how a growth-coupled design could significantly increase the kinetics of CVOMT1 toward phenol. Through a similar strategy, enzymes could be engineered with better kinetics toward formaldehyde establish-

ing these pathways *in vivo*.

As mentioned before, the ATLAS database has been used to construct novel C1 assimilation pathways [93][94]. One key feature in establishing these novel pathways was the usage of aldose reactions. Aldolases are enzymes with unrivaled efficiency for C-C bond formation [98]. Some show an unprecedented donor spectrum and have a broad range of aldehydes such as formaldehyde and its derived glycolaldehyde as acceptors [99]. The concept of sugar synthesis from formaldehyde, termed the formose reaction, is not a new concept. The self-condensation of formaldehyde to form a complex mixture of carbohydrates is already possible abiotically using high temperatures, or with high pH in the presence of catalytically active species [100][101]. Even cell-free chemoenzymatic starch synthesis has already been attempted using CO_2 as a feedstock. In this research, CO_2 was chemically reduced to methanol and the released formaldehyde was converted to the glycolytic intermediate dihydroxyacetone phosphate using the computationally designed formolase [96][102]. This approach is an important starting point to generate sugar feedstocks from methanol as a precursor for industrial biotechnology. This is especially relevant because the production of green methanol from CO_2 and electricity is already being scaled at an industrial scale [103]. So, if the feedstock is there, only the pathways to generate sugars from methanol remain to be engineered. Although very powerful, aldolases are quite promiscuous due to their broad product spectrum. Any aldose reaction could possibly lead to four different stereo configurations and would require further optimization regarding specificity and efficacy [94]. Once again, growth-coupled selection strategies could be the answer here. Auxotrophic strains can be generated to select new aldolase reactions based on kinetics and stereoselectivity. As I demonstrated in **chapters 2**, **3**, and **6**, the growth of these auxotrophic strains would become completely dependent on the introduced module and input, allowing fast characterization. As a plethora of microbial cell factories can utilize rich sugars, this novel assimilation pathway could potentially set up the feature of metabolic orthogonality: the ability to plug in metabolic architectures in any given host [44]. The produced sugars from these pathways could then enter native or novel catabolic pathways such as the GATHCYC, allowing full carbon conservation and increasing product yields [76][104].

Concluding remarks

We are on the verge of understanding the diversity that metabolism has to offer, and more specifically how we can leverage it. This knowledge will give us full control over metabolic networks, transplanting and creating metabolic traits how we desire. This knowledge will generate the next generation of microbial cell factories that will have a significant impact on realizing a sustainable bioeconomy. However, establishing these novel features in microbial cell factories is a time-consuming task. Connecting these features to microbial growth can dramatically expedite the traditional pace and performance of the DBTL cycle, creating novel cell factories with unprecedented speed.

Within this thesis, I aimed at expanding the metabolic repertoire of *P. putida* KT2440 by tailoring specific features using growth-coupled selections. The research in this work not only shows how these strategies can be used to establish synthetic assimilation pathways but also how they can be used to radically redesign the complete metabolic network. Moreover, it highlights the incredible potential of growth-coupled designs for the discovery and engineering of enzymes for new biochemistries. The acquired knowledge generated within this thesis will significantly aid in further improving the metabolic repertoire of *P. putida* and establishing it as a key player in industrial biotechnology.

Bibliography

1. Dupont-Inglis, J. & Borg, A. Destination bioeconomy – The path towards a smarter, more sustainable future. *New Biotechnology* **40,** 140–143 (2018).
2. Danielson, N., McKay, S., Bloom, P., *et al.* Industrial Biotechnology - An Industry at an Inflection Point. *Industrial Biotechnology* **16,** 321–332 (2020).
3. Nielsen, J. R., Weusthuis, R. A. & Huang, W. E. Growth-coupled enzyme engineering through manipulation of redox cofactor regeneration. *Biotechnology Advances* **63,** 108102 (2023).
4. Cros, A., Alfaro-Espinoza, G., De Maria, A., *et al.* Synthetic metabolism for biohalogenation. *Current Opinion in Biotechnology* **74,** 180–193 (2022).
5. Pimviriyakul, P., Wongnate, T., Tinikul, R., *et al.* Microbial degradation of halogenated aromatics: molecular mechanisms and enzymatic reactions. *Microbial Biotechnology* **13,** 67–86 (2020).
6. Chen, F. Y., Jung, H. W., Tsuei, C. Y., *et al.* Converting Escherichia coli to a Synthetic Methylotroph Growing Solely on Methanol. *Cell* **182,** 933–946 (2020).
7. Claassens, N. J., Bordanaba-Florit, G., Cotton, C. A., *et al.* Replacing the Calvin cycle with the reductive glycine pathway in Cupriavidus necator. *Metabolic Engineering* **62,** 30–41 (2020).
8. Gassler, T., Sauer, M., Gasser, B., *et al.* The industrial yeast Pichia pastoris is converted from a heterotroph into an autotroph capable of growth on CO2. *Nature Biotechnology* **38,** 210–216 (2020).
9. Gleizer, S., Ben-Nissan, R., Bar-On, Y. M., *et al.* Conversion of Escherichia coli to Generate All Biomass Carbon from CO2. *Cell* **179,** 1255–1263 (2019).
10. Kim, S., Lindner, S. N., Aslan, S., *et al.* Growth of E. coli on formate and methanol via the reductive glycine pathway. *Nature Chemical Biology* **16,** 538–545 (2020).
11. Femmer, C., Bechtold, M., Held, M., *et al.* In vivo directed enzyme evolution in nanoliter reactors with antimetabolite selection. *Metabolic Engineering* **59,** 15–23 (2020).
12. Luo, H., Hansen, A. S. L., Yang, L., *et al.* Coupling S-adenosylmethionine–dependent methylation to growth: Design and uses. *PLoS Biology* **17,** 1–13 (2019).
13. Cravens, A., Jamil, O. K., Kong, D., *et al.* Polymerase-guided base editing enables in vivo mutagenesis and rapid protein engineering. *Nature Communications* **12,** 1–12 (2021).
14. Zhang, X., Xu, G., Shi, J., *et al.* Microbial Production of L-Serine from Renewable Feedstocks. *Trends in Biotechnology* **36,** 700–712 (2018).
15. Bouzon, M., Döring, V., Dubois, I., *et al.* Change in cofactor specificity of oxidoreductases by adaptive evolution of an escherichia coli nadph-auxotrophic strain. *mBio* **12** (2021).
16. Cahn, J. K., Werlang, C. A., Baumschlager, A., *et al.* A General Tool for Engineering the NAD/NADP Cofactor Preference of Oxidoreductases. *ACS Synthetic Biology* **6,** 326–333 (2017).
17. Sellés Vidal, L., Kelly, C. L., Mordaka, P. M., *et al.* Review of NAD(P)H-dependent oxidoreductases: Properties, engineering and application. *Biochimica et Biophysica Acta - Proteins and Proteomics* **1866,** 327–347 (2018).
18. Orsi, E., Claassens, N. J., Nikel, P. I., *et al.* Growth-coupled selection of synthetic modules to accelerate cell factory development. *Nature Communications* **12,** 1–5 (2021).
19. Gurdo, N., Volke, D. C. & Nikel, P. I. Merging automation and fundamental discovery into the design–build–test–learn cycle of nontraditional microbes. *Trends in Biotechnology* **40,** 1148–1159 (2022).
20. De Jong, E., Stichnothe, H., Bell, G., *et al. Bio-Based Chemicals: A 2020 Update* 1–79 (2020).

21. Alter, T. B. & Ebert, B. E. Determination of growth-coupling strategies and their underlying principles. *BMC Bioinformatics* **20,** 1–17 (2019).

22. Chen, J., Wang, Y., Zheng, P., *et al.* Engineering synthetic auxotrophs for growth-coupled directed protein evolution. *Trends in Biotechnology* **40,** 773–776 (2022).

23. Von Kamp, A. & Klamt, S. Growth-coupled overproduction is feasible for almost all metabolites in five major production organisms. *Nature Communications* **8,** 1–10 (2017).

24. Van Rosmalen, R. P., Smith, R. W., Martins dos Santos, V. A., *et al.* Model reduction of genome-scale metabolic models as a basis for targeted kinetic models. *Metabolic Engineering* **64,** 74–84 (2021).

25. Kim, J., Salvador, M., Saunders, E., *et al.* Properties of alternative microbial hosts used in synthetic biology: Towards the design of a modular chassis. *Essays in Biochemistry* **60,** 303–313 (2016).

26. Bruinsma, L., Wenk, S., Claassens, N. J., *et al.* Paving the way for Synthetic C1 - metabolism in Pseudomonas putida through the reductive glycine pathway. *Metabolic Engineering,* 100585 (2023).

27. Dronsella, B., Orsi, E., Benito-vaquerizo, S., *et al.* Engineered synthetic one-carbon fixation exceeds yield of the Calvin Cycle. *bioRxiv* (2022).

28. Dvořák, P. & de Lorenzo, V. Refactoring the upper sugar metabolism of Pseudomonas putida for co-utilization of cellobiose, xylose, and glucose. *Metabolic Engineering* **48,** 94–108 (2018).

29. Jeong, D., Oh, E. J., Ko, J. K., *et al.* Metabolic engineering considerations for the heterologous expression of xylose-catabolic pathways in Saccharomyces cerevisiae. *PLoS ONE* **15** (2020).

30. Sun, X., Mao, Y., Liu, P., *et al.* Global Cellular Metabolic Rewiring Adapts Corynebacterium glutamicum to Efficient Nonnatural Xylose Utilization. *Applied and Environmental Microbiology* **88** (2022).

31. Liu, J., Wang, X., Dai, G., *et al.* Microbial chassis engineering drives heterologous production of complex secondary metabolites. *Biotechnology Advances* **59,** 107966 (2022).

32. Matsumoto, T., Tanaka, T. & Kondo, A. Engineering metabolic pathways in Escherichia coli for constructing a "microbial chassis" for biochemical production. *Bioresource Technology* **245,** 1362–1368 (2017).

33. Zhang, W., Zhu, X., Wang, Y., *et al.* Bacillus subtilis chassis in biomanufacturing 4.0. *Journal of Chemical Technology and Biotechnology* **97,** 2665–2674 (2022).

34. Martin-Pascual, M., Batianis, C., Bruinsma, L., *et al.* A navigation guide of synthetic biology tools for Pseudomonas putida. *Biotechnology Advances* **49,** 107732 (2021).

35. De Lorenzo, V., Krasnogor, N. & Schmidt, M. For the sake of the Bioeconomy: define what a Synthetic Biology Chassis is! *New Biotechnology* **60,** 44–51 (2021).

36. Nikel, P. I. & de Lorenzo, V. Pseudomonas putida as a functional chassis for industrial biocatalysis: From native biochemistry to trans-metabolism. *Metabolic Engineering* **50,** 142–155 (2018).

37. Ankenbauer, A., Schäfer, R. A., Viegas, S. C., *et al.* Pseudomonas putida KT2440 is naturally endowed to withstand industrial-scale stress conditions. *Microbial Biotechnology* **13,** 1145–1161 (2020).

38. Weimer, A., Kohlstedt, M., Volke, D. C., *et al.* Industrial biotechnology of Pseudomonas putida: advances and prospects. *Applied Microbiology and Biotechnology* **104,** 7745–7766 (2020).

39. Poblete-Castro, I., Becker, J., Dohnt, K., *et al.* Industrial biotechnology of Pseudomonas putida and related species. *Applied Microbiology and Biotechnology* **93,** 2279–2290 (2012).

40. Nikel, P. I., Fuhrer, T., Chavarría, M., *et al.* Reconfiguration of metabolic fluxes in Pseudomonas putida as a response to sub-lethal oxidative stress. *ISME Journal* **15,** 1751–1766 (2021).

41. Sánchez-Pascuala, A., Fernández-Cabezón, L., de Lorenzo, V., *et al.* Functional implementation of a linear glycolysis for sugar catabolism in Pseudomonas putida. *Metabolic Engineering* **54,** 200–211 (2019).

42. Roma-Rodrigues, C., Santos, P. M., Benndorf, D., *et al.* Response of Pseudomonas putida KT2440 to phenol at the level of membrane proteome. *Journal of Proteomics* **73,** 1461–1478 (2010).

43. Thorwall, S., Schwartz, C., Chartron, J. W., *et al.* Stress-tolerant non-conventional microbes enable next-generation chemical biosynthesis. *Nature Chemical Biology* **16,** 113–121 (2020).

44. Calero, P. & Nikel, P. I. Chasing bacterial chassis for metabolic engineering: a perspective review from classical to non-traditional microorganisms. *Microbial Biotechnology* **12,** 98–124 (2019).

45. Lu, C., Batianis, C., Akwafo, E. O., *et al.* When metabolic prowess is too much of a good thing: how carbon catabolite repression and metabolic versatility impede production of esterified α,ω-diols in Pseudomonas putida KT2440. *Biotechnology for Biofuels* **14,** 1–15 (2021).

46. Shachrai, I., Zaslaver, A., Alon, U., *et al.* Cost of Unneeded Proteins in E. coli Is Reduced after Several Generations in Exponential Growth. *Molecular Cell* **38,** 758–767 (2010).

47. Vernyik, V., Karcagi, I., Tímár, E., *et al.* Exploring the fitness benefits of genome reduction in Escherichia coli by a selection-driven approach. *Scientific Reports* **10,** 1–12 (2020).

48. Martínez-García, E., Aparicio, T., de Lorenzo, V., *et al.* New transposon tools tailored for metabolic engineering of Gram-negative microbial cell factories. *Frontiers in Bioengineering and Biotechnology* **2,** 1–13 (2014).

49. Volke, D. C., Friis, L., Wirth, N. T., *et al.* Synthetic control of plasmid replication enables target- and self-curing of vectors and expedites genome engineering of Pseudomonas putida. *Metabolic Engineering Communications* **10,** e00126 (2020).

50. MohammadiPeyhani, H., Hafner, J., Sveshnikova, A., *et al.* Expanding biochemical knowledge and illuminating metabolic dark matter with ATLASx. *Nature Communications* **13,** 1–12 (2022).

51. Leprince, A., de Lorenzo, V., Völler, P., *et al.* Random and cyclical deletion of large DNA segments in the genome of Pseudomonas putida. *Environmental Microbiology* **14,** 1444–1453 (2012).

52. Klompe, S. E., Vo, P. L., Halpin-Healy, T. S., *et al.* Transposon-encoded CRISPR–Cas systems direct RNA-guided DNA integration. *Nature* **571,** 219–225 (2019).

53. Rosenberg, J. & Commichau, F. M. Harnessing Underground Metabolism for Pathway Development. *Trends in Biotechnology* **37,** 29–37 (2019).

54. Blombach, B., Grünberger, A., Centler, F., *et al.* Exploiting unconventional prokaryotic hosts for industrial biotechnology. *Trends in Biotechnology* **40,** 385–397 (2022).

55. Bertsch, J. & Müller, V. Bioenergetic constraints for conversion of syngas to biofuels in acetogenic bacteria. *Biotechnology for Biofuels* **8,** 1–12 (2015).

56. Loakes, D. & Holliger, P. Darwinian chemistry: Towards the synthesis of a simple cell. *Molecular BioSystems* **5,** 686–694 (2009).

57. Szostak, J. W., Bartel, D. P. & Luisi, P. L. Synthesizing life. *Nature* **409,** 387–390 (2001).

58. Decoene, T., De Paepe, B., Maertens, J., *et al.* Standardization in synthetic biology: an engineering discipline coming of age. *Critical Reviews in Biotechnology* **38,** 647–656 (2018).

59. Porcar, M., Danchin, A., de Lorenzo, V., *et al.* The ten grand challenges of synthetic life. *Systems and Synthetic Biology* **5,** 1–9 (2011).

60. Kampers, L. F., Asin-Garcia, E., Schaap, P. J., *et al.* From Innovation to Application: Bridging the Valley of Death in Industrial Biotechnology. *Trends in Biotechnology* **39,** 1240–1242 (2021).

61. Coker, J. A. Extremophiles and biotechnology: Current uses and prospects. *F1000Research* **5,** 1–7 (2016).

62. Ye, J. W., Lin, Y. N., Yi, X. Q., *et al.* Synthetic biology of extremophiles: a new wave of biomanufacturing. *Trends in Biotechnology* **41,** 342–357 (2022).

63. Noll, P., Lilge, L., Hausmann, R., *et al.* Modeling and exploiting microbial temperature response. *Processes* **8** (2020).

64. Rivera, E. C., Costa, A. C., Atala, D. I., *et al.* Evaluation of optimization techniques for parameter estimation: Application to ethanol fermentation considering the effect of temperature. *Process Biochemistry* **41,** 1682–1687 (2006).

65. Chen, G. Q. & Jiang, X. R. Next generation industrial biotechnology based on extremophilic bacteria. *Current Opinion in Biotechnology* **50,** 94–100 (2018).

66. Uratani, J. M., Kumaraswamy, R. & Rodríguez, J. A systematic strain selection approach for halotolerant and halophilic bioprocess development: A review. *Extremophiles* **18,** 629–639 (2014).

67. Blaby, I. K., Lyons, B. J., Wroclawska-Hughes, E., *et al.* Experimental evolution of a facultative thermophile from a mesophilic ancestor. *Applied and Environmental Microbiology* **78,** 144–155 (2012).

68. Jarzab, A., Kurzawa, N., Hopf, T., *et al.* Meltome atlas—thermal proteome stability across the tree of life. *Nature Methods* **17,** 495–503 (2020).

69. Lonsdale, T. H., Lauterbach, L., Honda Malca, S., *et al.* H2-driven biotransformation of n-octane to 1-octanol by a recombinant Pseudomonas putida strain co-synthesizing an O2-tolerant hydrogenase and a P450 monooxygenase. *Chemical Communications* **51,** 16173–16175 (2015).

70. García-Granados, R., Lerma-Escalera, J. A. & Morones-Ramírez, J. R. Metabolic engineering and synthetic biology: Synergies, future, and challenges. *Frontiers in Bioengineering and Biotechnology* **7,** 1–4 (2019).

71. Erb, T. J., Jones, P. R. & Bar-Even, A. Synthetic metabolism: metabolic engineering meets enzyme design. *Current Opinion in Chemical Biology* **37,** 56–62 (2017).

72. Nielsen, J. & Keasling, J. D. Engineering Cellular Metabolism. *Cell* **164,** 1185–1197 (2016).

73. Banerjee, D., Eng, T., Lau, A. K., *et al.* Genome-scale metabolic rewiring to achieve predictable titers rates and yield of a non-native product at scale. *bioRxiv,* 1–33 (2020).

74. Bogorad, I. W., Lin, T. S. & Liao, J. C. *Synthetic non-oxidative glycolysis enables complete carbon conservation* 2013.

75. Lin, P. P., Jaeger, A. J., Wu, T. Y., *et al.* Construction and evolution of an Escherichia coli strain relying on nonoxidative glycolysis for sugar catabolism. *Proceedings of the National Academy of Sciences of the United States of America* **115,** 3538–3546 (2018).

76. Hellgren, J., Godina, A., Nielsen, J., *et al.* Promiscuous phosphoketolase and metabolic rewiring enables novel non-oxidative glycolysis in yeast for high-yield production of acetyl-CoA derived products. *Metabolic Engineering* **62,** 150–160 (2020).

77. Schwander, T., Von Borzyskowski, L. S., Burgener, S., *et al.* A synthetic pathway for the fixation of carbon dioxide in vitro. *Science* **354,** 900–904 (2016).

78. Diehl, C., Gerlinger, P. D., Paczia, N., *et al.* Synthetic anaplerotic modules for the direct synthesis of complex molecules from CO2. *Nature Chemical Biology* (2022).

79. Hadadi, N., MohammadiPeyhani, H., Miskovic, L., *et al.* Enzyme annotation for orphan and novel reactions using knowledge of substrate reactive sites. *Proceedings of the National Academy of Sciences of the United States of America* **116,** 7298–7307 (2019).

80. Lin, G. M., Warden-Rothman, R. & Voigt, C. A. Retrosynthetic design of metabolic pathways to chemicals not found in nature. *Current Opinion in Systems Biology* **14,** 82–107 (2019).

81. Noor, E., Eden, E., Milo, R., *et al.* Central Carbon Metabolism as a Minimal Biochemical Walk between Precursors for Biomass and Energy. *Molecular Cell* **39,** 809–820 (2010).

82. Lawson, C. E., Martí, J. M., Radivojevic, T., *et al.* Machine learning for metabolic engineering: A review. *Metabolic Engineering* **63,** 34–60 (2021).

83. Liao, X., Ma, H. & Tang, Y. J. Artificial intelligence: a solution to involution of design–build–test–learn cycle. *Current Opinion in Biotechnology* **75,** 102712 (2022).

84. Teixeira, L. V., Moutinho, L. F. & Romão-Dumaresq, A. S. Gas fermentation of C1 feedstocks: commercialization status and future prospects. *Biofuels, Bioproducts and Biorefining* **12,** 1103–1117 (2018).

85. Maitah, M. & Smutka, L. The Development of World Sugar Prices. *Sugar Tech* **21,** 1–8 (2019).

86. Keller, P., Reiter, M. A., Kiefer, P., *et al.* Generation of an Escherichia coli strain growing on methanol via the ribulose monophosphate cycle. *Nature Communications* **13,** 1–13 (2022).

87. Kim, S., David Giraldo, N., Rainaldi, V., *et al.* Optimizing E. coli as a formatotrophic platform for bioproduction via the 1 reductive glycine pathway 2 (2022).

88. Köpke, M. & Simpson, S. D. Pollution to products: recycling of 'above ground' carbon by gas fermentation. *Current Opinion in Biotechnology* **65,** 180–189 (2020).

89. Liew, F. E., Nogle, R., Abdalla, T., *et al.* Carbon-negative production of acetone and isopropanol by gas fermentation at industrial pilot scale. *Nature Biotechnology* **40,** 335–344 (2022).

90. Bar-Even, A., Noor, E., Lewis, N. E., *et al.* Design and analysis of synthetic carbon fixation pathways. *Proceedings of the National Academy of Sciences of the United States of America* **107,** 8889–8894 (2010).

91. Satanowski, A., Dronsella, B., Noor, E., *et al.* Awakening a latent carbon fixation cycle in Escherichia coli. *Nature Communications* **11,** 1–14 (2020).

92. Hadadi, N., Hafner, J., Shajkofci, A., *et al.* ATLAS of Biochemistry: A Repository of All Possible Biochemical Reactions for Synthetic Biology and Metabolic Engineering Studies. *ACS Synthetic Biology* **5,** 1155–1166 (2016).

93. Yang, X., Yuan, Q., Luo, H., *et al.* Systematic design and in vitro validation of novel one-carbon assimilation pathways. *Metabolic Engineering* **56,** 142–153 (2019).

94. Mao, Y., Yuan, Q., Yang, X., *et al.* Non-natural Aldol Reactions Enable the Design and Construction of Novel One-Carbon Assimilation Pathways in vitro. *Frontiers in Microbiology* **12** (2021).

95. Lu, X., Liu, Y., Yang, Y., *et al.* Constructing a synthetic pathway for acetyl-coenzyme A from one-carbon through enzyme design. *Nature Communications* **10,** 1–10 (2019).

96. Siegel, J. B., Smith, A. L., Poust, S., *et al.* Computational protein design enables a novel one-carbon assimilation pathway. *Proceedings of the National Academy of Sciences of the United States of America* **112,** 3704–3709 (2015).

97. Klein, V. J., Irla, M., López, M. G., *et al.* Unravelling Formaldehyde Metabolism in Bacteria: Road towards Synthetic Methylotrophy. *Microorganisms* **10** (2022).

98. Windle, C. L., Müller, M., Nelson, A., *et al.* Engineering aldolases as biocatalysts. *Current Opinion in Chemical Biology* **19,** 25–33 (2014).

99. Szekrenyi, A., Garrabou, X., Parella, T., *et al.* Asymmetric assembly of aldose carbohydrates from formaldehyde and glycolaldehyde by tandem biocatalytic aldol reactions. *Nature Chemistry* **7,** 724–729 (2015).

100. Cestellos-Blanco, S., Louisia, S., Ross, M. B., *et al.* Toward abiotic sugar synthesis from CO2 electrolysis. *Joule* **6,** 2304–2323 (2022).

101. Kopetzki, D. & Antonietti, M. Hydrothermal formose reaction. *New Journal of Chemistry* **35,** 1787–1794 (2011).

102. Cai, T., Sun, H., Qiao, J., *et al.* Cell-free chemoenzymatic starch synthesis from carbon dioxide. *Science* **373,** 1523–1527 (2021).

103. Stöckl, M., Claassens, N. J., Lindner, S. N., *et al.* Coupling electrochemical CO2 reduction to microbial product generation – identification of the gaps and opportunities. *Current Opinion in Biotechnology* **74,** 154–163 (2022).

104. François, J. M., Lachaux, C. & Morin, N. Synthetic Biology Applied to Carbon Conservative and Carbon Dioxide Recycling Pathways. *Frontiers in Bioengineering and Biotechnology* **7,** 1–16 (2020).

CHAPTER 8

THESIS SUMMARY

English and Dutch

Summary

Microbial metabolism has undergone billions of years of evolution, allowing microorganisms to adapt to changing environmental conditions and exploit new energy sources. This process has led to the development of diverse metabolic pathways, such as photosynthesis, fermentation, and respiration, enabling microorganisms to thrive in various environments. This evolution of life has provided a valuable source of microorganisms and enzymes that can be leveraged in industrial biotechnology. In recent years, advancements in genomics and synthetic biology have allowed for precise manipulation of microbial metabolism, enabling the creation of new industrial biotechnology applications. Currently, we can design and construct novel metabolic pathways and transplant them into potential microbial cell factories that don't normally utilize such features. In this way, more efficient and sustainable production processes can be developed, leading to the creation of new industrial biotechnology applications. This thesis entitled "Restoring life: Growth-coupled designs for synthetic metabolisms in *Pseudomonas putida*" aims to expand the metabolic repertoire of the industrially interesting soil bacterium *Pseudomonas putida*. As the title suggests, this metabolic expansion is primarily achieved through growth-coupled selection systems. To accomplish this, strains were engineered that rely on a particular metabolic module for growth.

Chapter 1 of my work begins with an account of the rise of industrial biotechnology and metabolic engineering. I then delve into the use of growth-coupled selection systems within these fields, which allow for faster development of cell factories through the swift selection and optimization of cellular metabolic pathways. By detailing the evolution of growth-coupled selection systems, my aim is to give readers a better understanding of the potential applications of these techniques. One particularly interesting application of growth-coupled selection systems is the installation of new metabolic features such as the ability to utilize alternative feedstocks. With the ongoing food vs fuel debate, there is a pressing need for alternative carbon sources that are not intended for human consumption. C1 compounds, for example, have emerged as a promising alternative due to their sustainable production potential. Incorporating C1 compounds into microbial processes via growth-coupled selection systems presents an exciting opportunity to

develop more sustainable and environmentally friendly bioproduction methods.

In **chapter 2**, I describe the partial assimilation of three C1 compounds: methanol, formate, and CO_2. In this study, we established a growth-coupled selection system based on the amino acids glycine and serine. Growth of this strain could only be achieved if the C1 compounds were converted to these amino acids by the introduced synthetic pathway. Of particular interest was the establishment of CO_2 assimilation, which was achieved through short-term laboratory evolution. By modulating the intracellular NAD^+/NADH ratio, a single mutation in complex I of the electron transport chain enabled the assimilation of CO_2.

In **chapter 3**, we continue exploring the potential of growing *P. putida* on CO_2 as the sole feedstock. The assimilation of CO_2 as an industrial microbial feedstock is quite an interesting concept as it doesn't compete with human consumption. However, CO_2 is quite a poor feedstock compared to sugar, and an additional energy source is needed for its assimilation. Therefore, in **chapter 3** I assessed candidates that could potentially fuel the cell with all its energy. For this purpose, I utilized another growth-coupled scenario, one in which the strain can no longer produce energy when it is growing on acetate as a carbon source. In this scenario, an extra electron donor is needed to supply the cell with energy. This tight selection system was validated using formate and then used to assess the electron donors phosphite, and hydrogen. Although the functionality of phosphite was proven, it was not powerful enough to provide the bacteria with enough energy to sustain growth. For hydrogen, a synthetic module was created, genetically integrated, and transcribed. However, more research regarding its functionality as an electron donor is required.

Apart from alternative microbial feedstocks, for a successful establishment of microbial processes in the industry, it is important that as much of the substrate ends up in the product. Yet, bacterial metabolism is not hotwired for production and contains steps that can lower the final yield. One of them is the CO_2-releasing step of the pyruvate dehydrogenase. Therefore, in **chapter 4**, we demonstrated a carbon conservation mechanism to circumvent this wasteful reaction by overexpressing a highly active phosphoketolase. The introduced mechanism increased cellular fitness on both glycerol and xylose as the sole carbon source, achieving

faster growth rates and higher cell densities. In addition, yields of mevalonate and malonyl-CoA on both carbon sources were improved

In **chapter 5**, we continue with growth-coupled selections to radically alter the main metabolism of *P. putida* to create a shikimate pathway-dependent catabolism (SDC). This pathway is the biochemical source of aromatic compounds. While numerous valuable molecules can derive from this pathway, its biotechnological exploitation remains a mounting metabolic engineering challenge. This anabolic pathway is often highly regulated and carries low fluxes. Here, we installed the shikimate pathway as the main catabolic pathway for growth using a pyruvate-releasing reaction from the said pathway. We created a strain auxotrophic in pyruvate to couple the shikimate pathway with cellular growth. For this purpose, we used a reaction that cleaves the final intermediate of the shikimate pathway into pyruvate and 4-hydroxybenzoate (4HB). However, a metabolic reconfiguration of this extent requires the usage of laboratory evolution. To aid the establishment of the shikimate pathway as the dominant pathway for growth, we used a selective 4HB biosensor. Evolution eventually resulted in a heterotrophic mix of mutants and from this pool we isolated SDC.1. We discovered that mutations on the regulatory genes miaA and mexT were present in all sequenced isolates. Reverse engineering of these mutations in the pyruvate auxotroph resulted in immediate growth. This highlights the tight regulation the shikimate natively possesses and how their removal aided in establishing SDC. To assess the flux going through the pathway, we measured the yield of 4HB. Through further rational and model-driven engineering, we created a strain that achieved 89.2% of the maximum predicted yield, indicating a major catabolic flux through the shikimate pathway. Lastly, we deliver a promising strain that can serve as a useful chassis to produce various shikimate pathway-derived compounds.

Continuing with the shikimate pathway, the work described in **chapter 6** focuses on the production of anisole. Anisole is an aromatic ether with many industrial applications, yet its production up until now was only possible through chemical synthesis. In this chapter, using a basil-derived enzyme, we demonstrated first-time biological anisole production from phenol. Through a modular approach, we were able to produce anisole from glucose as the starting point. However, the anisole-

producing enzyme still displayed low selectivity towards phenol, limiting the production. Therefore, we created a growth-coupled selection system to optimize *in vivo* the kinetic parameters toward phenol as a substrate. This selection system allowed us high throughput screening of a mutant library, and after a single passage, we isolated a new superior variant with a higher affinity towards phenol.

In **chapter 7** of this thesis, I provide a comprehensive summary of the key findings and insights gained throughout my research. I focus on the potential implications for the future of microbial chassis design and novel metabolic engineering processes, highlighting their potential to advance the fields of synthetic biology and metabolic engineering.

Samenvatting

Het microbiële metabolisme heeft miljarden jaren van evolutie ondergaan, waardoor micro-organismen zich hebben kunnen aanpassen aan veranderende omgevingsomstandigheden en nieuwe energiebronnen hebben kunnen benutten. Dit proces heeft geleid tot de ontwikkeling van diverse metabole routes, zoals fotosynthese, fermentatie en ademhaling, waardoor micro-organismen in verschillende omgevingen kunnen gedijen. De evolutie van het leven heeft gezorgd voor een waardevolle bron van micro-organismen en enzymen die kunnen worden gebruikt in de industriële biotechnologie. In de afgelopen jaren hebben vorderingen in genomica en synthetische biologie nauwkeurige manipulatie van het microbiële metabolisme mogelijk gemaakt, waardoor nieuwe industriële biotechnologische toepassingen kunnen worden gecreëerd. Momenteel kunnen we nieuwe metabole routes ontwerpen, bouwen en transplanteren naar potentiële microbiële celfabrieken die deze functies normaal niet kunnen gebruiken. Op deze manier kunnen we efficiëntere en duurzamere productieprocessen ontwikkelen, wat kan leiden tot nieuwe industriële biotechnologische toepassingen. Dit proefschrift getiteld "Restoring life: Growth-coupled designs for synthetic metabolisms in *Pseudomonas putida*" heeft tot doel het metabole repertoire van de industrieel interessante bacterie *Pseudomonas putida* uit te breiden. Zoals de titel suggereert, wordt deze metabole uitbreiding voornamelijk bereikt door aan groei gekoppelde selectiesystemen. Om dit te bereiken, heb ik stammen ontwikkeld die niet kunnen groeien tenzij er een bepaalde metabole module aanwezig is.

Hoofdstuk 1 van mijn werk begint met een verslag van de opkomst van industriële biotechnologie en metabole engineering. Vervolgens verdiep ik me in het gebruik van aan groei gekoppelde selectiesystemen binnen deze velden en hoe deze systemen een snellere ontwikkeling van celfabrieken mogelijk maken door de snelle selectie en optimalisatie van cellulaire metabole routes. Door de aan groei gekoppelde selectiesystemen in detail te beschrijven, is het mijn doel de lezers een beter begrip te geven van de mogelijke toepassingen van deze technieken. Een bijzonder interessante toepassing van aan groei gekoppelde selectiesystemen is de installatie van nieuwe metabolische kenmerken, zoals de mogelijkheid om alternatieve grondstoffen te gebruiken. Met het voortdurende debat over voedsel

versus brandstof is er een dringende behoefte aan alternatieve koolstofbronnen die niet bedoeld zijn voor menselijke consumptie. C1-substraten zijn naar voren gekomen als een veelbelovend alternatief aangezien ze op een duurzame manier kunnen worden geproduceerd. Het opnemen van C1-substraten in microbiële processen via aan groei gekoppelde selectiesystemen biedt een geweldige kans om duurzamere en milieuvriendelijkere bioproductiemethoden te ontwikkelen.

In **hoofdstuk 2** beschrijf ik de gedeeltelijke assimilatie van drie van deze C1-substraten: methanol, formiaat en CO_2. In deze studie hebben we een aan groei gekoppeld selectiesysteem opgezet op basis van de aminozuren glycine en serine. Groei van deze stam kon alleen worden bereikt als de C1-substraten via een geïntroduceerde synthetische route in deze aminozuren werden omgezet. Van bijzonder belang was het success van CO_2-assimilatie, die werd bereikt door korte laboratoriumevolutie. Door de intracellulaire NAD^+/NADH-verhouding te moduleren, maakte een enkele mutatie in complex I van de elektronentransportketen de assimilatie van CO_2 mogelijk.

In **hoofdstuk 3** gaan we verder met het verkennen van het potentieel van het kweken van *P. putida* op CO_2 als enige grondstof. De assimilatie van CO_2 als een industriële microbiële grondstof is best een interessant concept omdat het niet concurreert met menselijke consumptie. CO_2 is echter een vrij slechte grondstof in vergelijking met suiker en er is een extra energiebron nodig voor assimilatie. Daarom heb ik in **hoofdstuk 3** potentiële kandidaten beoordeeld die de stam met al zijn energie zou kunnen voorzien. Voor dit doel heb ik een ander aan groei gekoppeld scenario gebruikt, een waarin de stam geen energie meer kan produceren als hij groeit op acetaat als koolstofbron. In dit scenario is een extra elektronendonor nodig om de cel van energie te voorzien. Dit strakke selectiesysteem werd gevalideerd met behulp van formiaat en vervolgens gebruikt om de elektronendonoren fosfiet en waterstof te beoordelen. Hoewel de functionaliteit van fosfiet was bewezen, was het niet krachtig genoeg om de stam voldoende energie te kunnen geven voor groei. Voor waterstof is een synthetische module gemaakt, in het genoom geïntegreerd en afgeschreven. Er is echter meer onderzoek nodig naar de functionaliteit van waterstof als elektronendonor.

Naast alternatieve microbiële grondstoffen is het voor een succesvolle vestiging

van microbiële processen in de industrie belangrijk dat zoveel mogelijk substraat in het product terechtkomt. Toch is het bacteriële metabolisme niet gemaakt voor productie en bevat het stappen die de uiteindelijke opbrengst kunnen verlagen. Een daarvan is de CO_2-afgevende stap van het enzym pyruvaat dehydrogenase. Daarom demonstreerden we in **hoofdstuk 4** een mechanisme om deze verkwistende reactie te omzeilen door een zeer actieve fosfoketolase tot overexpressie te brengen. Het geïntroduceerde mechanisme verhoogde de cellulaire fitheid op zowel glycerol als xylose als substraat, waardoor snellere groeisnelheden en hogere celdichtheden werden bereikt. Bovendien werden de opbrengsten van mevalonaat en malonyl-CoA op beide substraten verbeterd

In **hoofdstuk 5** gaan we verder met aan groei gekoppelde selecties om het centrale metabolisme van *P. putida* radicaal te veranderen en een shikimaatroute afhankelijke katabolisme (SDC) te creëren. De shikimaatroute is de biochemische bron van aromatische producten. Hoewel tal van waardevolle moleculen uit deze route kunnen voortkomen, blijft de biotechnologische exploitatie ervan een steeds grotere uitdaging voor metabole engineering. Deze anabole route is vaak sterk gereguleerd en heeft van nature lage fluxen. In ons werk, hebben we de shikimaatroute geïnstalleerd als de belangrijkste route voor groei met behulp van een pyruvaat-afgevende reactie. We creëerden een stam die auxotroof is voor pyruvaat om de shikimaatroute te kunnen koppelen aan cellulaire groei. Hiervoor hebben we een reactie gebruikt die het laatste tussenproduct van de shikimaatroute splitst in pyruvaat en 4-hydroxybenzoaat (4HB). Een metabolische verandering van deze omvang vereist echter het gebruik van laboratoriumevolutie. Om de vestiging van de shikimate-route als de dominante route voor groei te helpen, hebben we een selectieve 4HB-biosensor gebruikt. Evolutie resulteerde uiteindelijk in een heterotrofe mix van mutanten en uit deze verzameling isoleerden we de eerste stam: SDC.1. We ontdekten dat mutaties op de regulerende genen miaA en mexT aanwezig waren in alle isolaten. Het herintroduceren van deze mutaties in de pyruvaat-auxotroof resulteerde in onmiddellijke groei. Dit benadrukt de strakke regelgeving die de shikimaatroute van nature bezit complex is en hoe de mutaties in deze genen hielp bij het tot stand brengen van SDC. Om de flux die door de shikimaatroute te bepalen, hebben we de opbrengst van 4HB gemeten. Door verdere rationele en modelgestu-

urde engineering hebben we een stam gecreëerd die 89,2% van de maximaal voorspelde opbrengst behaalde, wat wijst op een grote katabole flux door de shikimaatroute. Als laatste, leveren we een veelbelovende stam die kan dienen als een nuttig chassis om verschillende producte te produceren van de shikimaatroute.

Voortbordurend op de shikimaatroute, concentreert het werk beschreven in **hoofdstuk 6** zich op de productie van anisool. Anisool is een aromatische ether met veel industriële toepassingen, maar de productie ervan was tot nu toe alleen mogelijk door chemische synthese. In dit hoofdstuk demonstreerden we met behulp van een enzym afkomstig uit basilicum de eerste biologische productie van anisool uit fenol. Door een modulaire aanpak konden we anisool produceren uit glucose als uitgangspunt. Het anisoolproducerende enzym vertoonde echter nog steeds een lage selectiviteit voor fenol, waardoor de productie werd beperkt. Daarom hebben we een aan groei gekoppeld selectiesysteem gecreëerd om *in vivo* de kinetische parameters voor fenol als substraat te optimaliseren. Dit selectiesysteem stelde ons in staat om een mutantenbibliotheek met hoge doorvoer te screenen, en na een enkele passage een nieuwe superieure variant met een hogere affiniteit voor fenol te isoleren.

In **hoofdstuk 7** van dit proefschrift geef ik een uitgebreide samenvatting van de belangrijkste bevindingen en inzichten die ik tijdens mijn onderzoek heb opgedaan. Ik concentreer me op de mogelijke implicaties voor de toekomst van het ontwerp van microbiële chassis en nieuwe metabolische processen, waarbij ik hun potentieel benadruk om vooruitgang te boeken op het gebied van synthetische biologie en metabole engineering.

Appendices

Lyon Bruinsma

Acknowledgements

And now, dear reader, the story is over. Time flies when you're having fun, and what a fun time it was. Four years of doing research alongside wonderful people who share my love and passion for science. Although I must admit it was hard to drag myself out of the lab, I am happy that I started writing and that it resulted in the thesis you are reading right now. And after this, I will finally have the privilege to yell "Yes!" when someone asks if there is a doctor in the room. There is a certain beauty in that.

To all those who have played a role in my journey, whether large or small, I extend my heartfelt thanks. Your contributions have been immeasurable, and I could not have achieved this milestone without you. Yet, I would be remiss if I didn't give a special mention to the wonderful people who made these years unforgettable.

First, I would like to express my gratitude toward my supervisor, **Vitor**. At the start of the Ph.D., I was quite lost in which direction I should go, but you gave me the freedom to explore the unknown and pursue my putida ambitions. I deeply value the trust, guidance, and support you have given me over the years.

I would also like to take this opportunity to express my gratitude to the members of my thesis committee, **Diana Machado de Sousa**, **Marian de Mey**, **Sonja Billerbeck**, and **Maia Kisvaar** for taking the time to assess and evaluate my research work.

Although many people have been integral during my four years of research, there are three people that are in the top layer. My musketeers: **Christos**, **Enrique**, and **Maria**, with whom I spend countless hours, afternoons, and weekends in and out of the lab.

Christos, my μαλακα. You know how I am a fan of bad jokes, so with this I would like to compare you to an enzyme. Why you ask? Because you truly acted as a catalyst during my Ph.D. You were someone I could always share my metabolic engineering ideas with. You never said, "What if" but always said "Let's do it!". A positive feedback loop that I always loved. You truly are a metabolic Daedalus, coming

up with new ideas almost every second. Our collaborations have been fruitful ones and there are only many more to come.

Enrique(or maybe Camilo in disguise?). Even before my Ph.D. started, during the master thesis, you have been a mentor for me, and it has only intensified ever since. Together with Christos, you guys walked, so the rest of us could run, smoothing the path for my Ph.D. and now even for the Postdoc. You always look out for the best in anyone and try to make that person reach their full potential. Over the last few years, you have been a true comrade, a listening ear to talk to, and a great guide during my putivueltas. You truly are a remarkable friend.

Maria. Who knew such greatness could come in such a small, i mean, standard-sized package? You wanted me to write five pages of acknowledgments just for you, and I probably could. However, you forgot my pimentón in Barcelona three years ago, so as a punishment I shall only write this tiny paragraph. Anyway, I don't think there are enough words to express my gratitude to you. We go all the way back to the Master, where I still had hair and you were a fiery redhead. And now, look at us, you're a Morena, and I am Dwayne "the Rock" Johnson, minus the tattoos, tan, and muscles. Sometimes I am frightened about our telepathic abilities, but I am always happy that I can share anything with you. Although sometimes I wonder if you understand, as you always say: "I don't know what you're talking about".

Thanks, my musketeers. For the many moments of laughs, beers, parties, sunny trips, and many things more. I would say there's no greater gift than when colleagues turn into friends. It makes the work not even feel like work anymore.

I would like to thank all the other wonderful people in the lab of SSB who made the time spend there noteworthy.

Sara Moreno, part of the famous Salvaro™, you're a brilliant clever girl and a computational wizard. Every time you touch those keys, magic happens. It was such an honor to collaborate with you and above all to call you a friend. Unlike Maria, you actually brought me pimentón. If that's not friendship, then I don't know what is. **Sara Benito**, my Peliroja who secretly might be a Morena. You were my C1 – señorita, and I loved the discussions and moments we shared over the years. Moreover, you're an extremely clever scientist. Putting your e-mail in the middle

of a figure on a poster, so people can contact you. Just genius. **Efsun**, you're a delightful and kind person and moreover an amazing cook. Your yeast might be oily, but your food is divine. This is a kind reminder that it's still not too late to adopt me. **Sabientje**, your presence is an everlasting joy. You brighten up every room with your happiness and upbeat personality. And I'm happy that now I can enjoy it almost every day. That many puzzle breaks may be present in our future. **Alex**, jaaa. Mein Deutsche Schmetterling. I am sure you have already planned your whole life in a colorful planner. And although this planning is probably quite rigid, I'm happy you have the flexibility to go beyond the German stereotype and be the friendly outgoing person you are. It's a pleasure to work with you. **Marco C**. Güey! You joined us in the middle of the pandemic and I can't imagine it must have been easy to go from the sun to the rain. But you have managed yourself well. It's always a joy to work and talk with you. **Marco A**, my Italian brother. The greatest tragedy ever written is the story of how we only met in the last year of my Ph.D. and not in the first. We know the world was not prepared for us to make every party legendary, but just imagine how epic the world would be if we could. Unicum!

Silvia, thanks for all the help around the lab, you are a silent force until a mosh pit comes along, then you turn completely loca and I love it. **Tom**, our HPLC wizard, thank you so much for all the technical assistance over the years. **Willemijn**, thank you for all your organizational skills, already starting when I was still a student in Porto, all the way to booking the Ph.D. defence on a broken website. To my former office mates, **Nong**, **Rita**, **Luis**, and **Linde**, thanks for all the great chats and jokes we had along the way. **Bart**, thanks for all the help with analyzing the whole genome sequencing. **Peter**, thanks for seeing the potential in me during my thesis, which led to the start of my Ph.D. **Cristina** and **Rob**, thanks for all your help with the students. **Maria**, thanks for the nice chats and advice over the years. I think I never met someone who knows as much about any topic as you. I'm sure you will take SSB to great heights! To the rest of the SSB members, current and former: **Nhung**, **Rik**, **Henk**, **Jasper**, **Eduardo**, **Sanjee**, **Wasin**, **Archita**, **Sonja**, **Erika**, **Stamatios**. Thanks for all the fun times, including Christmas events, Cakes, Seminar drinks, High chocolates, and much more.

During the last few years, I had the pleasure and privilege of supervising many fantastic students and none of this work could have been done without them. **Kesi**, I feel blessed because I had the privilege of having you not once, but twice as my student. You were an integral part of setting up two of my research projects. You are an amazing researcher and one of the kindest people I have ever met. Moreover, you make the best tempeh! Terima kasih! **Simon**, we were so unlucky that on the day your thesis started the corona pandemic hit the Netherlands and we all had to quarantine. In the following homebound weeks, it became clear to me that you had tremendous potential that the pandemic simply wasted. Luckily, we could still squeeze in some days of labwork at the end of your thesis. You'll achieve great things, of that, I'm sure. **Marieken**, you were an incredibly determined person. When the experiments were beating you down, you just kept on working harder. In that way, I like to believe you took after your old supervisor, which probably also explains why we took so many breaks and had such fun wine hours. **Job**, when we met your skills were already on par with those of a Ph.D. student. Your ability to go beyond the scope of the project and elevate it to a higher level was amazing. The professor that gets you as a Ph.D. candidate will be a lucky person. **Imogen**, you were my final student and from the first meeting, I already knew our personalities were a great match. From then on, the lab was always filled with laughter. During your thesis, I saw you develop from a caterpillar to an imogenbutterfly.

Next, I would like to thank all the bonus IGEM students that I acquired over the course of my Ph.D. **Ben** and **Alba**, you were my first IGEM students ever and I loved coaching and working with you. I will especially remember the trip to Boston and becoming the runner-up at the IGEM jamboree. And then my other bonus students, my favorite cowgirls (Shania Twain starts playing – Let's go girls!), **Anemoon**, **Sanne** and **Sophieke**. It was an absolute blast having you girls in the lab. It was weeks full of joy, fun, parties, laughter and only fond memories to look back on.

Of course, there are many more wonderful people I have met over the year that I want to thank. Starting with the two people that make up my patented **Belenzo™**. **Belen**, you are one of the kindest souls there is out there. I thoroughly enjoyed all our times together, from the dinners, parties, and dozens of times we went plant

shopping. There is always a big smile on your face (if you're not home with covid again of course). But no need to worry, in the next pandemic, you can rely on me again to buy you toilet paper. **Lorenzo**, my friend. You're the only Italian who ever dared to utter my new Italian word "Grazione" and thereby tried to significantly improve the Italian language. One day we'll get there and transform Italy! And then we can also start building our dragon. I hope from the bottom of my heart, that you will once get your Godzilla. **Despoina**, like Maria, we have known each other since the Master and since then you two have swapped hair colors. You have been a great friend ever since. If only everyone would have your childlike sense of wonder, the world would be a happier place. May we twerk forever together! **Pilar**, also we met all the way back in the master and you have been a great friend ever since. Although we celebrated your veinitiochañera during the thesis, you have only become younger in spirit since then. Because of you, I am more Mexican, and that's why I always arrive an hour late at parties. But I still have some practice to do, as you still always arrive later than me. One day I will realize my dream, to record your sneezes and make the perfect and happiest morning alarm clock ever. Furthermore, I would like to thank **Fotis**, **Yahya**, **Dani** (Feo), and **Jeroen** for the many fun nights, trips, and adventures we shared over the years and the many more that will come.

My Greek muses, **Anastasia**, **Nancy**, **Kassiani** and **Menia**. Every time when I see you goddesses, my mood just elevates to a higher power. I'm so happy Zeus made you lovely ladies. It's never a Greek tragedy when anyone of you is around. You all have a special place in my heart and It's an everlasting joy to call you guys my friends. **Stephan** and **Isabelle**, you might be the most fun and crazy married couple I know. Thank you for all the random, yet amazing friday drinks that always ended up in the international club at night and unfortunately hangover in the morning. **Nico**, we started with a simple meeting to talk about C1, and from thereon, you became like a second supervisor to me. Your knowledge has been extremely helpful in further shaping one of my favorite projects. To **Iame** and **Sara**, thank you for all the help with anaerobic bottles and CO_2 experiments, I was a complete noob and you really showed me the way. **Marina**, my Italian-Brazilian karaoke star, your

joyful personality always managed to brighten my day. **Martha**, like any Indonesian person I ever met, you are an angel. One of the kindest persons in know with the biggest smiles on your face 24/7. **Miguel** (Feolito), when I called you Feo in our first e-mail and you appreciated it, I knew you were an amazing guy. You're often batshit crazy and that's exactly how I like my friends. And by hanging out with **Ricardo** (Feo dos or maybe Guapo for once?), I'm sure you two will only amplify each other's craziness. **Carina**, I loved how our gel room talks always quickly turned into a one-hour discussion about the great existential matters in the universe. To my MicEvo neighbours, **Patricia**, **Daniel**, **Burak**, **Guillaume**, **Jolanda**, **Stephan**, **Kassiani**, and **Yassin**. Nine out of ten times, when I walked to the canteen, you guys would be there and have time for a coffee and a chat. Thank you for those happy breaks. I would like to thank all the other people who made the time in Helix enjoyable: **Cristian**, **Carrie**, **Irene**, **Thomas**, **Prokopsis**, **Costas**, **Caifang**, **Chen**, **Evgenious**, **Suzan**, **Eric**, and **Ivette**.

I would like to thank my fellow organizer of the Ph.D. trip 2022 to California, **Carina**, **Peter**, **Max**, **Valentina**, **Maria**, **Lorenzo**, **Despoina** and **Anastasia**. It was not easy to pull off an amazing trip during a pandemic. But I am so happy we have managed to pull it off in the end. Thank you also to **Raymond** and **Michelle**, for being such amazing supervisors along this extraordinary trip. I wanna thank the synthetic metabolism and C1 team, **Nico**, **Miguel**, **Panos**, **Suzan**, **Vittorio**, **Olufemi**, and **Sara** for all the fruitful and intriguing lunch meetings we had over the last few years.

Next, I would like to thank **Alex**, **Antoine**, **Antonia**, **Carlos**, **Chunze**, **Claudia, Guniz**, **Henrik**, **Isa**, **Kari**, **Jenny**, **Jort**, **Julia**, **Laura**, **Miriam**, **Matic**, **Mels**, **Nicola**, **Noor** (Hear me Roar, Gezellig!!), **Nuran**, **Pedro**, **Tim**, **Wimar**, and all the other people at BPE. The introduction in your group was one of the easiest ever. The vibes are completely amazing, and I am looking forward to keeping on working in this great atmosphere.

Next to my colleagues, there are several other people who had the joy of having me in their life. These people made me leave the lab for them, which is already an indication of their significance in my life.

Rubén (Pedo Gordo aka Rub Rub), you might be one of the weirdest people I have ever met, and I fricking love it. Thank you for making me seem normal. Since the master, you have been one of my greatest friends. Sometimes it's like we share one brain, and it scares me. **Jim**, you were my introduction son all the way back during our bachelor's. And apart from throwing you on the roof and making you land on my bike; I like to believe I was a good parent. I love our dark humor talks about Karen's and whatever. **Lisa**, we met during our bachelor's, and since then you have never been able to get rid of me. We shared so much over the years, from countless coffees to amazing stories. You've always been there for me, and I know you will always be. And I am happy that you have met your Tonto. **Pablo**, you're one amazing kind and funny guy, although you already make the occasional bad dad joke. But I'll forgive you for that. Furthermore, I would like to thank **Annemarie** (224), **Carlos**, **Mei, Federica**, and **Stephane** for all the fun dinners, beers, and parties we had over the years.

A big thanks to my Ljouwert doebies: **Jennifer**, **Jentina**, **Rosan**, **Mike**, **Jose**, **Marleen**, **Kimberly, Reina**, **Klarinda**, **Hans**, **Marcel**, **Lydia**, **Wilco**, and **Jurjen** for all their support. With many of you, I started student life in the beautiful Leeuwarden over a decade ago (My god, we're old.…). Still, I feel so grateful to be able to enjoy your company. From the Covid-among us games and pubquizzes to the countless trips, sinterklaasjes, parties, and everything else we shared. Thanks for everything, Doebies!

Bedankt aan al mijn Klazienaveense waailapjes : **Yorick**, **Yoeri**, **Stefanie**, **Nina**, **Romy**, **Kevin**, **Ashley**, **Sharon**, **Stefan** en **Marc**. De meeste van jullie ken ik al decennia lang en ik kan geen tijd meer herinneren zonder jullie. Jullie steunen mij altijd door (heel erg) dik en dun en elke keer wanneer we samen zijn krijg ik buikpijn van het lachen. Ook al is mijn aanwezigheid nogal geminderd over de laatste jaren, echte vrienden blijven. Moar eem poar neem'n onnie?

Duizend bedankjes voor mijn geweldige familie, die mij van kinds af aan hebben geleerd om altijd het positieve en overal de lol in te zien. Zij zijn de reden waarom ik vooral om al mijn eigen grappen lach. **Opa en Oma Immink**, ook al denken jullie waarschijnlijk nog steeds dat ik een medische doctor word, jullie onvoorwaardelijke steun ongeacht van wat ik doe is het enige wat een kleinkind nodig heeft. Dank jullie wel. **Oma Bruinsma**, ook al bent u al heengegaan voordat ik mijn PhD begon, bij deze wil ik u toch bedanken voor alle steun die u mij al deze jaren gegeven heeft. Ook al was u grootste angst dat ik kou zou vatten omdat ik geen sokken droeg met mijn sandalen, u steunde mij altijd en overal. Dank u wel. Verder wil ik de twee aapjes in mijn leven, **Jaime** en **Roan**, bedanken. Het leven met jullie twee was nooit saai, er was altijd wel wat te beleven. En wat ma en pa ook zeggen, wij gedroegen ons altijd… nou ja ik dan. Verder ben ik helemaal verheugd dat jullie allebei een geweldige partner hebben gevonden om jullie onder de duim te houden. **Annika** en **Dagmar**. Jullie zijn beide geweldige dames en ik kan niet wachten om nog vele jaren met jullie door te mogen brengen.

Als laatste, zijn er twee mensen die alle lof in de wereld verdienen, mijn ouders **Anja** en **Martin**. Zelfs met een wetenschappelijke methode is niet vast te leggen hoeveel ik van deze twee mensen houd. Niet alleen hebben zij mij alle kansen gegeven die ik kan krijgen in het leven. Zij zouden alles opgeven, zodat ik en mijn broers een geweldig leven zouden kunnen leiden. En alleen dit feit al, kan niet beschrijven hoeveel ik van hen hou. Niet alleen voor de laatste jaren, maar voor mijn hele leven. Zij zijn altijd mijn steun en toeverlaat geweest en staan achter elke keuze die ik maak en het is niet in woorden uit te leggen hoe dankbaar ik ben voor alles wat zij mij hebben gegeven. Deze thesis zou niet mogelijk zijn zonder hun. Dank jullie voor alles!

About the author

Once upon a time, not too long ago, Lyon Bruinsma was born on the 4th of June 1994 in Klazienaveen, the Netherlands. Being a curious and rather nerdy kid, he always wanted to know how the world worked. During high school, this passion skyrocketed, which led him to study Biotechnology at the Hogeschool van Hall Larenstein in Leeuwarden.

For his BSc thesis, he relocated to the cold tundras in Finland to work at the University of Tampere. Here, he was working on studying the effect of the introduction of alternative oxidases in mitochondria for tissue regeneration.

Driven by his eagerness to learn more, he started his MSc studies in Molecular and Cellular Biotechnology at Wageningen University. This included a MSc thesis in the laboratory of Systems and Synthetic Biology, characterizing a citrate exporter in *Aspergillus niger*.

Unbeknownst at the time, this would also lead to the place where he would pursue his Ph.D. Though in between these two periods, he relocated to the sunny shores of Portugal for his MSc internship at the Instituto de Investigação e Inovação em Saúde da Universidade do Porto, in which he investigated the effect of salt stress on compatible solutes production in cyanobacteria.

Now knowing the true meaning of “Saudade”, Lyon moved back to the Netherlands to start his Ph.D. research project in September 2018 at the Laboratory of Systems and Synthetic Biology of Wageningen University under the supervision and mentorship of Professor Vitor Martins dos Santos. The accumulated work of this project can be read within the borders of this thesis.

Currently, Lyon is a Postdoctoral researcher at the group of Bioprocess Engineering at Wageningen University working on the development of novel enzymes for biomanufacturing purposes.

List of publications

- ✎ **L. Bruinsma**, S. Wenk, N. J. Claassens*, and V. A. P. Martins dos Santos*. Paving the way for synthetic C1 metabolism in *Pseudomonas putida* through the reductive glycine pathway. Metabolic Engineering, (2023) https://doi.org/10.1016/j.ymben.2023.02.004

- ✎ **L. Bruinsma**, M. Martin-Pascual, K. Kurnia, , M. Tack, , S. Hendriks, , R.van Kranenburg, and V. A. P. Martins dos Santos (2023). Increasing cellular fitness and product yields in *Pseudomonas putida* through an engineered phosphoketolase shunt. Microbial Cell Factories, 22(1), 1-9. https://doi.org/10.1186/s12934-022-02015-9

- ✎ M. Martin-Pascual*, C. Batianis*, **L. Bruinsma***, E. Asin-Garcia, L. Garcia-Morales, R. A. Weusthuis, R. van Kranenburg and V. A. P. Martins dos Santos. A navigation guide of synthetic biology tools for *Pseudomonas putida*. Biotechnology Advances 49, 107732 (2021) doi.org/10.1016/j.biotechadv.2021.107732

- ✎ T. Laothanachareon, **L. Bruinsma**, B. Nijsse, T. Schonewille, M. Suarez-Diez, J. A.Tamayo-Ramos, and P. J. Schaap, (2021). Global transcriptional response of *Aspergillus niger* to blocked active citrate export through deletion of the exporter gene. Journal of Fungi, 7(6), 409. https://doi.org/10.3390/jof7060409

- ✎ A. Andjelković, A. Mordas, **L. Bruinsma**, A. Ketola, G. Cannino, L. Giordano, and H. T.Jacobs, (2018). Expression of the alternative oxidase influences Jun N-terminal kinase signaling and cell migration. Molecular and Cellular Biology, 38(24), e00110-18. https://doi.org/10.1128/MCB.00110-18

* denotes equal contribution

Co-author affiliations

✉ Laboratory of Systems and Synthetic Biology - Wageningen University & Research

Wageningen, 6708 WE, The Netherlands

Maria Martin-Pascual, Vitor A. P. Martins dos Santos[a], Christos Batianis[a], Sara Moreno-Paz, Kesi Kurnia[b], Marieken Tack, Simon Hendriks, Job J. Dirkmaat

✉ LifeGlimmer GmbH

Berlin, 12163, Germany

Vitor A. P. Martins dos Santos [a]

✉ Laboratory of Microbiology - Wageningen University & Research

Wageningen, 6703 HB, The Netherlands

Nico J. Claassens, Richard van Kranenburg

✉ Corbion

Gorinchem, 4206 AC, The Netherlands

Richard van Kranenburg

✉ Bioprocess Engineering Group - Wageningen University & Research

Wageningen, 6700 AA, The Netherlands

Ruud A. Weusthuis

✉ Systems and Synthetic Metabolism Group - Max Planck Institute of Molecular Plant Physiology

Potsdam-Golm, 14476, Germany

Sebastian Wenk

Current addresses

a. Bioprocess Engineering Group - Wageningen University & Research

Wageningen, 6700 AA, The Netherlands

b. Faculty of Engineering and Natural Sciences - Tampere University

Tampere, 33720, Finland

Overview of completed training activities

Discipline specific	**Year**
EmPowerPutida 7th General Assembly	2018
EmPowerPutida 8th General Assembly	2019
Lost in Translation - Analysing SynBio	2018
SynBio WUR Impulse Seminar	2018
IGEM Jamboree	2019
5th Applied Synthetic Biology in Europe	2020
Metabolic Engineering 14, AIChE	2021
The 2nd International BioDesign Research Conference	2021
NBC22 Biotechnology Conference	2022
Microbial Biotechnology Symposium 8.0	2022
CO_2 Symposium: The expanding world of biological one carbon fixation	2022
General	
VLAG PhD week	2018
The Choice: Un-box your PhD process & take charge of your performance	2019
Scientific writing	2021
Presenting with impact	2021
Career perspectives	2022
Optional	
Preparation of research proposal	2017
PhD study tour to Boston and New York	2019
PhD study tour to California, incl. organising committee	2022
Weekly and monthly group meetings	2018-2022
iGEM	2019-2021

Colophon

The research described in this thesis was financially supported by the European Union Horizon2020 projects EmPowerPutida (grant agreement nr. 635536) and IBISBA (grant agreements nr. 730976 and 871118).

Cover by: Lyon Bruinsma
Printed by: ProefschriftMaken